Algorithms for Geometric Optimization and Enrichment in Industrialized Building Construction

by

Christopher Rausch

A thesis
presented to the University of Waterloo
in fulfillment of the
thesis requirement for the degree of
Doctor of Philosophy
in
Civil Engineering

Waterloo, Ontario, Canada, 2021

Examining Committee Membership

The following served on the Examining Committee for this thesis.

External Examiner	MOHAMED AL-HUSSEIN Professor, University of Alberta
Supervisor(s)	CARL HAAS Professor, Department Chair, University of Waterloo
Internal Member	SCOTT WALBRIDGE Professor, Director (ArchE), University of Waterloo
Internal Member	DANIEL LACROIX Professor, University of Waterloo
Internal-external Member	JONATHAN ENNS Professor, University of Waterloo

Author's Declaration

This thesis consists of material all of which I authored or co-authored: see Statement of Contributions included in the thesis. This is a true copy of the thesis, including any required final revisions, as accepted by my examiners.

I understand that my thesis may be made electronically available to the public.

Statement of Contributions

Chapter 4 includes core contributions that I have made in a publication for the Journal of Automation in Construction. As part of this publication, I wrote the entire manuscript, and I received assistance from the co-authors in the following way. First, for the experiments, I received assistance from an undergraduate research assistant Carol Liang who assisted with running several Monte Carlo simulations. In addition, I received editorial advice, feedback, and contributions for the manuscript from Prof. Carl Haas and Dr. Mohammad Nahangi.

Chapter 5 includes core contributions in a journal article that has been published in the journal of Construction Engineering and Management. For this publication, I wrote the manuscript in its entirety and conducted all of the experiments. The co-authors for this paper, Prof. Benjamin Sanchez and Prof. Carl Haas assisted by providing editorial advice, feedback, and contributions.

Chapter 6 includes core contributions in a journal article that has been published in the International Journal of Construction Management. For this publication, I wrote the entire manuscript and conducted all functional demonstrations. The co-authors provided assistance as follows. Dr. Ruodan Lu provided a brief write-up about geometric digital twins and Dr. Saeed Talebi provided a brief write-up and identification of dimensional tolerance requirements for some of the elements found in industrialized construction. Both Dr. Lu and Dr. Talebi, along with Prof. Haas provided additional editorial advice, feedback, and contributions.

Chapter 7 includes core contributions in a journal article published in the Journal of Automation in Construction. As part of this publication, I wrote the entire manuscript and conducted all experiments. My co-author Prof. Carl Haas provided valuable editorial advice, feedback, and contributions.

Chapter 8 includes core constructions made in several publications. First, I present core contributions made in a conference paper for an approach that automatically extracts semantic information for building assemblies required for disassembly planning. This work stems from initial research conducted by Prof. Benjamin Sanchez who developed a product recovery management framework. My contribution was developing an automated approach to obtaining the metadata required for this framework. I drafted the entire conference paper and received assistance from co-authors (Prof. Benjamin Sanchez and Prof. Carl Haas) in the form of editorial advice, feedback, and contributions. Chapter 8 also includes contributions I made in a second conference paper for ‘product cycling’ of industrialized buildings. I drafted this paper in entirety and developed the algorithm shown. I received

assistance from Prof. Benjamin Sanchez who drafted a section on life cycle impacts which is required in the algorithm. In addition, Chloe Edwards provided assistance by conducting a structural analysis of the foundations, which is part of the conceptual configurator presented in this work.

Abstract

The burgeoning use of industrialized building construction, coupled with advances in digital technologies, is unlocking new opportunities to improve the status quo of construction projects being over-budget, delayed and having undesirable quality. Yet there are still several objective barriers that need to be overcome in order to fully realize the full potential of these innovations. Analysis of literature and examples from industry reveal the following notable barriers: (1) geometric optimization methods need to be developed for the stricter dimensional requirements in industrialized construction, (2) methods are needed to preserve model semantics during the process of generating an updated as-built model, (3) semantic enrichment methods are required for the end-of-life stage of industrialized buildings, and (4) there is a need to develop pragmatic approaches for algorithms to ensure they achieve required computational efficiency. The common thread across these examples is the need for developing algorithms to optimize and enrich geometric models. To date, a comprehensive approach paired with pragmatic solutions remains elusive. This research fills this gap by presenting a new approach for algorithm development along with pragmatic implementations for the industrialized building construction sector.

Computational algorithms are effective for driving the design, analysis, and optimization of geometric models. As such, this thesis develops new computational algorithms for design, fabrication and assembly, onsite construction, and end-of-life stages of industrialized buildings. A common theme throughout this work is the development and comparison of varied algorithmic approaches (i.e., exact vs. approximate solutions) to see which is optimal for a given process. This is implemented in the following ways. First, a probabilistic method is used to simulate the accumulation of dimensional tolerances in order to optimize geometric models during design. Second, a series of exact and approximate algorithms are used to optimize the topology of 2D panelized assemblies to minimize material use during fabrication and assembly. Third, a new approach to automatically update geometric models is developed whereby initial model semantics are preserved during the process of generating an as-built model. Finally, a series of algorithms are developed to semantically enrich geometric models to enable industrialized buildings to be disassembled and reused.

The developments made in this research form a rational and pragmatic approach to addressing the existing challenges faced in industrialized building construction. Such developments are shown not only to be effective in improving the status quo in the industry (i.e., improving cost, reducing project duration, and improving quality), but also for facilitating continuous innovation in construction. By

way of assessing the potential impact of this work, the proposed algorithms can reduce rework risk during fabrication and assembly (65% rework reduction in the case study for the new tolerance simulation algorithm), reduce waste during manufacturing (11% waste reduction in the case study for the new panel unfolding and nesting algorithms), improve accuracy and automation of as-built model generation (model error reduction from 50.4 mm to 5.7 mm in the case study for the new parametric BIM updating algorithms), reduce lifecycle cost for adapting industrialized buildings (15% reduction in capital costs in the computational building configurator) and reducing lifecycle impacts for reusing structural systems from industrialized buildings (between 54% to 95% reduction in average lifecycle impacts for the approach illustrated in Appendix B). From a computational standpoint, the novelty of the algorithms developed in this research can be described as follows. Complex geometric processes can be codified solely on the innate properties of geometry – that is, by parameterizing geometry and using methods such as combinatorial optimization, topology can be optimized and semantics can be automatically enriched for building assemblies. Employing the use of functional discretization (whereby continuous variable domains are converted into discrete variable domains) is shown to be highly effective for complex geometric optimization approaches. Finally, the algorithms encapsulate and balance the benefits posed by both parametric and non-parametric schemas, resulting in the ability to achieve both high representational accuracy and semantically rich information (which has previously not been achieved or demonstrated).

In summary, this thesis makes several key improvements to industrialized building construction. One of the key findings is that rather than pre-emptively determining the best suited algorithm for a given process or problem, it is often more pragmatic to derive both an exact and approximate solution and then decide which is optimal to use for a given process. Generally, most tasks related to optimizing or enriching geometric models is best solved using approximate methods. To this end, this research presents a series of key techniques that can be followed to improve the temporal performance of algorithms. The new approach for developing computational algorithms and the pragmatic demonstrations for geometric optimization and enrichment are expected to bring the industry forward and solve many of the current barriers it faces.

Acknowledgements

Throughout the course of my graduate studies (both during my MASc and during my PhD), I had the great honour of being supervised by Professor Carl Haas. Over the years, your support, guidance, and friendship have not only made way for a productive academic journey, but also made for some incredible memories on the ski trails, on the tennis court, and travelling to and from conferences. I am indebted to your wise, loyal, and kind-hearted character.

I would like to acknowledge the financial support of the Natural Sciences and Engineering Research Council of Canada, Mitacs, Edge Architects, and the University of Waterloo. In addition, I want to acknowledge the in-kind support of FARO, Dimensional Control Systems, Edge Architects, and Z-Modular.

During the course of my PhD, I had the privilege to collaborate closely with numerous members from industry, who collectively helped to shape my research ideas and to gauge its pragmatism for implementation. In particular, I am grateful to Matt Bolen, Mike Trussell, Brian Pitts, Ann Bilodeau, Nicholas Gouthro, Darren Sippel, David Warne, Aziz Dhamani, Joshua Bigham, Brent Slawnikowski, and Scott Diaz. I also had the opportunity to collaborate with several academic researchers, who similarly helped to shape my research ideas, and who I worked closely with in the development of new publications. In particular, I am grateful to Dr. Benjamin Sanchez, Sheida Shahi, Dr. Ruodan Lu, Dr. Saeed Talebi, Dr. Mani Poshdar, Dr. Carl Schultz, Beidi Li, Yinghui Zhao, Chloe Edwards, Mahdi Sharif, Qian Chen, and Professor Bryan Adey.

I would like to thank my PhD committee members – Professor Mohamed Al-Hussein from the University of Alberta, and Professors Scott Walbridge, Jonathon Enns, Daniel Lacroix and Carl Haas from the University of Waterloo.

I am forever grateful for the support of my family and friends. Above all, I am thankful for my wife Emily, who has been my biggest supporter in life. Your loyal support and love are what has enabled me to write this thesis today, and what will motivate me in life's next chapters.

Preface

This thesis is the result of several peer-reviewed journal articles, conference papers and a book chapter. It has been structured into several core chapters, reflecting contributions made principally in journal articles.

It might be relevant to note that prior to commencing this PhD, the author worked for several years in the construction industry as a computational design specialist, where the development of automated workflows for virtual design and construction (offsite assemblies in particular) was undertaken. This opportunity provided a comprehensive perspective into the need for and development process behind much of the work presented herein.

Table of Contents

List of Figures

List of Tables

List of Abbreviations

ACM – aluminum composite material
AEC – architecture, engineering, construction
BCS – building coordinate system
BIM – building information model
B-rep – boundary representation (geometric schema)
CAD – computer aided design
CNC – computer numerical control (machine)
COP – combinatorial optimization problem
CSG – constructive solid geometry (geometric schema)
DfMA – design for manufacture and assembly
DfX – design for "x"
DLL – dynamic link library
EoL – end of life (stage)
GA – genetic algorithm
GD&T – geometric dimensioning and tolerancing
gDT – geometric digital twin
GWP – global warming potential
HVAC – heating, ventilation, and air conditioning
IBC – industrialized building construction
ICP – iterative closest point
IFC – industry foundation class
LCA – life cycle assessment
LOD – level of development
MEP – mechanical electrical plumbing (system)
MOP – multi-objective optimization problem
NURBS – non-uniform rational basis spline (geometric schema)
PED – primary energy demand
QA/QC – quality assurance/quality control
RANSAC – random sample consensus
RMS – root mean square
SA – simulated annealing
SIFT – scale-invariant feature transform
SOR – statistical outlier removal
VPL – visual programming language

Chapter 1: Introduction

1.1 Background

Despite the long-standing claim that construction productivity has been in decline for the past half-century [1-3], a report published by the U.S. Labor of Bureau Statistics challenges this, showing a positive trend in labour productivity for several construction sectors over the past three decades. In particular, multi-family new housing construction and industrial construction sectors have witnessed average productivity increases of 3.7% per year from 1987 to 2016 and 5.3% per year from 2006 and 2016, respectively [4]. Analysis of the underlying deflators for four of the largest sectors in construction (single-family new housing construction, multi-family new housing construction, industrial building construction, and highways, streets and bridges construction) reveals a positive trend in productivity [5], contesting the status quo. For each of the sectors examined in this study, the prevalence of industrialized construction (e.g., offsite manufacturing, modular construction, prefabrication) and advanced digital technologies (e.g., building information modelling) have become burgeoning pillars. The market share of industrialization has grown significantly in recent years (particularly within the commercial and residential sectors in particular). For instance, from 2015 to 2020, the combined size of the modular construction market in Canada and the United States has doubled, from 2.4% to roughly 5% of the total construction market [6,7]. Similar figures have also been reported for other countries alike [8]. Coupled with the growth of this type of construction, the use of advanced digital technologies is said to bring the single largest increase to productivity across construction [9]. For this reason, research that seeks to address the long-standing claim of negative productivity in construction focus on both industrialization and digital technologies such as BIM as the two single paradigms that must become ubiquitous [10]. Irrespective of the stance on productivity status[1], while industrialization and BIM are independently shaping the modern state of construction, it is clear that their combined presence on projects can garner unparalleled time and cost savings, evidenced through early identification of long-lead items, shorter procurement times, improved design exploration, prescient identification of fabrication issues, reduced coordination errors, enhanced quality control, etc. [9].

Yet while industrialized building construction is witnessing a renaissance within the industry, several objective factors still need to be addressed. These factors can be broadly grouped into technical (e.g., design, engineering and process requirements associated with the complex interfacing and logistics of such projects) and non-technical (e.g., attitudinal perception across stakeholders) [11]. Among the

[1] *It is well acknowledged that measuring productivity in construction is a challenging and potentially subjective endeavor due to intricacies associated with quantifying both output and hours worked for a given sector*

technical barriers, much of the problems encountered stem from trying to approach the design process in the same way as for traditional building construction [8]. As a result, challenges exist with respect to (a) design flexibility, (b) 'locking-in' the design early on, (c) optimization of material-use across the lifecycle, (d) efficient quality control practices, and (e) mitigating unique risks such as assembly misalignments during fabrication, assembly and onsite installation [11-16]. Many of these technical challenges stem from the degree of digitization employed during design and construction as evidenced below:

a) Design flexibility is often hard to achieve in industrialized building construction. For economic reasons, modules and assemblies are designed to achieve a high level of standardization, since offsite manufacturing relies on achieving economies of scale [17,18]. Yet, research has slowly started to demonstrate how advanced geometric algorithms can allow for increased customization, by focusing standardization on core interfaces between components [19]. Such approaches also depend on parameterizing a geometric model in order to establish the topological relations between components that are required to achieve this type of product configuration.

b) For industrialized building construction, it is necessary to 'lock-in' the design early in the project. This can be challenging, not only from a stakeholder process standpoint, but also for product design. Making any changes later in the project has a profound impact on project success – significantly more than for traditional construction [9]. Design for manufacture and assembly (DfMA) and parametric BIM are two modelling paradigms that have considerable promise for addressing the concerns associated with locking-in the design early in a project. On one hand, DfMA which is a design approach that establishes processes to ensure optimal manufacturability and "assemblability" can be used to ensure that certain design changes to suite the actual construction process are minimized. Paired with this, parametric BIM affords the ability to propagate changes in a geometric model automatically, without having to re-establish topological relations between components. Both approaches rely heavily on digitization early in a project.

c) It is well recognized that industrialized building construction has significant advantages with respect to minimizing waste, compared to traditional construction [8,20]. To this effect, numerous technologies continue to be introduced into the industrialized building process to minimize waste and optimize the use of materials [21]. While there is still a need to make improvements to material efficiency during construction [22], it is becoming increasingly important to address the use of materials at the end-of-life stage. This is because generally, industrialized buildings contain more materials than traditional buildings (roughly 10-15% more based on some studies [23]) in order to ensure there is

adequate strength and stiffness for transportation and handling of components and assemblies. Based on the unique attributes of industrialized buildings (i.e., they are often designed in a modular manner, with connections suitable for onsite assembly), they have the unique ability to be disassembled and potentially reused. Such opportunities will become more important as social imperatives concerning the circular economy become more prevalent. Promoting such concepts requires embedding important semantic information upfront in models in order to enable the prescient planning and reuse of industrialized buildings down the road.

d) Quality control practices in industrialized construction are critical for catching dimensional and geometric errors prior to onsite assembly. This is particularly where the use of laser scanning and BIM have been deployed for industrialized building construction [15]. While the comparison of laser scan data (e.g., point clouds) with BIM has been relied upon in industry for many uses cases, the challenge that still exists is localization, interpretation, and abstraction of discrepancies. While a 3D point cloud can be overlaid on a 3D model to produce a map of geometric deviations, this analysis by itself does not translate into distinct quality control improvement measures. The challenge of sensing and interpreting geometric deviations during fabrication and assembly is especially important in repetitive assembly workflows, such as modular construction, where parametric corrections to assembly geometry configuration (i.e., location, orientation, size of objects, etc.) can have a profound impact on manufacturing efficiency and reduction of rework due to dimensional variability.

e) Recurrent examples in the industry frequently reveal how project performance is directly tied to the management of geometric variability, which is a key characteristic of the physical geometry of components and assemblies [16,24,25]. In severe cases, the poor management of geometric variability can completely halt projects and be the single largest contributor to cost and time overruns – in some cases being in excess of millions of dollars of overruns and delays on the order of months and years [26].

What each of these important challenges have in common is that while they can be traced back to insufficiencies surrounding digitization, they are also inextricably linked to the maturity, optimality, and enrichment of (i.e., richness of data contained within) geometric models. While ongoing research is addressing some of these problems through a range of approaches, no studies to date collectivity address or categorize the level of maturity and quality of information required for geometric models in industrialized building construction. Existing approaches tend to be developed on a case by case basis or focus heavily on non-geometric factors (e.g., operational and process-based tactics) [16]. Much of the current research outlining gaps, barriers, and current challenges in industrialized building

construction present specific topics and objectives for researchers to focus on, but do not provide the specific pathway for getting there. This research addresses these gaps by focusing specifically on the optimization and enrichment of geometric models using computational algorithms.

1.2 Research Aims

This research develops algorithms to optimize and enrich geometric models used in industrialized building construction. It is beginning to be recognized that the design, analysis, and optimization of assemblies is founded upon abstracting physical geometry within a digital model; for which, computational algorithms have several substantial key advantages over manual approaches. First, they provide the ability to parameterize models. The development and optimization of parameters is key for configuring topology (i.e., spatial relations between components and assemblies, which are independent of changing shape, size, or position). On one hand, parameterization affords the ability to optimize material use during manufacturing [27] but is also fundamental in developing product configuration (i.e., allowing for more flexible design approaches). Secondly, computational algorithms provide for increased automation in industrialized building construction. Nascent practices such as digital fabrication (also referred to as file-to-factory systems) operate by seamlessly transferring data from design software to automated manufacturing equipment [28]. Such practices, which are important for realizing visions such as "Construction 4.0", rely quite heavily on achieving a high level of automation [29]. Finally, computational algorithms are agile and can be used to deploy powerful optimization and analysis techniques including stochastic simulation, enumerative combinatorics, and metaheuristic optimization. The ability to develop optimal or near-optimal solutions to complex geometric problems in industrialized building construction can translate into significant time, resource, and cost savings for the industry. This thesis explores such propositions by addressing the following basic research questions:

- How can complex geometric processes be codified based solely on the innate properties of geometry? Can the concept of parametric (or parameterized) geometry be exploited for automating complex geometric processes?

- What core assumptions can be made to ensure automated solutions are pragmatic for implementation in industry?

- In which situations are approximate optimization methods superior to exact methods in terms of achieving efficiency without sacrificing quality of end results.

Seeking to address these basic research questions is the focus of this present research, and it drives the specific objectives and the scope described in the following section.

1.3 Research Objectives and Scope

The overall goal of this work is to provide an integrated framework for the development and deployment of computational algorithms that optimize and enrich geometric models for industrialized building construction. In support of this goal, the following objectives have been defined:

- Conduct a review of existing methods used for geometric optimization and enrichment in construction in order to understand and address knowledge gaps.
- Establish an overall framework for developing new, pragmatic computational algorithms, including support for the use of visual programming languages[2].
- Investigate and compare the relative performance of stochastic sampling with algebraic models for geometric analysis.
- Investigate and compare the relative performance of metaheuristic with enumerative methods for geometric optimization.
- Develop an approach to automatically update geometric models during the construction process of industrialized buildings.
- Develop an automated approach to semantically enrich models for disassembly planning of buildings (to support end-of-life materials recovery).

While several of these research objectives are in fact applicable to numerous applications and sectors in construction, the case studies and demonstrations herein are specifically tailored to industrialized building construction. It is not the focus nor scope of this research to develop algorithms that will exhaustively perform all potential geometric optimization and enrichment demands for industrialized buildings. Such a goal is not feasible in one body of work and is further encumbered by the continuously evolving nature, needs and complexity of industrialized building construction. Rather, this work serves as a core body of work upon which other researchers and developers can draw upon in order to inform and provide examples for their own subsequent algorithms development. In addition, the case studies presented in this research focus on several key stages of a project: design, fabrication and assembly, onsite construction, and end-of-life. However, gaps within these stages inevitably occur, and it is not the intention, nor scope, to comprehensively cover every single aspect of an industrialized building project.

---

[2] *Visual programming languages provide the ability for construction industry practitioners to develop computational algorithms without needing a comprehensive computer programming background.*

Where applicable, comparisons between exact and approximate solving methods are used. Approximate methods developed in this work (e.g., stochastic sampling, metaheuristics, etc.) provide local optima in a suitable timeframe, whereas the exact solution alternatives provide global optima with no guarantee on convergence in a suitable timeframe. In other words, the scope of this research is focused on developing pragmatic algorithms that can be deployed directly in the industry, as evidenced by case studies. As noted by Greenough et al. [30], with the growing innovation in industrialized building construction, there is a dire need to ensure solutions are practical to elicit integration.

1.4 Thesis Organization

The overall organization of this thesis is outlined in Figure 1 and elaborated on as follows.

Chapter 1 presents relevant background about industrialized building construction, briefly outlining the current challenges and gaps with respect to the optimization and enrichment of geometric models. Building upon this background, the specific aims, objectives, scope, and methodology are also presented.

Chapter 2 presents a comprehensive literature review of relevant topics to this research including the state of industrialized building construction, a typological overview of geometric process requirements for industrialized building construction, and an overview of the types of algorithmic approaches that can be employed in computational algorithms.

Chapter 3 focuses on developing the overall framework for new algorithms. The first part of this framework is predicated on a parametric vs. non-parametric classification model. The purpose of this model is to categorize geometric data in such a way that can facilitate the optimal use of approximate or exact algorithm approaches. This is closely tied to the second aspect of the proposed framework which establishes the unique approaches for each of the developed algorithms based on computational complexity. In particular the notion of "functional discretization" is posited, which focuses on discretizing variable domains so that approximate analysis and optimization can be performed, as opposed to strictly relying on exact algebraic formulations. Finally, the use of visual programming languages is employed within the proposed framework as the primary mechanism for developing computational algorithms.

Chapters 4-8 outline the new algorithms developed in this research which are specifically targeted at key lifecycle stages across a project: design, fabrication and assembly, onsite construction, and end-of-life. As depicted in Figure 1, there are four algorithms, which are classified according to unique algorithm approaches (enumeration, metaheuristic optimization or stochastic sampling).

Chapter 4 presents the development of an algorithm to analyze dimensional tolerances for industrialized assemblies using the Monte Carlo method. This method, which is a form of stochastic sampling, is intended to simulate or model the effect of tolerance accumulation that can result from improper design specifications. Such a method is important in industrialized building construction for ensuring that assemblies do not exhibit undesirable geometric deviations. This algorithm is compared to prevailing exact algebraic models in order to benchmark its relative performance.

Chapter 5 presents an algorithm for optimizing the topology of architectural panels during fabrication. In particular, metaheuristic techniques are used to reduce the waste that can occur from 'unfolding' and 'nesting' panel geometry on 2-dimensional coils, which are cut by a router. This case study, while carried out for architectural panels, has significant relevance for all types of panelized buildings (*a type of industrialized building construction predominately practiced in Europe).* This algorithm is compared to an exact enumerative algorithm in order to benchmark its relative performance.

Chapter 6 presents the relevant background of a method for automatically updating geometric models during onsite construction of industrialized buildings. Such a method is also critical for dimensional quality control during fabrication and assembly (which happens to be the focus for this chapter). The background presented in this chapter comes in the form of an evaluation of state-of-the-art "geometric digital twining" methods. The chapter concludes with an assertion of the value of an *automated* parametric BIM updating method – which is the focus of Chapter 7.

Chapter 7 presents an approach for automatically updating geometric models using laser scan data. This is accomplished by postulating a parameterization framework, whereby the shape and pose of elements in a BIM can be automatically updated to best-fit the information contained in 3D point clouds.

Chapter 8 contains new algorithms for end-of-life support for industrialized buildings. The objective of this chapter is to develop new approaches for enriching geometric models in order to improve the circularity of industrialized buildings. First, an algorithm is developed that uses spatial parameterization to extract and enrich key information required for disassembly planning of buildings. Then, a conceptual application of this method is presented in the form of a product configurator for the "cycling" of modules within an industrialized building over distinct lifecycles.

Finally, chapter 9 presents the main conclusions, limitations, and future directions of this research.

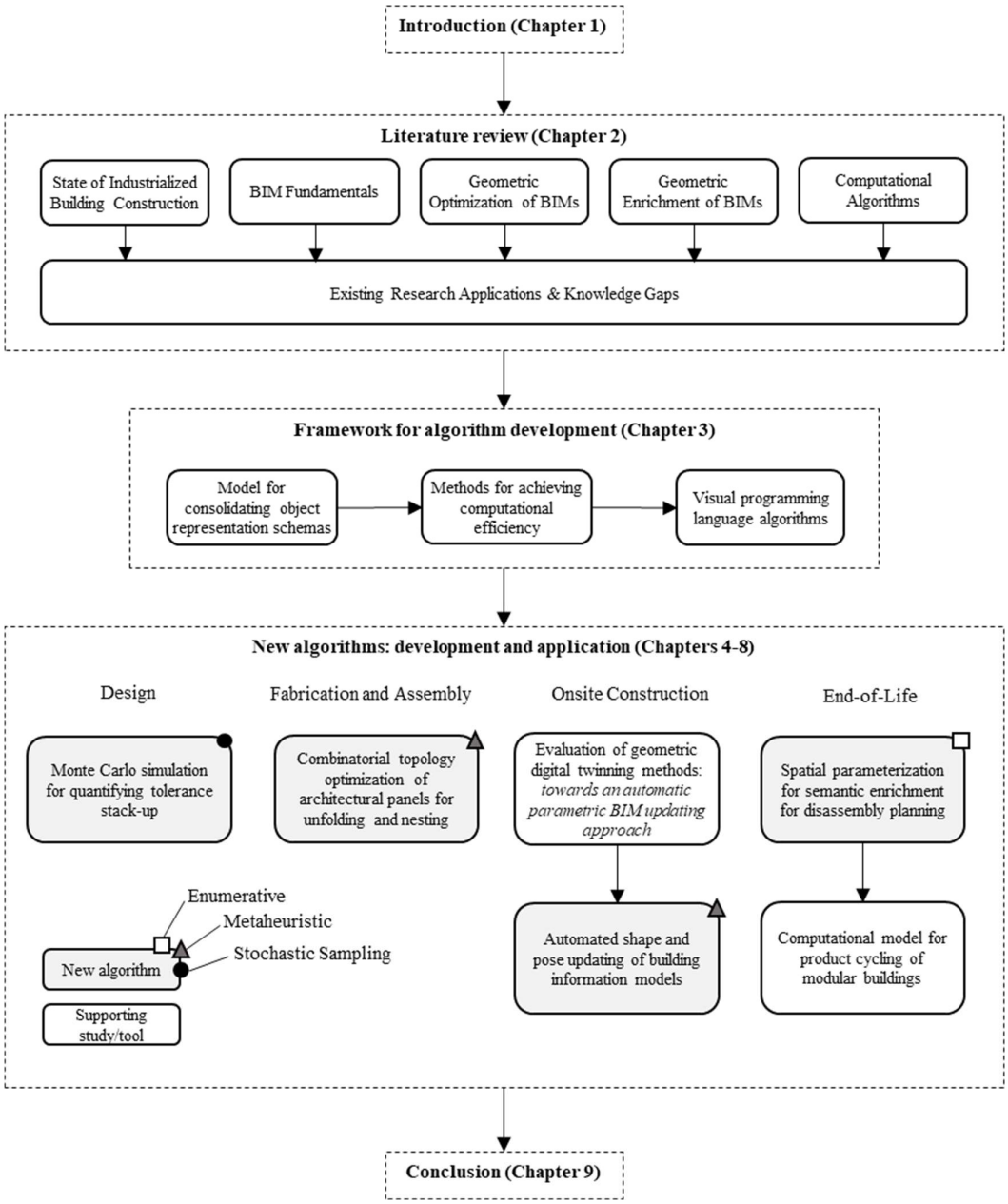

Figure 1: Thesis organization

Chapter 2: Literature Review

2.1 State of Industrialized Building Construction

Industrialized building construction (IBC) is the process of employing offsite manufacturing processes for the construction of buildings (residential, commercial, industrial). While this form of construction has been associated with many different nomenclatures such as offsite manufacturing, offsite fabrication, offsite construction, pre-assembly, prefabrication, modular construction, etc., [9] the term *industrialized building construction* is typology agnostic. The two most important defining principles of an industrialized building are prefabrication and standardization [31]. As a working definition, IBC includes fully volumetric pre-assembly such as modular construction (the de-facto approach in North America), as well as non-fully-volumetric pre-assembly such as panelized building construction (the de-facto approach in many European countries). In recent years, the state of standardization in industrialized construction is changing in two distinct ways. First, while the conventional approach to standardization saw very limited variants for components, assemblies and modules [32], recent advancements to digitization and automation are creating unique opportunities for mass customization. The proliferation of a fully autonomous manufacturing facility does not rely on the production of a standardized product[3], but rather a standardized process. Secondly, new design paradigms are creating new opportunities for mass customization. Research has begun to strategically focus not on assembly standardization, but on interface standardization [19]. Such paradigm shift has also paved the way for the nascency of product configurators and "kit-of-part" systems which codify the ways in which a catalogue of components and assemblies can be combined together to achieve customization [33]. In summary, while IBC may not be a new term, and while it may have several quasi-synonymous associations, advancements to digitization and design approaches are contributing to its resurgence in the industry.

In IBC, the majority of traditional site-based construction work occurs in a climate-controlled facility, allowing advanced production techniques to be used to prefabricate building elements, assemblies, and buildings in a highly efficient manner [15]. The overall construction process is typically discretized across a manufacturing line into distinct fabrication and assembly phases, e.g., (1) structural assembly, (2) mechanical, electrical, plumbing (MEP) subsystem, (3) walls, floors, partitions, (4) MEP fixtures, (5) finishes and millwork, and (6) enclosure and service tie-ins (Figure 2).

---

[3] *The robots executing work in an offsite manufacturing facility do not care if the code sent to it is the same or different for each assembly – they simply execute whatever codified instructions are sent to them. The author has observed such process firsthand for the fabrication of steel assemblies. Where complete customization will still take time for holistic implementation is execution of tasks such as drywalling, MEP, finishing, etc. which are still conducted in a predominately manual manner.*

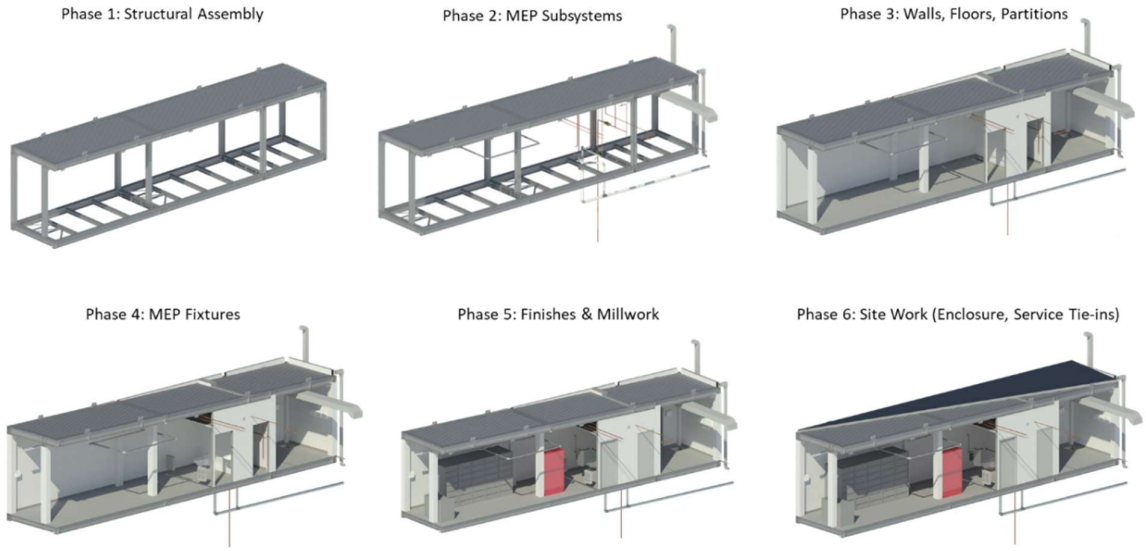

Figure 2: Key fabrication and assembly phases for industrialized building construction

Much attention has been paid to the state of industrialized construction in recent years. Within the industry, emerging strategies for improving the state of industrialized construction has been pursued in the form of vertical integration, development of spin-off ventures, and digital systems integration [34]. Such strategies are pragmatic solutions to mitigate the risk of innovation used to address the conventional problems or barriers associated with industrialized building construction. The past two years in particular (2019-2020) has witnessed manifold research review papers that cover various aspects of industrialized construction including the barriers, critical success factors, state of technology, trending research topics, innovative techniques or the use of BIM [8,10,11,15,35-37]. It is clear from these studies that much attention is being paid to industrialized construction, whether they point to inherent strengths, weaknesses, or future directions for development. One reason as to why this is, stems from the current and projected growth of this sector; some estimates predict industrialized construction will grow globally at a rate of 6% compounded annually between 2018 and the year 2023 [38]. In some cases, it has already become the dominant form of construction in counties such as Sweden, where over 70% of all houses are prefabricated [39]. In addition to the growth trajectory, another reason why much attention is being paid to industrialized construction stems from its ability to address the current shortage of building stock globally. Urbanization and increasing housing costs are key contributors to the growing need for mass production of building stock, for which industrialized construction is uniquely poised to serve [40].

In light of the growth trajectory, but more importantly, the promise of what industrialized building construction represents, it is important to understand where projects can go awry. One of the most cited projects in recent years which experienced significant issues was the B2 tower project, now named 461 Dean Street, in Brooklyn, New York [26,41,42], which was constructed in 2016. This

particular project, which was the tallest modular tower in the world at the time, ran into several problems during construction stemming in large part from geometric management challenges (during fabrication and onsite assembly). Installation challenges from geometric variability led to this project taking twice as long to erect, and cost overruns on the order of tens of millions of dollars. In addition, water leaks proliferated after initial installation; again, due in part to the geometric based problems encountered. While it is easy to observe many of the problems faced on this project through the very specific lens of 'bad control of geometry', this research duly notes that such postulation is not this simple. Truth be told that undertaking an unprecedented project of this scale, with such a prolific profile, is rife with manifold process, relational, labor, contract, design, and legal challenges. Yet, the intellectual learnings of such challenges have had a significant impact on the industrialized building construction industry, specifically with regards to the digital and physical management (i.e., analysis, optimization, enrichment, and control) of geometry. For instance, entire business lines of metrology organizations and new start-ups have targeted their practices towards dimensional inspection of offsite manufactured assemblies (e.g., FARO BuildIT Construction, Cintoo, Glove Systems, etc.). In addition, new innovation has been introduced to control geometric variability by standardization of core structural components (e.g., VectorBloc® system owned by Z Modular®). Finally, increasing attention is being paid to the development of new digital product configuration and "kit-of-part" systems which aim to optimize the product-process interface in industrialized construction (e.g., KitConnect® by ProjectFrog, and Riveia® by Splash Modular). This collective attention towards industrialized construction, and specifically to the digital and physical management of geometry indicates that the challenges faced on the B2 tower project are not anecdotal but represent a fundamental component to the success of industrialized building projects.

Building upon this motivation, the following section presents a comprehensive overview of the geometric process requirements in industrialized building construction, which serves as an important backdrop for the developments made in this research.

2.2 Core Attributes of a Building Information Model (BIM)

Establishing a formal definition of "BIM" can be challenging since it can be viewed as a process, a digital entity, or both. For instance, BIM has been defined as "the digital representation of physical and functional requirements of a facility" (i.e., digital entity), and as "modelling technology and associated set of processes to produce, communicate, and analyze building models" (i.e., process)

[15,43]. This research does not take an either-or stance on this definition but rather discusses geometric requirements that apply to both the process and well as the digital entity[4].

The most fundamental geometric requirement of a BIM is that it must contain parametric objects. As outlined by Eastman et al. [43], parametric objects have the following characteristics:

- They *must* be geometrically derived and defined (i.e., they must be computable)
- They *must* have the ability to link, receive, or export attributes and properties (i.e., they must be query-able)
- They *must* include semantic information (parameters) in the associative data, topology and material-specific data.
- They *cannot* contain geometric redundancies (e.g., different views, such as plan and elevation, must not present conflicting geometric properties about the object)
- They *can* have parametric associations that enable automatic changes (e.g., changing the parameter of a door width will automatically change the rough opening of the associated wall). Further, these parametric associations can be used to identify when violations exist for feasibility in terms of manufacturing, construction, installation, etc.

Based on this definition, BIMs are (1) geometric models that are (2) enriched with semantic information and (3) can include additional associative relations. Each of these three core attributes are broken into further detail by discussing the way that geometric models are built (geometric schema selection), what types of semantic information can be enriched, and the types of agents that can be employed for adding additional associative relations. Finally, a foundational discussion about BIMs would be incomplete without discussing how many of these concepts tie together from a modelling standpoint through the well-established level of development (LOD) framework employed during design.

2.2.1 Geometric Representation Schemas

The first step to developing a geometric model is the choice of which representation (i.e., geometric schema) to employ. The digital or virtual representation of physical objects in various modelling systems (e.g., computer-aided design, graphic design and as-built modelling) categorizes these representation methods based on ambiguity, directness, and compactness (Figure 3). Unambiguous

[4] For clarity "BIM" is used to denote "building information model" e.g., BIM, BIMs (plural), while "building information modelling" is spelled outright to avoid potential confusion.

(or complete) representations are used to describe the entirety of a physical object, and underlying primitives or descriptors can be inverted to recreate the exact same object being represented. In essence, this means that unambiguous approaches can be used to provide a one-to-one mapping between objects and their representation [44,45]. On the other hand, ambiguous representations are often used to distinguish between objects in a very efficient manner [45], even though the descriptors used cannot provide a one-to-one mapping between objects and their representation. For instance, wireframe models can be ambiguous, because the topology of faces and rules of which segments belong to which faces is not defined [44]. As such, ambiguous representations sacrifice completeness for computational efficiency, which is advantageous in applications such as object recognition. Within unambiguous representations, methods can be further classified into implicit and explicit representations. The key difference between these two approaches is the directness for which objects can be encoded. Indirect (or implicit) representations use intermediate geometric descriptors such as histograms of normals or curvature to describe objects [46] as compared to explicit methods which directly describe objects using surface (e.g., polysurfaces, meshes), or volumetric (e.g., constructive solid geometry) descriptors [46,47]. Since some features are innately represented better by either an explicit or an implicit approach, a hybrid modelling approach can be employed for representing a mixed set of features. For instance, regular features of an object (such as planar surfaces) could be represented explicitly, while irregular features (such as higher-order curvature) on that same object could be represented implicitly [47]. In this way, modellers do not need to sacrifice the benefits of one approach over the other if mixed representations are acceptable to use. A final division between approaches is parametric vs. non-parametric representations. While explicit methods can be either parametric or non-parametric, implicit methods are distinctly not a parametric form [48]. Parametric representations are more algebraically refined than non-parametric methods, however, they can be more computationally intensive to perform operations on [49]. While this may not be the case for simple primitives such as lines, circles and planes, it is especially true for representing complex geometry, using formats such as polysurfaces, Bezier curves, B-Splines, Non-Uniform Rational Basis Spline (NURBS), and piecewise functions. Non-parametric representations, in contrast, are more computationally efficient, however, they are more difficult to achieve accurate or exact geometric representation. A non-parametric representation can be implicit as in the case of differential properties of a surface of a given location [46], or can also be explicit as in the case of polygonal meshes. The conversion between parametric and non-parametric representations is discussed in [48]. The conversion from parametric to non-parametric is defined as *implicitization* and it is possible to perform for any rational parametric surface of curve. The reverse process, defined as *parameterization*, is not as easily executed and is not always possible to perform for higher-order descriptors. Parametric representations have become the "quasi-standard*"* for CAD modelling [49] due to algebraic topology capabilities, while non-parametric representations are preferred in machine

vision and as-built modelling systems [45,47] due to computational efficiency. A classification structure of the main types of geometric schemas used and sample filetypes is shown in Figure 3.

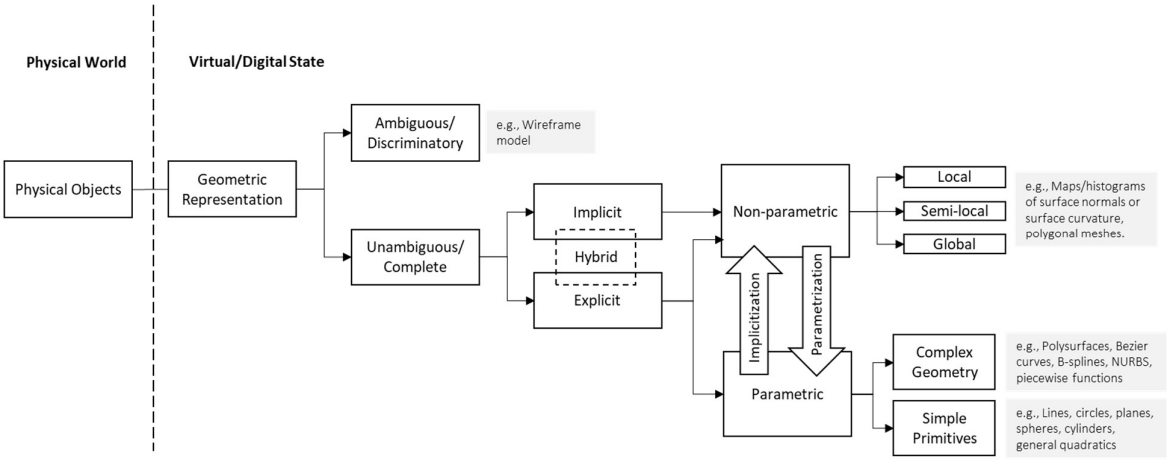

Figure 3: Classification of modelling approaches used to represent physical objects according to ambiguity, directness, and compactness (adapted from [50] using [44-49]).

2.2.2 Semantic Information

In addition to the process of creating geometric models based on representation schemas, the second aspect of BIM is the development of semantic information. This comes in the form of associated data, rules, topology and material-specific data [43]. Parameters are also used to classify objects into categories, families, types and instances, which is stored as data in the form of text, integers, numbers, area, volume, angles, URLs, or binary data [51]. This research pays special attention to the topic of topology, given its importance for creating and establishing strong parametric associations between components in an assembly. Put simply, topology describes the spatial relationships between elements that do not change based on changes to geometric parameters of those elements [52]. While topology is in fact unique from geometry, it is perhaps the most closely related semantic information to geometry. Topology can relate to the relationship between features of an element (e.g., face to edge), the relationship between elements (e.g., beam to column) or relationship between groups of objects or spaces (e.g., room to room). Topology plays a key role in the way architects and engineers understand the function and expected behaviour of building elements. Topology, geometric representation and material properties are distilled into the "semantics" of an object, which can be interpreted as the form, function and behaviour of objects and systems of objects [53]. Current modelling practice in construction emphasizes the creation and preservation of semantics by explicitly outlining that building information models must contain parametric intelligence, topological relationships, and object attributes [54], otherwise, they are considered no more than 3D geometric models.

2.2.3 Creating Additional Associative Relations - *Parametric Modelling Systems*

While all BIMs and parametric objects contained therein must contain semantic information as a minimum requirement, there are yet additional mechanisms to increase the intelligence and preservation of semantic integrity. Parametric modelling (also referred to as parametric design) involves the use of geometric rules and constraints to embed explicit domain knowledge into BIMs and provides a way for automated design regeneration [55]. It should be noted that there is a clear distinction between parametric modelling (i.e., employing parameters and constraints to build and maintain domain knowledge), and parametric geometry representations that utilize algebraic expressions to define geometry (e.g., NURBS and boundary representation, B-rep formats) [55]. While any CAD modelling system can contain a parametric representation of an object, the following characteristics differentiate parametric modelling systems: users can define customized relationships between features and objects, parameters between objects can be integrated into a system (i.e., a parameter of one object can be used for defining parameters on other objects), parametric definitions are compatible in a system or are otherwise mutually exclusive such that no two parameters create conflicting relationships; geometry should be object or feature-based [55]. A simple case of parametric modelling is a recorded script of commands based on geometric variables to create, position, or relate objects. This simple case forms the basis for history-based constraint modellers [56], which stores the sequence of commands used to create a model and allows for an updated model to be produced by changing operational parameters in the command sequence. This approach to modelling has become very popular in the manufacturing industry and is seen in software such as SolidWorks®. Constraint-based design requires all dimensions of features and parts to be parametrically defined, constrained, and related to other features [57], or it is otherwise considered under-constrained, and cannot be realized [56].

Parametric modelling in the AEC industry has adopted a less feature-constrained paradigm in order to expedite the overall design process (since feature-constrained parametric design is very time consuming). The manufacturing industry is often involved in mass-scale production of single assemblies which justifies a longer design process to ensure feature constraints are properly defined, whereas the AEC industry involves much more product customization, rendering feature-constraint design too time-consuming and tedious for many applications (e.g., residential house design is not as intricate from an assembly complexity standpoint as aerospace assembly design). This is one reason why much of the AEC industry has historically employed the use of constraint-free design paradigms, based on 2D drafting tools (i.e., AutoCAD, Sketchup, etc.) to develop digital designs. Constraint-free modellers offer tremendous flexibility and rapid design realization for designers but suffer from the absence of an underlying algebraic paradigm to derive geometric representation. This means that the process of integrating domain knowledge, topological relationships or making changes to design

iterations is tedious and manual. An intermediary class of modelling software can be classified as a hybrid-constraint design approach. In this class of modelling software, a user has the flexibility to create geometry without the necessity of constraining all object features, but the definition of key topological constraints and domain knowledge can still be instituted. Popular software for BIM is Autodesk® Revit®, which has become a standard in the AEC industry due to its user-friendly interface, focus on design communication (i.e., drawing generation), and vast object libraries containing parametric elements [43]. While Revit® does allow users to develop custom parametric objects, it is based on an idealized geometric editing paradigm that does not allow direct access to modify individual polygons (with some exceptions), since it is not based on a NURBS schema [58]. NURBS-based software allows for more complex geometries to be represented accurately, since they are mathematically driven, and objects can be interactively manipulated by changing the spatial position of control points [54]. As such, Revit® is used for regular/simple primitive representations and is challenged by higher-order parametric representation. In contrast, NURBS-based modellers such as Rhinoceros® are often used for complex geometries. Paired with a parametric scripting interface called Grasshopper®, it can achieve a greater degree of parametrization (Figure 4). It should be noted that while Revit® also has its own scripting interface called Dynamo, the NURBS-based paradigm employed in Rhinoceros® is what enables it to perform higher-order parametrization, due to finer granularity at the feature-level for designs.

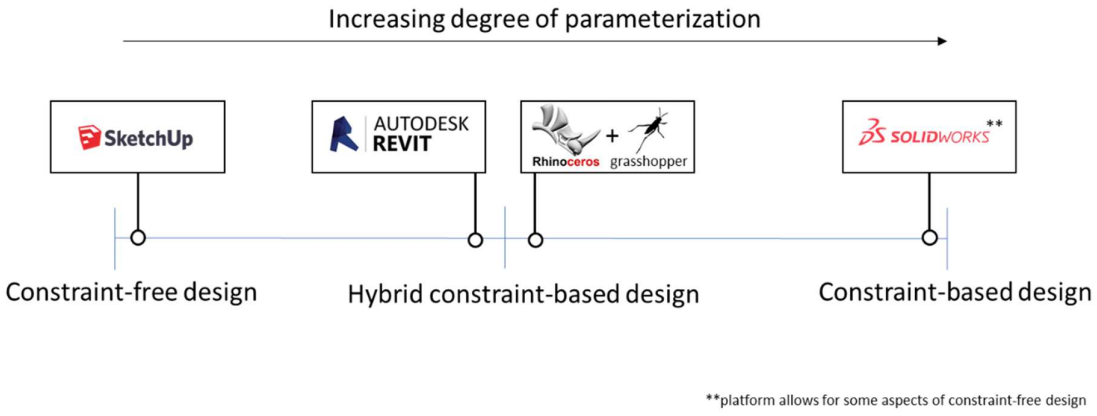

Figure 4: Ranging parametric capabilities of modelling software employed in the AEC industry

While constraint-free modellers are inherently fast and easy to use, they suffer from the lack of structured algebraic underlying paradigms for geometric representation. On the other hand, constraint-based modellers provide a sufficient algebraic representation structure but suffer from a time-consuming design process. Hybrid-constraint modellers provide for a natural middle ground solution but do also suffer from drawbacks. Users must rely on previously developed libraries of parametric objects, or modelling approaches that can be ambiguous since multiple sets of parametric rules can be used to develop the same set of objects [55,59]. Despite these challenges, hybrid constraint-based

modellers also employ powerful automated capabilities through the use of computational algorithms, which is explored in further detail in this research.

2.2.4 Level of Development (LOD) Framework

Models and drawings generated for the geometric representation of a project evolve during design according to distinct levels of maturity. It is important to identify the degree to which project teams can rely on the fidelity of geometric and semantic information provided by a model [60]. For 2D drawings, the reliability or maturity of this information can usually be interpreted from the specificity and quantity of dimensions being shown. However, for a 3D model (e.g., BIM), it can be difficult to differentiate a preliminary model from a highly developed model with exact specifications of project elements [61]. Level of Development (LOD) is a well-known framework for specifying the level of maturity for elements modelled in a BIM. The concept of LOD was first introduced by VICO Software Ltd. in 2005 for the goal of tracking cost estimates of projects. During this time, LOD was abbreviated for "Level of Detail". Later, the American Institute of Architects (AIA) evolved this concept to represent "Level of Development". To specify the level of development of model elements, AIA published distinct LOD categories in 2008, which have since been refined by BIMForum to comprise the following six categories [62,63]:

1. LOD 100 refers to a conceptual model that contains the schematic appearance of a building element with approximate size and can be used for very preliminary analysis (i.e., a rough estimation of the cost per unit of area).

2. LOD 200 represents a model at which the approximate geometry of a building elements is modelled. This model contains the approximate size, location, and systematic relationship of the most building elements, and is used to develop the construction documents. Although this model cannot be used for detailed construction planning and clash detection, it is fine for high-level planning.

3. LOD 300 refers to a model that contains the precise geometry (i.e., size, location, and systematic relationship) of all the objects that should be installed in the building during construction. This model can be used for detailed cost estimation, scheduling, and clash detection before starting the construction phase of a project.

4. LOD 350 represents a model with the level of maturity found in LOD 300, with the addition of details for building system interfaces. In this way, this model can be used to specify the parts needed for the coordination of elements required for supports and connections between objects.

5. LOD 400 represents a model that is used directly to fabricate or assemble building elements. This model contains precise information about all components belonging to an element, in which the element can reliably be fabricated based on them.

6. LOD 500 refers to an as-built model which should be delivered to the owners after construction. In terms of level of development, this model is the same as a design model with LOD 350. A model with LOD 500 is the updated form of LOD 350 design model to reflect scope changed during the construction phase.

2.3 Geometric Optimization of BIMs

There is an abundance of research surrounding the topic of optimization for design, planning, engineering, site layout, project management, etc. This section presents a condensed overview of the topic of geometric optimization as it pertains to building information modelling. Using the taxonomies and overviews provided by [64-66], a concept-map of categories, applications and objectives for geometric optimization can be formulated (Figure 5).

Figure 5: Concept map for geometric optimization applications and objectives in construction

The first category for geometric optimization explored in this section is project performance. Topology optimization is a freeform engineering methodology that optimizes the shape and layout of a system in order to optimize its structural performance (e.g., often to minimize the use of materials). Topology optimization is part a large body of knowledge for the optimization of structural systems, with particular focus on the use of finite element analysis and has applications in reinforced concrete, structural steel, architectural free-form shells [27,67,68]. Topology optimization is also becoming a core aspect to novel digital manufacturing applications. For instance, Nadal et al. demonstrate how the use of discretized geometry in the form of voxelization can be used to optimize material use (i.e., topology) for 3D printing [69]. Across these applications, geometric optimization is applied to structural systems and material use to ultimately reduce costs and environmental impacts of constructed assets.

The next set of geometric optimization applications within the category of project performance that are common in literature is directed towards energy use, thermal performance, and daylighting. These

objectives are often grouped in architectural-based multi-objective optimization frameworks. Traditionally, the type of geometric optimization being performed was only for very crude (or low level of detail) geometry parameters such as length, width, and height of walls, or window-to-wall ratios. However, recently researchers have developed much more sophisticated approaches through use of physics engines that can simulate environmental conditions (sunlight, temperature, wind, etc.). The result of this development had led to increasingly complex forms of geometric optimization (e.g., bespoke free-form shells, complex grammar-based parametric geometry, and forms referred to as "generative design") [70]. Since performance of building systems is only partly influenced by the optimization of geometry, a lot of attention is also paid to non-geometric parameters such as material selection, construction type, insulation values, reflectivity factors, etc. [71]. Generally, these large multi-objective optimization frameworks are developed during the conceptual design stage, with the ultimate goal of reducing environmental impacts (e.g., CO_2 emissions, embodied carbon, etc.), reducing operational costs, and improving user comfort [72,73].

The second category of geometric optimization relates to project management applications. One large area of research in this category is the planning of logistics on construction sites. While this type of application does not explicitly perform geometric optimization (i.e., the form of assemblies is not being optimized), in some cases, implicit optimization is performed for the temporal pose of objects and assemblies (i.e., optimizing the position of objects in a specific sequence). The analysis of geometry plays a key role in many logistics planning methods such as the optimal storage of materials on-site [74], facility layout planning [75], crane setup location and heavy-lift path planning [76], robotic assembly of components [77] and worker and equipment path planning, analysis and hazard prevention [78]. Across the various methods used for logistics and sequence planning, geometric analysis and optimization is ultimately used to increase safety, reduce project duration, or reduce project cost. Another application within project management where geometric optimization is often applied to is improving constructability. Constructability is a project management technique for identifying, resolving and optimizing processes with respect to fabrication, assembly and installation of components in order to reduce or prevent errors, delays and cost overruns [79,80]. Previously, research has implicitly targeted constructability by integrating it within structural topology optimization [81,82], but a burgeoning area of research within construction explicitly targets constructability through a concept called design for manufacture and assembly (DfMA). The premise behind DfMA is to improve overall constructability by evaluating a given design in terms of its downstream manufacturing and assembly processes [83,84]. Trade-offs need to be made between these two processes since a design optimized for manufacturing may not be optimized for assembly, particularly in terms of dimensional tolerance specification (i.e., large tolerances favour manufacturing, while small tolerances favour assembly) – this is where geometric optimization plays a key role. The ultimate goals of improving constructability are to reduce project duration and cost

(minimizing construction delays and cost overruns). Another related application to improving constructability is reducing waste during construction. This can be facilitated (once again) through structural topology optimization, but also through optimized geometric parameters for cutting and other production processes, dimensional coordination and standardization, and minimizing the number of components in an assembly [85-87]. Generally, the ultimate goal of reducing waste during construction is to reduce the environmental impact of material use and to reduce the cost associated with additional materials and waste disposal.

The final noteworthy application of geometric optimization relates to the management of data produced across the project lifecycle. This particular application tends to be sparse in the literature for construction but has growing importance based on the large amount of data being produced and exchanged between stakeholders and software. One method of geometric optimization focuses on the compression of datapoints within representation schemas. For instance, optimization can be carried out to preserve representational accuracy while compressing the number of vertices in mesh or B-rep schemas [65]. Such practices are quite common in computer graphics and machine vision [88], but less so in construction. This type of optimization proves especially challenging in the case where parametric representation schemas (BIMs produced during design) are combined with non-parametric schemas (e.g., point cloud data collected during construction to represent the "as-built" condition) [89]. Methods for maximizing data compression also tend to focus on ensuring data interoperability across the various stakeholders and building information modelling software employed. However, the focus on data interoperability rarely employs geometric optimization (though some examples do exist [90]), and instead, focus on the use of standardized schema-mapped data exchanges (e.g., Industry Foundation Classes, and Model Views Definition methodologies) [91].

The discussion in this section has focused on the unique applications of geometric optimization in construction. It is important to note that each of these applications can be carried out directly on a geometric model (i.e., BIM). Across all of the main applications (except for data management), optimization can be expressed in terms of two unique topologies: intra-object topology, and inter-object topology. For instance, structural topology optimization relates to the finite analysis of intra-object topology, whereas architectural optimization (material, energy, thermal and daylighting use) pertains predominately to meta-level inter-object topology. Construction process-related optimization (logistics) relates mainly to inter-object topology and finally, manufacturing (constructability, and waste reduction) relates to both inter- and intra-object topology.

2.3.1 Management of Geometric Variability

One of the areas that are particularly unique to industrialized building construction as it pertains to the optimization of geometry is managing geometric variability of components and assemblies as they

progress throughout construction and installation sequences. While this topic is relevant in construction as a whole, managing geometric variability is unique to industrialized building construction since the tolerances used range on the order of millimetres for factory-produced components to several centimetres for many site-constructed components [92]. Furthermore, the aggregation of sequential assemblies often creates tolerance accumulation concerns, which need to be effectively addressed and managed [13].

The author has previously conducted a series of studies to quantify the expected accumulation of dimensional variability in IBC projects [26,93,94]. Table 1 depicts a summary of critical sources of dimensional variability. As observed, a significant contribution stems from the manufacturing and assembly process. As such, a series of methods for managing geometric variability can be broadly grouped into product design and design execution (Figure 6). Ultimately, methods in both of these categories are needed to ensure an effective management strategy.

Table 1: Summary of critical sources of dimensional variability and corresponding impacts

Construction process	Largest deviations observed	Impact on dimensional quality
Fabrication of precast concrete panels	• Warping: 5 mm • Bowing: 5 mm • Smoothness: 6 mm	Warping, bowing, and smoothness impact the geometrical compatibility of panels with the floor frame. Aesthetics and serviceability are also impacted depending on extent of variability.
Fabrication of floor and roof frames	• Bowing: 17 mm • Tie-in plate position: • 5 mm	If steel frame dimensions are too large, concrete panels will not fit. If tie-in plates are not in correct position, modules cannot be connected on site. Aesthetics are also impacted if gaps are present.
Assembly of structural system	• Overall assembly deviations: 18 mm • Tie-in plate position out-of-plane: 17 mm	Aggregation is the critical impact when conducting non-compliance tests for dimensions, however if gaps are large enough, the aesthetics of the system are also impacted.
Temporary support conditions	• BLUCO framing table levelness: 9 mm along length • Shop floor levelness: 30 mm across 18 m by 5 m area • Cribbing elevation deviations: 8 mm • Elastic deflection of module: 30 mm at midspan	Deviations in framing table impact accuracy of fit-up processes. Modules can elastically distort if placed directly on the shop floor or if placed only at the 4 corner supports (if cribbing is elevated significantly off the shop floor). Geometric response of structure to loads can impact aggregation of sub-systems if fit-up in plant and final onsite conditions do not match.
Transportation and Handling Loads	• Overall assembly deviation: 3 mm	Small elastic deflections do not significantly impact the module or structure but can cause drywall cracking. Small plastic deflections do contribute to overall accumulation of variability.
Erection at Project Site	• Overall assembly deviation: 4 mm	Small elastic deflections do not significantly impact the module or structure but can cause drywall cracking. Small plastic deflections do contribute to overall accumulation of variability.

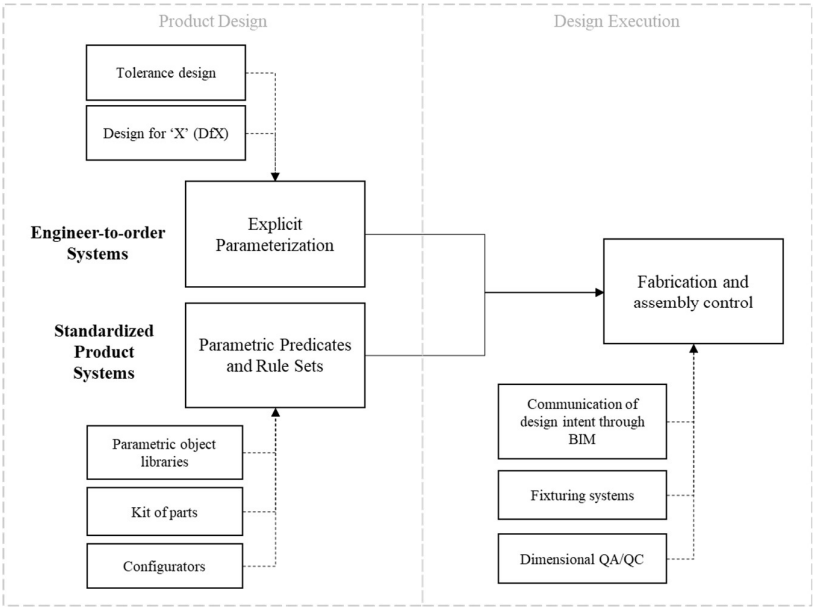

Figure 6: Processes for managing geometric variability in industrialized building construction

In product design, the aims of geometric variability management are to predict, analyze and design for variability sources (i.e., this is known as explicit parameterization), or to employ pre-defined digital products with known geometric compliance measures (i.e., these are parametric predicates and rule sets). The use of "parametric" in describing these systems is important since parameters are ultimately used to stipulate the allowable limits on variation.

Since construction product configurations range from engineer-to-order systems to standardized product systems [95], managing geometric variability can be examined in each of these configuration systems. In highly standardized product systems, parametric predicates and rule sets are employed. Parametric object libraries consist of predefined digital building objects, with semantic metadata and adjustable parameters to modify geometry. Parametric object libraries are typically developed for specific BIM software, such as Autodesk® Revit. Across libraries, the largest collection of parametric building objects is provided by BIMobject, with over 400,000 objects from over 1000 different manufacturers as of 2019 [96]. Open source, software agnostic efforts are also being made for the development of parametric object libraries. buildingSMART is creating a digital object database (data dictionary) where building parameters are assigned unique identifiers and stored with multilingual translations and a unified terminology across multi-trade disciplines. The use of parametric objects from these easily accessible libraries provides designers with the ability to take basic building blocks and achieve desired customization by modifying intrinsic parameters [97] that are typically set within manufacturable limits from various product suppliers. While parametric objects in these widely available libraries are either industry standards (e.g., I-beams of set sizes) or supplier-specific (e.g., doors within a company catalogue), product developers also create in-house parametric libraries for specific use cases and workflows. These types of bespoke parametric object libraries are often

referred to as kits-of-parts [98]. When integrated into a larger platform, these kits of parts along with associated processes, knowledge and relationships are defined as product platforms or configurators. A key benefit of configurators is the total control of a product's parameters [99], which is not solely limited to geometry but also applies to important project-related processes and relationships. Configurators are especially useful for the delivery of highly complex manufactured assemblies, where having process and product-related parameters mapped out in logical relationships is key to reducing conflicts [100], and the presence of non-parametric attributes. The disadvantage to product configurators is the time required to set up the platform and the design restrictions posed by standardization [101].

Outside of standardized product systems (which apply to parametric libraries, kit-of-parts and configurators), practitioners needing to achieve strict parametric primitives in product design can employ Design for "X" (DfX) methods. The "x" in DfX represents various terms such as assembly, manufacturing, transportation, construction, safety, etc. In this way, using a DfX-oriented architecture allows the design team to evaluate design parameters with respect to manufacturability, transportation and assemblability and other requirements. If problems are found in these stages, information is fed back into the component design for the optimization of parameters. In some cases, DfX has been used for the development of specific parametric libraries [102], but it can be used in engineer-to-order applications in construction (i.e., unique one-off projects) as well [84]. DfX functions by abstracting certain process capabilities and ensuring that design parameters are compatible. Building upon this idea, tolerance design goes one step further by analyzing and allocating process capabilities in the form of dimensional tolerances to determine conflicts for assemblability and violation of tolerance accumulation. In the context of tolerance design, process capabilities define the expected variation of a given process (e.g., steel frame welding, rebar placement, concrete pouring, component alignment, etc.), which in turn can be used to determine its probability of not exceeding the required tolerances [103]. Practitioners often rely on the use of pre-existing standards and codes to derive suitable tolerance values (e.g., CSA S16.1, AISC 360, CSA A23.1, ACI 117.1, ISO 1803, ISO 3443, ISO 4464), however these standards have been established for conventional construction and are not strict enough for industrialized building construction. In design, compatibility between tolerances and process capability is achieved using one of two approaches: tolerance allocation or tolerance analysis. Tolerance allocation can be illustrated using an example of a steel beam that has a specified tolerance of 3 mm. The processes affecting the length of that beam (e.g., cutting, measuring, grinding, etc.) must have a net variation of less than 3mm. In this case, the tolerance can be divided, or "absorbed" between compounding processes, however, the net variation of processes is what matters and must be less than the specified tolerance for the length of the beam (Figure 7a). On the other hand, tolerance analysis occurs where process capabilities are analyzed to derive a suitable overall assembly tolerance. This can be illustrated by the amount of adjustability required for the connection of a

prefabricated curtain wall system. The variability of the underlying building substrate as well as positional variability of the curtain wall must be analyzed in order to derive suitable tolerances (Figure 7b). Both tolerance analysis and tolerance allocation require some knowledge about the capabilities of processes in terms of their dimensional variability. While it may be difficult to determine the dimensional variability of construction processes, Milberg and Tommelein [25] demonstrate that failure to consider process capabilities can result in conflicts during installation on-site. Notwithstanding the ability for processes to meet their required tolerances, another fundamental issue is ensuring that the interaction of tolerances of the overall system does not create conflicts. For instance, if a series of prefabricated modules being installed in succession to each other are subject to an overall tolerance requirement, the accumulation of tolerances in and between each module must not exceed the overall tolerance of the system (Figure 8). Each of the tolerances shown in this example function as key parameters that must be properly accounted for, in ensuring the presence of highly parametric primitives. For this reason, tolerance design identifies, designs and optimizes the selection of critical geometric parameters.

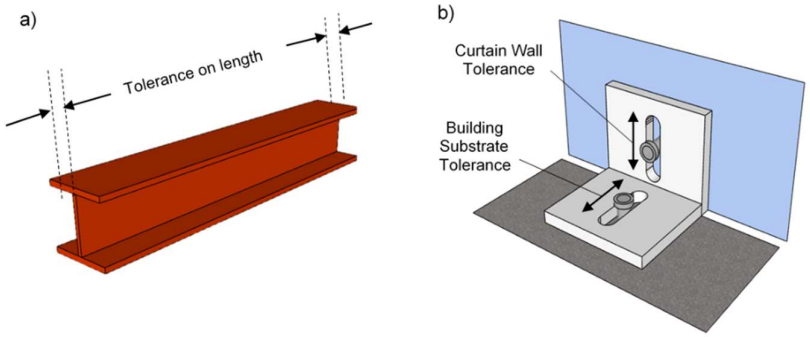

Figure 7: Examples of tolerance design approaches: (a) tolerance allocation for the variability on the size of a steel beam and (b) tolerance analysis of a connection for a curtain wall system.

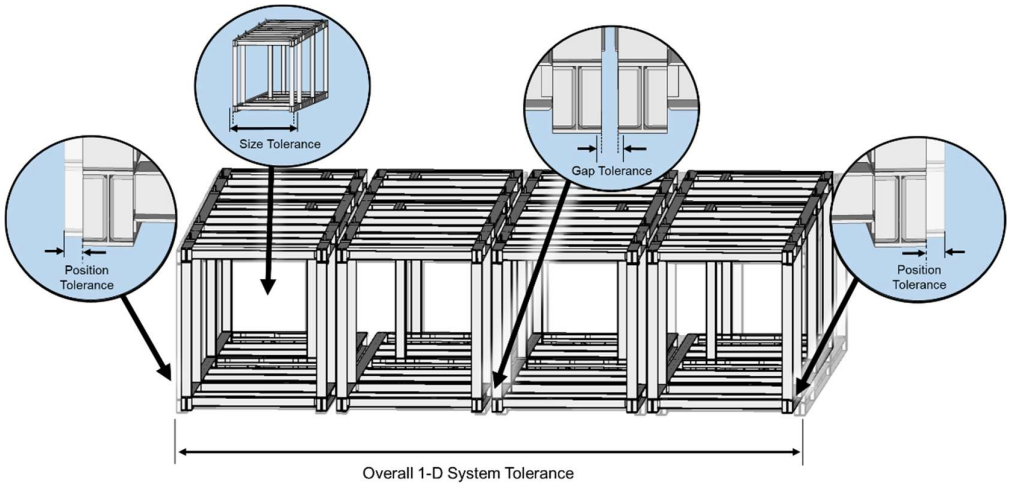

Figure 8: Interaction of tolerances for a modular structural system (position, size, and gap tolerances) which is subjected to an overall one-dimensional system tolerance.

After parametric primitives have been properly designed, their preservation in physical reality relies on methods during execution (i.e., fabrication and assembly), to ensure that these geometric parameters are not violated. In structural assemblies, proper fit-up between components is critical for ensuring there are no excessive gaps between interfaces. In the event of large gaps between interfaces, joining processes such as welding can introduce secondary stresses due to eccentric loading through the connection which can cause structural safety issues [104]. Fabrication control for other subsystems such as mechanical, electrical plumbing (MEP) include aspects such as adequate clearances between MEP services, no visual damage or debris on components, brackets installed correctly, flanges connected with the correct fasteners and to the required torque value, and required testing performed prior to commissioning [105]. One such proactive approach that has been employed within construction for this has been design coordination and communication through BIM. Clash avoidance and integrated project delivery are two features of BIM that aim to proactively mitigate potential design risks, such as dimensional control issues [106]. Studies into the root cause of clashes and tolerance problems observed during fabrication often trace issues back to design uncertainty, lack of specificity, design complexity, and design errors [107,108]. Yet an equally important factor is the control of parameters during fabrication itself. Existing research has developed novel methods to avoid defects during construction (including violation of geometric parameters) through the use of BIM and in-field visual tools [109]. Dimensional quality assurance and quality control (QA/QC) is also becoming common practice. The comparison of a 3D laser scan of the as-built assembly with the BIM of the as-designed assembly (i.e., scan-vs-BIM), has been shown in many studies to be a very important aspect of ensuring geometric parameters and tolerances are not exceeded during fabrication and assembly [110-112]. Aside from design intent communication and ground truth mechanisms for the preservation of parametric primitives, a range of methods is employed during production for controlling geometric parameters. For industrialized building construction, mechanical fixturing is the most common way for practitioners to ensure geometry is produced in a controlled (datum-referenced) manner [13]. While the manufacturing industry employs the use of more permanent jigs, the construction industry often favours the use of reconfigurable fixturing systems (in light of mass customization needs as opposed to the large economies of scale seen in manufacturing) [113].

Currently, many geometric variability management methods and workflows focus either exclusively on design (i.e., the development of parametric primitives), or on design execution (i.e., the control of geometry and established parameters). However, no works to date provide a framework for federating these efforts across the design and execution boundary. Furthermore, despite the best efforts made for the preservation of strict parametric primitives, previous research demonstrates that the presence of non-parametric geometry (i.e., dimensional variability exceeding tolerances) is unavoidable [92,114]. While this can be argued for the production of tightly controlled manufactured products, it becomes especially true when considering the unique processes related to site-work in industrialized building

construction [26]. Rather than trying to avoid non-parametric mediation, another alternative approach is to digitize and parametrize non-parametric objects and domains, which is covered in further detail in Section 2.4.2.

2.4 Semantic Enrichment of BIMs

While the topic of establishing semantic information for BIMs was previously covered in Section 2.2.2, this section outlines research being conducted for automated enrichment processes; herein referred to as "semantic enrichment". Semantic enrichment was initially conceived as "the process in which an expert system interference rule engine applies domain-specific rule sets to identify new facts about building objects and relationships in an input building model and adds them to the model" [53]. In general, it involves classifying objects in terms of their aggregation and grouping relations, along with populating unique identification and missing information where applicable [115]. This can be applied in two general thrusts: (1) inference of new domain knowledge or "facts" required to carry out a necessary process (e.g., establishing aggregation and grouping relations is essential for quantity take-off and cost estimation), or (2) updating the pre-existing "facts" (e.g., shape, material, mechanical properties and functional classification) to obtain new information about an asset (e.g., updating the geometric status of an asset during construction). Each of these thrusts is covered in the following manner. First, a general overview of approaches is presented. Then, the topic of as-built digitization is addressed, which is principally concerned with fusing real data from an asset (either constructed or being constructed) to a BIM for which the data currently does not exist or is outdated. Finally, the current application areas and domains for semantic enrichment are covered.

2.4.1 Semantic Enrichment Approaches

The first documented application of semantic enrichment was authored by Belsky et al. [53] and was developed specifically to facilitate the exchange of information (i.e., export and import) between building information modelling software. This particular tool, called "SeeBIM" (Semantic Enrichment Engine for Building Information Modelling) relies on inference rule sets and is applicable for any geometry that can be represented using axis-aligned bounding boxes (AABBs) – in other words, its only useful for very low LOD levels (refer to section 2.2.4). In light of this limitation, a second tool (SeeBIM V2) was developed to accommodate more complex geometric representations [116]. This method also relies on the use of inference rule sets (in this case linking to external data and shape features for complex geometry) but is applicable to higher LOD levels. While the approach of using inference rule sets has proved very successful for a number of applications, Bloch and Sacks posited and evaluated the use of machine learning for semantic enrichment [115]. They found that machine learning is especially useful for the analysis of spatial regions within buildings, and for the enrichment of more obscure and subjective information (e.g., building code interpretation). While the

methods listed thus far have developed semantic enrichment processes using the IFC schema (primarily since IFC is considered to be the de-facto schema), in recent years several aspects of the IFC schema have come to light which suggests it has limitations for interoperability. As such, Werbrouck et al. [117] proposed an approach that relies on Semantic Web technology (an alternative schema) in order to enrich BIMs generated from 3D point clouds. Their work improves interoperability and aims to incentivize the process for keeping a BIM up-to-date. This notion of maintaining the geometric fidelity of a BIM is closely related to the process of generating a BIM from real-world data (i.e., as-built digitization), which is covered in detail next.

2.4.2 As-built Digitization

As-built digitization is the process of representing physical geometry (objects, domains, etc.) digitally, and has been popularized in the construction industry through the term "scan-to-BIM". Scan-to-BIM involves the use of taking a 3D laser scan of as-built objects of interest, and processing this data (3D point cloud) by conversion to other non-parametric entities (such as meshes, which can be manifold as opposed to point clouds) or parametric primitives, in order to develop a digital model. Once digital objects are abstracted (either through manual or automated methods), a final step involves semantically enriching objects, as per BIM data fidelity requirements.

Scan-to-BIM can be very challenging with respect to representational accuracy in the context of parameterization of building features. For instance, consider the as-built modelling process of the wall shown in Figure 9. While as-designed features for this wall could be presented using simple parameters of height, length, depth and associated semantic parameters (e.g., wall composition, material, layers, etc.), the as-built wall may not conform to these limited parameters in an accurate manner. In plan-view, the wall will deviate from a nominal straight line at a specific scale (see Figure 9-D). Strategies for dealing with this non-parametric attribute in the scan-to-BIM process could include:

- Ignoring the deviations and modelling the wall as being flat/straight.
- Modelling a straight wall, but moving it to fit with the innermost point, midpoint (i.e., split the difference), or outermost point.
- Discretizing the wall and employing small-scale parametrization (Figure 10).

The end-use for as-built digitization of this wall should dictate which strategy is employed. For instance, if the digitization of this wall is to plan for the installation of architectural panels, then an outermost plane is preferable since shims can be used on the wall to account for 'negative' variability. On the other hand, if the purpose of as-built digitization is to create a rough model for spatial

planning/reconfiguration, then the fastest or easiest strategy can be employed. This example also demonstrates the challenge of relying on automated scan-to-BIM approaches versus manual methods.

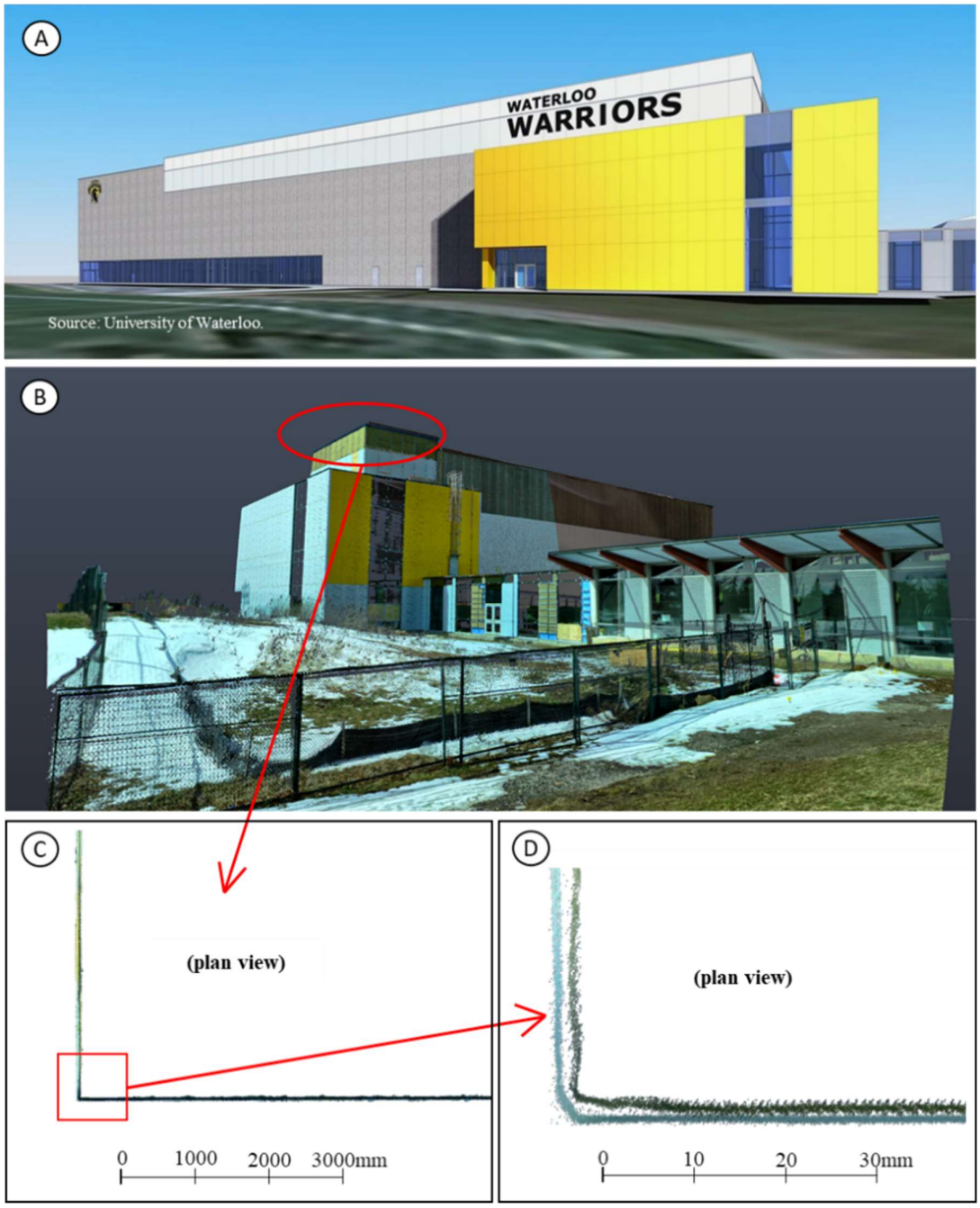

Figure 9. A: Architectural rendering with idealized (i.e., parametric) features. B: Laser scan of building under construction (scanned with FARO Focus M70). C: Plan view of the point cloud from the laser scan. At this scale, the walls can be characterized as parametric. D: At a smaller scale, building features no longer have parametric form.

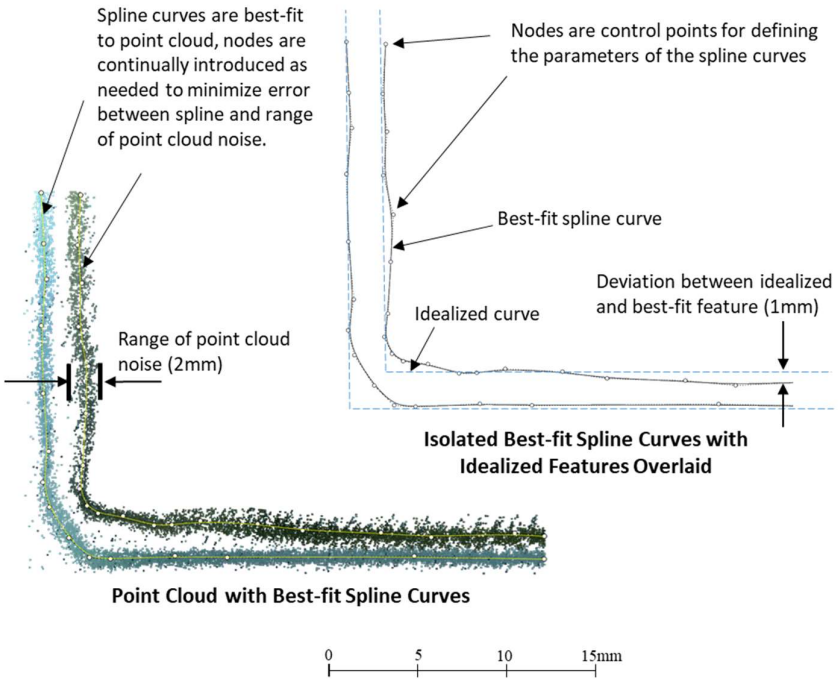

Figure 10: Demonstrating how non-parametric features can be represented by parametric primitives through discretization and feature-fitting at an acceptable level of accuracy.

Data format and fidelity are also important factors in as-built digitization. Practitioners often rely on NURBS-based approaches to achieve the greatest degree of parametric representation – as opposed to other modelling paradigms that are explicitly non-parametric (e.g., triangular meshes), or are only suited to very basic parametric primitives (e.g., CSG) [54,118]. In some cases, the conversion of non-parametric forms to parametric forms inevitably results in loss of accuracy. Rather than trying to focus on advanced parametric conversion methods, some research has instead adopted a hybrid-modelling approach, comprising both parametric features and non-parametric features. In this way, parametric features are used when accuracy thresholds can be met, and when they cannot, non-parametric features are employed. Examples of research in this area include the modelling of buildings (parametric) and underlying terrain (non-parametric) [119], modelling of historical buildings using both parametric and non-parametric forms [47], and complex industrial assemblies [120].

Over the past decade, many researchers have focused on automating the process of as-built digitization, primarily through the development of novel object recognition methods. There are several taxonomies used for categorizing the methods used for object recognition including local heuristics vs. global optimization, data-driven vs. model-driven, semantic segmentation vs. semantic registration being some of the most common [50,121,122]. While some researchers contend and focus exclusively on one of these taxonomies, a brief overview of each illustrates the range of methods employed in object recognition.

The central element of many object recognition methods is the identification of discriminate features that are used to distinguish between objects of interest in a point cloud scene and the remainder of the scene (i.e., clutter). Descriptors can be material-based including colour, texture, reflectivity, geometry-based such as surface normal or curvature, or some combination thereof [121,123]. Local descriptors are used to recognize object instances. This approach involves computing a distinct set of local descriptors from either a model object or select non-parametric object (e.g., mesh or point cloud). Then the scene for which objects are to be recognized within is searched for that unique descriptor set until a match is found. Various metrics can be used to compare fitting if there are numerous object instances in a database to select from. A common approach is the use of machine learning [124,125]. When identifying a match, fine-registration methods can be applied to optimize object pose parameters [46]. Global descriptors are used to recognize object classes. This approach is similar to the process of matching based on local descriptors, however, relies on overall patterns and is less sensitive to local variations. An entire set of objects belonging to a given class (i.e., doors, windows, MEP equipment, etc.) are characterized and used to search a given scene for instances of each class. Typically, global descriptors struggle with point cloud occlusion but are better suited to handle object shape variability [46].

Data-driven methods perform shape-, feature-, material-, and statistics-based matching with training data, whereas model-driven methods perform knowledge- and context-based matching using expert knowledge [121]. Perhaps the most common data-driven approaches employed for the extraction of simple features is use of Random Sample Consensus (RANSAC) and Hough Transform [126]. However, data-driven techniques which focus on purely numerical approaches cannot generate many of the objects found in real-world applications [46], especially when those objects contain very primitive features (e.g., planar, circular) that pose challenges for discriminate detection between like-feature objects (e.g., cabinets, doors, walls predominately have planar features). This has prompted the development of model-based techniques that can leverage auxiliary discriminate information such as “expert conceptions” and pre-existing building information model databases [123]. For instance, Son et al. [127] use a method whereby prior knowledge from scene, geometry and topology are all leveraged through the use of instrumentation diagrams and a 3D object database. Scene knowledge included a list of relevant objects to be found in a scene, geometry knowledge detailed characteristics of object properties (i.e., height, width, depth dimensions), and topology knowledge contained adjacency data between objects. Xiong et al. [128] use a context-based modelling process for recognition of core structural components (e.g., walls, floors, and ceilings). Their method consists of the following steps: voxelization to uniformly discretize data, planar patches extracted using a region-growing algorithm, patch classification using machine learning (stacked learning), and clutter removal. Finally, a ray tracing algorithm is used to label voxels extracted for each planar patch, and a support vector machine classifier is used to detect rectangular openings (e.g., doors and windows).

This particular study demonstrates the complexity and mixed array of methods that often need to be combined to derive bespoke accurate workflows in the automated creation of semantically rich BIMs.

Methods within the previous two taxonomies typically start by segmenting a point cloud into regions and clusters from which to extract and recognize objects. This is performed using some combination of prior rules, descriptors, or machine learning. This semantic segmentation process has several challenges revolving around the nature of captured point clouds including variable regional densities, surface roughness and reflectivity, scene clutter and occlusions. To address this, researchers are indeed improving segmentation approaches [125,129], however completely different approaches are also being formulated. Segmentation-free registration is an approach that does not rely on segmenting a point cloud in order to generate an as-built BIM. Most notable among this notion is the work by Xue et al., who have developed an approach to reassemble BIM elements into a model that is iteratively compared against a point cloud of a scene [122,130]. Their approach relies on derivative-free optimization between the fit of semantic BIM elements from a pre-existing library and the point cloud scene. Other approaches circumvent segmentation by polygonising the point cloud and performing template-based matching of candidate elements. Across segmentation-free methods, there is still a need for pre-existing semantically enriched BIM elements, which is time consuming, and must encapsulate a prescient understanding of the as-built geometry of constructed elements.

In summary, as-built digitization methods attempt to parameterize physical objects and domains through algorithms and approaches aimed at maintaining representational accuracy. Once parameterized, distinct features and relations between these features are used to establish the "semantics" of a model.

2.4.3 Application Areas for Semantic Enrichment Methods

Semantic enrichment processes have been developed for and or applied to the following applications[5]:

- Precast concrete elements [53].
- Concrete highway bridges – beam/girder, box girder, slab [116,131].
- Building interior spaces and furniture [132].
- MEP systems [129].

[5] It should also be noted that this list is not exhaustive, since the term 'semantic enrichment' is not always explicitly referenced in research works; even though in some cases semantic enrichment is in fact being performed. Best attempts have been made to identify such literature.

- Code compliance checking [133].
- Heritage buildings and architectural artifacts [117,134].
- Floor space classification [115].
- Retrofit building models [135].

This list represents a wide range of asset types and applications (i.e., what kind of assessment is being performed on an asset). The applications of semantic enrichment continue to evolve as the underlying object recognition and classification algorithms improve. These methods can be broadly grouped based on whether the starting point for carrying out semantic enrichment processes is solely based on a 3D point cloud or not. Methods that solely rely on a 3D point cloud as the starting point have more challenges with abstraction and classification. While seminal research is continuing to support these types of methods, it is clear that (when possible) a much more effective approach is to build up and maintain initial model semantics on parametric primitives [117], rather than trying to abstract it 'from scratch'.

2.5 Computational Algorithms in Construction

Computational algorithms are comprised of machine-readable workflows that execute a task in an automated fashion. In construction, the selection and modification of geometric parameters (e.g., position, orientation, and shape) and topological parameters (e.g., relations between objects, offsets between assemblies, etc.) can be exploited for many tasks such as design, simulation, and work sequencing. Often these geometric and topological parameters form dense and complex N-dimensional solution spaces when performing optimization and enrichment tasks. The following section provides background on the types of typical optimization problems and solution approaches suitable for applications in construction.

2.5.1 Optimization Problems

Optimization problems can generally be solved by either exact or approximate algorithms (Figure 11). Among exact algorithms are calculus-based methods, which can be further classified into indirect methods that solve for local extrema by setting the gradient of the objective function equal to zero, or direct methods that iteratively explore gradients through the entire search space [136]. The other type of exact algorithm is enumeration which searches every finite point contained within the domain of the objective function until the global extrema is found. Approximate algorithms are classified into heuristic or metaheuristic methods. A constructive heuristic is a step-by-step procedure starting from an empty solution that converges on a feasible (yet not necessarily the global optimum) solution,

while local search methods start with a complete (local optimum) solution and iteratively search locally for a potentially better solution. The other type of approximate algorithm is based on metaheuristic methods. The term metaheuristic has been popularized within the computer science and artificial intelligence communities as being a set of general (heuristic) techniques that can be applied to a range of problems, i.e., they are problem independent optimization approaches [137]. In some cases, the term metaheuristic has also been used as a process for guiding the use of local heuristics to improve the likelihood of finding a global optimal solution and avoiding getting 'trapped' in an inferior local optima [138]. To avoid potential confusion surrounding this term, this thesis deems metaheuristics as being problem-independent optimization techniques. Metaheuristic methods can be grouped into a wide range of classification structures (e.g., natural vs. synthetic, memory vs. memory-less, dynamic vs. static object, etc.), however one of the most common approaches is to classify according to trajectory vs. population-based [139]. In this classification, trajectory-based methods perform local searches between single solutions at a time (e.g., Tabu search, simulated annealing), whereas population-based methods perform search processes that involve evolutions between sets of solutions (e.g., genetic algorithm, particle swarm optimization).

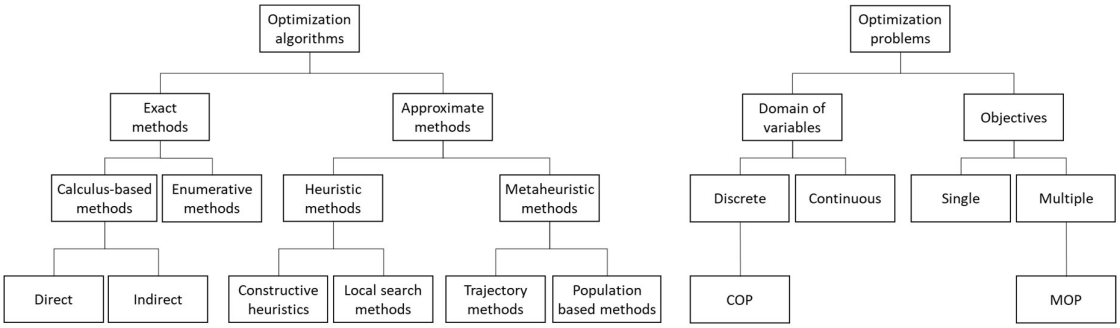

Figure 11: Classification of optimization algorithms and problems. Adapted from [136,140]

The classification of optimization problems can be done according to the structure of variable domains and the number of objectives being solved. This gives way to two common references in literature: combinatorial optimization problems (COPs) and multi-objective optimization problems (MOPs). While these two types of problems are not mutually exclusive, their prevalence in describing many real-world problems is cause for the elaboration of each to help structure background knowledge for this research. As is outlined in Chapter 3, COPs are a core focus of the algorithms developed in this research, and as such, much of the following discussion is geared towards this unique type of optimization.

Combinatorial analysis (combinatorics) is a branch of mathematics that counts the number of ways to arrange or configure items. This reliance on counting or enumerating is what distinguishes combinatorial analysis techniques from other branches of geometric and topological analysis [141].

Building upon this, combinatorial optimization uses these same underlying techniques to solve discrete optimization problems. The key difference is that combinatorial optimization is goal-oriented i.e., it can terminate its process when a certain objective or goal is met whereas combinatorial analysis only terminates when a constraint is met or when enumeration of the entire domain is exhausted. Combinatorial optimization is characterized by having discrete decision variables (as opposed to continuous variables), whereby the objective function can take on a linear or non-linear form [142]. A combinatorial optimization problem (COP) can be solved by iterating through a finite set of variables, which also have a finite set of variable instances. In other words, COPs are defined by having a finite search space. The general form of a combinatorial optimization problem, *P* can be represented as

$$P = (S, f)$$

Eqn. 1

where *S* is the solution space defined by a set of discrete variables $X = \{x_1, \ldots, x_n\}$ and f is the objective function to be minimized or maximized subject to a set of constraints [139]. When feasible, it is ideal to find the global solution, $s^* \in S$, where $f(s^*) \leq f(s)\ \forall s \in S$. Initially, finding the global solution to a given COP was solved using exact (complete) mathematical approaches; most notably through linear and integer programming [143]. However, as the emergence of complex COPs and corresponding methods to solve these problems have evolved, extensive areas of mathematics have been created for solving unique COPs. Some of the most common COPs that arise in many real-world applications include the travelling salesman problem, bin-packing problem, cutting stock problem, minimum spanning tree problem, knapsack problem, and branch-and-cut problem [144].

Generally, COPs are solved using one of two main approaches: exact mathematical methods or heuristic-based (approximate) techniques [145]. The use of metaheuristics (i.e., general, problem-independent heuristics, such as a genetic algorithm) has been shown to be favourable over exact mathematical methods in some cases [146], since exact mathematical algorithms such as linear programming cannot provide time-effective solutions when solution space domains become too dense. The drawback of heuristic or metaheuristic approaches is that convergence upon the optimal solution(s) is not guaranteed. As such, depending on the computational demand of a given COP, one must assess which optimization approach to pursue. With the ever-growing trend in computing power capabilities being at the disposal of practitioners in the construction industry, there is still an important role in the use of exact mathematical algorithms for COPs (even if they have a high computational demand). Similarly, hard COPs that might have been out of reach in terms of computing power even through the use of heuristics, are becoming more feasible to tackle.

Another optimization problem also appears in many real-world applications: multi-objective optimization problems (MOPs). As its name implies, MOPs are defined based on the number of objectives taken into consideration for a given optimization problem. As previously stated, MOPs and

COPs are not mutually exclusive, however consideration of multiple vs singular objectives does influence the approach taken for developing an algorithm. In many cases, not every objective can be simultaneously optimized, eliciting trade-offs. As with other industries, the construction industry has numerous examples of problems that are both multi-objective and combinatorial in nature. Perhaps the most well-studied example relates to multi-objective project scheduling [147]. In this example, many discrete variables are employed such as the number and assignment of resources, crews, activities, as well as activities' duration (in days), and choices of the construction method. This naturally creates the case for a discrete set of combinations from which to optimize according to objectives such as cost, duration, and quality.

2.5.2 Developing BIM-based Computational Algorithms

The input for computational algorithms comes from 3D CAD objects, existing BIM semantic data (metadata), user-defined inputs (parameter thresholds, tolerances, quantities, etc.) and heuristic objectives. Among the most common design software with computational algorithm capabilities are Grasshopper® for Rhinoceros® and Dynamo for Autodesk® Revit. These programming interfaces are integrated directly into their parent design software, and automation is carried out through custom user scripts and workflows. When applied to design, the use of computational algorithms is often referred to as parametric design and is described as being the combination of method, math, logic, geometry, and computer science [148]. The combination of these components enables computational algorithms to effectively automate menial design tasks, verify design iterations for building code compliance, detect localized or systemic geometric clashes and catch costly errors early in the design process. While architectural design has been predominately impacted by the introduction of computational algorithms (for use cases such as geometric rationalization, form-finding and conceptualization of design alternatives), the use of computational algorithms for construction and structural design is starting to also emerge [149-151]. Automation of tasks such as rebar layout, parametric dimensioning in 2D drawings, and as-built verification are beginning to emerge in the construction industry by way of automated workflows comprising computational algorithms.

Extracting geometric information from 3D objects in BIM is a relatively trivial endeavour, however the development of algorithms for higher-order metadata semantics and geometric optimization is a challenge and remains elusive in many spheres of the construction industry [152]. In current practice, computational algorithms are often created for and used in singular projects. This stems from the diversity of factors and challenges faced between projects [153], but also due to the difficulty of modifying existing computational algorithms. Therefore, despite the growing use of multi-objective optimization through computational algorithms, there is a need for a systematic approach to develop and refine these workflows [154] and approaches that enable easy modification to address unique project complexities.

2.6 Existing research for geometric optimization and enrichment in industrialized building construction

In light of the previous discussions, this section presents a comprehensive summary of the existing literature for geometric optimization and enrichment of BIMs, specifically in the domain of industrialized building construction. To do this, the prevailing journals within four major library databases (Wiley, Elsevier, ASCE and Taylor & Francis) were searched within: *Automation in Construction, Advanced Engineering Informatics, Journal of Construction Engineering and Management, Computer Aided Civil and Infrastructure Engineering, Journal of Computing in Civil Engineering, Journal of Structural Engineering, Journal of Architectural Engineering, Construction Research and Innovation, International Journal of Construction Management*, *Journal of Construction Management and Economics* and the *International Journal of Industrialized Construction*. The keywords used to identify the relevant research were amalgamated between the two knowledge domains: BIM-related keywords ("optimization", "BIM", "model", "enrichment", "optimal") and industrial building construction related keywords ("modular", "offsite", "prefab", "industrialized"). Combinations of concatenated keywords describe various focus areas pertinent to this research, e.g., "geometric **optimization** of building information **model**s for **industrialized** building construction", "semantic **enrichment** of **BIM** for **modular** construction", etc. In total, keyword searches produced a total of 3,625 articles, from which each title was examined for its relevance. If a given article was presumed to have potential relevance to the research topic, its abstract was examined (this resulted in approximately 250 articles). From this search, a total of 36 articles were deemed to have minor to significant relevance to the research topic of this thesis. A categorical summary of these articles is presented in this section and outlined in Table 1, as part of identifying the current knowledge gaps in the literature.

The first category examined in the relevant literature is grouped as design-related methods. Many of these methods are automated approaches to create design details and generate design alternatives. This is commonly referred to as "generative design", and the computational techniques used range from simple heuristics to metaheuristics. Alwisy et al. [155] developed a system to automate drafting details for modular construction manufacturing, and in doing so employ a heuristic rule-based system that is capable of minimizing waste. The use of design structure matrices and combinatorial algorithms were shown by [156] to generate high-level design alternatives for modular high ride buildings. In a similar fashion, the use of genetic algorithm, particle swarm optimization and energy modelling computation were previously shown to generate optimal design configuration for modular prefabricated wall/floor systems and high rise buildings [157,158]. Computational algorithms have also been used to automate the structural design process of industrialized buildings [30]. These design-centric methods often do not explicitly perform geometric optimization, but when they do,

they are often constrained to simple or high-level geometric details (e.g., room dimensions, module envelop dimensions, etc.). In the rare examples of when complex geometry is being optimized, the existing research studies have focused on extremely bespoke structures and have not been explicitly developed for industrialized building [159,160]. As such, there is still an opportunity to develop more generalized approaches that carry out geometric optimization for industrialized building construction.

Another common theme among design-related methods is the use of configuration systems to achieve design customization. Configuration in this context ranges from the establishment of semantically rich parametric object libraries [102], computer-aided design modules with architectural building objects [161], standardization of component interfaces [19], or geometric feature classifier based repositories [162]. Often, these methods are predicated on establishing semantic enrichment manually (i.e., building parametric objects manually, and archiving, classifying and depositing them into a repository). There is very little done by way of automatically developing semantic information required for downstream processes or outlining the ways in which industrialized objects and assemblies can be customized or configured. However, there is precedent in the literature on the use of heuristics and mathematical algorithms for codifying manufacturing knowledge and constraints to produce semantically rich BIM information for industrialized building construction [163]. Overall, the use of configurators for industrialized building construction does not explicitly carry out geometric optimization, however there is tremendous opportunity to develop approaches that can automatically produce semantically enriched BIM objects.

As evidenced in the number of relevant studies identified in this literature review (Table 1), one of the most common groups of methods for geometric optimization and enrichment is centred on manufacturing. This group of methods is very diverse, some of which are situated on the design-manufacturing interface (overlapping with methods that employ the use of DfMA techniques), others which focus on minimizing waste during cutting and fabrication processes, some that employ process-based incentives, and some that optimize production sequencing and factory layout [16,164-166]. While not all of these methods explicitly carry out geometric optimization or enrichment, a well researched classical geometric optimization application is the cutting stock problem. 1D stock cutting of steel and timber components for industrialized building construction has been solved using greedy best fit algorithm (i.e., a heuristic rule-based algorithm) [167,168], exact enumeration algorithms [22] and rule-based generative algorithms [169]. While these algorithms perform very well for the specific applications they have been developed for (predominately 1D cutting), since they rely on exact or heuristic techniques, they are computationally inefficient when the geometry is more complex (e.g., non-rectilinear 2D geometry), or when the number of objects being optimized becomes large. As such, there is a need to investigate the use of more approximate techniques (such as metaheuristics) and optimize more complex geometry. Where metaheuristics have been previously applied for

manufacturing, is for determining optimal design variances that minimize fabrication cost for prefabricated wall panels [170]. However, this application was only suitable for very large parametric variances (ranging from 1' (304.8 mm) to 20' (6096 mm)) and is not applicable for more granular tolerances.

Another group of methods centred on manufacturing for industrialized building construction relates to the enrichment of BIM objects with as-built information. There is a range of methods that perform automated dimensional quality verification and extraction of defect-related information. For instance, automated methods have been developed for cylindrical objects [171-173], planar objects [174], and entire 3D assemblies [110]; all of which are directly applicable to industrialized building construction. These methods employ use of several iterative and probabilistic computer vision algorithms such as Random Sample Consensus (RANSAC), principle component analysis (PCA), Hough Transform, and K-nearest neighbour algorithm. These methods perform enrichment directly from point clouds taken on as-built assemblies and are currently constrained by the degree to which semantic information can be automatically generated. In most cases, entirely new 3D geometry is generated (i.e., scan-to-BIM), which must be parsed into an existing BIM. This parsing process is very tedious, and in most cases, the use of scanning for industrialized building assemblies is used as an independent (off-line) quality control process, rather than being integrated into a more semantically rich BIM management process. In addition, currently the use of algorithms for dimensional quality control in industrialized building construction is almost entirely framed as a post-build check (i.e., semantically enriching the as-built quality), rather than being situated upstream during design.

A final group of manufacturing centric methods focuses on the topic of digital fabrication. With the growing use of automated and digital technologies being integrated into industrialized building construction, there is growing attention to producing machine-readable data. Montasser et al. previously developed an approach where knowledge-based enrichment was carried out to codify BIM objects for direct integration with CNC machines [175]. In a similar way, Rui et al. developed a comprehensive platform facilitating digital fabrication in industrialized building construction [176]. These approaches tend to be centred on capturing expert knowledge and developing format exchange processes so that BIMs can be directly developed for automated communication with digital fabrication equipment. With the advent of these digital systems, there is also growing research on verifying that the initial designs are compatible for digital fabrication. For instance, Shi et al. developed a computational approach to verify the manufacturability of designs using Ray casting algorithm, Graham's scan method, and other exact algorithms [32]. In these manufacturing centric approaches, geometric optimization and enrichment are typically not directly carried out, but they provide a framework and computational basis for developing such methods.

Computational methods have also been developed for industrialized building construction applications related to transportation, logistics and on-site assembly. Bani et al. used a genetic algorithm to optimize the transportation and assembly process of precast concrete elements [177], and while this approach does not explicitly optimize or enrich geometry, the temporal pose of geometry was taken into consideration. In other methods, the use of exact algorithms have also been used to optimize the sequencing and stacking of prefabricated panels [178] and a rule-based heuristic approach was used to discretize assemblies into smaller components in order to optimize transportation [179]. For onsite assembly optimization, numerical and mathematical algorithms have been developed by Hosein et al. to optimize crane path planning for the installation of industrialized building assemblies [180], and Rausch et al. demonstrated how geometric variability could be managed for the installation of interchangeable modules [181]. Across all of these methods, geometric optimization is not directly addressed, but rather an inter-object topology and temporal pose is the focus of optimization.

Finally, when trying to identify computational methods for the operations and end-of-life stages of industrialized building construction, such endeavour yields very little previous research work. Numerous studies have been done to either enrich BIMs with as-built information (similar to the previous discussion about the manufacturing stage) [182], or to identify the life-cycle opportunities for industrialized buildings [183]. With the advent of new methodologies for improving the environmental impact of new buildings through product recovery management [184], there is a growing need to develop new computational methods to semantically enrich industrialized building BIMs to support product recovery management. One approach this has been purposed is through the concept of design for disassembly (DfD), for which Eckelman et al. conducted Monte Carlo simulations of prefabricated buildings to assess the efficacy of different DfD strategies [185]. Given the nascency of this area of research, no other known methods have been developed specifically to enrich BIMs with data required for disassembly planning, reuse and extending the useful life of industrialized building construction.

In summary, across all of the identified relevant research, the following trends and observations can be made and reasserted:

- Analysis and optimization of geometry tend to be applied only to simplistic variants.
- Across methods, there is little to no comparisons between algorithmic approaches. For this reason, there is a need to provide better benchmarking and comparisons between the main approaches (i.e., exact vs. approximate algorithms)

- Manufacturing techniques that aim to minimize waste have focused on simplistic geometry and as such have employed exact enumerative algorithms or rule-based heuristics. As such, there is a need to develop more powerful techniques for more complex geometric optimization or for larger sets of objects.

- Computational methods in design are predominantly centred on automated parts of the typical design process ("generative design", drafting automation, etc.) instead of developing advanced geometric optimization methods. On a similar note, manufacturing methods have explored methods for managing geometric variability. It is clear that a prescient path forward is to focus on developing geometric management methods that can be employed during design for optimizing geometry, rather than simply reporting on the semantic quality observations of as-built assemblies.

- Very little research has been done to semantically enrich models for end-of-life management of industrialized assets.

Table 2: Analysis of Research Related to Geometric Optimization and Enrichment in Industrialized Building Construction

Method Title	Lifecycle Stage	Geometric optimization	Semantic enrichment	Computational approaches/details	Relevance & Gaps
Automated BIM drafting for modular construction manufacturing [155]	Design, Manufacturing	N	N	Scenario based analysis (rule based approach)	System can be used to carry out optimization to minimize waste. Geometric optimization and enrichment not directly addressed.
GA for manufacturing, transportation and assembly of precast construction [177]	Logistics, Construction	N	N	Genetic algorithm	Performs multi-objective optimization for resource scheduling. Geometric optimization and enrichment not directly addressed.
Design for Manufacture and Assembly-oriented parametric design of prefabricated buildings [102]	Design	Y	Y	A custom parametric library using DfMA principles	DfMA concepts codified into digital objects which are pre-emptively optimized. Algorithmic approach not employed.
A methodology for the optimal modularization of building design [19]	Design	Y	N	Codified system for standard interfaces	Geometric optimization and enrichment not directly employed.
Kit interface for refurbishment with 2D modules [186]	Construction	Y	N	Small-scale cyber physical system.	A physical configuration system to minimize dimensional variability. Method limited to localized application of 2D panels.
Optimized wall panel construction configuration [168]	Design, Manufacturing	Y	N	Greedy best fit algorithm	1D stock cutting problem for optimization. Research postulated future exploration of GA for optimization.
Configuration for industrialized house building platforms [161]	Design	N	N	Computer aided design modules used to link architectural objects	Design approach to facilitate configuration from an architectural perspective. No direct optimization or enrichment carried out.
Penalty and incentive based reduction of tolerance problems in offsite manufacturing [16]	Manufacturing	Y	N	Algorithm computes penalty and inventive rates based on performance	Method provides an indirect method (through production incentivization) to optimize geometric performance.
Prefabricated wall/floor optimization using metaheuristics [157]	Design	Y	N	Particle Swarm Optimization and finite element analysis	Optimal beam layout and wall placement. Method is limited to precast construction and cannot be adapted to complex geometry.
Dynamic waste allocation for panelized floor manufacture [167]	Manufacturing	Y	N	Simplified greedy algorithm	Method optimizes stock cutting for offsite manufactured components. This method is limited to 1D stock materials.
Combinatorial algorithm to minimize waste in wood framing [22]	Manufacturing	Y	N	Exact enumeration algorithm	Method optimizes stock cutting for offsite manufactured components. Exact enumeration may not be practical for more complex optimization.
Production sequencing of molds for prefabricated building components [165]	Manufacturing	N	N	Mixed integer linear programming model	Geometric optimization and enrichment not directly employed.

(Table 1 Cont'd)

Method Title	Lifecycle Stage	Geometric optimization	Semantic enrichment	Computational approaches/details	Relevance & Gaps
Optimal assembly planning for modular construction components [181]	Onsite Assembly	Y	N	Heuristic matching algorithm	Components to be installed must be interchangeable with non-negligible deviations.
Lean approach for prefabricated panel stacking, sequencing, and locating at site [178]	Logistics, Transportation	Y	N	Exact enumeration algorithm	Method does not perform geometric optimization directly but focuses on optimizing sequencing and productivity.
BIM semantics for digital fabrication [175]	Design, Manufacturing	N	Y	Knowledge based enrichment of BIM objects for CNC semantics	Method relies on codifying expert knowledge, rather than extracting information from intrinsic geometric parameters.
Big Data based DfMA repository for offsite construction [162]	Design	N	N	Geometric feature classifier and rest APIs to link suppliers databases	Method captures data produced by suppliers to enable semantically rich geometric objects for offsite construction to be generated.
CAD based simulator for factory performance in industrialized house building [164]	Manufacturing	N	N	Configuration system using object oriented CAD engine	Method facilitates simulations for factory optimization (labor and material use). However, system does not directly perform geometric optimization.
Automated spatial design of modular buildings [156]	Design	N	N	Unified matrix method and combinatorial algorithm	Method is used for automated design rather than performing geometric optimization or enrichment.
Material waste minimization for light frame boarding in offsite manufacturing [169]	Design, Manufacturing	Y	N	Rule-based generative algorithm for cutting stock optimization	This methodology is very comprehensive by providing design alternative analysis; however, the optimization is constrained to 1D stock geometry.
Modularization algorithm for prefabricated MEP building systems [179]	Transportation, Construction	N	N	Rule based spatial planning algorithm	System decomposition optimization used for delivery and installation of prefabricated components.
Spatial orientation and topology optimization of modular trusses [160]	Design	Y	N	Permutation matrix (exact enumeration using analytical expressions)	Method can be used to optimize complex geometry but is not directly applied to industrialized building construction.
Crane planning and optimization for modular construction [180]	Construction	N	N	Numerical and mathematical algorithms	Geometry optimization is indirectly addressed by simulating crane configuration and radius for installation processes.
An integrated system for providing mass customized prefabricated housing [163]	Design	N	N	Rule based heuristics and mathematical algorithms	Method codifies manufacturing capabilities into a configuration system. However, geometric optimization and enrichment not directly performed.
Prefabricated wall panels optimisation platform [170]	Manufacturing	Y	N	Non-dominant genetic algorithm with exact algorithms	Method balances trade-off between fabrication cost and design variance. The consideration of design tolerances are very large (+/- 1' to +/-20').

(Table 1 Cont'd)

Method Title	Lifecycle Stage	Geometric optimization	Semantic enrichment	Computational approaches/details	Relevance & Gaps
Site specific modular design optimization for high rise buildings [158]	Design	Y	N	Genetic algorithm with energy modelling algorithm	Method obtains optimal layout design, with focus on daylight and ventilation. Optimization is for high-level geometry rather than complex/granular level.
Integrating computational design to improve the design workflow of modular construction [30]	Design	N	N	Heuristic algorithm with structural analysis	This method performs automated design configuration, however geometric optimization is not directly performed.
BIM-based optimizer for assembly in offsite construction [166]	Assembly	N	Y	Parametric model linked with analytical hierarchy process based algorithms	This method is more focused on assessment of design alternatives than on optimizing geometry, however it produces semantically rich designs.
Design for disassembly assessment for prefabricated steel buildings [185]	Design, End of Life	N	Y	Monte Carlo simulation for analysis of DfD strategies	This method assesses the potential for prefabricated buildings to be disassembled; semantic enrichment of design indirectly addressed.
Multi objective optimization of modular structures: weight vs. geometric versatility [159]	Design	Y	N	Non-dominant genetic algorithm, and simulated annealing algorithm	Method performs optimization on very complex geometry but has been exclusively developed for bespoke structural frame system.
BIM enabled computerized design and digital fabrication of industrialized buildings [176]	Design, Manufacturing	N	N	Integrated digital platform with data driven optimization	Method is a holistic platform for facilitating digital fabrication for industrialized buildings. Geometric optimization is not explicitly carried out.
Geometric quality inspection of prefabricated MEP modules [173]	Manufacturing	N	Y	Convex hull algorithm, principal component analysis, RANSAC & others	Method used for verifying geometric quality, but indirectly enriches as-built models.
Automated verification of manufacturability of modular construction framing [187]	Manufacturing	Y	N	Ray casting algorithm, Graham's scan method, and other exact algorithms	Method is used primarily as a check but could be used to optimize geometry indirectly.
Adaptive tolerance analysis of prefabricated components [171,172]	Manufacturing	N	Y	Graph theory network (exact enumeration)	Method can be used to computationally track deviations, however, can only be used for discrete tolerance values.
3D reconstruction of surface defects of prefabricated elements [174]	Manufacturing	N	Y	K-nearest neighbor and Delaunay triangle algorithms	Method is used to enrich BIMs with defect related information.
Automated dimensional quality assessment of precast concrete elements [110]	Manufacturing	N	Y	Principle component analysis, Hough transform, RANSAC	Method is used to enrich BIMs by proposing to expand IFC schema to store defect related information.

2.7 Knowledge gaps

The knowledge gaps for this research are summarized in terms of key topics that were covered in the literature review. While some of these gaps are application-agnostic (i.e., they apply not just to industrialized building construction, but to construction or manufacturing), discussion of knowledge gaps is tailored towards industrialized building construction to fit the research scope.

2.7.1 Geometric optimization

- There is a need to develop novel approaches to predict the accumulation of dimensional variability so that proactive design optimization can be employed for industrialized buildings, rather than resorting to more time and resource-intensive remedial efforts during construction.

- There is a need to perform geometric optimization using more granularity than methods currently available (i.e., on the order of millimetres rather than centimetres) given the stricter dimensional requirements in industrialized building construction.

2.7.2 Semantic enrichment

- There is a need to develop ways in which to enrich or extract required semantic information for BIMs, but equally, there is a need to ensure that once this information is created, that it can be maintained. For fidelity of geometric information in BIMs, this means finding ways to preserve the accuracy of as-built representation for constructed works.

- The gap of current methods: expert knowledge is required to build and enrich, and this often cannot be inferred from the computational analysis of geometry alone.

2.7.3 Combinatorial algorithms

- Few studies compare the performance of exact and approximate optimization for COPs.

- Despite the prevalence of computational algorithms in construction, there is a need for a framework to simplify the solution approach, so that algorithms are more pragmatic for implementation.

Chapter 3: Methodology for Algorithm Development

This chapter outlines the methodology for developing new geometric optimization and enrichment algorithms in industrialized building construction (Figure 12). First, a model is presented which consolidates existing classification ontologies for geometric schemas using a parametric vs. non-parametric structure and incorporating the notion of semantic fidelity. Such a model is used in this research to inform the selection of geometric schema used in each algorithm. Then, the second aspect of the proposed methodology presents a series of methods used to achieve computational efficiency. Such methods are essential for ensuring that the developed algorithms are pragmatic for implementation. Finally, the proposed methodology relies on the use of visual programming languages (VPLs) to develop algorithms. As such, a brief section is provided to give background, rationale and a series of key steps used in developing VPL-based algorithms.

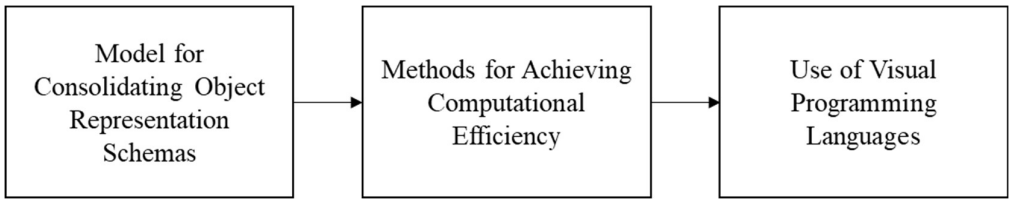

Figure 12: Core Aspects to the Methodology Used for Developing New Algorithms

3.1 Model for Consolidating Object Representation Schemas

The need for efficient computing for geometric modelling and analysis workflows often requires making trade-offs between the inherent advantages and disadvantages of different datatypes being generated and managed. This is notably observed in geometry reconstruction (e.g., scan-to-BIM, reverse engineering, etc.), where a trade-off often occurs between computational efficiency and the choice between increased semantic enrichment or increased representational accuracy (often both cannot be achieved simultaneously). This dichotomy can be generalized as a choice or trade-off between parametric and non-parametric object representation forms.

This section presents a model for characterizing object representations as being either “parametric” or “non-parametric”. While such a classification was partly addressed in Section 2.2.1, this section incorporates the notion of semantic fidelity as being a measure for classifying representation schemas. In doing so, this model consolidates the existing classification of object representations. This is particularly important for this research because it helps inform how algorithms should be developed, what assumptions can be made for pragmatism, and which solution approaches are best suited.

This research uses a conceptual model to help delineate between parametric and non-parametric geometric representations. This model is based on the distinction between analytical expressions and

digital approximations that appear in computer vision for pattern and shape recognition processes. As depicted in Figure 13, this model classifies parametric object representations as having many relations between individual datapoints or entities, and are by nature more abstract, while non-parametric object representations have a greater number of unstructured datapoints and are by nature more discrete or approximate.

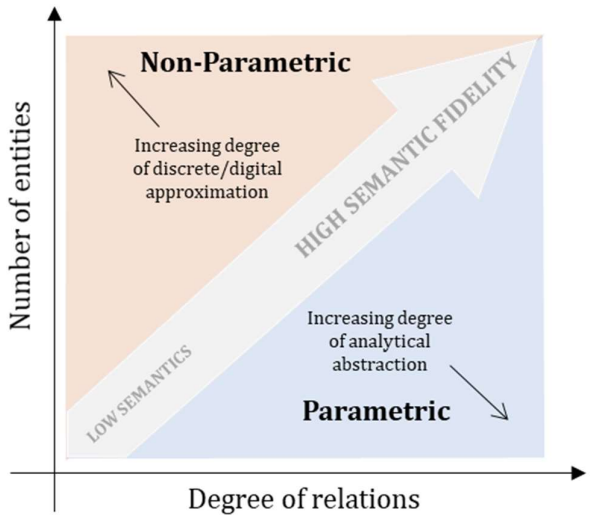

Figure 13: Conceptual model for characterizing the delineation of parametric and non-parametric object representations

In computer vision, various techniques for pattern recognition can be used to resolutely employ digital approximations of analytical expressions for recognition. One of the most common methods for shape detection in computer vision is the Hough Transform which detects curves by exploiting the duality between points on a curve and parameters of that curve [188]. It works by first considering the analytical expression of a curve, often in the parametric form (r, θ), and edge segments of an image given by (x_i, y_i). The transform is then implemented by discretizing the Hough parameter space over finite intervals of the image, or "accumulator cells". This technique takes an inherently parametric mathematical expression and discretely approximates it in a non-parametric manner to extract and transform information from an image (which itself can also be defined as a non-parametric data source).

Gaussian kernels are another example of discrete approximation used in computer vision to perform an analytical transformation on an image (Figure 14). A more general case of this is convolutional kernels and filters, which transform an expression into a discrete nxn matrix and is convoluted over an image. Discrete approximations such as kernels are efficacious in complex algorithms such as Scale Invariant Feature Transform (SIFT) due to the ability to perform analytical operations in a computationally efficient manner.

In the same way that many pattern recognition techniques transform analytical expressions into discrete approximations, this same analogy can be used to delineate between parametric and non-parametric object representations. On one hand, we can postulate a trend that the more abstract an expression or representation is, the fewer entities are required to relate components together. Conversely however, when these relations are broken and discretized, more discrete values are required to perform a similar level of approximation compared to its analytical counterpart.

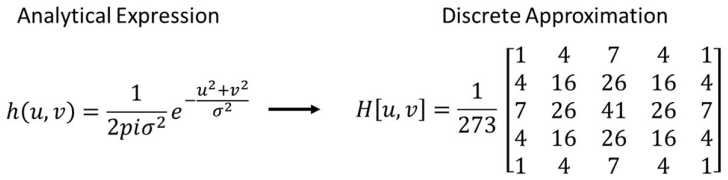

Figure 14: Analytical Gaussian Expression and the Digital Approximation (5x5 Kernel)

The final aspect of this model is characterizing the degree of semantic fidelity encapsulated in an object representation. The greater the number of entities and degree of relations between those entities, the greater the semantic fidelity of a representation. In practice, there is a trade-off that occurs between parametric and non-parametric object representations with respect to the degree of semantic encapsulation. This is perhaps most evident when representing "as-is" objects. While non-parametric object representations are positioned better for obtaining a higher degree of representational accuracy, they cannot be semantically enriched to the same level as parametric object representations. Despite the high level of abstraction in parametric representations and the significant advancements being made to leverage better parametric modelling approaches that maintain representational accuracy of as-is objects, the inability to achieve the same degree of representational accuracy as non-parametric representations restrict its ability to achieve the highest level of semantic fidelity. As such, a notable trade-off occurs between parametric and non-parametric representations with respect to semantics.

3.1.1 Populating the Model with Typical Geometric Representation Schemas

Previous research has provided information for assessing the trade-offs between geometric schemas (Table 2). Using this breakdown, a simple demonstration can be carried out for the representation of an I-beam element (Figure 15) to show how parametric representations tend to have fewer entities, which are more tightly related. The first digital representation in this figure is a point cloud, which can be obtained by performing sampling reconstruction of existing mathematical descriptions or from reality capture [189]. The other digital representations which are more structured than point clouds are triangular and polygonal (tessellated) meshes. As shown, the point cloud representation has 7296 datapoints (i.e., XYZ points), whereas the triangular mesh contains 1740 datapoints (i.e., triangle vertices), and in the most simplified case, the polygonal mesh structure has 108 datapoints (i.e.,

polygon vertices). These digital representations are also considered to be non-parametric. As opposed to regular shapes (e.g., rectangular, cylindrical, prismatic, etc.), non-parametric forms cannot be defined parametrically using a shape type and a limited set of parameter values that specifies the object [46]. Figure 15 also depicts two common mathematical representations. Non-Uniform Rational Basis Spline (NURBS) is a common boundary representation, which uses a series of surfaces to completely enclose and represent a given shape. Constructive Solid Geometry (CSG) is a mathematical representation that describes the volume of an object through the use of Boolean operations (e.g., addition and subtraction) of simple geometries to create more complex shapes. While CSG has been the preferred method for representing geometry in building information models (BIMs) due to its simplistic data structure [46], there are many applications where NURBS are preferred, since it can describe complex geometry more appropriately [54,118]. As shown for the steel beam, the NURBS geometry contains 56 datapoints (i.e., control points), whereas the CSG geometry contains 9 datapoints (3 extrusions built with 3 control points each).

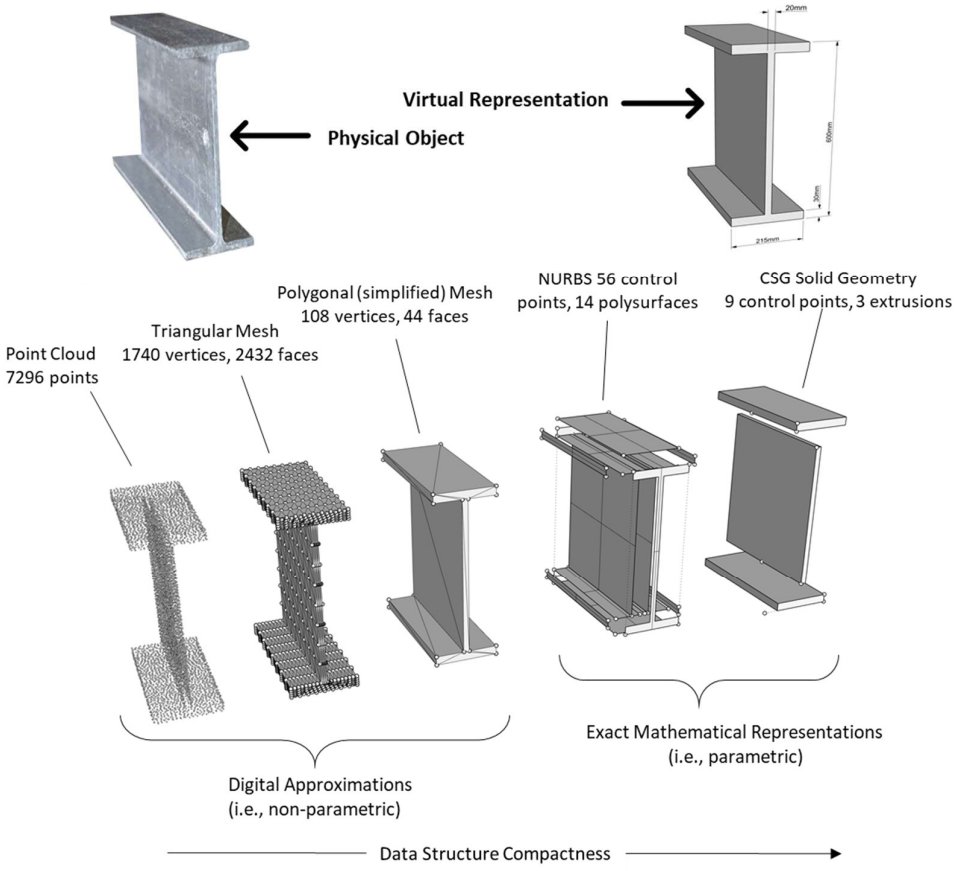

Figure 15: Digital Representation Schemas for a Physical Object (Steel Beam Element).

The general trend for this simple example is that as representation moves from approximate to mathematical or parametric, it becomes more compact, with fewer entities that are abstractly related. In addition, we can plot each of these geometric descriptors on the conceptual model (Figure 16). On

one hand, the point cloud representation is the most non-parametric with the highest number of entities (which are not related), while the CSG representation is perhaps the most abstract parametric representation. While not directly considered in this example, the Boundary Representation (B-rep) geometric schema is another parametric representation which arguably has the highest semantic encapsulation across all geometric schemas. This is because the B-rep schema is based on a hierarchical topological structure, with explicit relations between bodies, faces, edges and vertices (refer to [190] for a more detailed breakdown of this schema).

While this example demonstrates how geometric schemas can be characterized using the proposed model, the purpose of the analysis is not to provide a comprehensive (or exhaustive) classification of all possible schemas. However, certain schemas are better suited for more semantic fidelity than others. For instance, given how NURBS and B-rep can be discretized by adding additional control points without changing the initial geometry of an object, these representations potentially have the ability to harness the semantic fidelity requirements of a given application as opposed to those of CSG or non-parametric representations.

Table 3: Summary of the key trade-offs between geometry representations employed in AEC

Geometry Representation	Geometry Kernel Processing Demand	Continuity	Representational Accuracy (As-is)	Semantic Richness	Exactness for Complex Geometry	Sources
Point clouds	Slow (high computational effort)	Discretized	High	Low	Low	[89]
Mesh	Fast (no interpretation required)	Discretized	Med-High	Low	Med	[89]
B-rep	Med (interpretation required)	Exact, continuous	Med	High	High	[89,190]
CSG	Med (interpretation required)	Exact, continuous	Low-Med	High	High	[89]
NURBS	Med (interpretation required)	Exact, continuous	Med-High	High	High	[89]

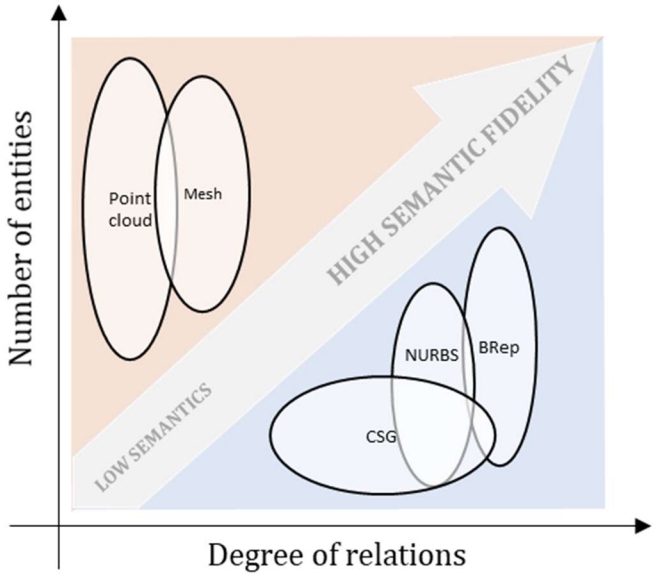

Figure 16: Depicting the Conceptual Model Using Geometric Schemas

3.1.2 Informing the Selection of Object Representations

This classification model helps to inform the selection of object representations used in each of the algorithms in this research. Given the compactness of their representation structure, parametric schemas are preferred when developing computational algorithms. However, in some cases, non-parametric representations are necessary to use in algorithms, especially when the representational accuracy of as-built objects is a priority. As such, the selection of geometric schemas for the algorithms in this research are informed as follows:

- When representational accuracy is a priority (e.g., methods for optimizing dimensional tolerances or for minimizing dimensional variability on site), one of the following approaches are used:

    1. B-rep is selected as the parametric schema since it has the highest semantic fidelity. Then, the final result of such a method is compared to point cloud representation, to quantify and generate a relative assessment of representational accuracy (since point clouds can produce the highest representational accuracy across geometric schemas).[6]

[6] This approach is adopted in *Chapter 4: Tolerance Analysis and Optimization using Monte Carlo Simulation* where B-reps can be used directly in the 3D-CAD simulation engine.

2. If it is desirable to assess computational demand with respect to representational accuracy, then both CSG and NURBS will be used. The final result of such a method is compared with point cloud representation, to quantify and determine which schema is more accurate compared to a point cloud representation.[7]

- When representational accuracy is not a priority (e.g., optimization or enrichment methods based solely on geometry obtained from an idealized BIM), only parametric schemas are used according to one of the following approaches:

    1. For algorithms where geometric optimization is being performed, B-rep is selected as the parametric schema, since this has the highest semantic fidelity, meaning that the resulting process achieves or preserves the highest degree of semantic fidelity.[8]

    2. For algorithms where semantic enrichment is being performed, NURBS is chosen since this schema has lower semantic fidelity than B-rep but is more granular in defining geometry than CSG. In order to be conservative, using a schema with an initial high semantic fidelity is not chosen since the core purpose of such algorithms is to demonstrate how semantic enrichment can be performed solely from the innate properties of geometry and topology. CSG (which has arguably the lowest upfront semantic fidelity) is not used in such algorithms since many objects cannot be represented using this overtly simplified schema.[9]

3.2 Computational Complexity Management

The notion of *functional discretization* is employed in this research as a way of converting complex continuous variable domains into discrete variable domains (where applicable) for the purpose of achieving a high level of computational efficiency. In other words, discretization is used to balance the accuracy and fidelity of an algorithm with its computational demand, to target pragmatism. Specifically, converting continuous variable domains to discrete variable domains involves the following:

---

[7] This approach is used in *Chapter 7: Automated Parametric BIM Updating* since B-reps cannot be parameterized in the same way that CSG and NURBS schemas can.
[8] This approach is used in *Chapter 5: Exact and Approximate Combinatorial Algorithms for Topology Optimization* so that additional semantics generated during design are preserved when performing topology optimization.
[9] This approach is used in *Chapter 8: End-of-Life Semantic Enrichment Algorithms for Industrialized Buildings* in order to demonstrate the semantic enrichment capabilities of developed algorithms using schemas which do not have the highest initial semantic fidelity.

- Continuous variables are converted into discrete variables for an algorithmic solver by selecting a suitable rounding limit (e.g., 0.001, 0.01, 0.1). The decision of a rounding limit for a given variable has a profound impact on the resulting number of possible variable instances for the algorithm to select from when solving. In other words, where possible, continuous optimization problems are converted into combinatorial optimization problems.

- Where appropriate, combinatorial optimization and analysis approaches are employed, since these approaches tend to have smaller decision variable domains than continuous optimization approaches. Furthermore, combinatorial algorithms are better suited for a wider range of algorithmic solving approaches (i.e., exact, and approximate solving methods – *not just exact*).

- Stochastic sampling (e.g., Monte Carlo method) is specifically investigated as an analysis technique to avoid the need for complex algebraic solving methods.

In addition to these techniques, it is important to briefly address the concern related to being trapped in a local optimum, which is applicable when using metaheuristics. Based on the two dominant metaheuristics adopted in this work (genetic algorithm, GA and simulated annealing, SA), generally SA is less prone to being trapped in a local optimum since it allows for up-hill moves in the iteration. In contrast, since GA is a population-based algorithm it can be more susceptible to being trapped in a local optimum – in which case, it is necessary to rely on properly calibrating cross-over and mutation variables, which affect the ability to move within a search space. In addition to these algorithm-specific methods for avoiding local optimum, another useful technique for stochastic based solving methods is to conduct a series of experiments and assess the range of outcomes. This is especially true for probabilistic methods such as Monte Carlo simulation, but also for the metaheuristic algorithms employed in this work. Finally, another strategy is to vary the starting point for each algorithm, which can affect the general area of a solution space that is explored.

3.2.1 Approach for Validating the Selection of a Given Class of Algorithm

Given the focus in this research on converting or simplifying continuous optimization problems into combinatorial optimization problems, it is useful to categorize COPs to help validate the correct class of algorithm is being chosen. Without delving into the highly contested computational complexity debate of whether P=NP, it is useful to categorize COPs in terms of increasing degrees of complexity (Figure 17). For many problems, this categorization can be presented as problems that are either NP-complete (i.e., solutions can be proved in polynomial time) or NP-hard (i.e., at least as hard as problems contained in

NP); the latter being more complex. Examples of NP-complete COPs include bin packing, knapsack problem, and integer programming, whereas NP-hard COPs include the travelling salesman, longest path, Hamilton Cycle and the min set cover problem [191]. It is well regarded that exact algorithms can be used to solve NP-complete problems [192]. Some NP-hard problems can be solved in polynomial time using heuristic-based approximate methods; however, the same problems may require exponential time for even the best exact algorithm. For such problems, it is more effective and pragmatic to employ approximate methods to converge on solutions in a reasonable amount of time. Nevertheless, depending on the size and complexity of a given COP, the use of exact algorithms can still be efficacious, as opposed to complex MOPs, which are often more suitably addressed through approximate methods.

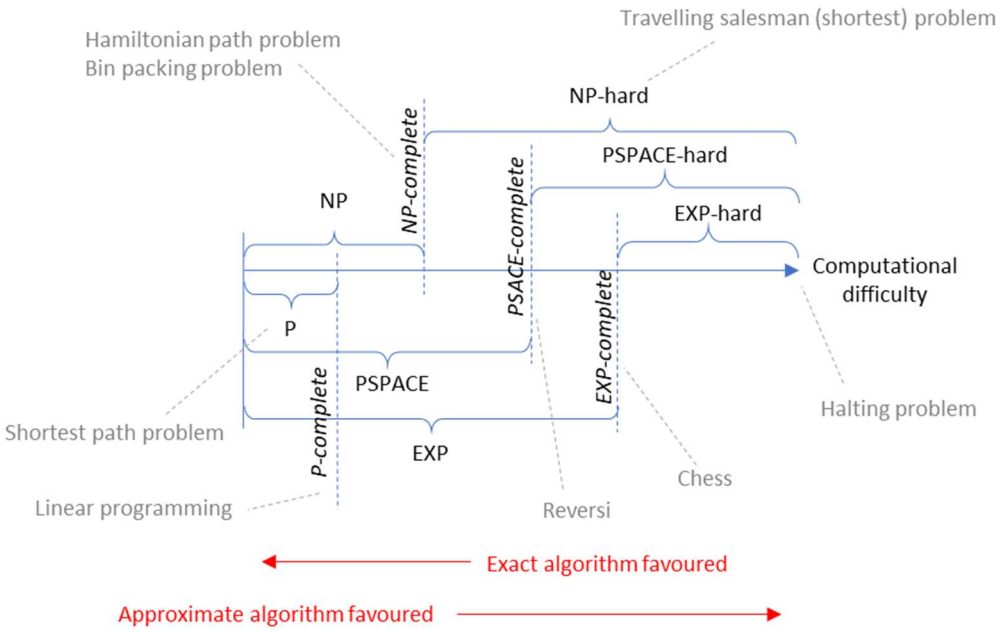

Figure 17: Categorization of computational problems according to increasing degrees of computational complexity

Rather than classifying COPs directly according to the computational complexity theory, this research adopts a more pragmatic approach by developing and comparing both exact and approximate algorithms (representing a range of enumerative, heuristic, metaheuristic and stochastic methods) as a pseudo approach for validating that the correct class of algorithm has been selected to solve a given problem.

3.3 Visual Programming Languages

This research uses visual programming languages as the primary method for algorithm development, given their ability to facilitate rapid prototyping over more conventional text-based programming. The following discussion is geared towards explaining the background behind visual programming languages

(VPLs), their burgeoning application in construction, and the development process employed in this research.

3.3.1 Background

Traditional automated workflows in construction require groups of experienced programmers and software companies to develop tailored solutions. This comes with high cost, long turnaround and required a highly coherent software team that understood construction processes deeply. However, the advent of visual programming languages (VPL) for computational algorithm development [193] has fostered a new way of developing custom software solutions for the construction industry. No longer are highly experienced programmers required for software development, as the ease with which computational algorithms are created can be tasked to design teams who have a basic understanding of process ontology (i.e., the idea of connecting functions together in a logical workflow). More frequently, design firms are harnessing the power and versatility of VPL-based computational algorithms so that rather than purchasing off-the-shelf software, they are developing automated workflows in-house.

VPLs have been traditionally met with resistance from the software development community since they lack the structure and process consistency required for code legibility [194], which can be problematic for troubleshooting or changing program functionality. To address these concerns, users must ensure that all programs are carefully vetted, documented and embedded with checks and balances throughout to flag operational faults. Despite the potential legibility concerns with VPLs, one of their strengths is the ease of creation for practitioners in the AEC industry. In this regard, visual programs can be created for highly customized processes with a quick turnaround as compared to equivalent off the shelf software[10].

Originally, many VPLs were designed to only handle intuitive design tasks such as architectural modelling or other basic geometry creation [195]. However, with increasing development in recent years and a concerted effort from the open-source community to develop advanced and customizable functionality, VPLs for construction design are beginning to be used for non-intuitive tasks. While most VPLs function by referencing DLLs (Dynamic Link Libraries), advanced functionality can be achieved through custom functions written in textual programming languages (C#, Python, C++, VB, etc.) which can also access platform APIs (application programming interfaces). This customization capability enables VPLs to be used for increasingly non-intuitive design tasks.

[10] For the purpose of this research, VPLs are deemed an acceptable approach for conducting agile development and or prototyping of proposed algorithms.

A conventional issue with VPLs has been that they lacked the tolerance granularity required in advanced geometric analysis (which is especially important in code compliance checking). VPL functionality and resulting accuracy is also based on the platform they operate on (unless they are platform-neutral). For instance, Autodesk® Revit has a polygonal-based representation of geometry, which is contrasted to the native NURBS (non-uniform rational B-spline) representation in Rhinoceros. Geometric representation type and interoperability conversion processes (e.g., converting a NURBS object to a polygonal object) are sources of inaccuracies. Furthermore, since most VPLs operate on CAD platforms that allow the creation of non-manifold geometry, achieving strict geometric tolerance adherence in VPL based programs is challenging. To overcome this issue, designers need to invest effort in ensuring that input geometry complies with manifold criteria and geometric tolerance requirements.

3.3.2 Development Process of VPL Algorithms

VPL-based computational algorithms must address three core areas of development: (1) computational functions, (2) programming syntax, and (3) data structure management. These three areas of development must be federated for an algorithmic workflow to be functional. Computational functions comprise a range of categories including geometric, arithmetic, Boolean, vector calculus, physics and heuristic optimization [196,197]. These core functions are deemed 'computational' by nature of how they compute, process, or transform geometry and associated metadata in an algorithmic fashion. It's worth noting that these functions comprise much more than just geometric transformation and analysis since, for every input object, there are numerous ways to extract quantitative and qualitative properties (metadata) which can be algorithmically computed [198].

Computational algorithms require proper programming syntax, which is platform-specific (e.g., Grasshopper and Dynamo each have their own unique syntax), or programming language-specific in the case of custom nodes (e.g., Python vs. C# syntax). Efficiency in script development is also important for improving the overall temporal performance of the algorithm. Finally, data structure management is a unique aspect of VPL computational algorithms that is required for proper functionality. Data management is platform-specific and governs the way that lists, groups and sub-groups of objects and attributes are handled through the program. For instance, Grasshopper VPL handles data management through lists of objects in 'trees'. Trees store data in a hierarchical manner with dimensional 'levels', where a tree can have any number of branches, and each branch can have sub-branches, etc. Items are stored in branches following the same hierarchical data structure as trees and branches (Figure 17). From this example of a data tree structure, it is important to note that when performing computational processes between tree items, their data structures must match. For instance, if item A in tree 1 is being tested for a

spatial clash against item B in tree 2, compatible tree structures could be {0;1;0} and {1;1;0} respectively, since they have the same dimensional levels and the last indices match. These same items would not be compatible if their tree structures happened to be {0;1;0} and {1;0;2;1} respectively since the second data tree structure has four 'levels'. Data structure management becomes complex for large sets of items and numerous trees. Linear algebra plays a critical role in ensuring compatible data structures in computational algorithms. Data structure management is optimized through the proper use of loops and parallel processing. Since computational algorithms handle large volumes of data and heavy computation, ensuring data management is developed efficiently is paramount. Algorithm development is preceded by an initial pseudocode derivation, where the key semantic processes and their relationships required in the algorithm are identified. This manual step drives the selection of computational functions. Pseudocode development is iteratively developed as results from the algorithm are validated through error identification/resolution and performance benchmarking. The general process for computational algorithm development is outlined in Figure 18.

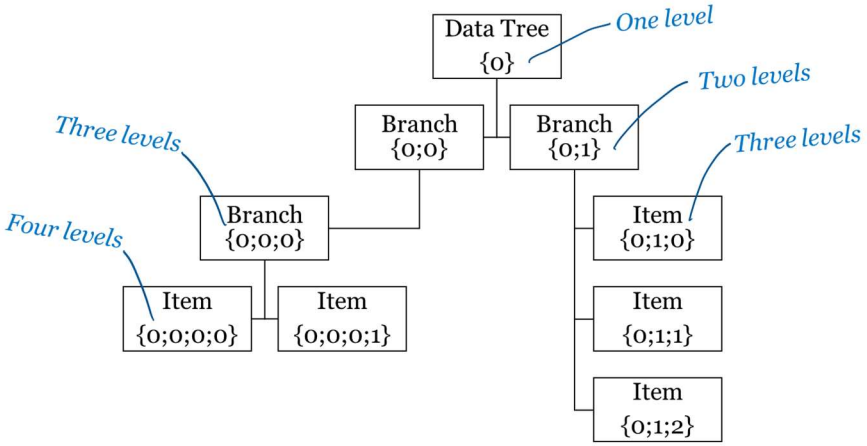

Figure 18: Example of data structure in computational algorithms.

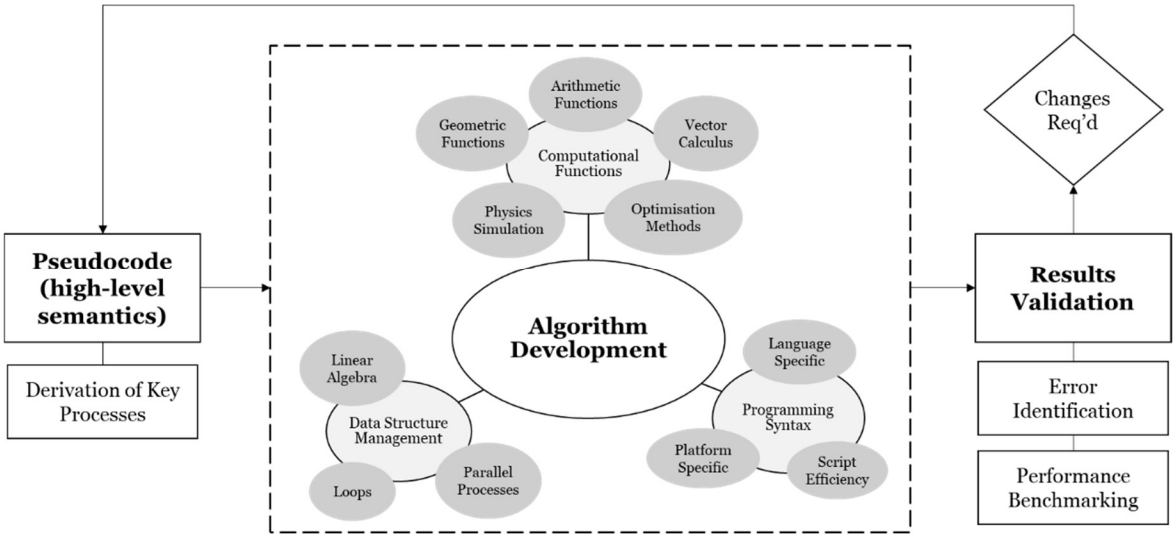

Figure 19: General process for the development of VPL-based computational algorithms for geometric optimization in BIM.

Chapter 4: Tolerance Analysis and Optimization using Monte Carlo Simulation

This chapter presents new developments made by the author that have been published in the journal of Automation in Construction [199]:

- Rausch, Christopher, et al. "Monte Carlo simulation for tolerance analysis in prefabrication and offsite construction." Automation in Construction 103 (2019): 300-314.

The purpose behind this work is to develop a computational method for optimizing the geometry of industrialized building assemblies through probabilistic simulation of dimensional tolerances. Such an approach is unique since existing techniques tend to solve tolerance-based problems during the onsite assembly stage, at the expense of large rework risk. This chapter uses an approximate method (Monte Carlo simulation) to obtain a more accurate tolerance accumulation mechanism compared to prevailing methods, which are predicated on discrete enumeration or analytical methods. A case study is carried out, where variations up to 37 mm are identified compared to as-built deviations which range up to 30 mm. Process optimization is also explored, where the risk of rework related to dimensional variability is reduced by 65.6% through the selection of alternate fabrication processes. To compare the Monte Carlo method to traditional analysis methods, a simplified 1-D tolerance analysis is used. Compared to an as-built deviation of roughly 11 mm, a probabilistic method produces a conservative value of 15.4 mm, while other traditional methods are either overly conservative (worst-case tolerance chain has a deviation of 19.8 mm), or overly ambitious (root sum square tolerance chain has a deviation of 4.6 mm). Tolerance analysis through Monte Carlo simulation is shown to be a proactive design tool with several key advantages for prefabricated and offsite construction. First, complex three-dimensional geometric interactions can be readily modelled using very basic tolerance configurations. Secondly, potential misalignments at key connection points can be identified and quantified in terms of a probability distribution of variation. Finally, design improvements can be achieved by comparing alternate construction processes to mitigate the risk of assembly rework.

4.1 Background

Due to the current fragmented practice of tolerance specification in construction [200], additional sources of dimensional variability in prefabricated and offsite construction (i.e., loads from transportation and fit-up on-site) increase the risk of rework [201]. Examples of rework risks include components being too small, too large, not level, excessive geometric changes, misalignments, and assembly fit-up conflicts [13]. While dimensional tolerances for prefabricated structures should comply with values outlined in governing standards [202], additional resources are used since tolerances from standards are not strict

enough for ensuring adequate alignment between prefabricated assemblies [171,181]. Engineers and designers must rely on tacit knowledge, libraries of case-specific tolerances, and ad-hoc strategies to derive tolerances for prefabricated structures. Since reliance on these resources does not always produce adequate tolerances, assembly geometry is still corrected during construction rather than being proactively addressed during design. This is why the current state of tolerance specification is described as an inefficient and reactive process [13,203], which is further compounded by the fact that associated rework typically delays activities along the critical path of a project.

4.2 Monte Carlo Simulation for Tolerance Analysis

Tolerance analysis is a favourable method for proactive dimensional control. In manufacturing, the design of mechanical assemblies must include a dimensional analysis as part of a complete quality assurance program [204]. Tolerance analysis methods have been developed over time to address assemblies that range in complexity. Common methods include dimensional tolerance chain models (or tolerance charts), statistical tolerance models, kinematic chain analysis (or vector loop models) and Monte Carlo simulation. It is useful to categorize these methods in terms of their ability to address varying degrees of assembly complexity: methods for 1-D or 2-D analysis and methods for 3-D analysis. Dimensional tolerance chain models aim to characterize the accumulation of tolerance in an assembly using a linear equation with worst-case tolerances or using a root sum square statistical equation. The challenge with tolerance chain models is that they are usually overly conservative (worst-case tolerance chains), or overly ambitious (root sum square) in their accumulation predictions [205]. To improve accuracy, statistical tolerance methods were introduced, comprising an equation of random variables that are solved using advanced techniques (e.g., Taylor series approximation, Croft's method, Hasofer-Lind index method, higher-order integration techniques, Taguchi's method, etc.). However, the increased accuracy requires developing and solving an assembly equation that can be very complex and not practical for many real-world applications [206]. Accordingly, due to limitations in either accuracy or analytic difficulty, tolerance chains and statistical models are often confined to only 1-D or 2-D tolerance analysis.

3-D tolerance analysis is more appropriately addressed using either a kinematic chain (or vector loop) analysis or simulation-based analysis. Kinematic chain analysis characterizes an assembly as a system of vectors connected at joints with translational and rotational degrees of freedom. Since kinematic chain systems are distilled into a series of matrices that often result in a non-linear equation, using them relies heavily on experience and insight [207,208]. Accordingly, simulation-based tolerance analysis is used when other methods are too cumbersome (e.g., statistical models or kinematic chain analysis) or do not provide sufficient accuracy (e.g., tolerance chains) [209]. Statistical simulation is carried out using the

Monte Carlo technique which compiles stochastic samples of probability distribution functions for individual components in the assembly. Despite the criticism of its potentially high computational demand, Monte Carlo simulation has been shown to be one of the simplest and most popular methods for solving complex tolerance analysis [210,211]. Recently, it has also been used to perform risk-based assessment on optimal strategies for tolerance management in modular construction [42]. In addition, research has proven the ease with which alternative production processes can be evaluated using the Monte Carlo method for optimal tolerance performance [212]. While the application of Monte Carlo simulation was initially limited to only dimensional tolerances, Yan et al. [210] developed an approach where geometrical tolerances (e.g., profile, planarity, roundness, concentricity) can be incorporated into the simulation process. This is particularly useful when trying to simplify the tolerance analysis process. Similarly, Sleath [213] describes a process of reducing an overall assembly into a subset of mating components that is representative of the assembly in terms of key geometric behaviour. These recent developments have helped to simplify large complex assemblies and to reduce the computational demand required when using Monte Carlo simulation.

4.3 Proposed Methodology

The proposed framework for tolerance analysis is shown in Figure 19 and has two primary modules. Module 1 is the tolerance identification process that involves decomposing the overall assembly into its core components, identifying the connections between these components, and configuring the corresponding tolerances at these connections. The second module is the tolerance simulation process, where results are expressed as probability distributions at critical measurement points. While the input to the framework is an initial 3-D design (including fabrication processes, tolerances, and a 3-D model), the output is a design that is optimized for tolerances and risk management. The success of the optimization process relies on the iterations involved with specifying part tolerances and fabrication processes that result in acceptable deviations at the critical measurement points.

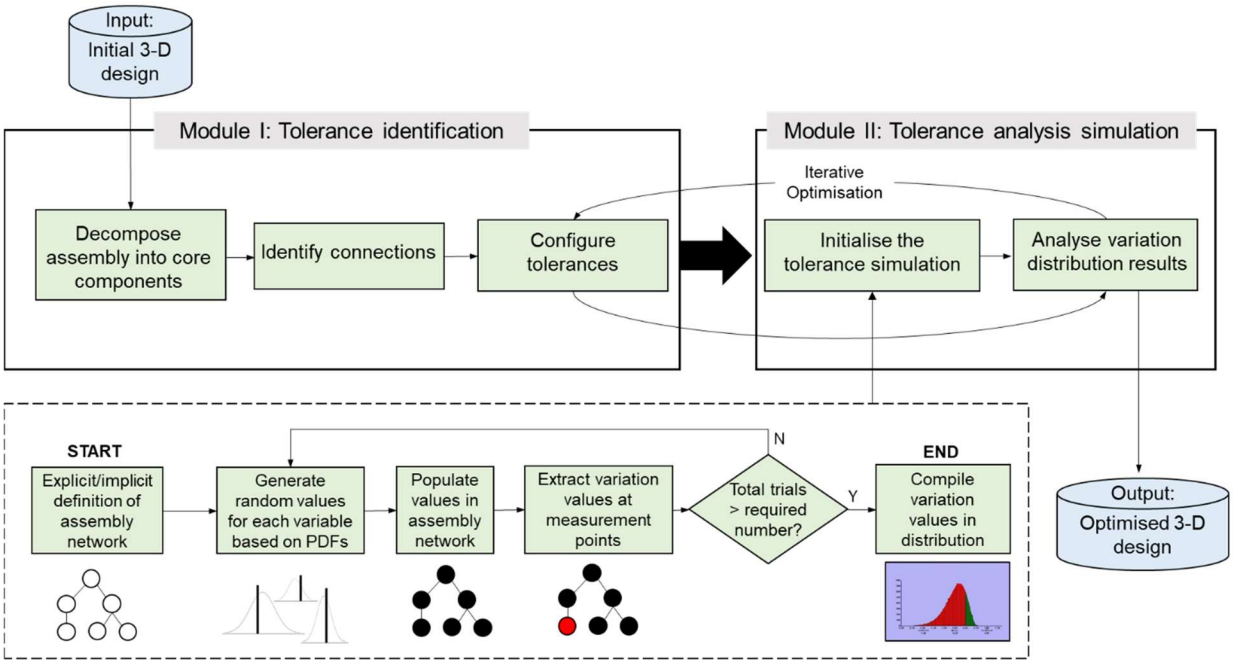

Figure 20: Overview of the proposed framework for simulation-based tolerance analysis of construction assemblies

The following types of tolerances are used in the proposed framework:

- **Size tolerances**, which express the difference between the actual length or width of a component and its nominal length or width.

- **Form tolerances**, which relate to the straightness of a linear feature (1-D profile of a component), or flatness of a surface. It should be noted that form tolerance is expressed as a linear dimension corresponding to the largest Euclidean distance between the profile of an actual line/surface feature to the nominal feature.

- **Positional tolerances**, which relate to the accuracy in location and are measured as a two-point distance from the actual position to the nominal position.[11]

When given no prior knowledge about a specific manufacturing process, it is generally assumed that its tolerance follows the normal distribution [214]. Previous tolerance considerations in construction have also relied on the normal distribution [25]. Since most construction tolerances are specified using a

[11] *It should be noted that orientation can be included within positional tolerances, since such variations can be significant drivers of rework in construction projects (especially for industrial applications)*

numerical ± value[12], it is necessary to explain how numerical tolerances can be expressed as statistical tolerances which are required for statistical simulation. In accordance with the principles of six-sigma methodology [215], a range of 6σ (six standard deviations) accounts for 99.73% of the entire normal distribution function. By expressing this statistical range as ±3σ centred on the mean of the standard distribution, it is possible to associate an initial ± tolerance to ±3σ of the normal distribution function (Figure 20).

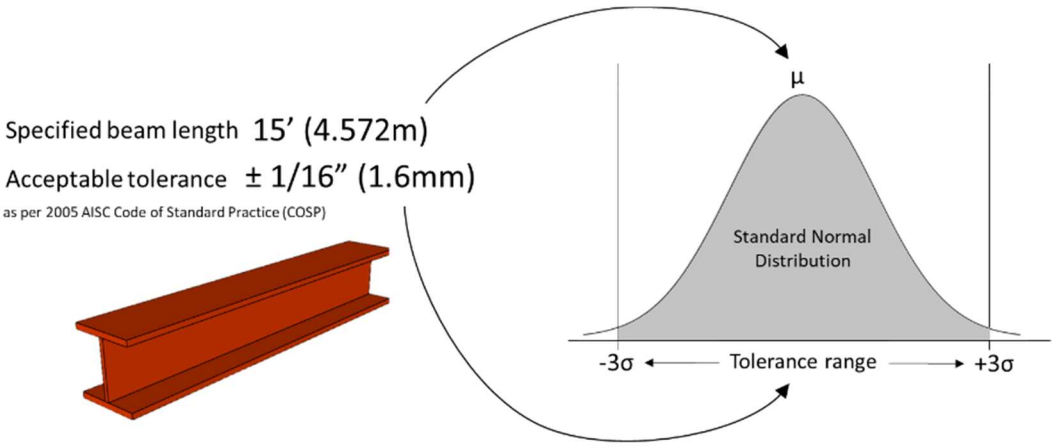

Figure 21: Demonstrating how numerical tolerance limits can be expressed in terms of statistical tolerance limits in accordance with six sigma principles.

The assembly network defines how each of the components is geometrically related. This process results from the decomposition of an assembly into the core subassemblies, as previously discussed, and results in a network of variables. The generation of the assembly network can be done explicitly (refer to [114] for demonstration of this using kinematics chains) or can be done implicitly using a 3D-CAD simulation engine (as was used in the functional demonstration shown in this chapter). Simulating non-rigid body deformations must be done by a "net rigid body effect", through the use of an equivalent dimensional variation. A key aspect of the assembly network creation is the inclusion of critical measurement points on the assembly, which are used to measure the overall compliance of the simulation process. For industrialized building construction, the following types of critical measurements can be included in an assembly network:

- **Gaps**: these can either be functional (i.e., required gaps between certain components), or can be resultant (i.e., gaps that should not be present, but are acceptable within certain limits).

[12] *While this research directly considers the case of a two-sided tolerance value (i.e., +/- X mm), it should be noted that the proposed method is also capable of handling one-sided tolerances (i.e., < X mm).*

- **Circle interference**: used to define acceptable alignment condition for bolted connections. This measurement type is covered in detail in a functional demonstration and is depicted in Figure 22.

- **Feature position**: used to define conditions of fit (i.e., the absolute or relative position of one feature to another) or are used to define appropriate inspection requirements for the overall geometry of an assembly.

Through the use of the Monte Carlo technique, the assembly network is then populated with values using a random value generator for each simulation trial. The accuracy of the simulation process is related to the number of simulation trials. It is generally very difficult to compute the minimum number of simulations required since this depends on the complexity of the deterministic model, variance of input and required accuracy of output. However, since the Monte Carlo method is a statistical measure, the number of required simulations can be roughly estimated using the central limit theorem and the confidence bounds of the normal distribution according to [216] as,

$$\boldsymbol{N = \left(\frac{Z_{\frac{\alpha}{2}} \left(\frac{\sigma}{\mu} \right)}{\frac{Er(\mu)}{\mu}} \right)^2}$$

Eqn. 2

where N is the number of simulations, $Z_{\alpha/2}$ is the standard normal statistic, σ is the sample standard deviation, μ is the sample mean, $Er(\mu)$ is the standard error of the mean and the expression $Er(\mu)/\mu$ is the margin of error in percent format. The challenge when calculating the minimum number of Monte Carlo simulations is that an initial set of simulations must be run in order to obtain the sample mean and standard deviation before a final set of simulations are run. After running this second set of simulations, the minimum number of simulations should be recalculated to verify that the increased precision of the sample statistics has not changed the accuracy of the initial estimation. To avoid this potentially cumbersome and iterative process of calculating the minimum number of simulations, this research employs a different approach. Instead, a predefined number of simulations are used, and the resulting margin of error is calculated and analyzed. If the resulting margin of error is deemed unacceptable, then a subsequent set of simulations can be carried out. Previous research has found that a limit of 10,000 simulations is generally sufficient for the purpose of tolerance simulation [217]. Using this value, and a predefined confidence interval, Eqn. 2 can be rearranged to solve for the margin of error:

$$\left(\frac{Er(\mu)}{\mu}\right) = \frac{Z_{\frac{\alpha}{2}}\left(\frac{\sigma}{\mu}\right)}{\sqrt{N}}$$

Eqn. 3

The confidence interval can be obtained by solving for the significance level α, using a Z-statistic table. For the purpose of this study, a confidence interval of 95% (on the margin of error) and 10,000 simulations are used. The only drawback to this approach of calculating the margin of error is that employing a predefined number of simulations can be potentially computationally expensive. However, the simplifications employed in this methodology (e.g., reducing an overall assembly into a smaller subset of mating components), reduce the computational demand of Monte Carlo simulation as evidenced in the functional demonstration, where simulation results are obtained very quickly.

Pseudocode for the Monte Carlo algorithm employed in this research is shown below. The basic premise of this algorithm is to compute specific tolerance chains that result from the aggregation of parts in an assembly. Then, for each critical dimension, these tolerance chains are continually generated according to the normal distribution for the computation limit (10,000 samples).

Algorithm 1 Monte Carlo Algorithm for Computing Dimensional Variation Stackup of Key Dimensions

Inputs: Assembly parts, $P_i \rightarrow$ B-rep objects with topology defined by curves, faces and vertices
Part tolerances $\rightarrow T_i[]$ for parts i to n, where T[] $\in$ size (+/- dim), form (1D limit), position (+/- datum)
maxIter = 10,000
$Crit\_dim_j$ = critical dimensions (j = 1 to m)
Initialization: s = 0
$Chain_j = Crit\_dim_j(f[P_i])$ – this defines the tolerance chain based on specific parts P_i
    WHILE s < maxIter **DO**
        j = 1
        FOR j = 1 to m
            $Chain_j = \sum normdist(0,T_i[])$
        RETURN $Chain_j$
    $Crit\_dim_j(s) = Chain_j$
    $Chain_j = 0$
END

4.4 Functional Demonstration of the Methodology

During an industrialized building project which was introduced in Rausch et al. [114], several challenges emerged during the fabrication and assembly of prefabricated structures. These challenges stemmed from dimensional variability issues that arose as the result of improper tolerance specification and geometric controls during construction. The accumulation of dimensional variability ultimately created large gaps between module tie-in plates and created challenges during fabrication and assembly. Data collected from this project is used to demonstrate how the proposed framework can detect and resolve geometric assembly conflicts. In this demonstration, the structural assembly of a module is assumed to be comprised

of three types of subassemblies (base frame, columns, and a roof frame), which are aggregated using bolted connections. During this project, once the columns were installed to the base frame, a scan-vs-BIM analysis [112] was used to quantify compliance to an as-designed BIM model. As-built data from a FARO laser scanner (which has an accuracy of ± 2 mm for the scanning distance in this project) was registered using Autodesk ReCap to produce a 3-D point cloud which was then overlaid on a BIM model in CloudCompare. This scan-vs-BIM analysis highlights several key column misalignments, ranging in magnitudes up to approximately 30 mm.

4.5 Simulation 1: Detecting Assembly Conflicts

An initial tolerance simulation is used to detect the presence of immediate assembly issues that result from the interaction between the geometric configuration and dimensional process capabilities. For simplicity, the base frame and roof frame are considered to be rigid and free from significant manufacturing deviations (e.g., from welding distortion). As-built deviations for the base and roof frame used in this project were quantified through a scan-vs-BIM analysis and were shown to be less than 5mm (Figure 21). The manufacturing deviations of the frames are small since the contractor utilized "fixturing tables" for fabrication. While this is effective in controlling the 2-D alignment of an assembly, there were no geometric controls for fixturing the 3-D alignment of the overall module structure (outside of measuring overall length and column verticality using tape measures, levels and laser meters). The ability to assemble the roof frame on the module, therefore, relies on several key tolerances: tolerances for placement of bolt holes in the base frame and columns, size tolerance of bolt hole diameter, size tolerance on bolt diameter, tolerance on the straightness of columns, and tolerance on the length of columns. To incorporate each of these tolerances into the simulation, several resources [92,218] and rules of thumb were used to obtain tolerance values, distribution type and range. Each of the tolerances is assumed to be normally distributed, and have the values as indicated in Table 3. The acceptable range for each tolerance corresponds to the ± 3σ (where σ is the standard deviation) limits of the normal distribution function, which contains 99.73% of all variations.

Table 4: Tolerance input values used in the simulation of the module structure assembly

Tolerance	**Tolerance Type**	**Tolerance Range (± 3σ)**
Bolt hole location (drilling)	Positional tolerance	±1/32" (0.8 mm)
Bolt hole diameter (drilling)	Size tolerance	±1/32" (0.8 mm)
Bolt diameter	Size tolerance	±5*thou* (0.12 mm) *
Column straightness	Form tolerance	±5/64" (2 mm) **
Column length	Size tolerance	±5/64" (2 mm)
*Since this tolerance is very small and has a near negligible effect, it was not considered in the tolerance analysis simulation.		

**The net effect of the column straightness is a positional tolerance at the top of the column. The tolerance value corresponds to the absolute horizontal deviation at the top of the column with respect to the base.

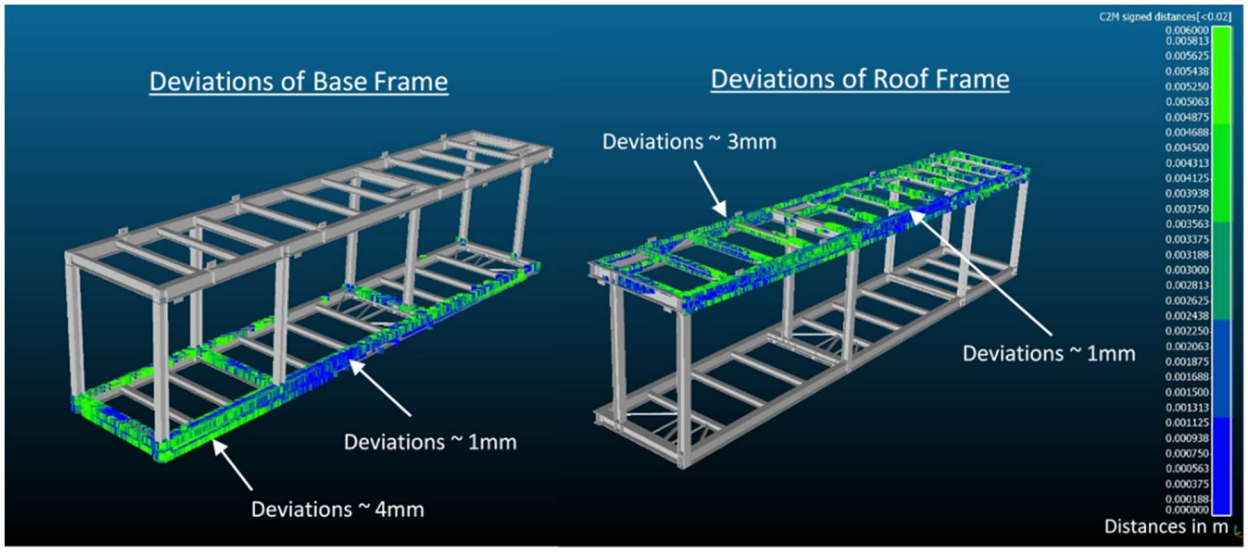

Figure 22: Deviations of the base and roof frames for this project. Laser scans obtained for both the frames were fit to the 3D BIM model, and scan-vs-BIM deviations were obtained using CloudCompare. Deviations for the fabrication of base and roof frames were less than 5mm.

Since the assembly sequence is characterized by key connections between subassemblies, the critical measurements for this tolerance simulation are at the bolted connections for the base frame and roof frame. In manufacturing, a specific measurement type called circle interference is used to assess the minimum clearance for pin/hole assemblies. This measurement can also be used for describing the condition of acceptable bolt-assembly alignment since it closely resembles a pin/hole assembly. In this regard, acceptable alignment occurs when there is a gap (or positive "circle interference" value) between the bolt surface and the hole surface (Figure 22). To account for varying degrees of rework in cases where a bolt-assembly does not align, a threshold is used where misalignments greater than 2 mm indicate a large amount of rework (realignment required), while misalignments less than 2 mm indicate a low degree of rework (where reaming or forced assembly can likely be used). While it might initially seem like a 2 mm threshold is quite small for large bolted connections in construction, it is important to note that most connections comprise multiple bolts in a specific pattern. If all bolts at a given connection experience the same misalignment vector, then a 2 mm threshold is likely to be overcome with a small amount of rework. However, to account for the condition where bolts at a given connection experience different misalignment vectors, it becomes increasingly more difficult to align them when their individual misalignments exceed 2 mm in different directions. In this simulation, the bolt diameter was ¾" (19 mm) and the bolt hole diameter was 25/32" (20 mm), leaving a maximum uniform gap of 0.5 mm when the

bolt is perfectly centred in the bolt hole. Based on the definition of circle interference, acceptable alignment occurs when the clearance between a bolt and bolt hole is within -2 mm and +0.5 mm. In total, 32 critical measurement points were defined in the tolerance simulation, corresponding to the top and bottom connections of the 4 outermost corner columns (there are 4 bolts at each connection)[13]. A key assumption in this analysis is that each bolt hole is drilled independently of each other (i.e., no jigs were used for hole alignment between the bottom of a column and the base frame or top of column and roof frame). Running the tolerance analysis for 10,000 Monte Carlo simulations only took 189 seconds and resulted in a variation distribution for each of the critical measurement points. Figure 23 shows a sample result for the variation distribution at one bolt connection. Negative circle interference values are shown in red and represent the condition where the bolt does not fit within the bolt hole. Only values outside of the -2 mm circle interference condition represent a high degree of rework[14]. Each variation bar chart contains the population mean, standard deviation and a best-fit probability distribution function.

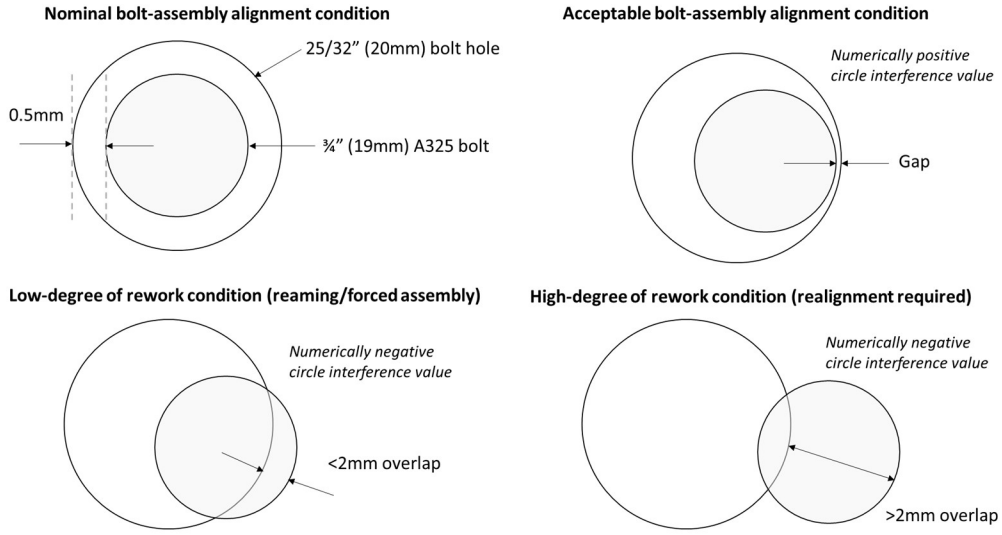

Figure 23: Nominal bolt-assembly alignment for this functional demonstration and conditions to describe acceptable alignment and rework conditions for misalignment.

[13] *For the purpose of this study, measurement of these 32 points was not directly captured since it is often challenging to directly capture bolt hole features from laser scanners – such measurement is more appropriately conducted using a laser tracker for instance. As such, these deviations are assessed by abstracting the deviations of columns and frames at these connection points.*

[14] *It should be noted that while this research considers these rework limits in a deterministic manner (i.e., $X < -2$ mm and -2 mm $< X < 0$ mm), these limits could also be probabilistic limits.*

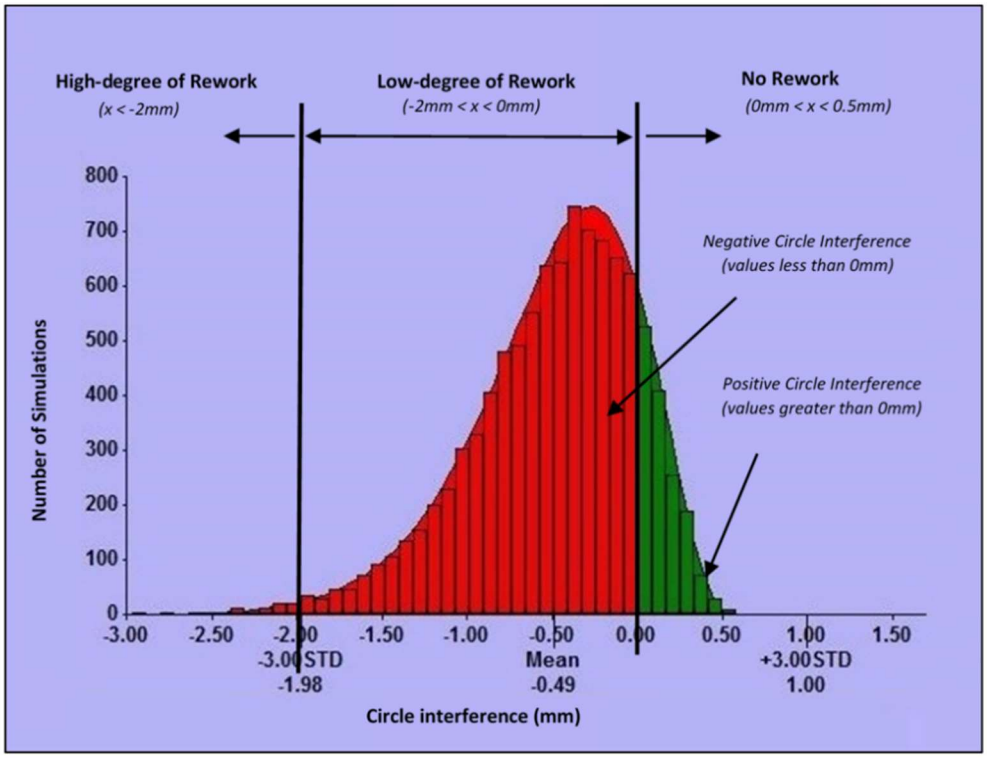

Figure 24: Sample variation bar chart of a bolted connection. Red values indicate rework conditions, where circle interference values between -2 mm and 0mm are a low-degree of rework and circle interference values outside of -2 mm represent a high-degree of rework. Green values indicate acceptable alignment between bolt and bolt hole, which requires no rework.

4.6 Assessing Probability of Rework

In this simulation, each variation bar chart best matched a Pearson Type I distribution function, which is a generalized case of the Beta distribution (with more arbitrary shifting and scaling parameters). Normally, it is not necessary to extract the specific function pertaining to each variation distribution since tolerance simulation software such as *3DCS Variation Analyst* provides a large set of analytics pertaining to the probability of non-conformance. However, for this chapter, the probability function was extracted in order to derive custom probabilities pertaining to the conditions of adequate bolt-alignment. Due to the complexity of modelling a Pearson Type I distribution, an equivalent Beta distribution was graphically fit to the data in each variation bar chart, and a cumulative distribution function was then used to derive the specific probabilities corresponding to each rework condition. The result of extracting these rework probabilities (Table 4) shows that the base connections are likely to experience only a low-degree of rework while the upper connections are likely to experience a high-degree of rework. While each of the lower connections has a mean circle interference between -0.1025 mm to 0.055 mm, the upper

connections have circle interference values up to -36.68 mm, which are much greater than the limit for rework at -2 mm (note that the negative values only indicate misalignment and do not correspond to the numerical value).

Calculating the overall system reliability (i.e., probability that no rework is required for any connection) is complex when accounting for the conditional probabilities between connections. For instance, there will be conditional probabilities between connections on the roof frame since a misalignment at one connection is likely to increase the chance of misalignment at another connection (assuming the misalignment is in the opposite direction of the other connection). For simplicity, by neglecting the potential conditional probabilities that may exist and only considering the high degree of rework, then the overall system reliability becomes,

$$P[rework]_{system} = 1 - P[no\ rework]_{system}$$

$$P[rework]_{system} = 1 - \prod_{i=1}^{n} P[1 - \ rework\ at\ connection]_i$$

Eqn. 4

where i ranges from 1 to 32 (for all connections), and $P[rework]_{system}$ relates to at least one event of a high degree of rework for the overall system. Calculating the probability of rework for this module with selected process capabilities results in a 99.98% probability. This is a logical result following from the specification of rework condition (circle interference outside of the 2 mm threshold) and since three connections have misalignments greater than 15 mm. To reiterate, a key assumption in this analysis is that the bolt holes are drilled independent of each other, which in fact increases the likelihood of misalignment at a given connection. In practice, jigs ensure that bolt hole patterns align better between column endplates and frames. However, the purpose of this work is to demonstrate the simulation capabilities and advantages for tolerance analysis.

The final step to this simulation is estimating the margin of error for a given confidence interval using Eqn. 3. Using a confidence interval of 95%, the maximum margin of error for the governing sample statistics in Table 4 was found to equal 5.7%. Since the margin of error is linearly related to the ratio of sample standard deviation over the sample mean, the governing measurement is the one with the largest ratio (in this case Column 1 at Base). It is important to note that this method of determining the margin of error is based on an approximation of the sample statistics using the central limit theorem and confidence bounds according to the normal distribution. Since the largest margin of error for all statistics in Table 4 is 5.7%, this is the estimate of the overall margin of error for this first simulation.

4.7 Simulation 2: Process Evaluation for Optimizing Module Assembly

A second simulation was used to reduce the high degree of rework in the first simulation by considering a new fabrication process for cutting bolt holes: waterjet cutting using a computer numerical control (CNC) machine. A cruder method of drilling bolt holes was initially selected in simulation 1. Water jet cutting is typically more expensive but results in a tighter tolerance with respect to the size and position of the bolt hole (0.2 mm vs. 0.8 mm) due to the accuracy of a CNC machine. Following the same procedure for tolerance analysis used in the first simulation, the result of "tightening" the positional and size tolerances for bolt holes has a profound effect on the rework associated with adequate assembly alignment. This time, running the tolerance analysis for 10,000 simulations only took 55 seconds. As seen in Table 5, there is no longer any probability of a high degree of rework event for any connections in the assembly. The overall probability of a low degree of rework event for the assembly using Eqn. 3 results in a 34.4% probability, meaning that the overall likelihood of no rework for this assembly is 65.6%. Again, it is important to note that a low degree of rework event is considered to be a minor amount of reaming and forced assembly, both of which are still viewed by contractors to be normal assembly requirements. Similar to simulation 1, the margin of error for a given confidence interval can be estimated. Using the same 95% confidence interval, the maximum margin of error for the governing sample statistics (Column 3 at Roof) in Table 5 is equal to 1.3%. As such, the estimate of the overall margin of error in this simulation is 1.3% with a confidence interval of 95%.

Table 5: Results for the process of drilling bolt holes. Average values at each bolted connection are shown for the distribution mean, standard deviation, and probabilities for varying levels of rework.

Key Fabrication Process - Drilling Bolt Holes **Location tolerance = ±1/32" (0.8 mm), bolt hole size tolerance = ±1/32 (0.8 mm)**					
Critical Measurement	Average Distribution* Mean	Average Distribution* Standard Deviation	Approximate Probability** of No Rework	Approximate Probability** of Low degree of Rework	Approximate Probability** of High degree of Rework
Column 1 at Base	-0.1025	0.355	30%	70%	0%
Column 2 at Base	-0.1025	0.3525	30%	70%	0%
Column 3 at Base	-0.105	0.3525	50%	50%	0%
Column 4 at Base	0.055	0.1375	70%	30%	0%
Column 1 at Roof	-0.1725	0.375	20%	80%	0%
Column 2 at Roof	-15.395	12.1875	0%	10%	90%
Column 3 at Roof	-33.18	25.985	0%	5%	95%
Column 4 at Roof	-36.6775	28.7125	0%	5%	95%
For each connection, the average distribution results for all 4 bolts are shown.** * Probabilities are approximated using graphical comparison to a beta distribution function.**					

Table 6: Results for water jet cutting bolt holes. Average values at each bolted connection are shown for distribution mean, standard deviation, and probabilities for varying levels of rework.

Key Fabrication Process – Water Jet Cutting Bolt Holes **Location tolerance = ±8 *thou* (0.2 mm), bolt hole size tolerance = ±8 *thou* (0.2 mm)**					
Critical Measurement	Average Distribution* Mean	Average Distribution* Standard Deviation	Approximate Probability** of No Rework	Approximate Probability** of Low degree of Rework	Approximate Probability** of High degree of Rework
Column 1 at Base	0.1575	0.09	100%	0%	0%
Column 2 at Base	0.16	0.09	100%	0%	0%
Column 3 at Base	0.1575	0.09	100%	0%	0%
Column 4 at Base	0.16	0.09	100%	0%	0%
Column 1 at Roof	0.14	0.11	90%	10%	0%
Column 2 at Roof	0.14	0.11	90%	10%	0%
Column 3 at Roof	0.1375	0.11	90%	10%	0%
Column 4 at Roof	0.14	0.11	90%	10%	0%
***For each connection, the average distribution results for all 4 bolts are shown. ** Probabilities are approximated using graphical comparison to a beta distribution function.**					

4.8 Comparison of Combinatorial Sampling with Exact Mathematical Approaches

To base the results obtained for stochastic tolerance analysis with other tolerance analysis methods, the following methods are examined and contrasted: a worst-case tolerance chain, a root sum square tolerance chain, and kinematic chain analysis.

As identified in the literature, dimensional tolerance chain methods (worst-case and root sum square) are generally limited in their use to just 1-D or 2-D tolerance analysis. To reflect this, a simplified 1-D analysis is carried out for a worst-case tolerance chain and a root sum square tolerance chain. A cross-sectional diagram of columns 1 and 2 in the assembly depicts the accumulation of variations in the form of a 1-D tolerance chain analysis in the x-direction (Figure 24). In this figure, column straightness, bolt hole size tolerance, nominal joint slippage (i.e., the gap between the bolt and bolt hole), and bolt hole position all contribute to the alignment between the column shown on the right and the roof frame assembly. Worst-case tolerance accumulation and root sum square tolerance accumulation are calculated according to the following equations

$$T_{WC} = \sum_{i=1}^{n} T_i$$

Eqn. 5

$$T_{RSS} = \sqrt{\sum_{i=1}^{n} T_i^{\,2}}$$

Eqn. 6

where T_{WC} is the worst-case tolerance accumulation, T_{RSS} is the root sum square tolerance accumulation, and T_i are individual tolerances for n number of chain elements. Using the chart in Figure 24, tolerance accumulation along the 1-D chain in the x-direction results in the following calculations for tolerance accumulation:

$$T_{WC} = 2A + 8B + 3C + 8D = 19.8\,mm$$

$$T_{RSS} = \sqrt{2A^2 + 8B^2 + 3C^2 + 8D^2} = 4.6\,mm$$

where A is the column straightness, B is bolt hole size tolerance, C is nominal joint slippage, and D is bolt hole position tolerance. The tolerance values used in this calculation correspond to bolt hole drilling as the key fabrication process (as per the tolerances outlined in Simulation 1). An equivalent deviation using the Monte Carlo method between column 2 and the roof frame was found to be 15.4 mm while the as-built deviation at the top of column 2 was found to be roughly 11mm. From these results, we can see that the worst-case tolerance chain method produces a more conservative (i.e., larger) accumulation than the Monte Carlo method, while the root sum square has an overly ambitious tolerance accumulation value. While the Monte Carlo method also produces a conservative result compared to the equivalent as-built deviation, it is important to note that in terms of tolerance analysis, conservative results are superior to ambitious results for identifying potential misalignments. The comparison of Monte Carlo with worst-case and root sum square tolerance chains match the conclusions observed in the literature. In addition, dimensional tolerance chain methods do not account for rotational errors that result from deviations in higher-order degrees of freedom (i.e., rotations in the Z direction). Even slight rotational errors at connections at one end of a module can lead to significant misalignments at the far end, which is being accounted for in the Monte Carlo simulation that in essence estimates a joint confidence limit (re. [219]). For these reasons, the Monte Carlo method is superior to tolerance chains for 3-D tolerance analysis on large complex structural assemblies.

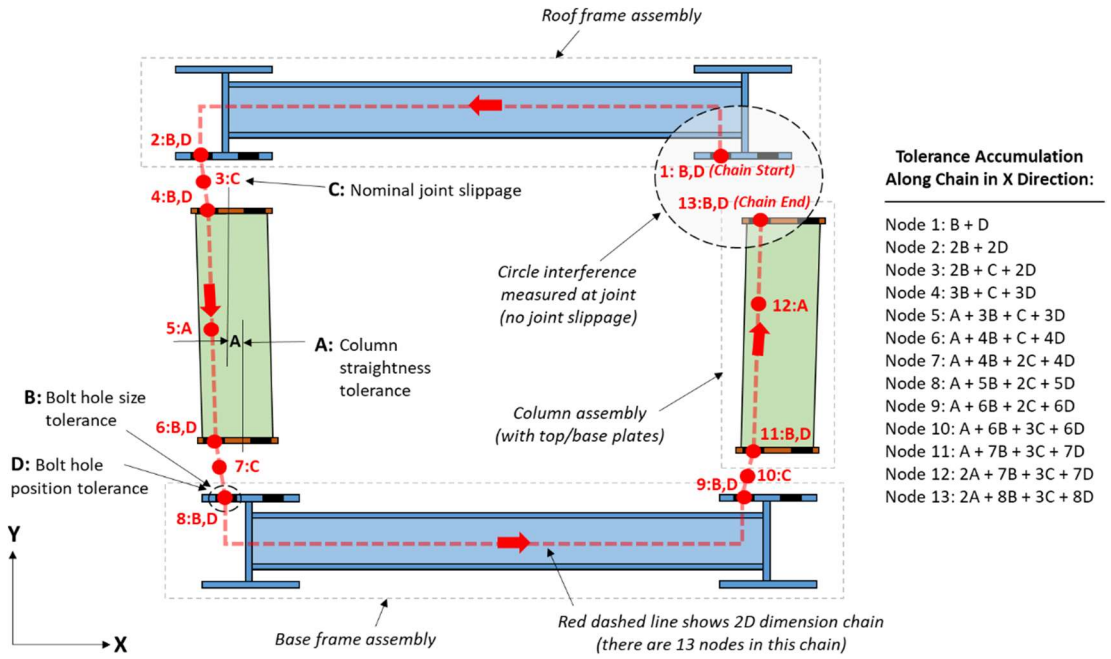

Figure 25: Simplified accumulation of variability and tolerances using a 1-D dimension chain in the x-direction illustrated in elevation-view.

In a previous study [114], the author demonstrated the use of kinematic chain analysis on an industrialized building assembly that came from the same project that was explored in this chapter. While this assembly was not the exact same one analyzed in this study, the structural configuration is very similar. In our previous study, we found that kinematic chain analysis could predict 3-D tolerance accumulation between a reference datum point on the bottom of the assembly to tie-in plates on the top of the assembly, which function as "end-effectors" in a kinematic chain. Since kinematic chain analysis relies on rotational and translational degrees of freedom, accounting for more complex interactions, such as gaps at joints, is challenging. To overcome this, several assumptions and simplifications were required. For instance, the kinematic behaviour of the roof frame was confined to rotation about the vertical axis alone. Another key assumption was that the entire base frame with columns was assumed to be one subassembly with negligible tolerances. The propagation of tolerance was thus attributed to two mechanisms: (1) deviations of each tie-in plate on the roof frame, and (2) deviation of the roof frame on the base frame and column subassembly. This means that in order to apply the kinematic chain method for the same 3-D analysis simulated using the Monte Carlo method in this study, a highly-variate kinematic chain equation would be required. Furthermore, the assumption that the base frame and columns function can be taken as one subassembly is not valid for two reasons. First, the as-built deviations of the columns with respect to the base frame were shown to be non-negligible. Second, discontinuities will exist when comparing the kinematic chains between each column to the connection

points on the roof frame. It is therefore too complex to use kinematic chain analysis at the same granularity of 3-D tolerance analysis that the Monte Carlo method is capable of. Similarly, the consideration of other tolerance analysis methods (e.g., tolerance mapping and statistical models) are also too cumbersome and complex to accurately predict 3-D tolerance accumulation in the way that Monte Carlo simulation can.

In summary, compared to other tolerance analysis methods, Monte Carlo simulation has many desirable attributes in the context of industrialized building construction. First, it is capable of handling complex three-dimensional relationships between components that other methods such as tolerance chain methods, kinematic chain analysis and tolerance mapping cannot. While other tolerance analysis methods may rely on the user having a fundamental understanding of graph theory and or comprehensive manufacturing tolerance nomenclature (e.g., GD&T), tolerance simulation can be carried out using simple tolerance configurations. Finally, it is shown to be a very effective design tool for comparing various fabrication processes based on tolerance performance and rework risk management.

4.9 Conclusion

This research is the first of its kind to demonstrate that tolerance behaviour and process capability can be simulated and optimized for industrialized building construction. Conventional tolerance chain methods are either too conservative or too ambitious in their prediction of tolerance accumulation. Other methods such as kinematic chain analysis, statistical methods or tolerance mapping methods are too challenging to use given the complexity in accounting for systematic behaviour in 3-D construction assemblies. Tolerance analysis through Monte Carlo simulation is proactive, applicable for complex 3-D assemblies and can reduce rework associated with correcting geometry during fabrication and onsite assembly. Traditionally, predicting misalignments at joints was elusive due to the complex 3-D interaction between components and the inability to model tolerance accumulation in such systems. However, utilizing process capability data in the form of statistical tolerance distributions, simulations can be used to model, predict and correct misalignments that may occur at critical joint locations.

The ability to predict how parametric construction objects can become non-parametric as the result of fabrication and assembly processes is important for ensuring proper aggregation and performance of industrialized building construction assemblies. In this case, the control of non-parametric deviations needs to be confined to tolerance limits in order to avoid the risk of rework. By selecting alternate fabrication processes, mediation can be achieved by ensuring that the changing state of an assembly remains tolerably parametric, thereby facilitating aggregation of subsequent (parametric) components.

Chapter 5: Exact and Approximate Combinatorial Algorithms for Topology Optimization

This chapter presents new developments made by the author that is in an article published in the Journal of Construction Engineering and Management [220]:

- **Rausch, C.,** Sanchez, B., Haas, C. (2020). Topology optimization of architectural panels for minimizing waste during fabrication. Journal of Construction Engineering and Management (accepted), Dec 2020.

The purpose of this work is to develop algorithms for optimizing the topology of prefabricated 2D panels to minimize waste during fabrication. While this chapter focuses on the domain of architectural panels and this is not strictly an application of industrialized building construction as defined in the background section, the argument is made that the methods can be suitably adapted for 2D panelized building construction (which is in fact a form of industrialized building construction).

5.1 Background

The use of thin-metal panel systems is a popular approach for cladding modern buildings. Often, these panels are used to provide an adequate rainscreen while giving a distinctive architectural design to a building. The emergence of large-scale free-form shapes has traditionally been challenging to manufacture in a cost-effective manner due to increasing architectural interest to proliferate geometric complexity [221]. File-to-factory systems (i.e., digital fabrication) have been introduced as a solution to automate the design and production of architectural panels [222]. Not only do such systems enable architects to increase the degree of geometric complexity that can be achieved, but this digitization process elicits unique opportunities for optimizing the topology of panels for reducing waste during fabrication. Aluminum composite material (ACM) panels in particular are among the most popular metal cladding systems [223], since they are lightweight, corrosion-resistant, easily manufactured and have a very long lifespan compared to other façade systems. For ACM panels, it is imperative to reduce waste during manufacturing, since the base material has very large CO_2 emissions [224]. The same can also be said for other common panel materials such as stainless steel, copper, etc. An efficacious way to reduce waste of panels without imposing significant geometric design constraints is optimizing the process of unfolding and nesting panel geometry on metal coils during fabrication.

This chapter presents a series of optimization algorithms for configuring architectural panel topology to reduce material waste during fabrication. While many optimization methods have been developed for the burgeoning area of industrialized construction, no optimization methods have been developed for

reducing material waste during the panel unfolding and nesting process. First, enumerative and metaheuristic algorithms are developed to minimize material waste for panel unfolding. Since this problem has not been solved, two alternative algorithms are developed to help classify the problem in terms of computational complexity. Then, a subsequent metaheuristic-based algorithm is developed to optimize the nesting of sample panels. To assess individual and comparative performance of these algorithms, a series of 3D panels from a typical residential construction project was used as a case study. The results demonstrate that by configuring panel topology and generating optimal nest configurations, material savings up to 11% compared to the current state-of-the-art can be achieved. Furthermore, the proposed approach provides for an automated file-to-factory system for architectural panel fabrication.

5.2 Optimization of Prefabricated Architectural Systems

Existing optimization research for building façade and architectural panel systems has been primarily developed for the design stage, with some applications also being seen in manufacturing and assembly. During design, it is often necessary to develop alternatives that achieve optimal performance in terms of building energy performance, daylighting, and fabrication cost, while meeting structural analysis and manufacturing constraints. For instance, Said et al. [170] developed an optimization platform that optimizes panel design and layout according to total fabrication cost, productive vs. non-productive labour hours and a design deviation index. The platform performs structural analysis and design in order to effectively size panels, studs, and other assembly components. This multi-objective problem is solved using a non-dominant genetic algorithm that outputs a series of Pareto-optimal design configurations. In a similar fashion, Montali et al. [225] developed a more general framework that takes into account the metrics of “architectural intent”, “required performance” and design constraints. In this framework, very specific indices can be automatically compared and evaluated during the conceptual design stage. This MOP accounts for both continuous and discrete variables (i.e., certain aspects are combinatorial in nature), and the overall framework is solved using a combination of heuristic rules and metaheuristic optimization.

A common theme in these existing design optimization frameworks is the use of metaheuristics. This method of optimization has become the de-facto choice for solving a wide range of COPs across the construction industry. In particular, metaheuristics have been developed for construction site layout [140,226], building layout planning [227], crane planning [228], time-cost optimization [229], resource levelling and allocation [227,230], engineering design [138], and numerous other applications [146]. Architects have been using metaheuristics to guide conceptual design for quite some time. In contrast to simply mimicking bio-inspired shapes and forms for their aesthetic attribute, the use of metaheuristics is

starting to be used in more of a hybrid manner to consider both architectural intent and specific design objectives. For instance, Agirbas [231] outlines an approach to conceptual façade design where swarm intelligence is used to generate non-Euclidean geometry which is also optimized for daylighting. Such approaches have also been shown to be solved through more specific heuristic algorithms, such as the approach in Pantazis and Gerber [232].

Despite optimization approaches being comprehensively applied to the conceptual design stage in building façade and architectural panel systems, there are far fewer applications tailored to optimizing the manufacturing process. With the modern capabilities of BIM, a nascent area of automation is focused on generating shop drawings to aid in the manufacturing and assembly process. Many of these applications are heuristic in nature but do not require performing any optimization. Yet, given the complexity of producing an optimal number of 3D isometric views without providing duplicate or missing information to manufacturers, Deng et al. [233] developed an algorithm based on graph-theory to producing optimal drawing views for panel manufacturing. Design for Manufacture and Assembly (DfMA) is another nascent BIM-enabled practice across industrialized construction and manufacturing, which is predicated on balancing ease of manufacturing with ease of assembling a component. While DfMA has been applied to the case of architectural panels, it is often used as constraints in optimization approaches, rather than as the sole objective focus of such methods [170,234]. Recently, a metaheuristic algorithm was developed to determine the optimal placement of robots for picking and placing panels on-site (i.e., the assembly aspect of DfMA). This method, developed by Ali et al. [235] solves the MOP of balancing time, reachability difficulty and collision avoidance of a robot while also populating optimal panel geometry configurations. While such an advanced framework has particular relevance for 3D printed façade systems, it does not address conventionally produced panels. One of the few studies that specifically focus on manufacturing optimization was done by Lee et al. [236], who evaluated more than 1000 unique curtain wall designs in order to establish a heuristic procedure for reducing aluminum material use by up to 40%. Yet this study is still situated primarily within the design stage, with only some manufacturing-based criteria being explored and considered. No known optimization methods have been applied specifically to optimize the manufacturing of architectural panels.

5.3 Applications of the 2D Cutting Stock Problem

The 2D cutting stock problem is a COP focused on optimizing the fit of 2D shapes within a rectangular sheet and has been addressed in a number of industrial applications including sheet metal cutting, shipbuilding, HVAC ductwork, structural steel plates, furniture parts, automotive bodywork, and bespoke glass panels [237-239]. Various techniques have been developed to address specific variants of this COP.

When constrained to just 1D optimization (or when a low number of rectangular objects are considered), this COP can be addressed using exact algorithms [22,240,241]. However, as the complexity of the problem increases (e.g., consideration of irregular shapes, non-convex geometry, or constraints such as guillotine cutting), metaheuristics quickly become much more favourable [237,242].

The 2D cutting stock problem is particularly relevant for the manufacturing of architectural panels (thin-metal in particular), yet no methods have addressed this problem using panel topology optimization. This particular application is unique from other industrial applications since the process of unfolding panels (i.e., converting the three-dimensional panel into a two-dimensional cut shape) involves selectively unjoining certain edges on the three-dimensional geometry, resulting in a large combination of possible nested shapes. A computer numerical controlled (CNC) router machine cuts panels according to the 2D unfolded geometry, after which, the panels are folded and welded along seams to produce the 3D final geometry. During fabrication, it is necessary to optimize the toolpath distance for the CNC router (i.e., the total travel distance the end-effector of the machine takes to cut and create bend-lines on a panel) in order to minimize fabrication time, as well as minimize the amount of waste that occurs when nesting panels. This problem is a compounded combinatorial problem since each panel can comprise a set of combinations, and each nest configuration can comprise a set of discrete combinations. Despite the existence of panel nesting software, they are predicated on performing semi-automated nesting and are subject to predefined 2D panel drawings [243]. In other words, the panel topology must be predefined in such software, which impedes the degree of material savings that can be achieved.

5.4 Knowledge Gaps

After review of the relevant literature (Table 6), the following knowledge gaps can be identified:

- Few studies compare the performance of exact and approximate optimization for COPs.
- Topology optimization has not been explored in architectural panel manufacturing, while it has in several other construction and manufacturing applications [244].
- Metaheuristics have been applied to a range of complex COPs in construction, yet none have been directed towards the process of unfolding and nesting architectural panels.
- Existing panel nesting approaches only perform optimization on pre-determined 2D panel geometry, which does not allow for topological variants of panels.

This chapter aims to address these gaps by developing combinatorial optimization algorithms that can configure panel topology specifically to reduce waste during fabrication without modifying the architectural intent of the panel layout on the building.

Table 7: Relevant studies that detail procedures for solving optimization problems related to the proposed research

Relevant Studies	Study Purpose and Relevance	Project Stage	COP, MOP, or Both	Solution Approach[a]		
				E	H	M
Industrialized construction and manufacturing						
[244]	A modified traveling salesman problem for topology optimization of prefabricated steel frames to minimize weight.	Design[b]	COP			●
[245]	Comparative evaluation of optimization algorithms for batch production of sheet-metal for prefabricated HVAC systems.	Manufacturing	Both	●		●
[246]	Sequential optimization approach using simulated annealing for nesting and cutting sequence in laser cutting	Manufacturing	COP			●
[241]	2D strip packing of rectangular industrial objects with branch-and-bound algorithm.	Manufacturing	COP	●		
[238]	2D cutting stock of arbitrarily shaped objects using a heuristic algorithm	Manufacturing	COP		●	
[242]	2D strip packing of irregular industrial objects using particle swarm algorithm.	Manufacturing	COP			●
[240]	Comparing methods for 1D cutting stock of construction objects (e.g., rebar).	Manufacturing	COP	●		●
[22]	1D and 2D cutting stock of wood components for prefabricated houses.	Manufacturing	COP	●		
[165]	Mixed-integer linear programming model to optimize the production sequencing and resource utilization of molds for prefabricated building components.	Manufacturing	COP	●		
[178]	Lean approach for prefabricated panel stacking, sequencing, and locating at site.	Transportation	Both	●		
[181]	Heuristic algorithm to find the best arrangement of modules with non-negligible deviations to minimize overall assembly dimension.	Assembly[b]	COP		●	
Building façade and architectural panel systems						
[232]	Multi-agent conceptual design to evaluate façade alternatives.	Design	MOP		●	
[225]	Model for optimizing façade design based on manufacturing knowledge and technical performance.	Design	MOP		●	●
[170]	Optimization model for minimizing fabrication cost of prefabricated panels based on architectural design intent, structural analysis, and fabrication processes.	Design	Both			●
[231]	Daylight optimization of façade design using particle swarm algorithm.	Design	COP			●
[247]	Dimensional optimization of façade panels for daylighting and energy performance.	Design	Both			●
[236]	Optimizing layouts and specifications of curtain wall extrusions to reduce waste.	Design, Manufacturing	COP			●
[234]	Façade cladding optimization based on design for manufacture and assembly.	Design, Manufacturing	MOP		●	
[233]	Automatic generation of fabrication drawings for façade mullions and transoms using a graph-theory based algorithm.	Manufacturing, Assembly	COP		●	
[235]	Optimized location of robot for façade picking and placing during assembly.	Assembly	Both			●

[a] solution approaches categorized as exact (E), heuristic (H), or metaheuristic (M)

[b] relevant research in design and assembly of industrialized construction systems is not exhaustive, but presented here to provide context for proposed research

5.5 Methodology for Topology Optimization of Architectural Panels

The manufacturing process for thin-metal panels in architectural cladding systems starts with a digital file containing unfolded 2D panel geometry. To properly unfold a panel, select edges must be unjoined in the 3D geometry. Depending on the combination of edges that are unjoined, the resulting 2D shapes can incur a range of material efficiencies. The file containing 2D geometry is often produced by a construction design firm, which digitally unfolds 3D panels into 2D shapes with bend lines and router cut lines. These unfolded shapes are then nested on a piece of rectangular coil (e.g., aluminum for ACM panels). The configuration of these nested shapes is constrained by a maximum coil width dimension, and a maximum coil length dimension, within which the unfolded panel(s) must fit within in order to be made from a single piece of aluminum (note: depending on the architectural intent, some panels may need to be produced from multiple pieces of aluminum, however such a case is not considered in this work). Depending on a given nest configuration, material waste is calculated by subtracting the overall area of a rectangular coil and the combined areas of nested panels. While the process of unfolding panels can be efficient to do manually for small sets of simple geometry, for large and or complex panel geometry, an algorithmic approach can bring significant time savings. Furthermore, by codifying the process of 2D panel geometry nesting, a file-to-factory system can be both automated and optimized in order to reduce material waste. The current process in the industry is heuristic, relying on the intuition of designers, however, combinatorial optimization algorithms can be used to optimize this process, as outlined in Figure 25.

The proposed approach starts with 3D panel geometry which is converted into 2D unfolded geometry via a panel unfolding algorithm. The details for this algorithm are presented in the following section. Depending on the shape of the resulting unfolded geometry, a bounding rectangle can be used (if material waste for such conversion is minimal) which helps to reduce the computational complexity of nesting. Such conversion is generally possible for rectangular panels. However, if material waste for this convex geometry conversion is non-negligible, then top-performing geometry variants can be stored and evaluated further in panel nesting. Once all geometry is converted into 2D shapes, a panel nesting algorithm is used. This metaheuristic algorithm is predicated on genes or variables for panel sequence permutations, orthogonal rotations (only orthogonal rotations are considered to reduce computational complexity), and panel geometry variants as applicable. The output of this algorithm is optimized panel topology, defining which panel edges must be unjoined, and panel nest configurations which can be

directly imported into a CNC machine. Such a process reduces waste during fabrication and can also minimize the toolpath distance of a CNC, which is a secondary objective.

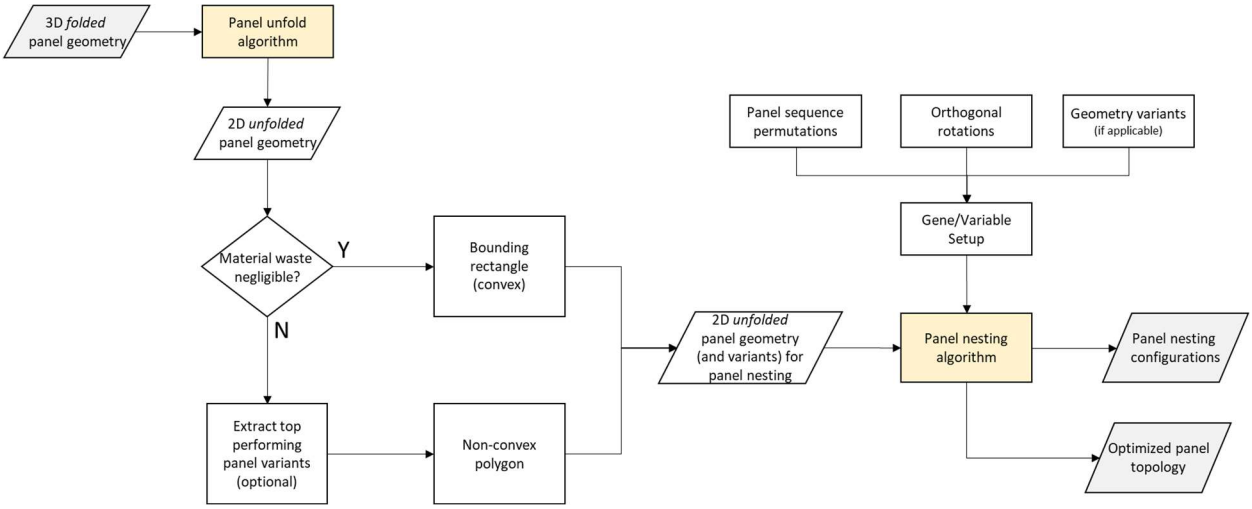

Figure 26: Workflow for topology optimization of architectural panels using a panel unfolding algorithm and a modified panel nesting algorithm.

5.6 Panel Unfolding Algorithm

The development of this algorithm was conceptually presented by the author in [248], and is expanded upon in this chapter. To demonstrate different combinations for unjoining panel edges, Figure 26 shows a simple panel with 13 panel edges that can be unjoined. Four different unfolded shapes demonstrate a range in material efficiencies ranging from 6660 mm x 1367 mm (least efficient) to 1292 mm x 2239 mm (most efficient). Furthermore, each shape has a range in toolpath distance (i.e., how far the CNC must move in order to create cut lines and bend lines) between 15.20 m (most efficient) to 19.75 m (least efficient). In this example, material efficiency and toolpath efficiency provide the same order classification for the 2D shapes considered, however this may not always be the case across all possible unfolded shape combinations. The total number of unfold combinations (U) can be calculated through the summation of the binomial coefficient:

$$U = \sum_{k=1}^{n} {}_nC_k = \sum_{k=1}^{n} \frac{{}_nP_k}{k!} = \sum_{k=1}^{n} \frac{n!}{k!\,(n-k)!}$$

Eqn. 7

where n is the number of panel edges, k is an iterator over n, C is the number of combinations, and P is the number of permutations. For 13 panel edges, there are 8191 different unfold combinations for this

panel. Rather than determining which class of computational complexity this problem belongs to (i.e., NP-hard, NP-complete, etc.), this research jointly develops an exact and approximate solution for panel unfolding and subsequently evaluates the most effective approach based on the number of edges for a given panel.

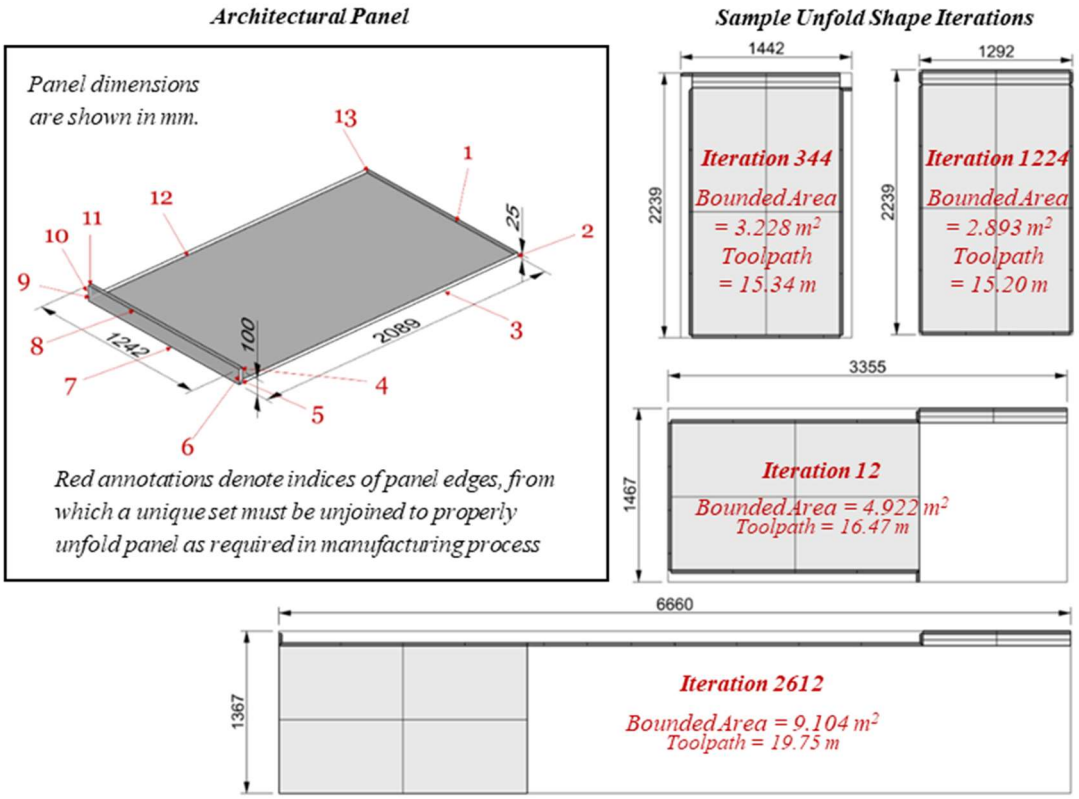

Figure 27: Demonstration of four unfolded panel geometries (ranging in material efficiency and toolpath distance) that can be used to generate the same 3D panel geometry.

There is not a universal set of rules to follow in order to properly unjoin panel edges. However, there are a unique set of constraints that cannot be violated in order to produce unfolded shapes that can be properly cut by a CNC router: the unfolded shape cannot contain self-intersecting curves, the unfolded shape must fit within the coil, and the result of unjoining edges cannot sever a panel into two separate pieces. When these constraints cannot be respected for a given panel – there are indeed cases where this occurs depending on geometric complexity – a designer must use experience and consultation with the architect to determine how to best configure panel topology and geometry to ensure the panels can be properly fabricated. The optimization goals for this process are to minimize the bounding area of an unfolded panel (for nesting purposes), and to minimize the toolpath distance (i.e., the length of router and cut paths for the CNC).

To develop an algorithm that automatically unfolds panels, it is helpful to determine whether this multi-objective COP is NP-complete or NP-hard. Since this is not a trivial task, a simpler approach is to develop an enumerative algorithm that searches all possible combinations, and a metaheuristic algorithm that searches the solution space in an efficient (yet non-exhaustive) manner. By experimenting with different panels of increasing numbers of edges, it is possible to evaluate which approach is more pragmatic based on the complexity of a given panel. The first algorithm provides an exact approach to unfolding panels. First, it computes all permutations of unfolding combinations for the specific number of panel edges according to Eqn. 7. Based on the coil dimension constraints (width and length), it unfolds all possible combinations, returning the set of panel edge indices which have the smallest bounding rectangle area. Since multiple combinations can have the same bounding area, toolpath distance is also computed, and used to sort the remaining unfold panel geometry. Finally, the resulting unfolded shape with the smallest toolpath distance is returned. A pseudocode for this algorithm is shown below:

Algorithm 2. Enumerative algorithm for determining optimal panel unfolding

```
Inputs: x_blank = maximum coil width dimension
y_blank = maximum coil length dimension
Panel → accessed as a B-rep object with topology defined by curves, faces and vertices
Variables: e() = indices of interior edges (shared between two surfaces on panel)
n[] = unique set of edge index combinations for e() [Eqn. 7]
t() = toolpath length for interior (i.e., router lines) and exterior (i.e., cut lines) for unfolded panel
c() = boolean return for constraints violations
01      FOR each panel
02        OBTAIN all panel edges e()
03        FOR i = 1 to n[].length
04          EXECUTE command {unjoin edges e(i)}
05          EXECUTE command {unfold panel}
06          r(i) = bounding rectangle on unfolded shape
07          x(i) = r(i) max x dimension #blank size x dim
08          y(i) = r(i) max y dimension #blank size y dim
09          t(i) = sum of exterior and interior edges
10          c(i) = boolean result of self-intersecting lines or multiple unfold shapes occurance
11          if x(i) <= x_blank && y(i) <= y_blank && c(i) == FALSE
12            area(i) = x(i)*y(i)
13          else
14            area(i) = 'null'
15        i_optimum() = RETURN indices of min in area()
16        t_optimum() = RETURN toolpath for i_optimum()
17      END LOOP
18      SORT n[i_optimum] by t_optimum()
19      RETURN n[i_optimum].firstindex
20      EXECUTE command {unjoin edges e(i_optimum)}
21      EXECUTE command {unfold panel}
22      END
```

The second algorithm has a similar setup to the first algorithm, but instead of computing all possible combinations of panel edges, binary variables or genes are used for each panel edge. A multi-criteria fitness function, *s* is then built, which accounts for constraint violations, bounding area and toolpath distance of unfold shapes:

$$s_{unfold} = {A_{unfold}}^{\alpha} * {t_{path}}^{\beta} * [1 + bool(sInt) + nU + bool(dimV)]$$

Eqn. 8

where A_{unfold} is the area of the unfolded shape, α is a scaling parameter for A_{unfold}, t_{path} is the toolpath distance, β is a scaling parameter for t_{path}, *bool(sInt)* is the boolean occurrence of whether the unfolded shape has self-intersections (0: no occurrence, 1: occurrence), *nU* is the number of unfold shapes and *bool(dimV)* is the boolean occurrence of whether the coil width or length are violated. The fitness function is structured as a metric (since area and toolpath distance are multiplied), where the occurrence of constraint violations scale the function in a linear manner. In addition, scaling parameters (α, β) can be configured to ensure the fitness function gives priority to unfold area over toolpath distance since different units can be used which affects the relative magnitude between unfold area and toolpath variables[15]. The method for solving this fitness function could be approached through a range of metaheuristics, however this work considers genetic algorithm and simulated annealing. These two metaheuristics are chosen, because they are the most popular methods for solving hard COPs based on their unique approaches (i.e., population-based and trajectory-based). A pseudocode for an algorithm based on simulated annealing is shown below:

[15] *It should be noted that these parameters are currently heuristically defined, but future research could investigate how to more objectively define these parameters in order to give preference to unfold area vs. toolpath distance.*

Algorithm 3. Metaheuristic (Simulated Annealing) algorithm for optimal panel unfolding

Inputs: Panel → accessed as a B-rep object with topology defined by curves, faces and vertices
maxIter = maximum number of iterations
Initialization: s = random starting point
s_best = best performing solution
t = temperature of fitness function
nU = number of resulting unjoined shapes
sInt = occurrence of self-intersection event on unfolded shape
dimV = dimensional constraint violations of width or length of coil
A = bounding area of unfolded shape
tPath = toolpath distance
α = scaling parameter for unfold area
β = scaling parameter for toolpath distance

```
WHILE t > minTemperature DO
    i = 0
    WHILE i < maxIter do
        s' = A(i)^(α) * t_path(i)^(β) * [1 + bool(sInt(i)) + nU(i) + bool(dimV(i))]   Eqn. 3
        Δ = f(s') – f(s)
        IF Δ < 0 THEN
            s_best = s'
         ELSE IF rand(0,1) < e^(-Δ/t) THEN
            s = s'
        i = i +1
    t = t(1-α)
RETURN s_best
EXECUTE command {unjoin edges based on s_best}
EXECUTE command {unfold panel}
END
```

The result of running the algorithms presented here for unfolding panels is an optimal combination of panel edges to unjoin along with a 2D unfolded panel shape. As outlined in Figure 25, depending on the degree of material waste associated with a bounding rectangle, multiple unfolded shapes can also be fed into the panel nesting algorithm, as outlined next.

5.7 Panel nesting algorithm (modified 2D cutting stock problem)

While cutting and packing problems have been associated with various names in literature such as trim loss, cutting, bin packing, strip packing, nesting, knapsack, etc., the problem formulated for nesting of prefabricated architectural panels is a *2D* cutting stock problem according to the comprehensive typologies outlined by [249] and [144]. When the shapes to be cut are overtly simple (i.e., rectangular) and low in quantity, this problem is NP-complete [242] and can be suitably solved using an exact algorithm. However, when the shapes become more complex (e.g., irregular, non-convex polygonal, etc.) or when the number of items increases, the problem quickly becomes NP-hard, requiring approximate solving techniques [250]. Accordingly, for the purpose of this chapter, an approximate metaheuristic

algorithm is developed in order to handle cases where prefabricated panels are geometrically complex and nested in high quantity configurations.

The formulation of the panel nesting algorithm starts as a 2D non-convex cutting problem [251], which can be reduced to a convex bounding rectangular cutting problem when material waste is expected to be minimal. In projects where the geometry of panels is strongly rectilinear with a low degree of bespoke architecture, this assumption is valid. However, when the geometry becomes more complex (e.g., multi-planar, non-orthogonal angles, etc.), it may be necessary to frame this nesting problem as a non-convex 2D cutting problem to minimize waste. The purpose of enacting the convex geometry assumption, when possible, is to reduce the computational complexity during nesting. The other key consideration for such an algorithm is whether to incorporate the guillotine constraint. This constraint assumes that material cuts must span the entire coil dimension (e.g., large brake presses cut a sheet into two separate pieces). Since thin-metal panels are typically cut from a CNC router, this assumption is unnecessary to embed into the algorithm. This algorithm has the following two constraints: (1) items must fit within a given rectangular coil, and (2) all items must not overlap each other. The algorithm has the same objective goals as the unfolding panel algorithm (minimize waste and minimize toolpath distance), except in this case, the objectives are applied to sets of coils.

This research employs a bottom-left placement strategy, where panels start at the top-right corner of a coil, and are then moved down as far as possible, and as far left as possible. In addition, each unfolded shape is allowed to rotate orthogonally in 90° increments; more discretized rotations are not considered in order to reduce the computational complexity. Determination of panel sequence is based on a permutation of panels where for a given sequence if a panel no longer fits on a coil, it is automatically placed on a new coil. This is repeated until all panels are placed on coils. The total number of panel nest configurations, N is computed as:

$$N = p! * k * \sum_{m=1}^{p} j_m$$

Eqn. 9

where p is the number of panels, k is the number of discretized rotations a panel can experience (i.e., 90° rotations would have a k value of 4), and j is the number of unfold variants for each panel. It should be noted that the value of j is determined by inspecting the initial results of the panel unfolding algorithm. If the unfolded shape can be represented by a bounding rectangle, then waste is minimal, and a single variant can be used for nesting (i.e., j = 1). However, if a bounding rectangle generates non-negligible

panel waste, then the user should inspect the top panel unfold variants and use tacit knowledge to select the possible number of viable panel variants to include in the nesting process (i.e., j > 1). Similar to the metaheuristic solver for panel unfolding, this problem is solved using both genetic algorithm and simulated annealing. A multi-criteria fitness function is formulated as:

$$s_{nest} = (C - resC - p)^2 * t_{path} * [1 + bool(o) + bool(dimV)]$$

Eqn. 10

where *C* is equal to the cumulative area of rectangular coils required, *resC* is the usable residual area of the coils, measured by the full-coil-width rectangles that can be extracted and used for subsequent panel creation, *p* is the combined area of all nested panels, *bool(o)* is the Boolean occurrence of overlapping panels, and *bool(dimV)* is the Boolean occurrence of any dimensional constraint violations of the coil (e.g., width or length). In this fitness function, the area-based terms are squared in order to weight the objective more towards minimizing the waste over optimizing toolpath. A pseudocode for the simulated annealing algorithm is shown below:

Algorithm 4. Metaheuristic (Simulated Annealing) algorithm for optimal panel nesting

Inputs: Panels → accessed as a B-rep objects with topology defined by curves, faces and vertices
maxIter = maximum number of iterations
Initialization: s = random starting point
s_best = best performing solution
t = temperature of fitness function
sInt = occurance of self-intersection event on nest configuration
dimV = dimensional constraint violations of width or length of coil
A = bounding area of unfolded shape
tPath = toolpath distance

```
01    WHILE t > minTemperature DO
02        i = 0
03        WHILE i < maxIter do
04            s' = A(i) * t_path(i) * [1 + bool(sInt(i)) + nU(i) + bool(dimV(i))]   (Eqn. 10)
05            Δ = f(s') – f(s)
06            IF Δ < 0 THEN
07                s_best = s'
08             ELSE IF rand(0,1) < e^-Δ/t THEN
09                s = s'
10            i = i +1
11        t = t(1-α)
12    RETURN s_best
13    EXECUTE command {unjoin edges based on s_best}
14    EXECUTE command {unfold panel}
15    END
```

5.8 Case Study

This case study demonstrates the workflow for optimizing panel topology on a set of exterior aluminum clad panels on a residential construction project. While these types of panels are used on a wide range of projects, residential and commercial construction tend to have more complex geometry than industrial buildings (which are often more uniform and repetitive in nature). Residential projects are unique from large commercial projects in that small batches of panels are designed and fabricated. On small residential buildings, a common architectural feature is the wrapping of panels around fenestration systems (e.g., windows, curtain walls, doors, etc.). Figure 27 shows a condition where panels wrap around a large rough opening for a set of windows. To mimic such configuration, a comparable panel layout was generated using typical panel sizes. The author has previously worked as a computational design specialist for a large multi-national architectural panel contractor based in Toronto, Ontario. This experience was drawn upon for configuring typical panel sizes, reveal gaps, and mounting hardware requirements (e.g., panels must have *returns* of a set size to mount clipping extrusions). This panel layout is shown as an isometric view in Figure 28, with eight different panel types. In addition, a sample panel (Type C) from this layout has been isolated for which the edge topology is shown, denoting the unique edges that adjoin two surfaces. A combination of these edges must be unjoined on the 3D panel geometry in order to manufacture in a 2D router process. Algorithms in this case study were developed in Rhinoceros® software using the visual programming interface Grasshopper® (Grasshopper scripts are provided in Appendix A). This is a common software among construction design firms, where panel geometry is in boundary representation (B-rep) or non-uniform rational basis spline (NURBS) and can be directly accessed and computed in a visual programming algorithm.

Figure 28: Recent Residential Construction Projects in Toronto, Ontario with Aluminum Exterior Panel Systems (photos obtained from Google Maps)

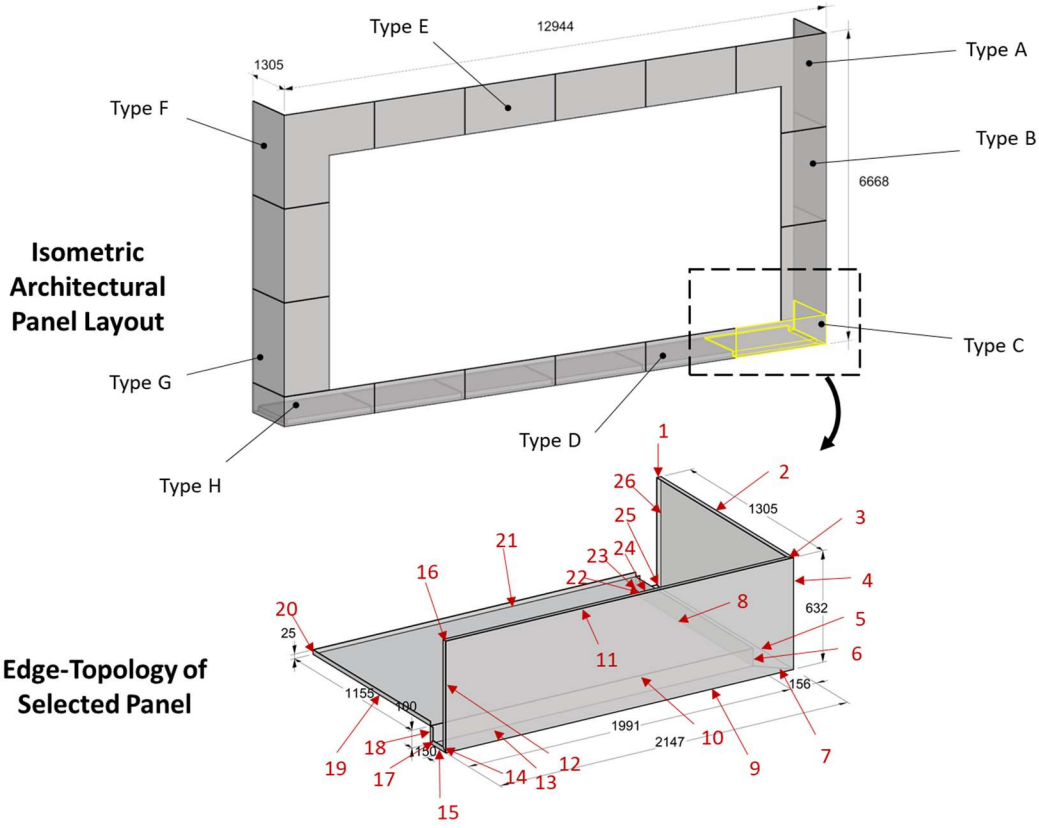

Red annotated arrows denote panel edges that adjoin two surfaces. All dimensions in mm.

Figure 29: Isometric panel layout and edge-topology structure for a panel Type C

5.9 Panel Unfolding

In the first set of experiments, five panel types were unfolded using three different algorithms: an enumerative algorithm that exhaustively generates all panel unfold results, a simulated annealing algorithm and a genetic algorithm that performs approximate searching. The results for this set of experiments is shown in Figure 29. The enumerative algorithm was programmed using a custom Python script which computes combinations in a loop sequence using the *itertools* module and the *combinations()* function. The simulated annealing and genetic algorithm solvers were programmed using binary variables/genes for the number of panel edges and the *Galapagos Evolutionary Solver* block in Grasshopper® [252]. For reporting computational performance, the machine employed in this research has an Intel Core i7-8650U CPU.

Each of the panel types examined in this experiment range in computational complexity from 8 panel edges to 27 panel edges (255 to 134,217,727 panel unfold combinations, respectively). Since simulated annealing and genetic algorithm perform stochastic searching, a series of 5 iterations were computed for each in order to quantify the average computational performance and variance of results. For this experiment, identification of the optimal panel unfold variants was achieved based on execution of the enumerative algorithm. As such, the fitness function values corresponding to these optimal panel unfold variants were used to evaluate the relative performance between the simulated annealing and the genetic algorithm methods (in terms of time required to achieve these values). As shown, the enumerative algorithm was superior when the number of panel edges is less than 13, however simulated annealing was superior when the number of panel edges exceeds this value. Overall, simulated annealing performed better than the genetic algorithm, both in terms of lower variance and in terms of temporal performance. For the simplest panel (Type E) the enumerative algorithm computed all unfolded shapes in only 2s, while the simulated annealing algorithm required an average of 17.6s and the genetic algorithm required an average of 25.2s. This was the only set of experiments (Type E) where the variance of simulated annealing was greater than the genetic algorithm. However, given the relative speed of both algorithms (i.e., both computed results in under 30s), the variance is not as important for this panel type. Where the large differences between the algorithms appear is for larger panel edge combinations. For panel Type C, the enumerative algorithm was unable to generate all possible combinations. After 24h, the solver had to be abandoned[16], at which point the result of computing the binomial coefficient (Eqn. 7) was only on

[16] *Note that while a range of potential stopping criterion can be employed, a pragmatic time limit was used in this research.*

iteration 13 of 27. However, using approximate optimization, simulated annealing generated a set of optimal results in an average of 707.6s and the genetic algorithm produced similar results in an average of 3,956s.

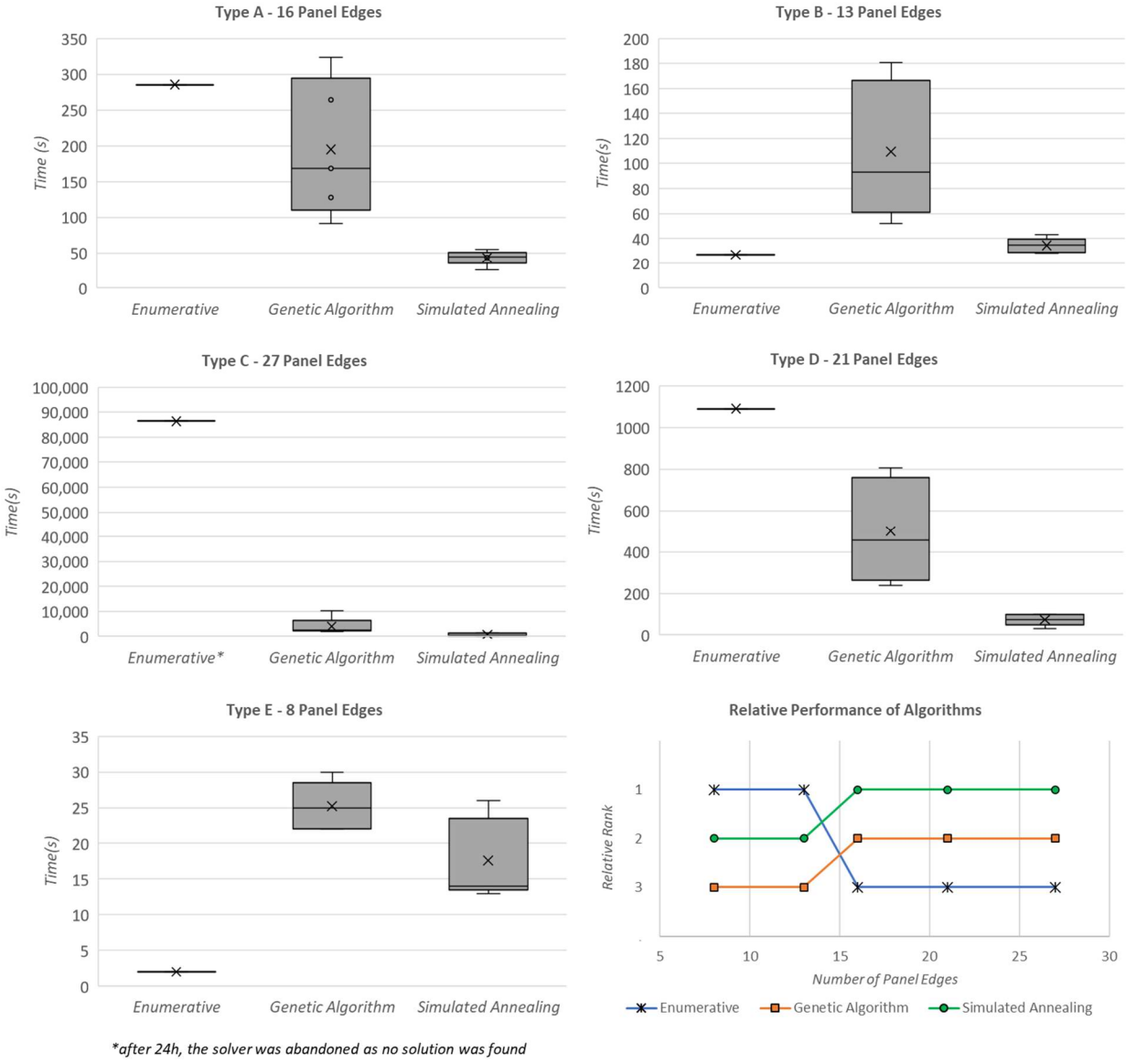

Figure 30: Relative performance and computational time required to unfold panel Types A to E using each algorithmic approach (enumerative, simulated annealing and genetic algorithm).

5.10 Panel Nesting

Similar to the first set of experiments, the panel nesting algorithm was developed in Grasshopper® and solved using the *Galapagos* solver. The bottom-left placement strategy was performed using the

OpenNest plugin developed by Petras Vestartas. Two experiments were carried out using this algorithm: the first quantifies the material efficiency of considering both rotational variations and unfold panel variants on a small sample, and the second quantifies the performance of this algorithm compared to the current state of the art (i.e., no unfold variants considered) for all panels in the layout shown in Figure 28. The first experiment for the panel nesting algorithm was performed on the same panel types used in the panel unfolding experiment. Rectangular coils with dimensions 10' by 40' (3,048 mm by 12,192 mm) were used to generate panel nest configurations. Five panel variants were produced for Type C, since these geometries had non-negligible waste when placed in a bounding rectangle (i.e., the convex geometry assumption was deemed not acceptable). The total number of possible nest configurations according to Eqn. 10 is 2,400. In this case study, both simulated annealing (Algorithm 4) and the genetic algorithm were used to compute nest configurations. Two different nest configurations were produced to highlight the performance of this algorithm compared to a non-optimal nest configuration (Figure 30). The non-optimal configuration does not include rotational variations or unfold panel variants, whereas the optimal configuration considers both. The difference in these two configurations is a net material savings of 9.50 m^2 which equates to 24% of total coil material. Furthermore, two coils are required for the non-optimal configuration, compared to only one for the optimal configuration. The relative performance of simulated annealing vs. genetic algorithm in this experiment was comparable since both produced the same optimal nest configuration in under 120s.

In a second experiment, all sixteen panels shown on the layout in Figure 28 were processed through the new nest algorithm. In this case, the total number of possible nest configurations according to Eqn. 10 is equal to $2.09x10^{15}$. In this experiment, both simulated annealing and genetic algorithm produced nest configurations in under 600s; simulated annealing slightly edging out the genetic algorithm in terms of nesting efficiency (residual useful material of 4859.88 mm by 3048 mm for simulated annealing, compared to 4655.56 mm by 3048 mm for the genetic algorithm). The total area of panels to be cut in this case is equal to 70.59 m^2. Assuming that a minimum residual coil length of 1000 mm is required for subsequent panel cutting, it is possible to quantify the material waste savings of the proposed algorithm compared to a random configuration and the best configuration from the current state-of-the-art method. Each of these configurations is shown in Figure 31. Since the current state-of-the-art methods for panel nesting (i.e., the software installed on CNC routers) is developed in proprietary software, it is unknown what the precise method employed is for optimizing the nesting process. However, this research considers the best possible nest configuration (through metaheuristics) that excludes the unfold variants (i.e., all panel shapes predetermined prior to nesting). The random configuration produces 44.09 m^2 of waste, requires four coils and has one residual piece of material that can be reused to cut additional panels. The

state-of-the-art method produces 29.38 m^2 of waste and has potentially two residual pieces that can be used to cut additional panels. Finally, the proposed algorithm produces only 26.08 m^2 of waste and has a single residual piece of coil that can be used to cut additional panels. Compared to the current state-of-the-art method, the proposed algorithm produces 11% less waste.

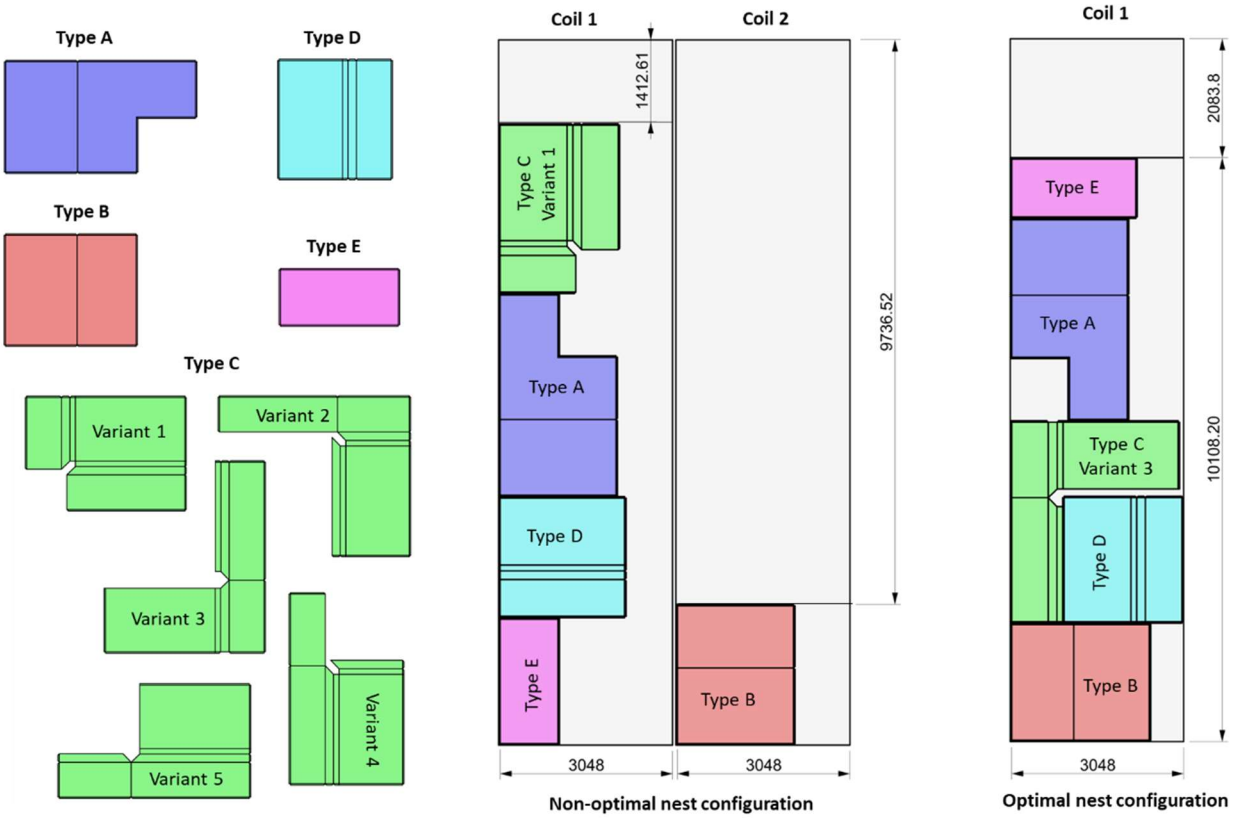

Figure 31: Panel unfold variants for Types A-E and two distinct nest configurations for the first experiment (panel colors shown for visualization purposes, all dimensions in mm).

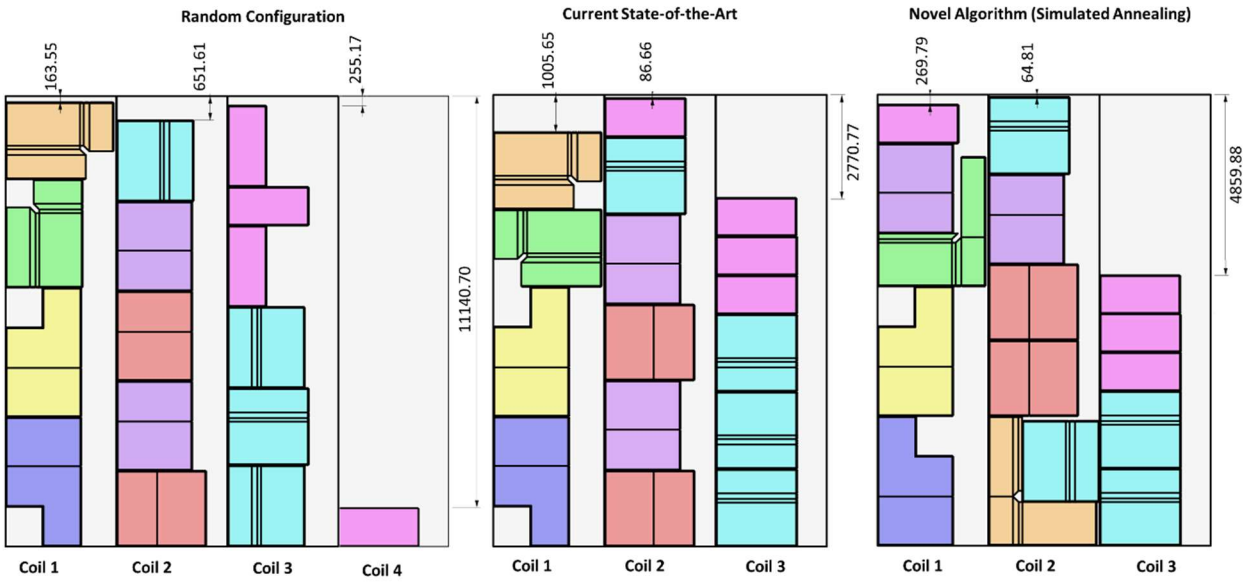

Figure 32: Comparison of configurations produced for the second experiment through random trial, current state-of-the-art, and the proposed algorithm (panel colours shown for visualization purposes, all dimensions in mm).

5.11 Discussion

The result of running each of the developed algorithms for panel unfolding shows that either enumerative optimization or simulated annealing optimization is preferable under the parameters explored. When panel geometry is simple (i.e., number of panel edges is less than 13, or total combinations under 8191) enumerative optimization is shown to be preferable. Above this threshold, simulated annealing is preferable. While one could argue that simulated annealing should be used for all panel unfolding applications (since enumerative optimization is only better for a small number of panels), most industrialized buildings comprise primarily simple panels. In such applications, enumerative optimization can provide sizeable time savings. For instance, unfolding 1000 panels with 8 edges could be performed in 2,000s (~0.5h) using enumerative optimization compared to 17,600s (~5h) for simulated annealing optimization. Furthermore, enumerative optimization guarantees the optimal unfold result is obtained, whereas there is a risk that sub-optimal results are generated using simulated annealing.

The modified 2D cutting stock algorithm for panel nesting is shown to perform optimally when considering panel rotational variations and unfold variants. This algorithm was not compared to an enumerative approach since existing research into the 2D cutting stock problem for non-convex geometry validates the efficacy of approximate (i.e., metaheuristic) techniques [242]. In addition, it is well regarded that the 2D cutting stock problem with non-convex geometry is an NP-hard COP, which is why the

proposed algorithm was derived for metaheuristic optimization. Both genetic algorithm and simulated annealing were explored in this chapter for the multi-criteria fitness functions, and it was found in both algorithms that simulated annealing performed better, both in terms of processing time required and optimization of the fitness functions. It should be noted that the purpose of this work was not to exhaustively or comprehensively explore all possible metaheuristic techniques to find the optimal approach. Rather, this chapter categorically compares and postulates efficient algorithms that can optimize architectural topology in a manner suitable for automation within a file-to-factory system.

It is important to highlight the factors that affect the expected performance of the algorithms presented in this chapter. While material waste reduction of 11% was achieved, this is based on the quantity and geometric properties of panel unfold variants that existed. Since the specific optimization methods of the current state-of-the-art software in practice are not divulged, this work cannot make any inferences of the relative performance of the proposed nesting algorithm. However, it is conclusively shown that by considering panel unfold variants that sizeable material waste reductions can be achieved. As the quantity and geometric diversity of unfold variants increases, so will the expected material savings.

Finally, it should also be noted that a key simplification made in this work was excluding the process of accounting for bend-allowances when unfolding panels. When folding thin-metal, bend allowances are important contributing factors to 2D cut shape and the final 3D folded panel. For pragmatic reasons, such allowance is not accounted for, but should be addressed in future work.

5.12 Conclusion

This chapter presents a series of algorithms for geometric optimization of 2D panels to minimize material use during fabrication. While the domain considered for the functional demonstration was architectural panels, this research has relevance to industrialized building construction since the use of 2D panelized assemblies is quite common in industrialized construction. Compared to existing approaches that perform 1D and 2D geometric optimization for the cutting stock problem, the algorithms developed in this research can be used for more complex geometry. By comparing the use of approximate algorithms such as a genetic algorithm and simulated annealing algorithm, it is possible to quantify their pragmatism over exact enumerative approaches (which many of the currently available methods tend to employ). The result of such comparisons equates to significant time savings while still achieving upwards of 11% material waste reduction. This can also equate to significant cost savings for the industry.

Chapter 6: Evaluating Geometric Digital Twinning Methods for Industrialized Building Construction: Towards Automated Parametric BIM Updating

This chapter presents developments made by the author that are in an article that has been published in the International Journal of Construction Management [253]:

- **Rausch, C.,** Lu, R., Talebi, S., Haas, C. (2021). Deploying 3D Scanning Based Geometric Digital Twins during Fabrication and Assembly in Offsite Manufacturing. International Journal of Construction Management. Accepted Feb 2021.

While the previous two chapters focused on various types of geometric optimization, this chapter pivots towards the development of semantic enrichment algorithms. Based on the review of the literature presented in the background section, the topic of managing a BIM during fabrication and assembly as well as preparing a final as-built BIM are intrinsically supported and aided through semantic enrichment processes. This chapter explores the concept of maintaining a "geometric digital twin" (gDT) for the dual purpose of verifying dimensional compliance during fabrication and assembly as well as exploring mechanisms for as-built BIM creation. This chapter compares three distinct gDT approaches for use during fabrication and assembly in IBC: (1) a scan-vs-BIM approach, (2) a scan-to-BIM approach and (3) a parametric BIM updating approach. Results from an industrialized building project reveal that scan-vs-BIM is the most accurate approach, parametric BIM updating produces the most semantically rich gDT, and scan-to-BIM is a middle-tier option balancing accuracy for semantic enrichment. This chapter lays the foundation for the new algorithms developed in Chapter 7, which automatically update BIMs using parameterization as a way of achieving semantic enrichment.

6.1 Introduction

As the complexity of projects utilizing IBC increases, so does the need and reliance on BIM for proper fabrication and assembly control. A previous survey found that the most likely IBC projects to utilize and benefit from BIM were high-rise buildings and industrial facilities due to the complexity of designing and constructing vast quantities of aggregated parts and the physical separation of offsite production and onsite assembly [14]. In these projects, reliance on a tightly controlled fabrication process is essential for ensuring adequate aggregation capabilities; both during offsite manufacturing and during onsite erection [16,18,254]. Increasingly, BIM and digitization techniques can be used to facilitate a more robust fabrication control process [9]. Recently, the term "digital twin" has been popularized in academia and industry, referring to the complete digital replica of physical assets, systems, and processes [255]. Digital

twins are intended to span the lifecycle of a product or system in order to simulate, collect information and create a feedback loop for continuous design, production and operation improvements [256]. The ability to create and maintain a geometric digital twin (gDT), i.e., the geometric component of a digital twin, during fabrication and assembly enables dimensional quality control to be done digitally and in a prescient manner. gDTs can be efficacious for ensuring key criteria are met such as fit-up, component aggregation, structural safety, subsystem coordination, clash avoidance, detection of excessive dimensional stackup, and building system performance compliance. In general, digital twins provide a mechanism for stakeholders to simulate, optimize and perform timely adjustments during production to correct for out-of-tolerance issues [257]. For these reasons, gDTs have great potential as quality control tools during fabrication and assembly in IBC.

This chapter demonstrates how geometric digital twinning can be employed in industrialized building construction during fabrication and assembly. Three distinct twinning approaches are examined using state of the art laser scanning based processes, namely: scan-vs-BIM, scan-to-BIM and parametric BIM updating. The current state of geometric digital twinning in construction relies on as-built data collection (e.g., laser scanning, photogrammetry, structured light imaging, etc.) and 3D geometry from a building information model (a BIM). While there is extensive literature surrounding the development and application of scan-vs-BIM and scan-to-BIM, no studies to date demonstrate or compare these approaches as part of maintaining a gDT. Furthermore, the concept of updating a BIM parametrically is only alluded to in existing research [258,259] but has not been demonstrated or evaluated in the context of maintaining the as-built status of constructed works.

6.2 Background

6.2.1 Dimensional Quality Control in IBC

The control of dimensional quality in IBC has myriad purposes including safety, constructability, aesthetics and functionality [93]. Dimensional errors are inevitable in IBC as a result of assembly complexity, human and equipment precision, and capabilities of dimensional inspection processes [260]. In structural assemblies, proper fit-up between components is critical for ensuring there are no excessive gaps between interfaces. In the event of large gaps between interfaces, joining processes such as welding can introduce secondary stresses due to eccentric loading through the connection which can cause structural safety and performance issues [16,104]. Dimensional deviations in prefabricated piping systems have a profound impact on the operation of plants and building systems [261]. As such, it is imperative to utilize robust dimensional quality control processes.

Quality inspections for IBC are conducted manually in many projects [15] using stage inspections, random controls, checklists, tape measures and contact measurement devices [16,173] which are employed during three key stages: production, post-production and onsite installation [261]. Of the main reasons for clashes between sub-systems in building construction, one of the most common causes stated by industry respondents in a recent survey was due to inconsistency between the design intent and fabrication requirements [108]. By capturing the as-built status of systems during construction and comparing it to the as-designed intent, it is possible to detect potential clashes proactively (among many other quality control items). This is predominately where the use of a geometric digital twin can be employed to address many of the current challenges faced by manual dimensional quality control practices in IBC. The next section provides a brief review of geometric digital twinning followed by current methods for creating and maintaining them in construction.

6.2.2 Geometric Digital Twins (gDTs)

While digital twins are in vogue, academia and industry are burdened by competing definitions [255,262]. The geometric digital representation of a real-life object has existed for decades despite the not-yet aligned terminology of digital twins. The role of geometry in digital twins is essential – without geometric representations, digital twins do not have a predicate for initializing or developing further [190]. As such, Lu & Brilakis [263] recently coined the term "gDT" ("g" for geometric), which is used for presenting this fundamental attribute of a digital twin. The concept of gDT is not new but is part of a comprehensive digital twin, stemming from the manufacturing industry [264].

Notwithstanding, there is no "one-size-fits-all" for gDTs that need to be developed to fit for purposes, application scenarios, and end-users. The end-users range from owners to asset managers, from architects to constructors, and from inspectors to maintenance teams. Their expectations and requirements in terms of the abstraction and accuracy of a gDT are different from one to another. For asset inventory management, smart city development, conceptualization, and design, it is not necessary to mirror every element or to digitally replicate all irregularities, textures, and physical anomalies to millimetre precision. This means the accuracy of the corresponding gDTs in this context is not overly stringent. In contrast, for operations and maintenance (O&M) and for fabrication and assembly control in IBC, accuracy as well as the level of granularity and sophistication of the resulting gDTs is more imperative [265]. While a BIM functions as a static digital representation, created to certain levels of detail during the design-construction lifecycle (e.g., BIM LOD 100, 200, 300, 350, 400 and 500), the role of a gDT is to be a dynamic geometric representation, based on BIM, but also incorporating geometric data collected during

the construction and operation of an asset (Figure 32). As such, a gDT evolves and updates as the geometric status of an asset changes over time, i.e., gDT_1, gDT_2, gDT_3, …, gDT_n.

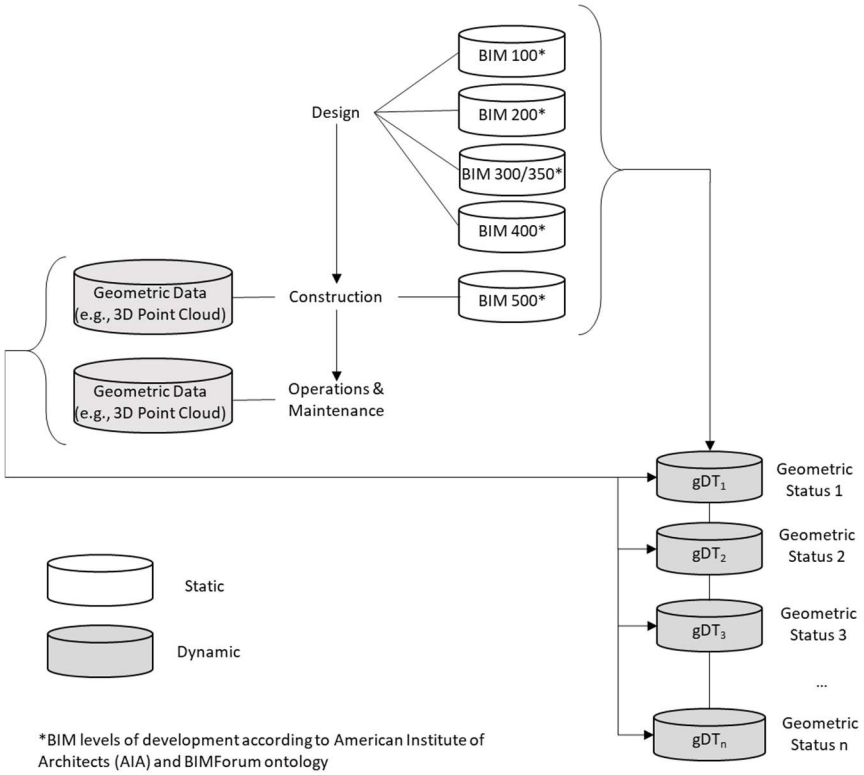

Figure 33: Context for a geometric digital twin (gDT) with respect to project stages, BIM and geometric data collected during the asset lifecycle

6.3 Mechanisms for Creating and Maintaining gDTs

There is no one single solution or platform used to create or maintain a gDT. As an interpretation process, twinning is about the procedure and methodology employed. This chapter derives three unique approaches for geometric digital twinning, which are based on collecting geometric data from laser scanning and tailored specifically towards fabrication and assembly control in IBC. These approaches are based on scan-to-BIM, scan-vs-BIM and parametric BIM updating.

6.3.1 Scan-to-BIM

With the development of 3D data acquisition technologies, scan-to-BIM has emerged as a process to collect as-built information to generate geometrically accurate BIMs using laser scanning. This process contains three main steps: (1) scanning, (2) registration, and (3) modeling. During the first two steps, the

3D as-built conditions are captured and distilled into a 3D point cloud. Object geometry modelling, object categorization (e.g., walls, doors, and pipes), and definition of object topological relationships (e.g., adjacency, connectivity, and membership) are three main activities that should be conducted during the modelling step [46,266]. Since many of these steps must be conducted manually (which is time consuming, tedious and error-prone), several research and industrial focus areas are dedicated to automating the modelling process [112,267,268]. The process of automated geometry modelling includes the following three tasks: (1) spatial correlation, which is the process of meshing the point cloud to approximate the complex geometries with polygonal meshes, (2) object recognition, which is the process of recognizing distinct objects, and (3) object classification and size fitting, which assigns parametric primitives to the recognized objects [46,50]. Object recognition is the critical task of automated geometry modelling and many research studies have utilized different methods and assessed their ability to recognize objects with different shapes.

6.3.2 Scan-vs-BIM

This approach is related to scan-to-BIM, except rather than converting a 3D point cloud into a new BIM, the data is directly overlaid on a BIM to quantify discrepancies. This method is sometimes referred to as "deviation analysis" and has been used in the construction industry over the past decade [269]. Deviation analysis has become the de-facto approach for dimensional inspection in IBC [261], with the most common applications being applied to structural systems, industrial piping and other MEP systems [93,173,261,270]. The general approach for this method involves registering (aligning) the 3D point cloud to a BIM using feature-based or global best-fit (i.e., through iterative closest point) methods. Then, discrepancies between the two datasets are colourized based on the Euclidean distance between individual points in the point cloud and the closest features in the BIM [271]. This type of analysis cannot produce discrete or 'parametric' deviations but is rather used as a pragmatic solution for depicting general out-of-tolerance issues in IBC [93].

6.3.3 Parametric BIM Updating

A third approach is based on the parametric attributes of BIM. The advent of 3D parametric modelling brought significant value to the construction industry: savings of up to 84% were initially realized for drafting costs and up to 51% for engineering costs [272]. These benefits continue today [14] and are maximized in projects with a high degree of complexity and repetition. In building information modelling, the classification of objects as being "parametric" extends beyond just representational form and has unique attributes to facilitate use across the entire construction lifecycle. In addition to geometric

attributes, parametric objects must also include semantic information in the form of associative data, rules, topology and material-specific data [43]. Parameters are also used to classify objects into categories, families, types and instances, which is stored as data in the form of text, integers, numbers, area, volume, angles, URLs, or binary data [51]. Parametric BIM affords the ability to propagate global changes in a model through local changes of driving parameters. This is perhaps most notably realized through the specification of parametric topology.

Parametric BIM has only very recently been posited as a gDT method [273], however it has long since been used as a powerful design tool [43]. Given how the modification of parameters can propagate changes to update a pre-existing BIM to match as-built conditions, it has the ability to dynamically assess potential assembly conflicts in near real-time. Previous research has investigated how such an approach has significant advantages for the construction industry [258], and how laser scanning can be used as the basis for propagating changes [274]. However, no research to date has explored or demonstrated how this approach can be used as a gDT.

6.4 Research Approach

This research outlines the necessary requirements of deploying gDTs for fabrication and assembly control in IBC and for producing an as-built BIM, where feasible. This is accomplished in three steps: (1) conducting a review to identify the necessary geometric accuracy and semantic requirements of gDTs, (2) identifying the existing capabilities of gDT methods with respect to step 1, and (3) conducting a series of functional demonstrations from a previous IBC project to assess how each gDT method can be deployed in fabrication and assembly processes. Based on the inherent strengths and weaknesses of each gDT method, the authors explore the trade-offs between geometric accuracy and semantic enrichment to understand where one gDT method might be favoured over another.

6.5 Requirements of gDTs for Fabrication and Assembly Control in IBC

6.5.1 Geometric Accuracy Requirements

The accuracy of a gDT should capture the maximum permitted deviations in elements and features outlined in codes, standards, and design practice guides. Quality inspections for structural systems in IBC include verifying component interface dimensions, component orientations, individual member tolerances, surface flatness, weld quality and distortion, cross-section dimensions and deformations, and required clearances and offsets [13,275,276]. Fabrication control for piping and mechanical, electrical,

plumbing (MEP) systems include verifying adequate clearances between MEP systems, fixtures, and physical interfaces [173]. Table 7 highlights key maximum permitted deviations (i.e., tolerances) for structural systems, walls, floors, partitions, MEP components and overall envelope requirements in prefabricated assemblies. A review of these tolerances reveals that the strictest dimensional requirements are typically placed on the structural system of IBC assemblies (note: tolerances for onsite structural components are much larger). This is important not only for the structural safety of an assembly but also for controlling deviations in typical construction sequencing since error propagation and or tolerance stackup of the final assembly is heavily influenced by the geometric state of the structural system.

While construction tolerance requirements for structural systems are well documented and outlined in numerous sources, the same cannot be said for other building subsystems. One possible reason for this is that performance of these systems is typically not tied to strict adherence to installation tolerances. For instance, wire gauge is often not modelled upfront in the BIM, since the inherent flexibility enables it to avoid in-field clashes as opposed to wiring conduit and cable trays which are modelled to resolve potential clashes with building components [43]. In some cases, HVAC and MEP guides and codes provide specific cases where building performance is directly tied to dimensional compliance. Naturally, these specific dimensional tolerance requirements need to be captured by the accuracy of a gDT. In plumbing systems, drains must have a minimum slope for proper drainage, which must be dimensionally verified during fit-up and installation. Proper fit-up between MEP system interfaces is governed by spatial layouts determined during design using clash avoidance and subsystem coordination. The implicit tolerances used in establishing clearances in clash avoidances need to be kept during fabrication to avoid both soft and hard clashes. Since many MEP systems such as plumbing pipe networks can accommodate a range of building tolerances (as observed in Figure 33), a gDT of these systems does not need to be as accurate as for the structural system.

Table 8: Maximum permitted deviations for select features, components, and assemblies in IBC

Element/feature dimensional	Subsystem	Maximum permitted deviations (tolerances)	Source
Fit-up of bolted connections	Structural	2mm once interfaces have been joined	[104]
Cast steel connection defects	Structural	Defect depth <5mm with length <10mm	[277]
Length of structural members	Structural	2mm (due to mill processes), 3mm (due to fabrication processes)	[104]
Position of fittings (critical to load transfer)	Structural	3mm	[104]
Position of fittings (non-critical to load transfer)	Structural	5mm	[104]
Camber deviation from intended curve	Structural	L/500 or 6mm (whichever is greater)	[104]
Position of bolt holes	Structural	2mm	[104]
Structural member position on baseplate eccentricity	Structural	5mm	[104]
Squareness of plate girder cross section	Structural	4mm	[104]
Twist in plate girder section from welding distortion	Structural	L/700 or 4mm (whichever is greater)	[104]
Precast column alignment from design-based gridline	Structural	9mm	[92]
Concrete floor slab thickness (cast in place or precast)	Structural	6mm	[92,278, 279]
Precast concrete	Structural	5-10mm	[110]
Concrete slab on grade	Structural	19mm	[92,279]
Position of concrete foundations	Structural	30 mm	[280]
Position of slab edges	Structural	10 mm	[280]
Position of core walls	Structural	At base 10 mm, at any other level 25 mm	[280]
Position of openings in core walls	Structural	Relative to grid 25 mm, relative to nearest point of reference on core 15 mm	[280]
Wood partition wall stud position and plumbness	Walls, Floors, Partitions	6mm	[92]
Steel partition wall stud position and plumbness	Walls, Floors, Partitions	3mm	[92]
Floor framing flatness (wood-framed)	Walls, Floors, Partitions	6mm	[92]
Gypsum wallboard plumbness and levelness	Walls, Floors, Partitions	6mm	[92]
Rough openings for doors and windows	Walls, Floors, Partitions	1mm to 5mm *(additional flexibility since caulking gaps range up to 20mm)*	[92]
Drainage pipe minimum slope	MEP subsystem	1 in 50 (e.g., 20mm for every 1000mm length)	[281]
Positional deviation of MEP component from	MEP subsystem	10mm	[173]
Deviation (angular and positional) between interfaces of prefabricated MEP systems.	MEP subsystem	3mm or 1% of outer diameter of pipe. *Adaptable module joints, threaded rods and other flexible coupling devices can be employed.*	[105]
Positional accuracy of plumbing systems, including the final position of interfaces for fixtures.	MEP subsystem	Connection elements (i.e., flanges that connect pipes and fixtures) require precise alignment (1-2mm error) since these connections are often watertight through threaded flanges. The pipe assembly leading up to a connection point can accommodate larger variations in the spatial position of the fixture (>10mm).	Refer to Figure 33.
Horizontal out-of-alignment due to manufacturing (for overall module envelope)	Overall assembly (in modular construction)	6mm	[18]
Vertical out-of-alignment due to manufacturing (for overall module envelope)	Overall assembly (in modular construction)	3mm	[18]

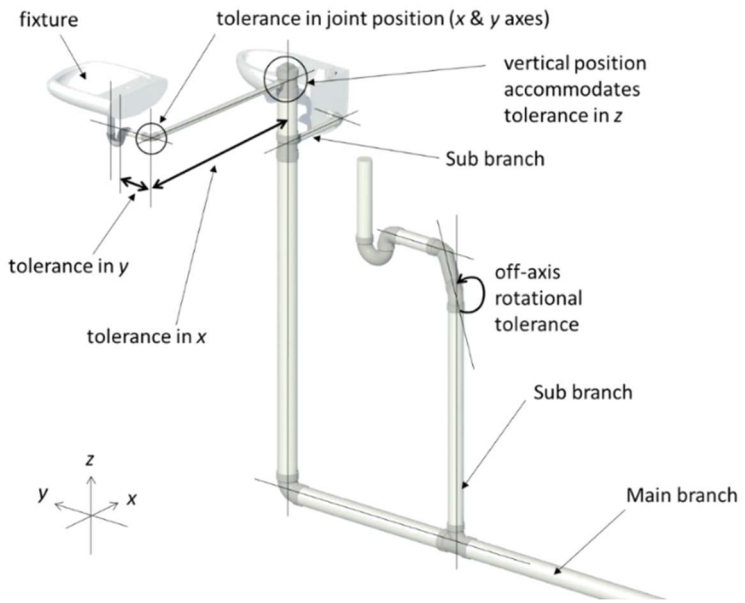

Figure 34: Dimensional tolerances from the main branch to sub-branches and fixtures in plumbing systems.

6.5.2 Semantic Requirements

Apart from the geometric accuracy requirements for gDTs in IBC, raw geometric information must also be interpreted and assessed in a highly semantic manner as per fabrication and assembly control requirements. For instance, verifying a component has been correctly installed is not solely a matter of verifying accurate placement, but is also based on verifying correctness in terms of its material, visual integrity, connection requirements, etc., which are semantically derived. In MEP systems, it is necessary to ensure there is no visual damage or debris on components, that brackets are installed correctly, flanges are connected with the correct fasteners and to the required torque value, and required testing performed prior to commissioning [105]. The semantic verification of offsite manufactured assemblies can be inferred from a geometric digital twin, as long as adequate fidelity of geometry and texture information is available.

6.5.3 Classifying IBC Systems According to Data Fidelity Requirements

Geometric digital twins for fabrication control should focus on high fidelity updating of aggregation features which have the greatest impact on the fabrication and assembly processes. Features in a model which require either highly accurate assessments or very strict semantic assessments are subjected to high fidelity capture (e.g., critical structural connections). Other items that are not constrained by strict fidelity requirements but are nonetheless important items to verify (e.g., rough stud placement and count) can be

subjected to low fidelity capture. The distinction between high and low fidelity twinning reflects the specification of tolerances in IBC, which should not be over-specified, as this can unnecessarily increase production costs [83].

In order to perform high fidelity twinning, the initial 3D model from the design stage must have a sufficient level of detail (e.g., LOD 400: information sufficient for fabrication as per AIA and BIMForum ontology [62,63]) of critical features so that as-built data can be directly overlaid, compared, and abstracted for dimensional and or semantic comparison purposes. High fidelity updating is then characterized by very accurate and feature-rich digitization of assembly features such as connection points between structural components.

Low fidelity updating is characterized by fast, simple methods for verification (i.e., such as methods presented in [282]). If these objects already exist digitally in a building model before fabrication, they often do not rely on extremely accurate methods for digitization (i.e., scan-to-BIM) to verify their fabrication quality. This is necessary for ensuring twinning efficiency in complex assemblies since fully automated methods for scan-to-BIM are elusive, and manually modelling the as-built geometry is time-consuming, tedious, and often not necessary in the scope of fabrication control.

While a distinction between high and low fidelity twinning methods is made in this research, for demonstration purposes, only high fidelity twinning is studied. Future research should study and incorporate a more holistic twinning framework with low fidelity methods and other auxiliary technologies (e.g., machine vision from photogrammetry paired with laser scans).

6.6 Outlining the Capabilities of Existing gDT Methods

This research considers three unique gDT methods that can be used for high-fidelity geometric digital twinning based on the approaches identified in the background section of this chapter. Guo et al. [173] outline the approaches for using laser scanning to perform quality assessments on prefabricated assemblies: without an as-designed model, with a CAD model (i.e., only the geometric information) or with a semantically rich BIM. In this work, these approaches are further refined into (1) scan-vs-BIM gDT, (2) scan-to-BIM gDT, and (3) parametric BIM updating gDT.

In the first approach, at each stage of production where the geometric status of the assembly needs to be geometrically twinned, a 3D laser scan is collected. Then, this data is registered to a pre-existing geometric model (BIM). A scan-vs-BIM deviation analysis is carried out for the subsystem of interest in order to assess the dimensional quality. Then, the parts of the geometric model that pertain to the

subsystem that was scanned are replaced by the 3D point cloud. A subsequent assessment is conducted to identify clashes with remaining subsystems in the geometric model. Despite the directness of this gDT approach, it does not provide a reliable mechanism for maintaining semantic information. Further, it does not directly generate an updated as-built BIM. It is strictly used to determine the dimensional quality of fabricated components and to assess if clashes with downstream subsystems will occur.

In the second approach, a 3D laser scan is collected in a similar temporal manner as the first approach. However, rather than directly overlaying the 3D point cloud with the pre-existing geometric model (BIM), a new model is generated using scan-to-BIM. This re-created assembly is then compared with the isolated subsystem of interest in order to visualize the dimensional quality. In addition, this recreated model is replaced to form a hybrid model that can be used to assess potential clashes with downstream processes. This particular approach has become feasible given the progression in automated scan-to-BIM methods, which continue to improve. Furthermore, many BIM software (e.g., Revit®) provide automatic error messages when trying to fuse models together when clashes result. This particular method might not be as accurate as the first approach since errors accrued during scan-to-BIM must be accounted for. However, this approach can be used for as-built BIM generation.

The third approach builds upon the two previous ones, by taking information generated by a 3D point or a re-created assembly[17], and rather than simply replacing this data in the initial geometric model (BIM), parametric updates are instantiated. The core benefit of this approach is that semantic information contained in the initial geometric model is preserved. This method takes advantage of not only the evolving status of scan-to-BIM and the fidelity of information generated in scan-vs-BIM, but also that of the parametric attributes of BIM.

A summary of each gDT method is shown in Figure 34. In this illustration, a gDT is developed for the geometric status of a particular subsystem of interest after its fabrication is complete, prior to commencing subsequent subassembly fabrication. There are two key assessments depicted here: (A) a deviation analysis for the system of interest, and (B) an impact assessment for downstream production.

[17] *The choice between using a scan or a model to drive these parametric updates is dependent on a user's discretion. At the point of establishing this research, it is not fully certain if there is an approach that is superior for all situations.*

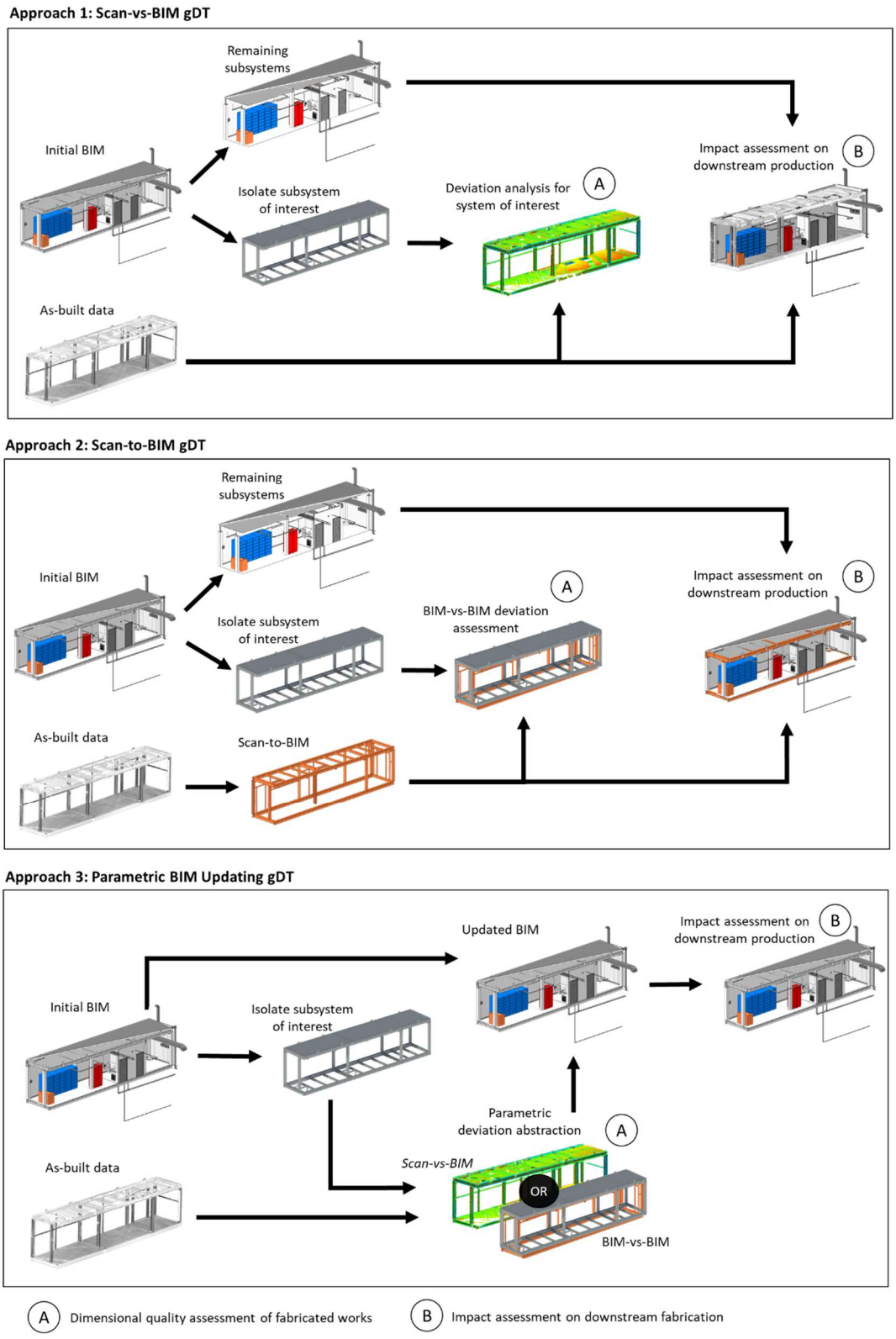

Figure 35: Geometric digital twinning approaches to support fabrication and assembly control assessments in IBC using as-built data capture and BIM

6.6.1 Enumerating the Factors Affecting Geometric Accuracy

Accuracy of a 3D scanning based gDT is based principally on the as-built data collection process, which is subject to device calibration errors, environmental conditions, and device measurement errors [269]. Accuracy is also based on the registration of datasets. For scan-vs-BIM, the alignment or registration of the point cloud with the BIM will accrue errors. Depending on the approach used for registration, such as best-fit alignment or feature-based alignment, different errors can occur. In addition, the alignment of geometric models (such as in a BIM-vs-BIM analysis) are also a potential source of error.

Another factor affecting the accuracy of a gDT is the characteristics of elements being twinned [283]. Unique material conditions (texture, shape, colour, reflectivity, etc.) may impact the accuracy of as-built data capture, especially for lidar laser scanners [269]. In addition, the geometric characteristics of elements also play a role. Since most BIM software tools employ use of rigid-body (idealized) parameters for defining construction elements (e.g., universal parameters defining cross sectional shape, and length, width, and height parameters), the ability to model or capture non rigid-body deformations is very challenging. While finite element analysis and multi-physics engines can be used to predict elastic and plastic distortions in materials, current digitization workflows that produce parametric objects such as scan-to-BIM cannot capture distortion such as bowing in a beam, welding distortion in steel frames, or bent flanges on pipe spools. Consequently, one solution is to ‘best-fit’ parametric idealized shapes to distorted shapes, at the expense of representational accuracy.

Where appropriate, the BIM level of development (LOD) also plays a key role in the ability to assess the accuracy of fabrication. For instance, if the LOD for a typical interior wall assembly is at LOD 300, then an overall thickness for the assembly is shown along with major penetrations for doors, windows and large mechanical equipment are detailed [63]. At this level of detail, individual components such as studs, bracing, insulation, sheathing and smaller penetrations for MEP equipment are not provided and as such cannot be parametrically updated. Without these additional details (which would be included at LOD 400 for instance), the accuracy of verifying fabrication for items such as wall penetrations which are important for MEP coordination and clash avoidance cannot be measured. In lieu of a model with sufficient LOD, scan-to-BIM and a subsequent deviation analysis can be used [269] to assess the accuracy of digitization of construction works.

To date, no known studies have derived an amalgamated error function for gDTs. This likely stems from the fact that the objective factors affecting accuracy are difficult or not feasible to homogenize since some factors are only available as average, standard deviation or absolute (i.e., maximum/minimum) values.

For instance, laser scanner manufacturers often report ranging error in terms of absolute upper/lower limits (e.g., +/- 2 mm), noise errors as standard deviation values, and registration errors as root mean square (RMS) values. This creates obvious challenges for trying to establish a single amalgamated error function. In some research, a point cloud is used as a the single 'ground truth' metric, however as explained in detail by [263], such approach requires abstracting local model features (e.g., quadratic model surfaces) since direct computation methods such as nearest neighbor have flaws (point cloud sparsity and noise erroneously increase deviations). Rather than proposing a homogenization strategy, this research uses the following abstracted function for reporting the error of 3D scanning based gDTs (E_{gDT}):

$$E_{gDT} = f(E_{AB}, E_{DC}, E_{RD}, E_{LOD})$$

Eqn. 11

where E_{AB} is the overall error resulting from the raw as-built data (e.g., scanner accuracy, registration error, noise, occlusions, etc.), E_{DC} is the error from data comparison (i.e., alignment of scan with BIM), E_{RD} is the rigid deformation abstraction error (difference between the as-built rigid deformations and the accuracy capabilities of the gDT method), and E_{LOD} is the error introduced from discrepancies between model LOD and as-built geometry LOD. Depending on the gDT method being employed, not every factor in this error function is applicable. As mentioned, due to intricacies and potential interrelations between these factors, it may not be feasible to derive an explicit algebraic expression (as factors may not always be mutually exclusive). As such, when investigating errors of gDT methods, this paper presents each of the individual terms listed in Eqn 11.

6.7 Functional Demonstrations of each gDT Approach

The following demonstrations emphasize high fidelity twinning of key 'driving' assembly features. Given the strict tolerance demands placed on structural elements, it is important that these components are digitally updated during fabrication and assembly stages [93]. As such, the structural system of a previous industrialized building is used to demonstrate each gDT approach. This particular project is comprised of prefabricated assemblies with steel chasses that are subsequently fitted with other building systems (MEP, walls, floors, fixtures, finishing and millwork).

An initial BIM was created using Autodesk Revit®, and as-built data was collected using a FARO laser scanner at key fabrication stages. Two commercial software packages were used for supporting the gDT approaches: FARO® BuildIT Construction and ClearEdge3D® Edgewise. Given its ability for highly customized feature-based registration, FARO® BuildIT Construction was used to perform scan-vs-BIM analyses. Feature-based registration is important for IBC, since datums are employed during fabrication

for controlling and measuring dimensional variability. Performing a global best-fit registration, such as through the *Iterative Closest Point* algorithm, does not account for datums on the assembly even though it does yield in global minimization of errors between the point cloud and BIM. In contrast, feature-based registration enables a user to localize key features and using primitive fitting on the point cloud for a series of features such as planes, extract coordinates that can be used for registration. ClearEdge3D® Edgewise was used to perform scan-to-BIM processes. While there is a range of existing research into automated scan-to-BIM processes, ClearEdge3D® Edgewise was chosen for this particular study given its graphical user interface and intuitive review process for verifying the dimensional fit between idealized 3D model features and the raw unstructured point cloud data.

6.7.1 Approach 1: Scan-vs-BIM gDT

In this approach, the structural subsystem in the initial BIM was first isolated. Then a deviation analysis was performed by scanning the fabricated structural system and registering the resulting point cloud to the BIM. Feature-based registration was used by extracting intersection points from three planar features located at each of the four bottom corners of the structural system. This deviation analysis revealed that variations of the structural system ranged up to 25.4 mm. In order to determine the impact of these variations, a subsequent assessment was undertaken to identify clashes that may occur for the next subsystem to be fabricated; in this case the installation of doors. Using a simple clash detection algorithm, it was found that the position of one particular beam resulted in a clash with a door assembly by roughly 20 mm (Figure 35). Other smaller clashes were also identified for gypsum wallboard elements that wrap around the vertical columns. Based on the information generated by this type of gDT, the fabricator has the ability to make informed, prescient decisions as to whether to correct the position of parts of the structural system or to adjust the position or form of the downstream components that result in a clash.

Enumerating the accuracy of this gDT is performed as follows. According to the laser scanner manufacturer, the maximum ranging error is equal to +/- 2mm at a distance of 25 m, and the standard deviation of ranging noise is between 0.5 mm and 1.35 mm for surface reflectivity of 90% and 10% respectively [284]. Both of these factors contribute to the raw as-built data error. The error in extracting planar features (required for registration) from the point cloud were reported in FARO® BuildIT Construction as 0.75 mm. Then the error in registering the point cloud to the BIM was quantified as 2.45 mm. It should be noted that both planar feature extraction and BIM registration are properties of the physical assembly and not based on the software employed. While there is no explicit error associated with parametric feature extraction, both previous enumerated errors are implicit forms of parametric

feature extraction. For this gDT, there are no errors associated with the BIM LOD, since the BIM was developed to a fabrication level of detail (i.e., LOD 400).

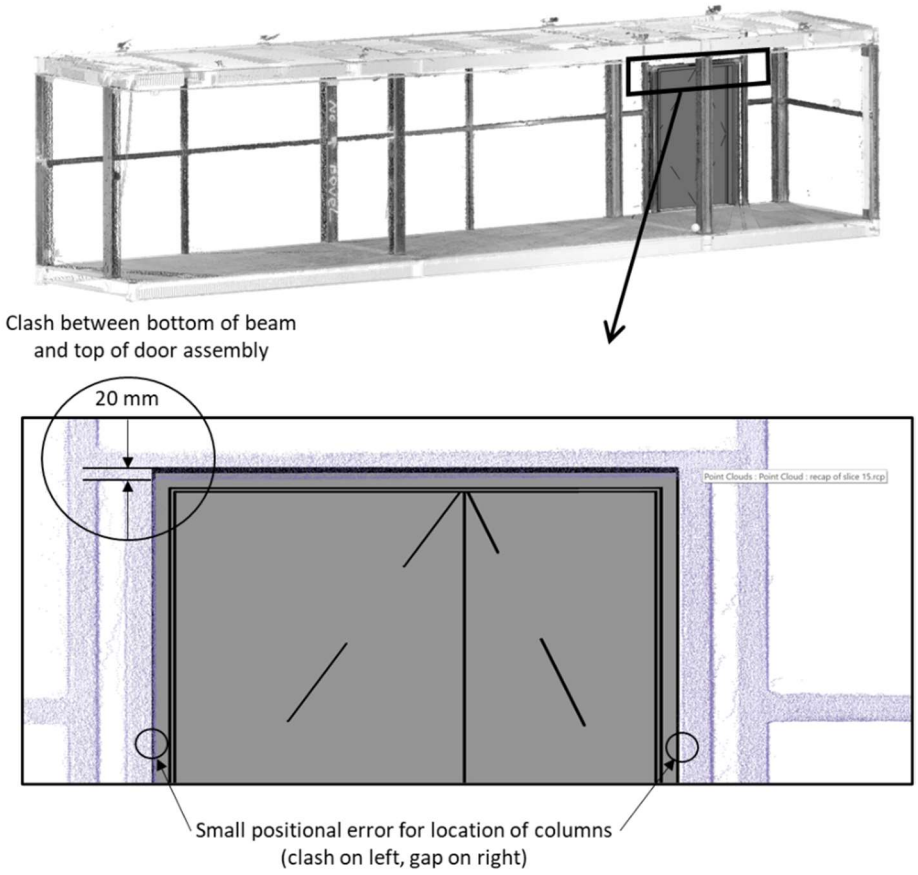

Figure 36: Scan-vs-BIM gDT: identification of a clash between a beam and door assembly.

6.7.2 Approach 2: Scan-to-BIM gDT

In this approach, the structural system was scanned in the same manner as the first approach. However, rather than directly using the resulting point cloud to overlay on the BIM, a subsequent model was (semi) automatically generated in ClearEdge3D® Edgewise. The result of this scan-to-BIM process was validated by manually confirming the parametric primitive fitting process of each structural component. This recreated model of the structural system was then aligned to the original BIM. The alignment procedure was done by using features on the base frame that correspond to the datum used during fabrication. After alignment, an assessment was performed between the two models (the as-designed and the as-built). This assessment was conducted by extracting parameterized deviations (i.e., positional deviations in each of the principal component directions) for the main structural components as shown in Figure 36. As depicted in the table portion of this figure, deviations for the beams and columns range up

to 25 mm, which is similar to the information produced in the scan-vs-BIM assessment of the first gDT method. However, an additional part of this assessment is the parameterized deviation extraction of interface plates (used as inter-module connections). Based on the way deviations are produced in scan-vs-BIM, when components have gross positional errors (e.g., larger than 50 mm) or if deviations cannot be captured using Euclidean distance measurement (e.g., if a window is shifted "in-plane" rather than "out-of-plane"), these cannot be captured in the typical heat-map visualization produced in scan-vs-BIM [269,285]. However, when performing a BIM-vs-BIM assessment as in this gDT approach, one-to-one comparisons between all elements is made. In this case, the fabricator incorrectly placed two interface plates P4 and P5 by 281 mm and 142 mm, respectively. Having access to such information directly after fabrication of the interface plates gives the fabricator the ability to correct the placement before enclosing in the structure further, and before invoking much larger rework costs downstream. In terms of assessing clashes with downstream processes, the initial model of the structural system was replaced by the recreated model. Then, clash detection was performed in a similar manner to the first gDT approach. This clash detection captured the same issue with the doorway assembly, and well as clashes with gypsum board elements as shown in Figure 37.

The enumeration of the accuracy of this gDT is as follows. The same raw as-built data errors from the first gDT apply. After performing scan-to-BIM, the resulting model was compared back to the point cloud according to the process outlined by Anil et al. [269] to quantify the accuracy of the process for generating the as-built BIM. In this case, the scan-to-BIM error was quantified as 8.89 mm. Finally, the alignment process (of the recreated BIM to the original BIM) was reported to have an error of 4.11 mm – this was determined by the average Euclidean distance between the outermost points on the base frame.

		X	Y	Z
Columns	C1	8.5915	-8.5985	4.3395
	C2	8.088	-6.548	3.7095
	C3	20.7515	-1.522	12.5895
	C4	19.4625	6.692	9.2965
	C5	-7.751	11.3685	6.112
	C6	-22.0125	-5.2065	11.958
	C7	3.3475	17.366	4.437
	C8	-7.597	15.739	-20.2615
Beams	B1	-5.624	-3.822	0.024
	B2	-1.799	-2.5855	1.3935
	B3	-2.8305	7.152	-0.0295
	B4	-7.396	-0.8725	0.036
	B5	-11.488	12.9655	0.524
	B6	-12.2625	2.4195	-19.9915
	B7	-8.479	5.029	-0.0775
	B8	-25.457	0.417	-25.3655
Interface Plates	P1	1.0225	18.514	6.3355
	P2	0.997	18.2845	8.0905
	P3	14.519	17.9265	8.8615
	P4	281.182	9.355	0.468
	P5	142.334	7.513	-3.506
	P6	-0.627	19.067	-5.078
	P7	-2.485	17.305	-2.195

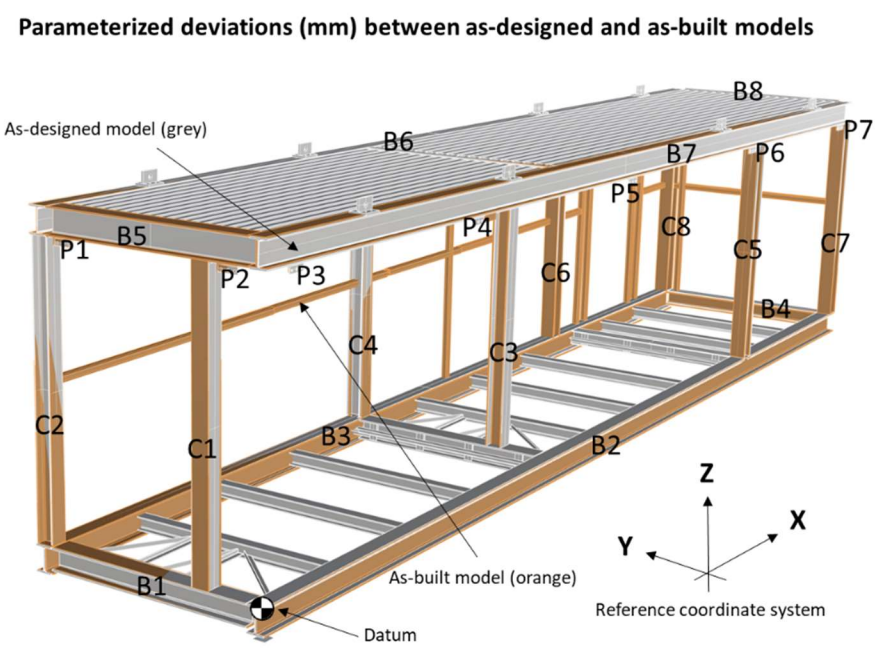

Figure 37: Parameterized deviations for main structural components by comparing a 3D model of the as-built state captured through digitization and registered to the as-designed state using a reference datum and best-fit rotations about the reference coordinate system axes. All deviations are in mm.

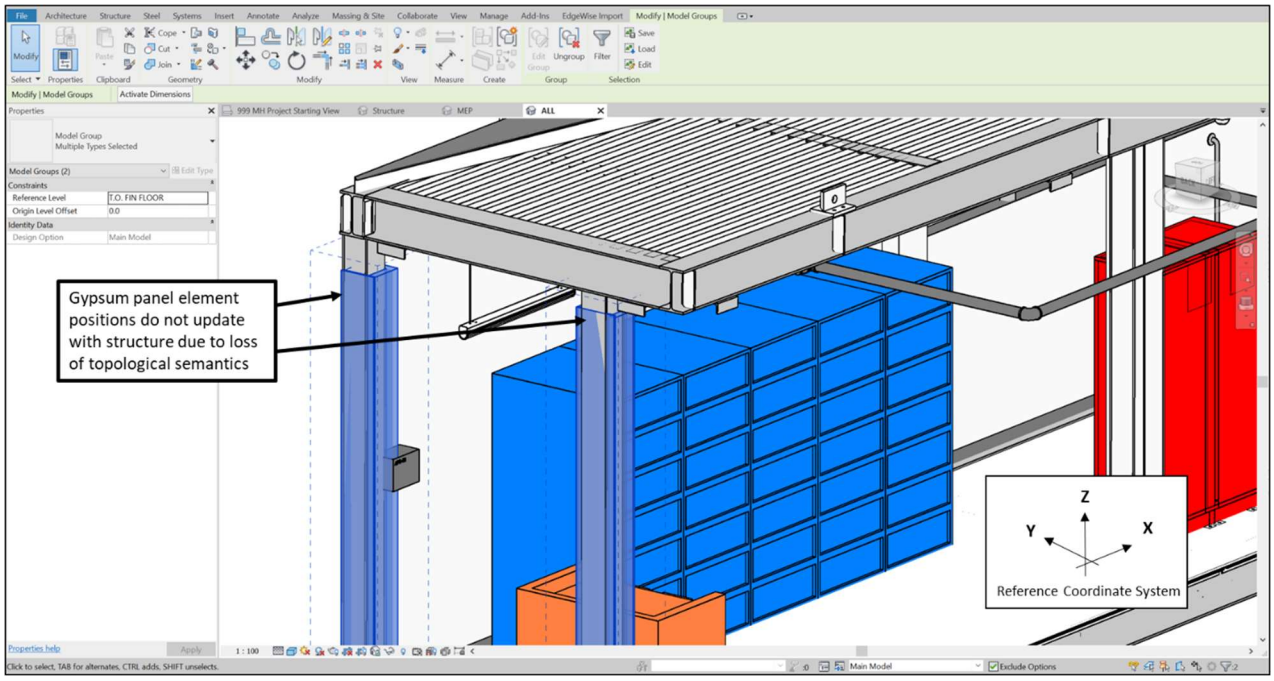

Figure 38: Depicting clashes captured using scan-to-BIM approach. Note how topological relations between gypsum elements do not update when the structural system is replaced in the BIM.

6.7.3 Approach 3: Parametric BIM Updating gDT

The final gDT approach performs parametric updates to an initial BIM. While deviations can be extracted using either a scan-vs-BIM approach or a BIM-vs-BIM approach as per Figure 34, this particular demonstration uses the BIM-vs-BIM approach, where two separate 3D models are overlaid, and parameterized deviations extracted along the main axes (Figure 36). In the scan-to-BIM process, elements are best fit to the point cloud, but are kept as idealized objects (i.e., only pose deviations captured). This means that if there are non-rigid deformations in elements such as welding distortion, these errors are 'smoothed' by best-fitting idealized elements to the point cloud.

Since Autodesk Revit® was utilized for the creation of the initial BIM and given the nature of parametric relationships between elements, all geometric deviations were constrained to transformations about the axes used in the creation of the initial 3D model (these axes are displayed in Figure 36). This ensures that the previously established topological relations that are defined parametrically are maintained during the updating process. Since subsystem components are based on geometric and spatial attributes of the structural system, updating the as-built geometry of the structure enables an update of subsystems in order to analyze fabrication control issues pre-emptively. Clashes can be detected for groups of objects that are not parametrically related or in cases where Autodesk Revit® creates error messages, indicating that certain relationships cannot be maintained based on changes to geometric and spatial configurations (Figure 38).

Enumerating the accuracy of this gDT is as follows. The same raw as-built data errors from the previous approaches apply. Since scan-to-BIM is used to generate parametric updates, the same error from the scan-to-BIM process applies (average error of 8.89 mm) as well as the error from aligning the recreated BIM to the initial BIM (average error of 4.11 mm). One additional source of error stems from constraining the parametric updates about the axes used to construct the initial BIM. This error is quantified by manually comparing deviations between elements, which resulted in an average error of 5.5 mm. Both the parametric update constraint and the scan-to-BIM error are combined into one overall error for rigid deformation (E_{RD}) of 14.39 mm.

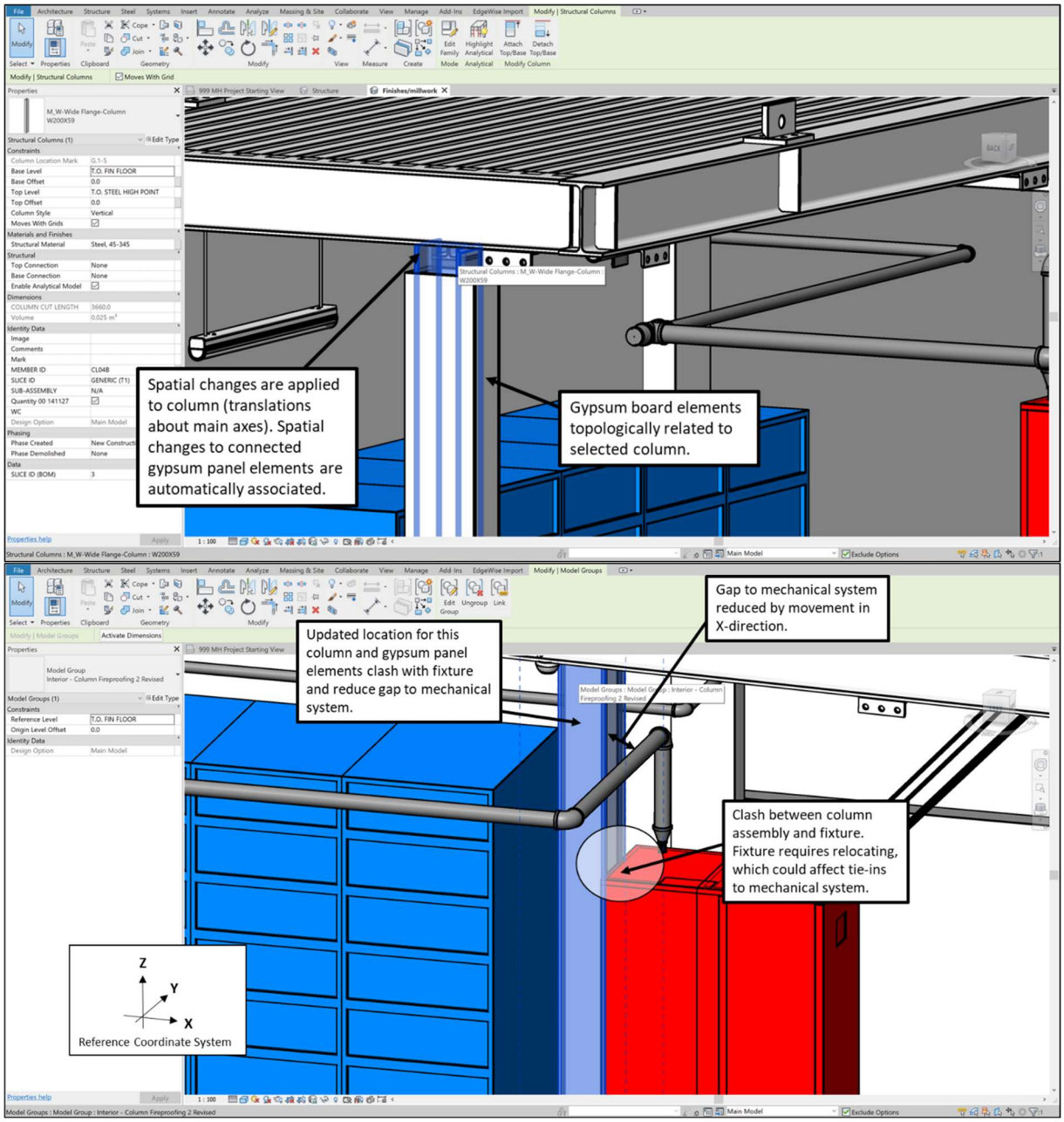

Figure 39: Automated changes propagate in BIM through parameter updating (top), are used to predict hard clashes (i.e., physical conflicts) and soft clashes (i.e., gap violations) in the assembly (bottom).

6.8 Comparison and Summary of Results

Each gDT approach can be compared and evaluated based on the following criteria: the ability to capture non-rigid deformations (as per discussion in Section 6.6.1), estimated average accuracy, level of data

fidelity (i.e., semantic preservation), and ability to directly facilitate as-built BIM creation. A summary of these metrics is provided in Table 8.

Of the three gDT approaches, scan-vs-BIM is the only one to capture non-rigid deformations. This is because scan-to-BIM and parametric BIM approaches currently do not support modelling of deformation for elements (all elements are assuming to prescribe to parametric primitives). As such, a scan-vs-BIM gDT must be used when trying to quantify non-rigid deformation such as welding distortion. This approach also achieves the best overall accuracy, since the other gDT approaches rely on making parametric assumptions which impact accuracy. Each of the gDT approaches have the same error from raw as-built data, but as shown in Table 9, scan-to-BIM and parametric BIM gDT approaches have larger data comparison errors (E_{DC}), and the parametric BIM gDT has the largest overall error. Based on the laser scanner used in the case study, even the most accurate gDT (scan-vs-BIM) has larger errors than several of maximum permitted deviations for various OSM elements – especially for the structural system (Table 8). Even by employing one of the most accurate terrestrial laser scanners on the market (e.g., +/- 1mm), the overall error would still larger than key deviations in Table 8. As such, for elements requiring very precise dimensional verification (< 5 mm), additional measurement devices such as laser trackers must be deployed. However, these devices cannot produce the same rich data from laser scanners, which is why 3D scanning based gDT approaches are still efficacious. The parametric BIM updating gDT boasts the highest fidelity, since all initial semantics associated in the as-designed BIM are preserved. This also means that it can produce the most semantically rich as-built BIM and as such it can simultaneously be used for fabrication and assembly control and for generating an as-built BIM. The scan-to-BIM gDT is positioned as a middle tier approach , and while it does not have the best overall accuracy, it can generate an as-built BIM in a more accuracy manner than the parametric BIM updating gDT (albeit at the expense of lower semantic richness). It is also the best positioned gDT for capturing missing components since a one-to-one comparison between design elements and as-built elements is performed.

Table 9: Summary and comparison of the gDT approaches used in the case study

gDT Approach	Scan-vs-BIM gDT	Scan-to-BIM gDT	Parametric BIM gDT
Enumerated accuracy factors	E_{AB}: $R_E = \pm 2$ mm[A] 0.8 mm < R_N < 1.4 mm[B] E_{DC}: 2.45 mm[C] E_{RD}: 0.75 mm[C] E_{LoD}: NA	E_{AB}: $R_E = \pm 2$ mm[A] 0.8 mm < R_N < 1.4 mm[B] E_{DC}: 4.11 mm[C] E_{RD}: 8.89 mm[C] E_{LoD}: NA	E_{AB}: $R_E = \pm 2$ mm[A] 0.8 mm < R_N < 1.4 mm[B] E_{DC}: 4.11 mm[C] E_{RD}: 14.39 mm[C] E_{LoD}: NA
Non-rigid deformation capture	Yes	No	No
Data fidelity	Low	Med	High
As-built BIM creation	No	Yes	Yes

A: absolute ranging error (R_E), B: standard deviation of noise error (R_N), C: average error

6.9 Conclusions

The geometric framework of a digital twin, (a 'geometric digital twin', or gDT) has been the focus of several research studies which employ use of 3D scanning to obtain accurate and dense information from a physical asset. The way that raw data is used to produce meaningful information and to update the geometric status of an asset becomes the 'twinning' method. This research explores three distinct ways that 3D scanning data can be used to produce a gDT. Each of these approaches have unique advantages and disadvantages based on the ability to capture non-rigid body deformations, accrual of error, fidelity or richness of semantic information, and the ability to generate an as-built BIM. This chapter presents the requirements for using gDTs in industrialized building construction based on geometric accuracy semantic information requirements. Using a case study, the capabilities of each gDT approach are presented in terms of how they can be deployed for distinct analyses, their ability to generate as-built BIM and enumerated factors that affect their accuracy.

The case study found that scan-vs-BIM produced the highest average accuracy since it eliminates potential errors accrued through reconstructive processes in twinning. Furthermore, this approach can capture non-rigid body deformations such as from welding distortion (e.g., Figure 40 depicts the ability for each gDT to capture and abstract non-rigid deformations for a particular beam with non-negligible midspan deflection – for which, scan-vs-BIM is superior). The main disadvantages of this gDT approach are its inability to directly to create an as-built BIM and inability to produce semantically rich information – currently these must be generated manually. On the other hand, the parametric BIM updating gDT was found to generate the most semantically rich as-built BIM since it can preserve initial semantics (the original geometry is updated parametrically). The main downside with this approach is its inability to accommodate shape-based parametric adjustments resulting in a lower overall accuracy. While this gDT method can be used directly for as-built BIM creation, it is significantly more challenging to use for generating information required for fabrication and assembly control. Finally, the scan-to-BIM gDT had balanced trade-offs with respect to the other gDTs. It has a slightly better accuracy than the parametric BIM updating, and likewise can directly produce an as-built BIM (albeit not to the same semantic richness).

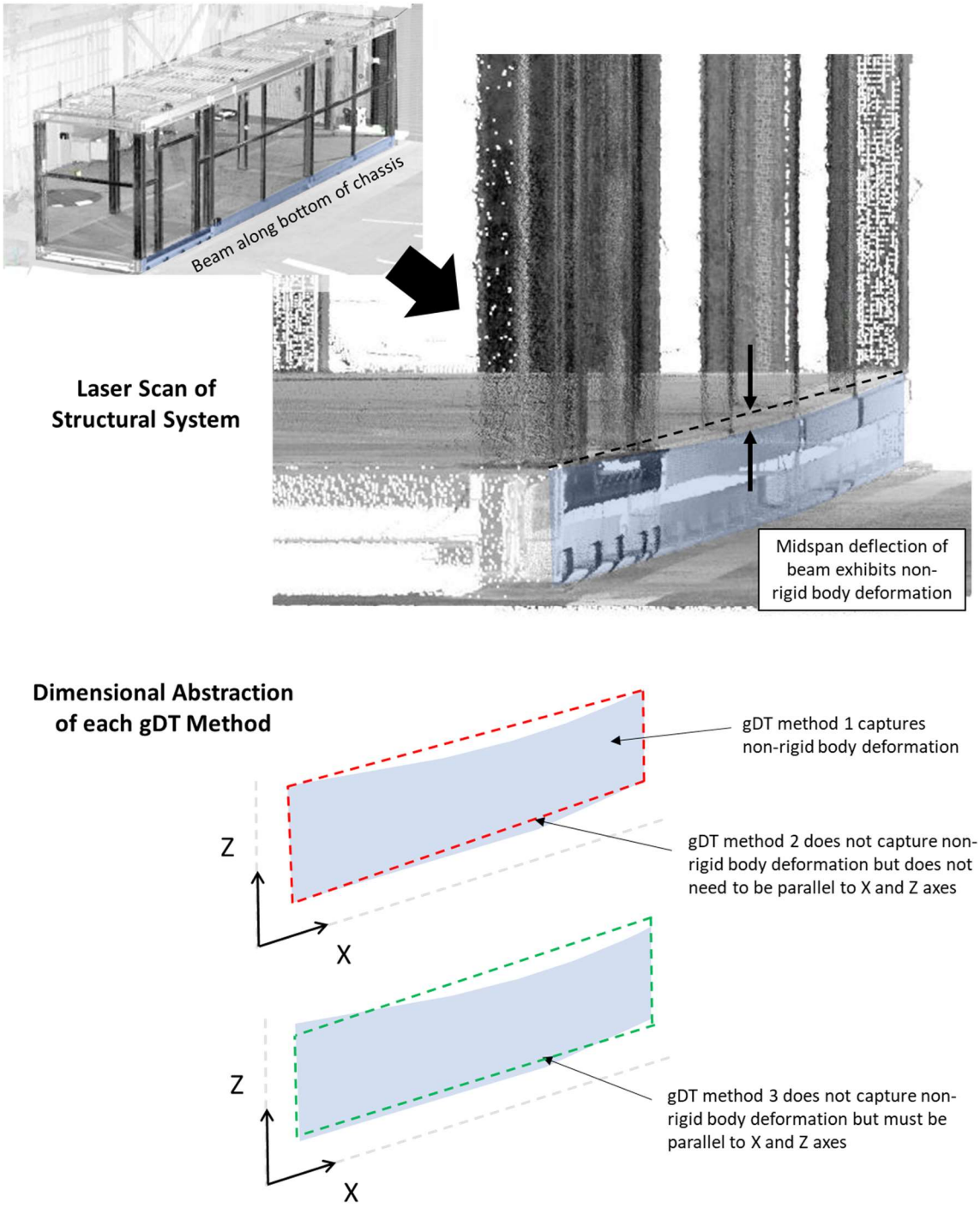

Figure 40: Depiction of each gDT's ability to capture (and abstract) non-rigid body deformation of a beam with midspan deflection located at the bottom of a chassis.

6.9.1 Limitations

The main limitation of this research relates to the method for quantifying dimensional accuracy. Since the enumeration of accuracy is based on several factors that are difficult or not feasible to homogenize (some factors are only available as average values, while others are absolute), it is not feasible to establish an overall amalgamated accuracy value for each gDT.

The other key limitation deals with the way in which parametric updates are executed in BIM. Depending on the nature of the geometric changes that need to be made, the topological relations and constraints cannot be maintained. Errors can occur for off-axis transformations, resulting in loss of topological semantics. In such a case, it can be challenging or not feasible to make updates to BIM.

6.9.2 Towards an Automated Parametric BIM Updating Method

The process of employing scanning based gDTs for fabrication control is comprised of a range of automated, semi-automated and manual steps, which should be automated in order to be more beneficial to projects given the amount of effort required to apply specific changes. Given its rich preservation of semantic information, parametric BIM updating is the most compelling gDT method for generating an as-built BIM. As such, the next chapter examines how to improve the dimensional accuracy of this approach and to develop an automated approach to perform parametric updates.

Chapter 7: Automated Parametric BIM Updating

This chapter presents developments made by the author that is being published in the journal of Automation in Construction [286]:

- Rausch, C., Haas, C. (2020) "Automated shape and pose updating of building information model elements from point clouds." Automation in Construction. Accepted Dec 2020.

The purpose of this chapter is to develop a computational approach for updating BIMs using a parameterization framework and the use of metaheuristics. Such an approach is particularly beneficial to industrialized building construction during the onsite construction process. Due to the strict dimensional quality requirements, it is necessary to obtain an updated model of the site components prior to the installation of offsite-produced assemblies. The case study employed in this chapter demonstrates how the geometry of cast in place concrete footings can be automatically updated in the BIM, while preserving the initial semantic information, in order to verify compliance prior to installation of building modules.

7.1 Background

Many workflows outline the process of digitizing a built asset and transforming non-parametric data such as 3D points clouds into a semantically enriched parametric building information model (BIM). However, this process has several onerous barriers and challenges corresponding to accurate object recognition, data associativity and semantic enrichment. While some applications necessitate this “ground-up” digitization process, there are other applications where it is possible, and in fact advantageous, to update a surrogate parametric BIM (“proto-BIM”) using as-built data. Despite related research, no methods to date outline and demonstrate the process of updating a parametric BIM considering pose and shape parameters of objects and assemblies. This article provides a new approach to managing the as-built status of constructed assets by exploiting the parametric capabilities of BIM, the accuracy of data provided by 3D point clouds and the computational dexterity of metaheuristics. A case study carried out for cast-in-place concrete footings shows how the error between BIM and the as-built conditions can be reduced from an overall average deviation of 50.4 mm for the as-designed BIM to 9.75 mm for feature-based parameterization and 5.69 mm for control point-based parameterization. The significance of this chapter is the development of an approach to progressively capture accurate as-built conditions in BIM, predict and resolve potential assembly conflicts in a prescient manner while maintaining the initial semantics and fidelity of an as-designed BIM. As such, this method functions as a reliable mechanism for realizing digital twins of constructed assets.

7.2 Parametric Model Updating: BIM and CAD Context

Previous research has studied and posited the case for parametrically updating BIMs. In 2008, Akcamete et al. [258] performed a gap analysis of current parametric CAD software to assess limitations for updating parameters in models. Using an experiment, the authors explored geometric changes in the form of length, location, angle, element connectivity, connection point, and decomposition (splitting objects into numerous parts) for floor and wall objects. These parametric changes were manually applied in order to investigate topological and geometric preservation in resulting IFC files. From this study, the authors noted that current software was not mature enough to support a reliable mechanism for updating BIMs in a parametric fashion. In a subsequent study [259], the authors created a taxonomy for the changes exhibited in two construction projects: localized (e.g., "changing a single value in the model will be enough to update it", and non-localized (e.g., further mechanisms required to ensure topology between affected elements is preserved). The authors then focused on evaluating opportunities for computational support for capturing a history of changes made between model versions, since this is deemed important for the knowledge of the as-built facility. Despite these early attempts at positing the use of parametric BIM updating, no studies since have developed and demonstrated a viable framework to this end.
In response to these early studies outlining the motivation for updating BIMs in a computational manner, there have been a handful of more recent studies that support this notion. Gao et al. [274] developed a methodology for combining progressively captured point clouds for BIM updating. Support is also found for the non-geometrical aspects to BIM. Since laser scanners are not capable of capturing semantic information required in BIMs, Lin et al. [287] proposed a "Final As-built BIM Model Management" framework to update the non-geometric information to collect inputs from correction/inspection forms. In this approach, information is centralized and sent to BIM engineers to update an initial BIM to match the as-built status. An approach to update an initial model to match existing conditions for cultural monument and heritage preservation purposes was proposed by Zvietcovich et al. [288]. Solid models and point clouds are converted into meshes, registration between datasets performed, and a distance function calculation made in order to segment and encapsulate a region of interest. Then conversion of the mesh to a solid model is done to update the initial solid model. In this approach, the initial 3D solid model is updated by adding to or subtracting from the initial solid using Boolean operations. This approach of 'growing' or 'shrinking' regions of interest results in mesh-like features being created, which is suitable for the applications targeted such as cultural heritage monuments for engineering analysis, visualization and restoration planning. However, this process does not provide the means for updating an initial model in a parametric way conducive to BIM requirements in the construction industry.

Within the domain of civil engineering, the only studies for the geometric updating of existing BIMs has been proposed by Bosche et al. [112,289]. At the conclusion of a study on tracking the built status of MEP works, Bosché et al. proposed a system that integrates scan-to-BIM and scan-vs-BIM in order to prompt the update of BIM during construction, operations, and maintenance stages of a project [289]. In this work, the actual BIM updating process is proposed to be carried out in a "semi-automated" manner using supervised learning. In a subsequent study, the authors build upon this proposed process and demonstrate its value in a case study [112]. The developed approach employs the use of Hough transform-based detection of circular cross-section building elements (e.g., pipes). An initial BIM model is transformed into a virtual "as-planned" point cloud, circular cross-sections from both as-built and as-planned point clouds extracted and compared with each other in order to infer the "recognition/identification" of planned elements. Finally, an as-built model "can be" generated (methods to do this are proposed) from the recognized poses of the as-built elements. Despite the obvious value posed by this system, it only works for circular cross-section elements. The authors also report limitations including limited orientation of sensed elements (i.e., pipe runs must be in "pre-determined directions") and the occurrence of false positives and false negatives in the recognition process. Furthermore, while the resulting as-built BIM can be created automatically for circular elements, entirely new BIM elements are instantiated which does not preserve the initial semantics of the as-designed BIM. Another key aspect to the work conducted by these authors is the consideration of object pose only, rather than object shape variability. In an earlier study, Bosché simplifies the task of object recognition by assuming "each objects' as-built shape dimensions already comply with the specified tolerances" [290]. This study concludes with the recommendation that future studies do, in fact, need to account for object shape variability as part of a more accurate representation of as-built status.

Outside the civil engineering domain, a small collection of research studies has explored methods for using *a priori* parametric models to fit to point clouds in an attempt to generate associative, accurate 3D models. Buonamici et al. proposed a novel approach for reverse engineering, whereby a parametric CAD template (with basic parameters associated with shape) is aligned and fit to a segmented point cloud [291]. The steps followed are: (1) development of an initial CAD template, whose parameters comply with the object being reconstructed, (2) pre-alignment of the template to as-built data using inertial properties, (3) corresponding surfaces between template and data are manually identified by a user, (4) optimization for minimizing the global fitting error between template and data is carried out using a Particle Swarm Optimization (PSO). The authors apply this framework to the reconstruction of mechanical assemblies (flange, pin, bracket, plate) and achieve a sub-millimetre accuracy overall. In a subsequent study [292], the authors develop a more efficient optimization process and compare the

Genetic Algorithm (GA) and PSO. In a related study, Shah et al. employ use of Simulated Annealing (SA) algorithm to fit a parametric model template to point clouds [293]. Parameters considered include part features (lengths, diameters, and angles) and assembly parameters (position, orientation of parts). Part feature parameters are first optimized using SA. Then iterative closest point algorithm is used to obtain position and orientation parameters (i.e., pose). Part topology (perpendicularity and parallelism) and assembly topology (contact between parts, constraints between parts) are addressed manually in this approach. The use of metaheuristics in these studies provides an efficient way to compute iterations of a large number of parameters. However, the approach of first modifying feature parameters and then using ICP to perform rigid pose alignment assumes that the discrepancies created from the difference in shape parameters are larger than pose. This is well suited for aligning a template model to a PC, but it does not necessarily work for updating an initial BIM where the as-built deviations of an object do not have as large feature-based (shape) deviations compared to a template of arbitrary size.

7.3 Proposed Methodology

The knowledge gaps stemming from the literature review are twofold: (1) no studies to date document and or demonstrate a process for accurately updating a BIM which preserves the initial model semantics, and (2) no methods in the civil engineering domain detail a procedure for parameterizing a BIM in order to account for shape variability. To address this, the proposed methodology details a workflow for updating BIMs, and a parameter optimization framework using metaheuristics. The contribution in the process-level workflow is the initial parameterization of the BIM, which considers shape parameters (something not considered in any previous works). The parameter optimization framework is based on existing approaches for CAD template fitting to point clouds and model-based vision.

7.3.1 Process level workflow

In the proposed workflow (Figure 41), a building coordinate system (BCS) must first be established in order to align point clouds generated from the site (construction site, offsite manufacturing facility, etc.) with the BIM. A common approach for doing this is to have permanent targets placed on site, which are surveyed using a total station. Then, these targets are captured in the point cloud of a laser scan and used to align the measured coordinate system with the BCS. An alternative strategy is to use specific structural elements as alternative survey landmarks [289] to ensure the point cloud is aligned with the BIM. This first step is important and cannot be substituted for local registration methods (as is often used in progress tracking), as the point cloud must provide the BCS-based (i.e., global) positions of features in the BIM. Next, the BIM must be parameterized in order to obtain a parametric associative model, i.e., changes

made to parameters propagate throughout the model in a holistic manner. The process for parameterizing BIM is presented in Section 7.3.2. After obtaining point clouds (which is proposed through the use of laser scanning), a series of post-processing steps can be done in order to improve the efficiency of the parameter updating process. These steps include performing feature-based segmentation of the point cloud through random sample consensus (RANSAC) or other methods in order to filter out parts of the point cloud that are not relevant for feature matching to BIM elements. For instance, it may be advantageous to extract planar or curvature-based features if the BIM to be updated comprises these specific features. This type of feature segmentation can be approached through an optional step of analyzing components of interest from the BIM in order to assess the distinct classification of features present. In addition, noise reduction can also aid in the updating process and can be approached through methods such as statistical outlier removal (SOR). After post-processing, a point cloud, components from the BIM can be extracted, compared with the point and updated through the proposed parameter optimization module which is outlined in Section 7.3.3.

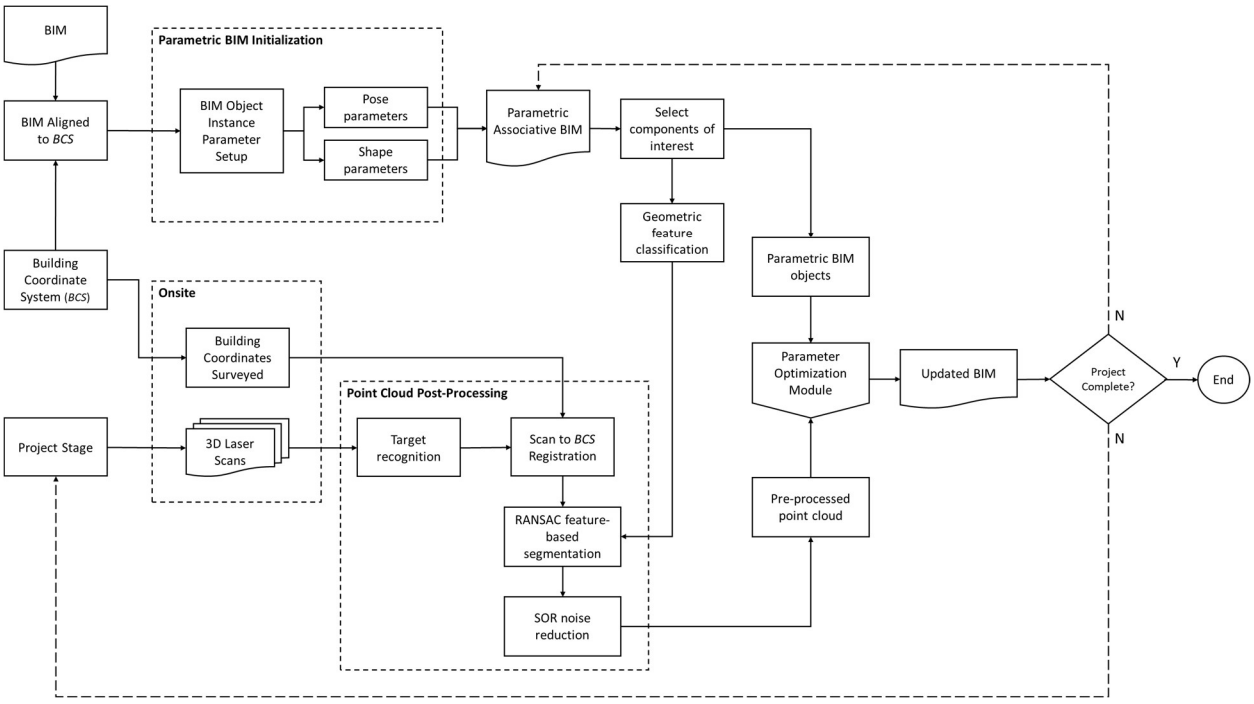

Figure 41: Process Level Workflow for Automated Parametric BIM Updating

7.3.2 BIM Parameterization

The proposed method relies on the formulation of rigid transformation for object pose parameters, which is based on six degrees of freedom (translations and rotations about the principal Cartesian axes). Pose

parameterization is a relatively straightforward process. However, shape parameterization is a complex task, since we must anticipate the behaviour and degree of deformation *a priori*. This unintentionally restricts the degrees of freedom for an object [294]. While one solution could be to perform extremely localized parameterization, this places too much computational demand on optimization processes, which are often *NP-hard* problems. As such, a balance must be struck between the degree of parameterization and geometric manipulation ability. Methods for parameterization include basis vector, domain element, discrete boundary, polynomial and spline (e.g., NURBS), CAD (e.g., CSG), analytical function, and partial differential equation, among others [295]. While many of these approaches are developed and applied in multi-disciplinary shape optimization (in aerospace design for instance), we focus on two common approaches based on the representation schemes used in BIM: feature-based (i.e., CSG) and control point-based (i.e., NURBS).

7.3.2.1 Pose parameterization

In mechanics, the degrees of freedom for an n-dimensional rigid body is comprised of rigid transformations that describe its pose in terms of translations and rotations in Euclidean space. Rotational degrees of freedom can be described in terms of constraints to an object's origin through principle axes or about arbitrary axes. Despite the derivation of rotation about an arbitrary axis, this can be simplified in terms of rotations given by:

$$R_x(\theta_X) = \begin{bmatrix} 1 & 1 & 0 \\ 0 & \cos(\theta_X) & -\sin(\theta_X) \\ 0 & \sin(\theta_X) & \cos(\theta_X) \end{bmatrix}$$

$$R_Y(\theta_X) = \begin{bmatrix} \cos(\theta_Y) & 0 & \sin(\theta_Y) \\ 0 & 1 & 0 \\ -\sin(\theta_Y) & 0 & \cos(\theta_Y) \end{bmatrix}$$

$$R_Z(\theta_Z) = \begin{bmatrix} \cos(\theta_Z) & -\sin(\theta_Z) & 0 \\ \sin(\theta_Z) & \cos(\theta_Z) & 0 \\ 0 & 0 & 1 \end{bmatrix}$$

Eqn. 12

where R_x, R_Y, R_Z are rotations about the X, Y, and Z axes by degrees θ_X, θ_X, and θ_Z respectively. Building upon rotational degrees of freedom, we can also incorporate translational degrees of freedom t_x, t_y, and t_z in the X, Y, and Z directions respectively. The degrees of freedom for rigid body transformation can then be expressed in an overall homogeneous transformation matrix, T as

$$T = \begin{bmatrix} r_{11} & r_{12} & r_{13} & t_x \\ r_{21} & r_{22} & r_{23} & t_y \\ r_{31} & r_{32} & r_{33} & t_z \\ 0 & 0 & 0 & 1 \end{bmatrix}$$

Eqn. 13

where r_{nm} are the rotational matrix components, and the scaling factor is equal to 1. Collectively, these rigid body degrees of freedom can be assigned to both rigid and non-rigid bodies in order to describe the way that an object translates and rotates in 3D space (Figure 41).

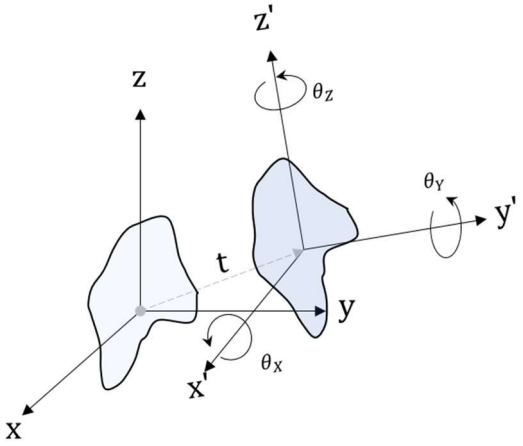

Figure 42: Depicting Rigid Body Degrees of Freedom for Rotations and Translations in 3D Space

7.3.2.2 Shape parameterization

Next, we outline two distinct types of shape parameterization, which correspond to non-rigid transformations that can be applied to an object. Since the choice of geometric representation is directly tied with shape parameterization, we present two distinct approaches which encompass the main types of geometric representation employed in BIM: (1) a feature-based scheme, where a user specifies the unique parameters associated with an object – this is achieved using constructive solid geometry (CSG) representation – and (2) a control point-based scheme using NURBS, where the boundary of an object and its topology to surrounding features and objects are distilled into a series of 3D points.

Feature-based scheme

Parameterization using this scheme occurs through the selection of discriminative geometric features by the user. In CSG representation, a set of 3D geometric primitives can be combined using Boolean operations to create customized geometry. We can represent the process of creating a CSG model object, M as the combination of Boolean operations performed on a set of n base geometric primitives:

$$M = \sum_{i=1}^{n} \sum_{j=1}^{n} b_i \, (G_i, G_j)$$

Eqn. 14

where b_i are the set of possible Boolean operations (addition, intersection, subtraction, and null for self-intersection cases), $G_i,\ G_i$ are the set of n primitive geometries (e.g., blocks, cylinders, spheres, tori, etc.) used to create the overall model assembly. This formulation assumes that there are null operations performed for self-intersection of geometries (e.g., there is no operation performed on $G_{i=1}$ to $G_{j=1}$, for instance). Further, only one unique Boolean operation is performed on any two geometric primitives (e.g., $G_2 \cup G_5 = G_5 \cup G_2$ as per the commutative law in Boolean algebra). While we present the process of creating a CSG model as a formulation (Eqn. 14), the resulting geometry is not unique (many primitives can be combined to create the same solid), which is often why CSG is represented in a tree structure as shown in Figure 42. The choice of primitives, and how they are initialized dictate the way that the resulting object's shape can be manipulated parametrically.

Each primitive geometry G in Eqn. 14 can be further defined according to a set of discriminative control parameters, $p_K,\ K \in \{1, \dots, N_K\}$ which correspond to either dimensions or angles. For instance, the dimensions A, B, and C in Figure 42 are explicit primitive parameters. In addition, we can define a set of assembly parameters, $a_l,\ l \in \{1, \dots, N_l\}$ for an assembly structure A used to establish topology between objects in a model; again in the form of discriminative dimensions or angles. An example of a topological parameter could be the offset between two parallel features on separate primitives. Take for instance the I-beam shown in Figure 42. Rather than explicitly defining the height of block 2, it could be derived topologically (i.e., implicitly) as a function of the offset between features on block 1 and block 3. As such, both explicit primitive parameters and implicit topological parameters can be used to create and define CSG-based objects. Modification to these parameters can be invoked directly, or indirectly through the use of reference points which some modelling software provides. For the purpose of this study, we consider feature-based parameters directly for describing an object's shape.

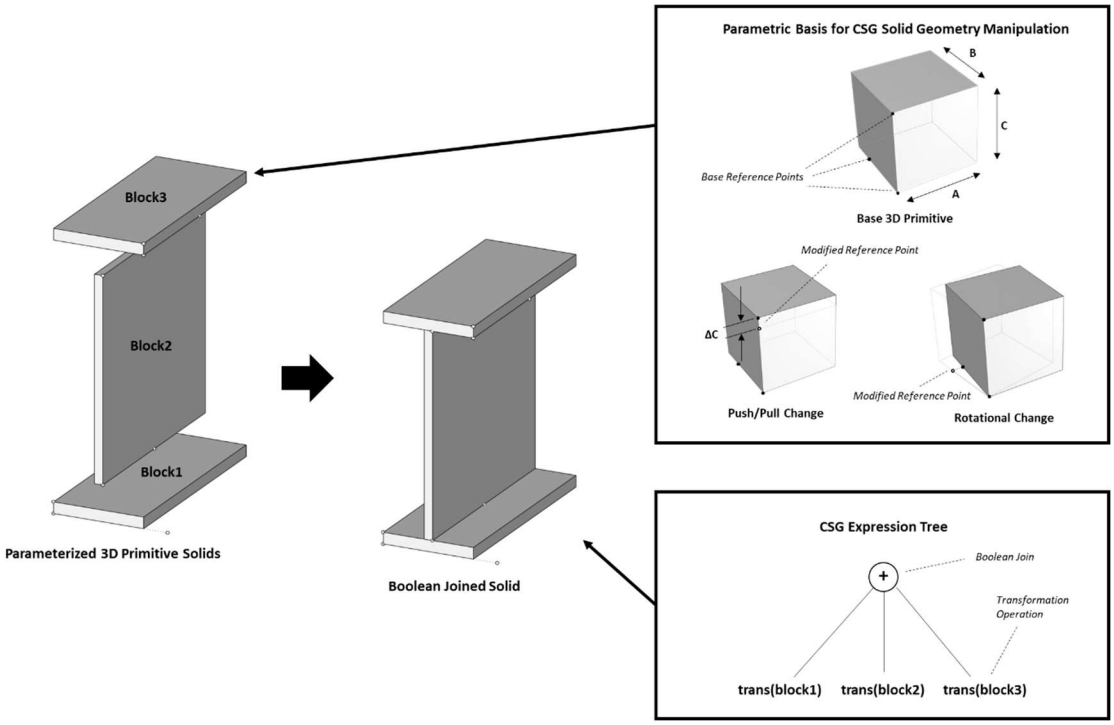

Figure 43: Parameterization for Feature-based (CSG) Representation of an I-beam Element

Control point-based scheme

While a range of geometric representations could be used for mathematical parameterization, we focus on Non-uniform rational B-splines (NURBS) since it has become the quasi-standard for geometric representation in 3D modelling due to its ability to represent both free-form shapes and common analytical shapes [296]. Unlike other parametric curvature representations (e.g., B-spline and Bezier), NURBS has four types of degrees of freedom (degree, control points, weights and knots) which affords the ability to represent closed curvature in addition to planar polysurface geometry. Given a set of $(n+1)$ control points, a p^{th}-degree NURBS curve is defined as:

$$C(u) = \frac{\sum_{i=0}^{n} N_{i,p}(u) w_i P_i}{\sum_{i=0}^{n} N_{i,p}(u) w_i} \qquad a \le u \le b$$

Eqn. 15

where P_i are the control points, w_i are the weights and $N_{i,p}$ are the pth-degree B-spline basis functions defined by the nonuniform knot vector,

$$U = \{a, \dots, a, \quad u_{p+1}, \dots, u_{m-p-1}, \quad b, \dots, b\}$$

Eqn. 16

In this case, by assuming that $a = 0, b = 1$ and $w_i > 0$, we can use rational basis functions $R_{i,p}(u)$ as follows:

$$R_{i,p}(u) = \frac{N_{i,p}(u)w_i}{\sum_{j=0}^{n} N_{j,p}(u)w_j}$$

Eqn. 17

in order to achieve the following compact expression,

$$C(u) = \sum_{i=o}^{n} R_{i,p}(u)P_i$$

Eqn. 18

This compact formulation allows us to express NURBS curves as piecewise rational basis functions and corresponding control points. This proves very efficient in terms of modifying basis curves by only considering control points as parameters. In general, NURBS shape modification is achieved by changing the knot vector, moving control points or changing the weights [297]. In this case, however, we can efficiently reduce the parameter space by only considering a modification to control points of predefined-degree curves. The notion of not considering knots in parameter modification is supported in literature since they do not carry a clear geometric meaning nor have an intuitive mathematical formulation [298,299]. There are essentially two types of geometry in practice where NURBS can be expressed in rational and non-rational forms. For polyhedral (i.e., planar surface) geometry which comprises the majority of objects in construction, NURBS curves can be assigned control point weights equal to 1 (i.e., this is the non-rational condition, which is equivalent to B-spline curves). On the other hand, control point weights can be varied (not all equal to 1) which creates the rational condition for NURBS to describe closed curvature features such as circles and ellipses (i.e., pipe geometry). In both the rational and non-rational case, we can rely solely on control point manipulation to achieve shape modification, without having to modify control point weights or knots. As depicted in Figure 43, control points on base (simplified) geometry can be manipulated through vector translation, and through insertion and subsequent translation. Relying solely on control point translation in some cases can cause undesirable local deformations, which prompts the insertion of additional control points. NURBS curves (like other parametric forms) have the unique characteristic that any number of additional control points can be added to the base geometry without modifying its shape [299]. NURBS curves also allow for unique modification abilities for polygonal geometry. In Figure 43, the cross-section of the I-beam can be changed to a different curvature degree (from degree 1 to degree 3) without changing the base shape. We see the effect this brings when translating control points – the result is a smoother shape. As the degree of

curvature and number of control points increase, the finer resolution and corresponding representational accuracy can be achieved.

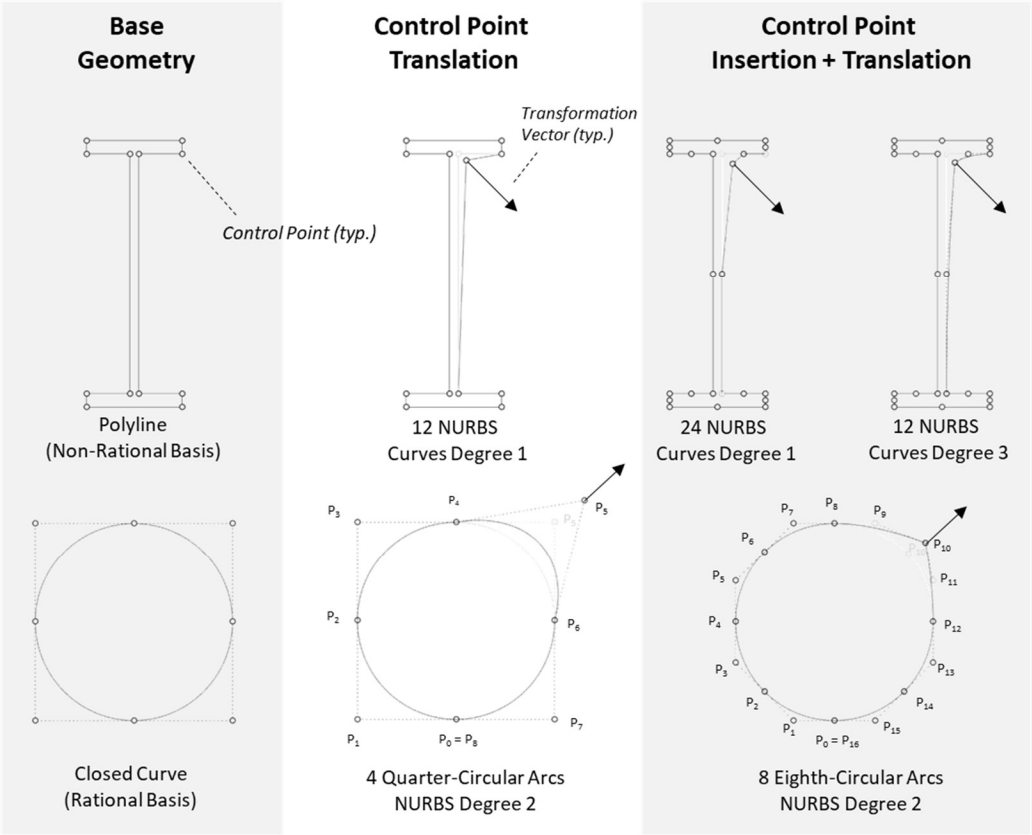

Figure 44: Control Point Manipulation for Polygonal and Closed Curve-Based 2D Geometry (note: control point weights and knots not shown for clarity)

According to Piegl [299], for each curve in a NURBS polysurface, translations to a given control point $P_k, 0 \leq k \leq n$ results in a new point, $\widehat{P_k}$ defined by the vector $V = \widehat{P_k} - P_k$. This produces a new curve, $\widehat{C_u}$ that is based on C_u from Eqn. 9, where all other control points are unaffected:

$$\widehat{C_u} = C_u + P_{k,p}(u)V \qquad u \in [u_k, u_{k+p+1}]$$

Eqn. 19

Piecewise NURBS curves can be used for modifying both polygonal and closed curve 2D geometry, however additional topological constraints must be introduced for handling 3D geometry (i.e., polysurfaces). Using a tensor product of NURBS curves (refer to Figure 44), we can express a NURBS surface $S(u, v)$ as a function of degree (p, q) in the respective directions (u, v) as follows:

$$S(u,v) = \frac{\sum_{i=0}^{n}\sum_{j=0}^{m} N_{i,p}(u)N_{j,p}(v)w_{i,j}P_{i,j}}{\sum_{i=0}^{n}\sum_{j=0}^{m} N_{i,p}(u)N_{j,p}(v)w_{i,j}} \qquad 0 \le u,v \le 1$$

Eqn. 20

where $P_{i,j}$ is the bidirectional control point net with weights $w_{i,j}$ and $N_{i,p}(u)$, $N_{j,p}(v)$ are B-spline basis functions defined on the knot vectors:

$$U = \{0,\dots,0, \quad u_{p+1},\dots,u_{r-p-1}, \quad 1,\dots,1\}$$
$$V = \{0,\dots,0, \quad u_{q+1},\dots,u_{s-q-1}, \quad 1,\dots,1\}$$

Eqn. 21

where $r = n + p + 1$ and $s = m + q + 1$. By using piecewise rational basis functions as shown in Eqn. 18 we can reach the following compact expression:

$$S(u,v) = \sum_{i=o}^{n}\sum_{i=o}^{m} R_{i,j}(u,v)P_{i,j}$$

Eqn. 22

There are two principles for modification of NURBS surfaces that need to be considered: (1) unnatural shape creation, and (2) tangency continuity. Moving a single control point normal to the surface of a (3+) sided polygon will create a surface that is no longer planar. As shown in the parametric topology constraints in Figure 44, modification of control point $P1'_1$(point 1 on surface 1) creates a non-planar condition. This premise leads to unnatural shape creation, which must be handled using topological rules and constraints [300]. One solution is to move complete sets of control points for a given surface to maintain planarity constraint (i.e., the "offset" surface approach). However, this approach requires additional surfaces to be created and/or potentially complex modifications to adjacent surfaces. Another approach is to split this surface into two separate planar sections (triangulation). This is problematic since creating more surfaces requires review and population of new semantic information. Both approaches also assume that the deformation of the object engenders a planarity condition, which is not always the case (e.g., large cast-in-place concrete surfaces can be non-planar). Therefore, rather than deriving complex topological constraints, we adopt the approach whereby each control point for a shape is free to translate in 3D space, so long as tangency continuity with adjacent surfaces is maintained. This in effect changes an initial planarity condition into a free-form curvature case. While this may be undesirable in some cases, this approach is much simpler than splitting surfaces or making complex adjacent surface modifications.

For most objects in BIM, the intersection of surfaces takes on a G^0 tangency continuity condition, where surfaces have a common linking curve. This condition creates sharp corners for planar feature-based geometry, as opposed to G^1, and higher-order G^n conditions which have filleted/smooth boundary conditions. As shown by [301], two adjacent surfaces $S_1(u,v)$ and $S_2(u,v)$ are G^0 continuous if (and only if) the following condition is satisfied:

$$BC(v) = \overline{BC}(v) = \frac{\sum_{i=0}^{n} N_{i,p}(u) w_i P_i}{\sum_{i=0}^{n} N_{i,p}(u) w_i} = K \frac{\sum_{i=0}^{n} \bar{N}_{i,p}(u) \bar{w}_i \bar{P}_i}{\sum_{i=0}^{n} \bar{N}_{i,p}(u) \bar{w}_i}$$

Eqn. 23

where $BC(v)$ and $\overline{BC}(v)$ are the boundary curves of the first surface and second surface respectively (derived from Eqn. 1), and K is a positive real number. Therefore,

$$P_i = \bar{P}_i,\ w_i = K\bar{w}_i \qquad i = 0,1,\dots,n$$

Eqn. 24

This formulation means that all control points P_i on the first surface must equate to the coincident points $\bar{P}_i$ on the second surface after any changes are made. In cases where a higher-order continuity condition is required, Zheng et al. provide further derivation for such G^N conditions [302]; however, for simplicity, we do not directly consider this condition in this work.

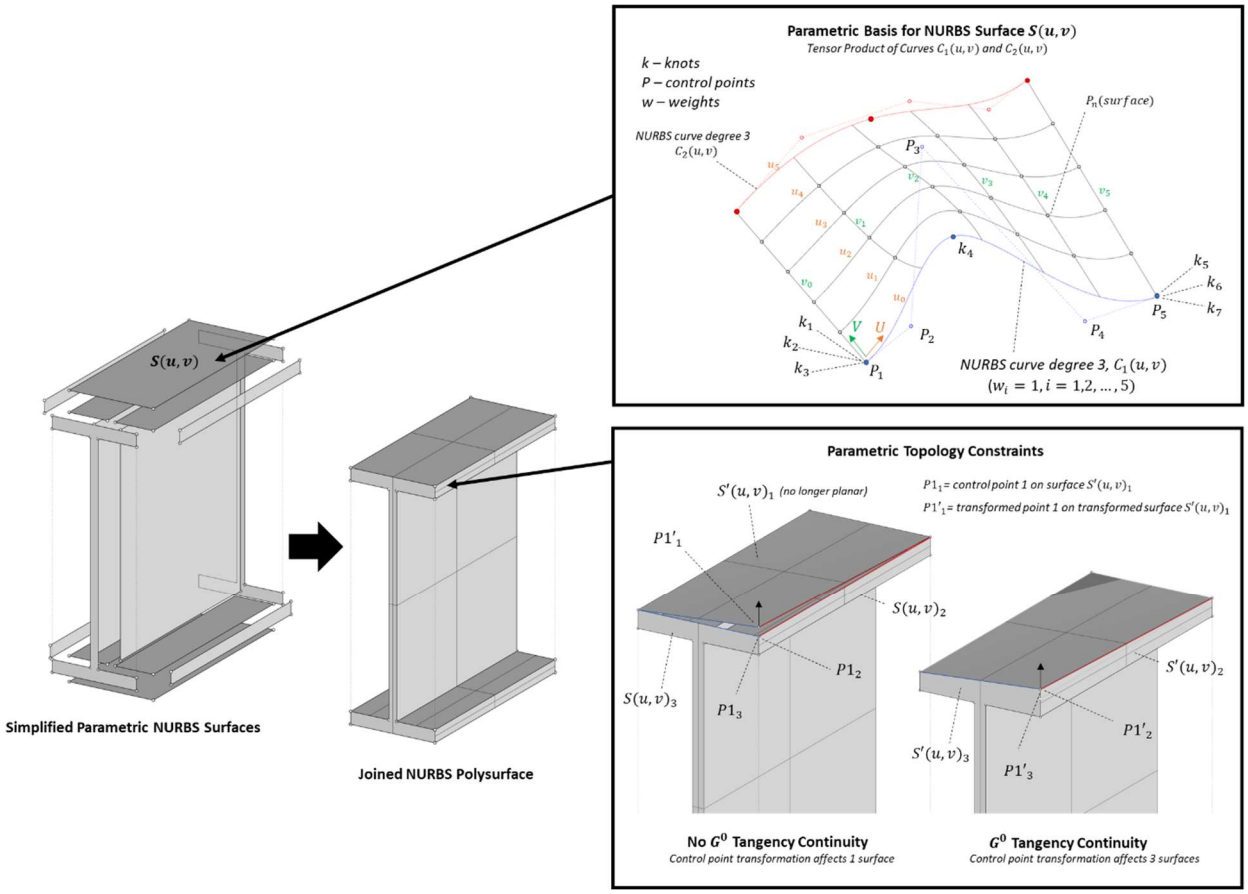

Figure 45: Parameterization for Control Point-Based (NURBS) Representation of an I-Beam Element

7.3.2.3 Summary of Shape Parameterization Schemes

In summary, according to the two most popular representations in BIM, shape parameterization can be approached through feature-based specification using CSG, or through control point-based specification using NURBS. On one hand, CSG tends to have fewer parameters and produces a more simplified geometric representation than NURBS. However, CSG can be more tedious to parameterize topological constraints (which must be done explicitly) such as ensuring base primitives maintain contact relationships after modifications are made. On the other hand, NURBS can implicitly handle topological constraints using continuity conditions such as G^0 tangency. NURBS tends to favour greater representational fidelity (which is demonstrated in the case study and discussion of this chapter) since a base NURBS polysurface can be discretized by adding additional control points as needed without modifying the initial shape.

7.3.3 Objective Function Formulation

The objective function, f in this method finds the optimal BIM parameter instances, x that minimize the root mean square (RMS) of the Euclidean distance, d between each BIM surface and the input point cloud according to

$$min\ f = \sqrt{\frac{1}{T}\sum_{t=1}^{T} d^2\left[M_t\left(x_{t_i}\right), PC_t\right]}$$

Eqn. 25

where T is the total number of model surfaces, $M_t\left(x_{t_i}\right)$ is a given model surface defined by control parameters x_{t_i} and where PC_t is the point cloud segmented for the given surface under evaluation. Using this objective function, the parameter update process is as follows: parameter instances drive model changes, for each instance, the model is converted into a mesh representation to compute distances to nearest points in the point cloud, then the RMS is computed, followed by the use of a metaheuristic to update parameter instances. This process is repeated until the desired threshold is met.

The process described above mirrors model-based vision, where parameterized models are projected into 2D and fit to images. In model-based vision, an initial set of parameters are used to associate model and image features. The solution is then solved when the parameter values enumerated enable a minimum least-squares calculation. Newton's method and the Levenberg-Marquardt method are often used to compute a vector of corrections (using local linear approximation) after each squared distance calculation and to ensure convergence of the solution to a local minimum [303]. The types of optimization methods employed in registration between datasets are grouped as local deterministic methods (e.g., gradient descent, ICP), global deterministic (e.g., graduated assignment, spectral method), stochastic (e.g., genetic algorithm, RANSAC), and constrained search (e.g., geometric hashing) [304]. Rigid alignment transformations (i.e., pose parameters) can be efficiently solved using local search algorithms such as Iterative Closest Point (ICP). For non-rigid alignment (i.e., shape parameters), a more approximate method is relied upon due to the higher dimensional nature of the problem [305]. The challenge of using ICP for non-rigid alignment is the tendency to lock into a local minimum since the algorithm follows a single path. This is where metaheuristics can be particularly useful, especially where there are sufficient constraints to guide the optimization process.

7.3.4 Metaheuristic Optimization

This research employs the use of two well-known metaheuristics to perform optimization of BIM parameters: genetic algorithm (GA) and simulated annealing (SA). These metaheuristics function differently in that they represent two distinct approaches for performing combinatorial optimization: namely, population-based, and trajectory-based [139]. Trajectory-based approaches function by searching between neighbourhood structures imposed on the members in a search space, whereas population-based methods incorporate an implicit learning component by evaluating and filtering out members in a solution set. While the focus of this work is not to explore a comprehensive set of metaheuristics, we employ GA and SA since they have been previously shown to be efficacious in solving similar objective functions with the number of parameters [292,293] to that shown in this chapter.

GA mimics the process of 'survival of the fittest' in a population and has been used as a proven way to solve hard optimization problems since their inception in the 1970s [306]. In GA, the parameters of the search space (genes) are encoded into chromosomes, which are contained in a population sequence and represent a given point in the search space. Iterations are carried out, whereby the population of a set size of chromosomes gives preference to the best performing chromosomes with respect to a fitness function. In the case of the proposed method, the BIM parameter instances, x are the genes in each chromosome. Biologically inspired operators such as crossover and mutation are used to generate new chromosomes to find better regions in the solution space. GA is initialized by selecting the desired population size, the number of generations (or a convergence threshold), crossover rate and mutation rate.

SA is said to be one of the oldest metaheuristics and is inspired by the annealing process of metal and glass, where an energy configuration is minimized through successive heating and cooling [137]. SA is based on random sampling and avoids poor local optima by allowing occasional hill climbing through a pair of nested loops which favour hill descent over hill climbing by some probability (i.e., the Boltzmann distribution is typically used, $\exp\left(-\frac{f(s\prime)-f(s)}{T}\right)$ where $f(s')$ is the new solution, $f(s)$ is the current solution and T is the temperature of the function). This probability that a hill climb occurs decreases over time since a cooling ratio $(0 < r < 1)$ is used to decrease the temperature after each new iteration [307]. SA is thus initialized by selecting the initial temperature, the cooling ratio and the sampling process between each solution iteration.

The final step to using metaheuristics for optimization involves specifying the stopping criteria, which relates to a state of convergence. Since both GA and SA operate by successively refining solutions across numerous generations, the stopping criteria become an important factor of the resulting solver efficacy. In

general, stopping criteria can be a temporal limit, a maximum number of generations to compute, a numerical threshold for the fitness function to reach, or a numerical threshold in the change of the fitness function or all parameters across successive generations/iterations. Pseudocode for feature-based parameterization and control point-based parameterization using a genetic algorithm are shown the following algorithms (rather than providing similar pseudocode for an approach using simulated annealing, the reader is directed to Algorithms 3, and 4 which outlines an optimization approach using simulated annealing).

Algorithm 5. Feature-based parameterization using a genetic algorithm

Inputs:
Element[] → accessed as CSG object with topology defined by prismatic variables
PC = cropped point cloud for object to be updated
Genes: G[] *the following genes are shown for illustrative purposes based on the case study*
G1: length_var = variance on length dimension (length_min < length_var < length_max)
G2: width_var = variance on width dimension (width_min < width_var < width_max)
G3: depth_var = variance on depth dimension (depth_min < depth_var < depth_max)
G4: rot_var = variance on rotation in XY plane (rot_min < rot_var < rot_max)
G5: x_pos_var = variance on x position (x_pos_min < x_pos_var < x_pos_max)
G6: y_pos_var = variance on y position (y_pos_min < y_pos_var < y_pos_max)
Objective Function:
f() = root mean square between BIM object surfaces and Euclidean distance to nearest points in pc

```
01  WHILE time < limit OR f()I < convergence limit
02  DO
03      Select individuals from G[] (fitness proportionate)
04      Randomly generate individuals from G[]
05      Apply mutations
06      Re-evaluate f() =
07      G[]i+1 ← newly created individuals
08      I = i+1
09  FOR each species evaluated
10  DO return best performing individuals from G[] → G[]optimal
11  RETURN f() for G[]optimal
12      END
```

Algorithm 6. Control point-based parameterization using a genetic algorithm

Inputs:
Element[] → accessed as B-rep object with topology defined by control points
PC = cropped point cloud for object to be updated
Genes: G[] *the following genes are shown for illustrative purposes based on the case study*
G1: control point 1 x-position variance
G2: control point 1 y-position variance
G3: control point 1 z-position variance
G4: control point 2 x-position variance
G5: control point 2 y-position variance
G6: control point 2 z-position variance
…
G22: control point 8 x-position variance
G23: control point 8 y-position variance
G24: control point 8 z-position variance
Objective Function:
f() = root mean square between BIM object surfaces and Euclidean distance to nearest points in pc

WHILE time < limit **OR** $f()_i$ < convergence limit
DO
    Select individuals from G[] (fitness proportionate)
    Randomly generate individuals from G[]
    Apply mutations
    Re-evaluate f() =
    $G[]_{i+1} \leftarrow$ newly created individuals
    i = i+1
FOR each species evaluated
DO return best performing individuals from G[] → $G[]_{optimal}$
RETURN f() for $G[]_{optimal}$
    END

7.4 Case study

During the construction of an industrialized building (Figure 46), it was necessary to obtain accurate measurements of the cast-in-place footings to assess geometric compliance for connected piers, and more importantly, for the structural connections used to fasten stacked modules (Figure 45). As such, the proposed methodology was implemented to generate an accurate as-built BIM and for progressively providing required geometric compliance assessments. Laser scanning at the project site was conducted after the forms for the concrete footings were removed. Permanent targets were surveyed using a total station and subsequently referenced in the resulting 3D point cloud obtained from laser scanning. Once the 3D point cloud was aligned with the building coordinated system specified in the as-designed BIM (using Autodesk® Revit), the BIM was parameterized for the concrete footings, which are rectangular prisms with overall dimensions of 7'8" (2337 mm) wide by 7'8" (2337 mm) long by 16" (406 mm) tall and have reinforcing steel at a cover of 2" (51 mm).

Figure 46: Industrialized building used for case study analysis

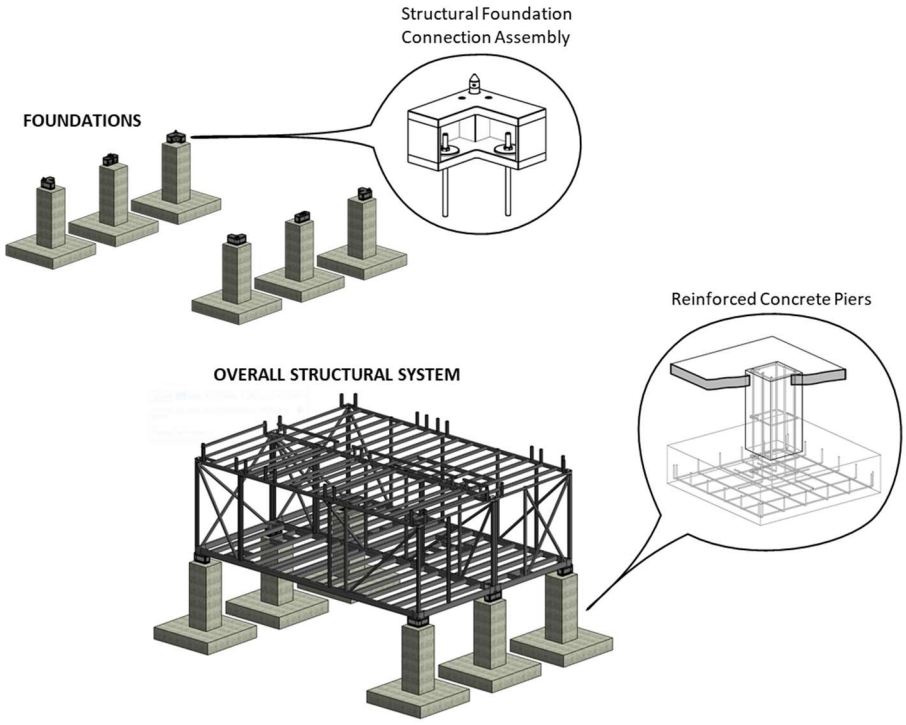

Figure 47: Connection of Cast-in-Place Concrete Foundation to Structural System

7.4.1 BIM Parameterization

Feature-based parameterization was done with CSG representation native to Revit® using the following parameters: length, width, depth, position in X, position in Y, position in Z, and rotation about Z. These parameters were created within the Revit® object *Family Type* editor, so that object instances can be set for each object independently, while still having the same set of parameters. As shown in Figure 46, all parameters except for position in Z are directly assigned within the *Family Type* – position in Z is parameterized separately using the properties tab in Revit® since this parameter is topologically related to other BIM objects. In other words, parameters created in the *Family Type* are intrinsic to an object, whereas additional parameters that are extrinsically related to other objects and features are parameterized outside of the *Family Type*.

Control point-based parameterization follows a simpler process since a user does not need to develop custom instance parameters that are required for feature-based parameterization. In this case, the control points of the base geometry are directly accessed and then translated in space in order to manipulate the geometry. Using NURBS, geometry does not need to be explicitly parameterized, but rather, control points used to establish an object's surfaces can be deformed. For simplicity, we only transform control points as parameters to modify, rather than knots, weights, and B-Spline curve degrees. As such, there are a total of 8 BIM parameters related to each of the corner control points for the rectangular prismatic footing geometry.

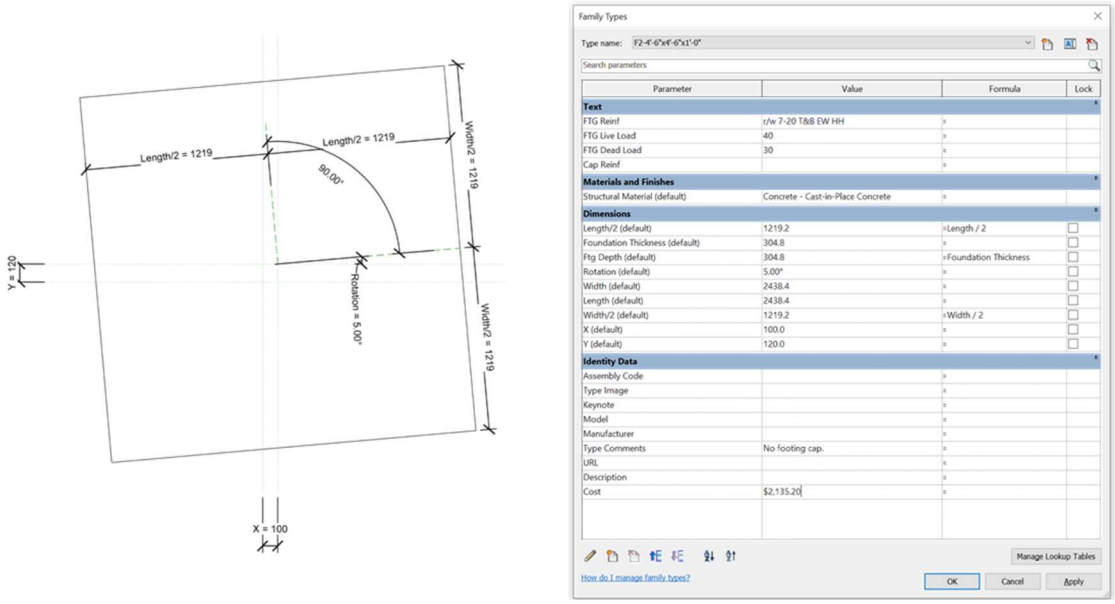

Figure 48: Revit® Family Type Editor for Footing Objects, Parameterized According to Feature-Based Scheme

7.4.2 Parameter Optimization

The optimization process was developed as computational algorithms using Grasshopper® (the reader is directed to Appendix A for these scripts). Using Rhino.Inside®, which is an open-source project that enables the use of Grasshopper in Revit®, both feature-based and control point-based schemas are addressed in a single programming environment. For the feature-based schema, Rhino.Inside® affords the ability to access and manipulate Revit® object parameters directly, while the control point-based schema is run entirely on the Rhinoceros® platform. Parameters for each schema are instantiated using numerical sliders that allow the user to specify domains, which function as limits on the parameter space. The setup of these sliders is important for ensuring that the solution is computed locally; i.e., during metaheuristic optimization, the solver explores solutions across the parameter space, which could result in fitting an object to the wrong location in the point cloud. In this case study, the sliders for dimensional parameters are specified with +/- 150 mm limits, which is large enough to allow for site tolerances, while still less than the nominal gap between each footing of 3' 6 ½" (1080 mm). The slider for the angular parameter in the feature-based schema was set to +/- 5°. The optimization engine, whether solved using GA or SA, takes a series of inputs (genes for GA, variables for SA) which relate to the BIM parameters. While translations and rotations can be used directly as inputs, feature dimensions (e.g., length) and control point positions must be instantiated as numerical variations, in order to use batch constraints rather than unique constraints for each gene or variable. In total, there are 6 genes/variables for the feature-based schema and 24 genes/variables for the control point-based schema as outlined in Figure 47.

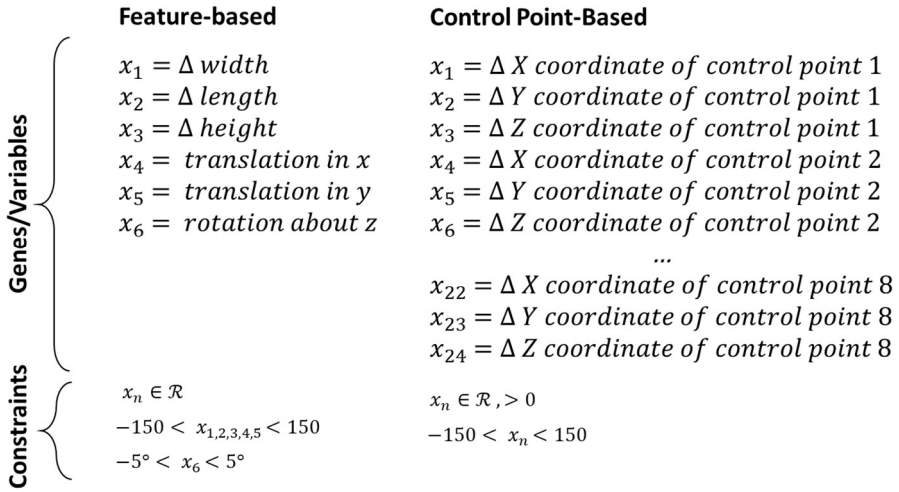

Figure 49: Enumeration of Genes (Genetic Algorithm)/ Variables (Simulated Annealing) and Numerical Constraints for Case Study Example

Prior to performing parameter optimization, the point cloud of the footings was post-processed in order to reduce noise and clutter, which improves the temporal performance of the optimization. CloudCompare was used to remove both noise and non-planar features from the point cloud (through RANSAC). Another key step for point cloud processing occurs within the computational algorithms, where for each footing, the overall point cloud is cropped to just the vicinity of a given footing. This ensures that data from other footings, or from remaining noise and clutter do not impact the optimization process. Voxel-based downsampling is performed to ensure that each face of the footing has roughly the same density. Without this step, the algorithm has a tendency to focus locally on regions in the point cloud with higher density and skews the results of the fitting process. Then, GA and SA optimization are performed using *Galapagos* [252], which is a dedicated metaheuristic solver. For GA, the required setup involves the selection of the population size (set to 30), criteria for aborting the solver (a threshold of 1 mm on the fitness function), and factors for changing the population across generations (maintaining 5% of the population and inbreeding by 75% between each generation). For SA, the required setup involves selecting the initial temperature (set to a logarithmic percentage of 100%), the cooling decay factor (set to 0.95), and the drift rate (set to 25%). It should be noted that these setup parameters for both GA and SA were determined by testing the best rate of convergence during the optimization process. The fitness function was derived using a mesh-compare function provided in the *Volvox* plugin [308], which computes the Euclidean distance between each point in a cloud and a corresponding mesh. In this case, we create a temporary mesh of the input geometry (which can be done for both the CSG and NURBS geometries without loss of fidelity), in order to efficiently compute deviations. Finally, these deviation values are used to generate an RMS value, which is taken as the fitness function.

The stopping criteria for each optimization approach were approached in slightly different ways. It is generally difficult to use the same stopping criteria for both GA and SA for comparison purposes, given the fact that these metaheuristics operate in unique ways. While we could use an absolute convergence value for the fitness function (e.g., stop the solver when the fitness function value is less than 2 mm), this restricts a given optimization approach from its representational accuracy. The problem of solely using a temporal limit is it restricts the ability to understand the computational efficiency of each method. To address this, we adopt two approaches that attempt to capture whether a given method is approaching convergence. For GA, a threshold was employed, where the solver was stopped when the variance in the value of all chromosomes in a given generation was less than 2 mm for, up to a maximum run time of 60 mins. For SA, a minimum of 3 annealing tracks was run. During this, the solver would be stopped when two sequential annealing tracks performed worse than the third-prior annealing track, up to a maximum run time of 60 min.

7.4.3 Results

For each of the 6 footings, experiments were carried out using both GA and SA to update the parameterized BIMs. The deviation between the as-built data described by the 3D point cloud and the as-designed BIM had an average discrepancy between 21.71 mm (the least error) and 109.82 mm (the largest error)[18]. The contractor noted during construction that the placement tolerance for formwork was equal to +2"/-0.5" (+51 mm/-12 mm) in any given direction (X, Y, Z). The way to interpret this tolerance is that more concrete would be added in a conservative case, and in the worst-case scenario only 0.5" LMC (least material condition) would occur. This was approached pragmatically by adding an additional 1" to the required dimensions for each footing. Generally, this tolerance was respected, with the exception of one footing that had a large vertical deviation, which was lower than nominal by roughly 4" (102 mm). Even despite the ability to achieve site tolerances, updating the BIM in an accurate manner was important for predicting downstream issues with adjoining piers, the height and coverage of rebar, and for the global alignment in the placement of structural foundation connections. Each experiment conducted was assessed in terms of the reduction in the final deviation between the as-built data and updated BIM. In addition, the time required for optimization was recorded in order to assess computational efficiency (the machine employed has an Intel Core i7-8650U CPU). The results of the final average deviation, reported in terms of RMS, is shown in Figure 49. The vertical axis in this figure is split into two distinct scales in order to visually enhance the spread of the initial and final deviations of the BIMs for each footing.

The first set of observations to note deals with the variance of the final deviation across all footings. For footing 1 and footing 2, the final spread of deviations is compact, as compared to footing 5 and footing 6. This is because the as-built geometry of the first two footings maintains its topology between surfaces closer to the nominal 90° as opposed to the last two footings, which has noticeably skewed angles. Figure 50 shows a top-down view of the point cloud for footing 5, along with the CSG-GA and NURBS-GA optimization approaches. As shown, the CSG-GA approach maintains topology at 90° whereas relaxing this constraint for the NURBS-GA approach enables it to yield in a better fit to the point cloud (6.72 mm compared to 15.34 mm). Both of these GA methods do, however, result in a substantial decrease in the final model fit compared to the as-designed BIM.

---

[18] *The errors reported in this research are specifically discrepancies between the point cloud and the resulting BIM pose and shape – the error between the 3D point cloud and the physical objects is not directly considered here but will contribute to the global errors of this framework.*

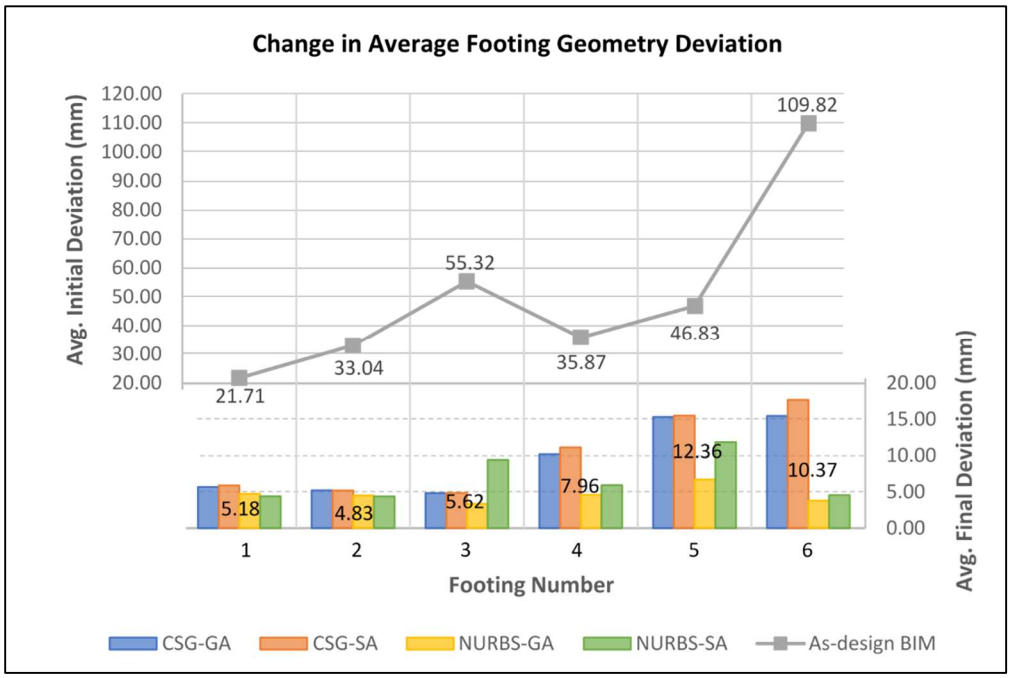

Figure 50: Change in average deviation between as-design BIM and parametrically updated BIM to the as-built conditions described by the 3D point cloud

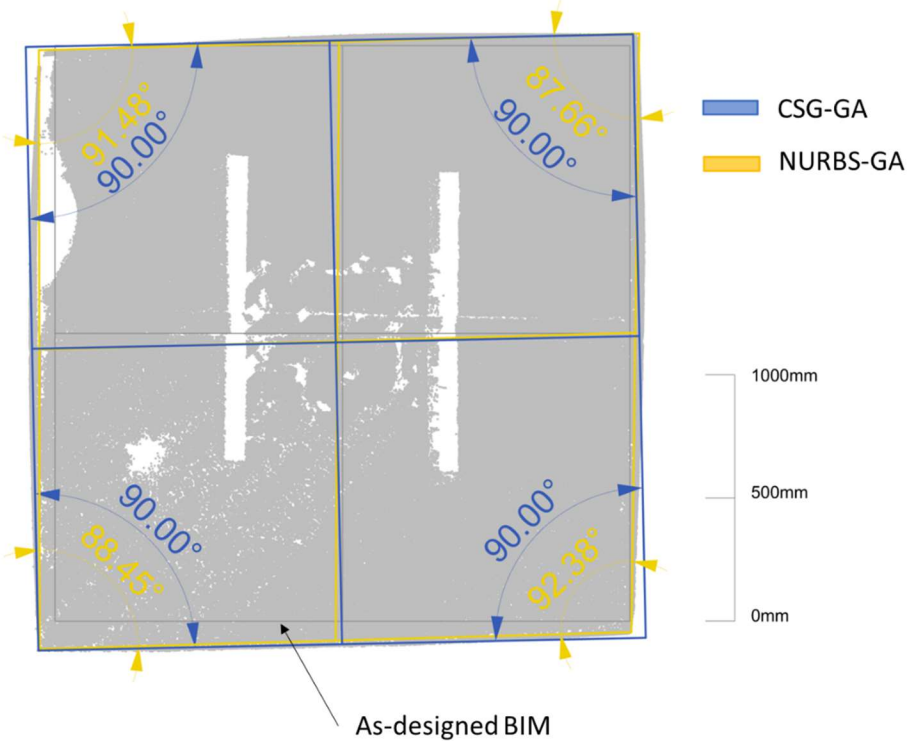

Figure 51: Plan-View Comparison of Geometric Fit for Genetic Algorithm Optimization for Footing 5.

The next observation relates to the representational accuracy between a feature-based and control point-based schema. For every footing, CSG parameterization generally had larger final deviations compared with the NURBS parameterization. Again, this relates to the ability of the NURBS method to relax its topological constraints implicitly. In order to achieve a higher representational fidelity using CSG, a more complex parameterization process is necessary.

When comparing the performance of GA to SA, we see the general trend that GA outperforms in terms of representational accuracy, whereas SA outperforms in terms of computational efficiency. When presenting the results of each method in terms of average final deviation and time for computation, we see across all 6 footings that CSG-GA achieves 9.46mm at 10mins, CSG-SA achieves 10.04 mm at 6 mins, NURBS-GA achieves 4.63 mm at 22 mins and NURBS-SA achieves 6.75 mm at 18 mins, respectively (Figure 51).

The final observation noted during these experiments is based on the point cloud coverage of footings. Due to the inability to capture the bottom of the footings, the Z-axis based parameters across the experiments exhibited a lot of variability, and in many cases, errors were introduced. In an ideal experiment, complete coverage of an object to be updated would be captured in the point cloud. However, this is challenging to accomplish, especially in the case where an object sits on highly variable terrain (as in this case study). The control point-based schema (NURBS) is very sensitive to missing data in the point cloud as was observed for setting the height of the footings. A feature-based schema (CSG) is less sensitive to missing point cloud data since it can utilize its topological constraints (e.g., all surfaces are locked at 90°, or a single height parameter for an object) to mitigate the impact of missing data. Regarding the vertical faces of the footings, complete coverage around the entire perimeter at the base of the footings is required for NURBS to generate accurate geometry. On the other hand, only one region of the footing base is required for CSG to generate accurate geometry. As such, there are inherent trade-offs between representational accuracy that need to be considered when accounting for point cloud coverage and the parameterization schema.

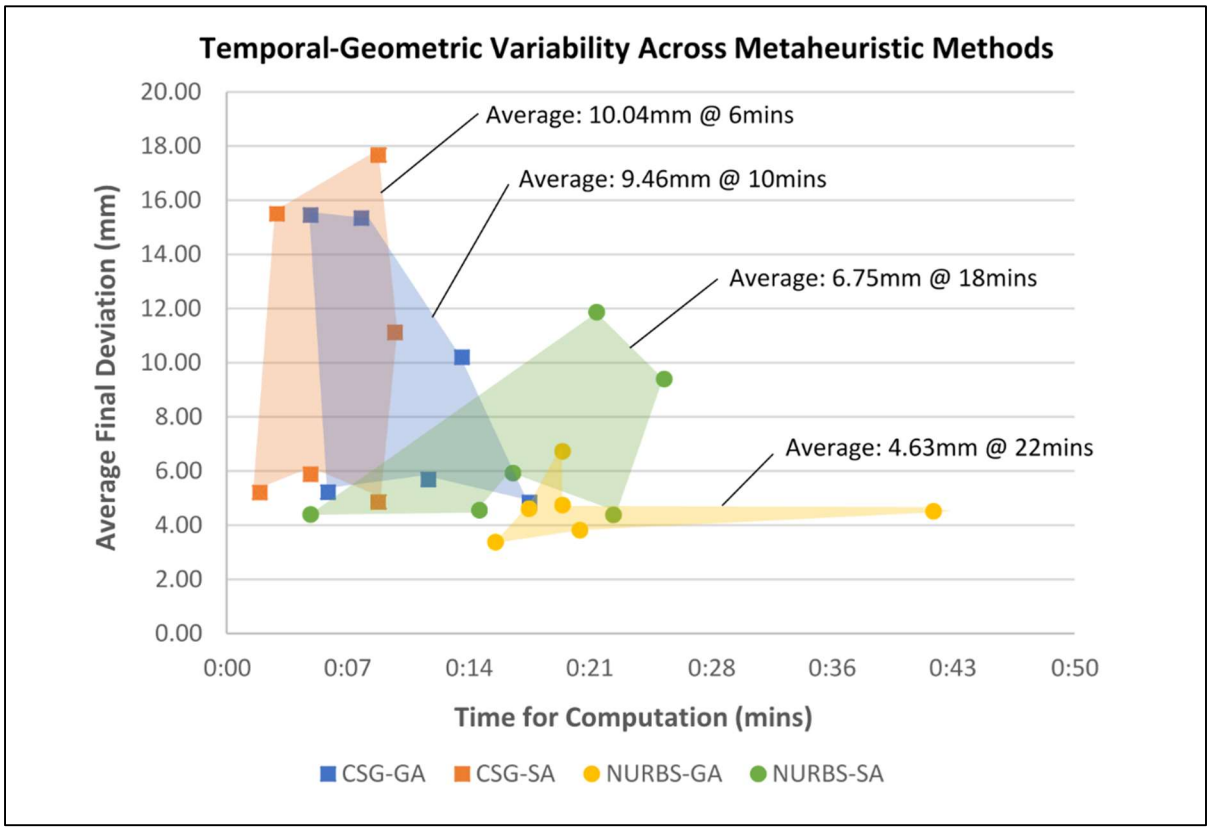

Figure 52: Performance of each metaheuristic method for updating BIM in terms of time for computation and average final deviation with the as-built condition

7.5 Discussion

This case study demonstrates how metaheuristic optimization can be used to update a BIM parametrically to represent the as-built conditions described by a 3D point cloud. The efficacy of each optimization approach is reported in terms of computational time and an average final deviation value. This deviation value is a measure of the Euclidean distance between the point cloud and the final resulting BIM geometry. It is important to note that this deviation value cannot be used as a global indicator of the performance of a given optimization method. In cases where the as-built geometry experiences complex non-rigid deformation (e.g., local cavities, non-planar buldging, etc.), the final deviation value can be non-zero, despite the best attempts at parameterization and despite the ability for a metaheuristic method to perform optimally. One could argue, however, that at some level of granularity, the right parameterization of geometry could be used to describe any type and degree of non-rigid deformation. This is not feasible to perform in many cases, due to the level of complexity and computation required. On the other hand, missing data in the point cloud can skew the accuracy of the final geometry, which may not be reflected in the average final deviation value (i.e., in theory, a deviation value of 0mm could

be achieved for an erroneous resulting geometry). As such, it is important to visually inspect the results of the proposed methodology. Despite these challenges, we have shown through two distinct parameterization schemas, that the proposed methodology can still achieve an accurate final representation of as-built geometry in a computationally efficient manner.

This study also explored the unique tradeoffs between parameterization schemas and metaheuristic optimization methods with respect to non-rigid deformation. NURBS tends to favour greater representational accuracy since a base NURBS polysurface can be discretized by adding additional control points as needed without modifying the initial shape. This means that NURBS geometry can engender greater localized adjustability, which is important for minimizing errors to the as-built state when updating a BIM. The discretization of NURBS geometry can also be handled automatically using computational algorithms, whereas this is much more difficult to perform on CSG geometry. While NURBS affords this benefit of discretization, naturally NURBS representation tends to have more control parameters which translate into greater computational demand during optimization. In general, it is best to minimize the number of control parameters since optimization with shape parameters is a computationally expensive process [294]. As such, it is recommended to adopt CSG when localized adjustability can be crude (i.e., desired accuracy on the order of centimetres), and simplified NURBS representation when more granularity (i.e., desired accuracy on the order of millimetres) is required. As a final experiment, we explored the use of a discretized NURBS schema to assess its ability to achieve greater representational accuracy than a simplified NURBS schema. Since footing 5 had the most profound occurrence of non-planar surface deviations, this object was selected. By discretizing the NURBS surfaces at the midpoint of each boundary curve (i.e., B-spline curves were changed from degree 2 to degree 3), using a genetic algorithm the average final deviation was reduced from 6.72 mm to 4.54 mm at a run time of 120 mins (after 60 mins, the average deviation was at 5.50 mm). Midpoint discretization increased the number of genes from 24 to 60, which increased computational demand. As expected, we observe a general trend that representational accuracy increases at the expense of greater computational demand across CSG, NURBS, and discretized NURBS schemas (Figure 52). Future research should explore optimal methods for discretizing control points in order to balance computational complexity with representational accuracy for updating BIM elements.

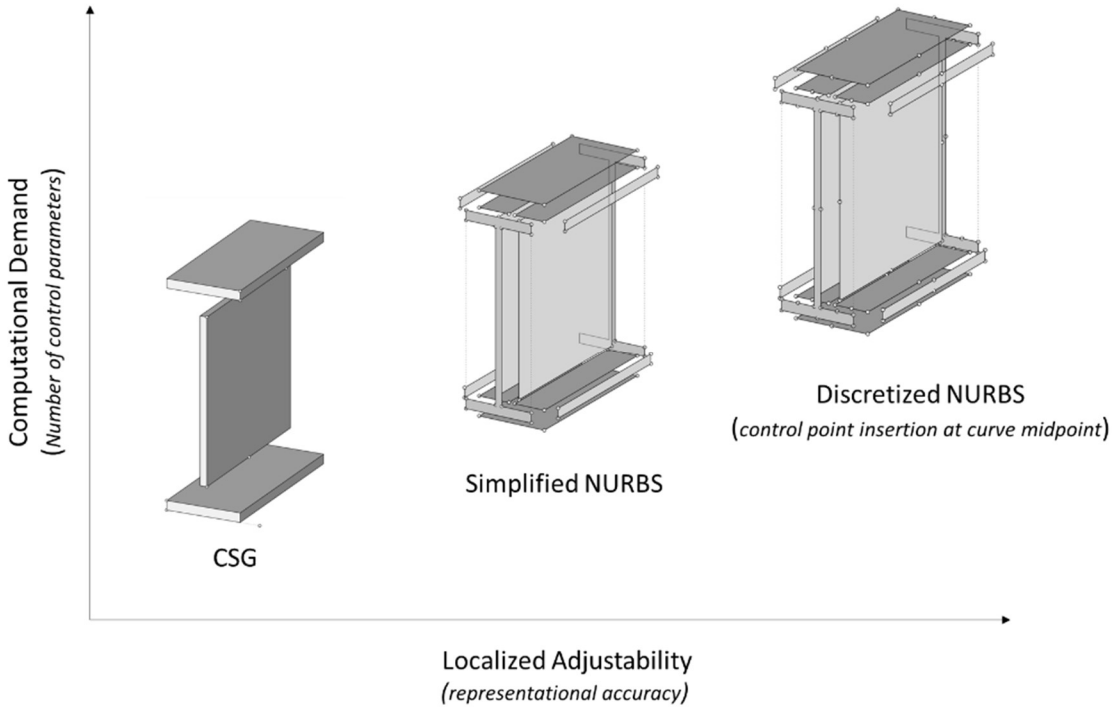

Figure 53: Generalization of the Trade-off Between Computational Demand and Localized Adjustability for CSG, Simplified NURBS and Discretized NURBS Geometric Representations

Automated BIM updating has great potential, particularly for industrialized building construction. This is because there is an increasing degree of semantic information being developed upfront during design. Rather than having to recreate all of this information during dimensional quality control and as-built BIM creation processes, this framework has the ability to only update the existing geometric data, while preserving semantic information.

Chapter 8: End-of-Life Semantic Enrichment Algorithms for Industrialized Buildings

This chapter presents developments made by the author which have been published (or are in the process of being published) in the following articles and conference papers [309,310]:

- **Rausch, C.,** Sanchez, B., & Haas, C. (2019). Spatial Parameterization of Non-Semantic CAD Elements for Supporting Automated Disassembly Planning. Modular and Offsite Construction (MOC) Summit Proceedings, 108-115.

- **Rausch, C**., Sanchez, B., Edwards, C., & Haas, C. (2020). A computational model for product cycling of modular buildings. ASCE Construction Research Congress, Tempe Arizona.

- Sanchez, B., **Rausch, C.,** Haas, C., (2020). Feature-constraint modelling for configurable and adaptable modular buildings. Submitted Dec 1, 2020. Advanced Engineering Informatics.

This chapter presents algorithms for semantically enriching geometric models used in industrialized building construction for activities occurring at the end-of-life stage. This topic remains elusive in existing literature and given that the uptake of IBC is expected to continue well into the future, it is inevitable that the end-of-life stage will need to be addressed for these assets. As the background section presented below will explore, industrialized assets have a unique opportunity for disassembly, which opens a range of applications for a circular economy. Compared to previous chapters, the algorithms presented herein are much more difficult to validate, since comparison with 'ground truth' measurements is not directly feasible. However, the purpose behind these algorithms is to demonstrate that many of the same approaches to the previous algorithms (i.e., exploitation of innate geometric and topological properties of assemblies) can be used to generate semantic enrichment processes.

This chapter begins by highlighting the background for the need to develop computational tools for addressing the end-of-life stage of industrialized buildings. In addition, the reader is also directed towards Appendix B, which presents a study outlining the potential that industrialized buildings afford with respect to the reduction of life cycle impacts as well as business models that can be used. This chapter then presents a computational algorithm that automatically extracts metadata required for an existing disassembly planning framework, initially developed by Benjamin Sanchez. This chapter then presents the computational basis for implementing 'product cycling' which is a functional way to extend the useful life of industrialized buildings by adding or subtracting modules to an existing building.

8.1 Background

Closing material-loops has been traditionally difficult to achieve within the construction industry. This is primarily because buildings are often custom made by a large group of participants and lack fundamental rules for supporting circularity such as ensuring buildings can be suitably deconstructed and enabling products to be easily reused [311]. This is predominately where industrialized building construction can offer sizeable advantages. Given the nature in which industrialized buildings (e.g., modular buildings) are brought together at the job site, they also have desirable attributes for disassembly. Even apart from the inherent advantages of disassembly, simply the ability to relocate modular assets has been shown to improve circularity by facilitating extended usability, and thus providing an alternative to otherwise hastened linear material flows [183]. The past five years have seen significant growth in the modular construction industry. From 2015 to 2020, the size of the modular construction market in North America has doubled, from 2.4% to roughly 5% [6,7]. As this growth trajectory is continued to proceed well into the future, there are significant opportunities to view the modular and prefabrication industry as a catalyst for realizing a circular economy.

In life-cycle management of existing buildings, there is a growing interest to improve performance holistically from cradle to grave (i.e., from manufacturing to end-of-life). This is required to improve sustainability and to create the conditions necessary for a circular economy [312], which is a model that moves away from a linear product usage (i.e., disposal at end-of-life) towards increasing levels of reuse and product recovery [313]. One way to address end-of-life product recovery in construction is adaptive building reuse which involves restoring and or changing the use of buildings entering their disuse stage. Adaptive reuse can maximize the residual utility and value of our ageing building stock, bringing significant environmental and sustainability benefits. Disassembling components according to a specific sequence of steps (i.e., “disassembly sequence planning”) is a key part of the adaptive reuse process [314]. Disassembly sequence planning is common in the manufacturing industry, where it is used to extract and repair defective components in an assembly or for recovering salvageable components at a product’s end-of-life. Due to a lack of updated information, disassembly sequence planning in manufacturing is performed using incomplete data between the overall assembly and sub-assemblies [315]. Similarly, in construction, updated data for components is not available since as-built models are often not current nor contain the required semantic information. As a result, disassembly planning relies on manual processes for defining relationships between components. Previously, the authors developed a novel framework for adaptive reuse of buildings based on the disassembly graph model [314,316]. This framework is the first of its kind to apply disassembly planning in construction in order to target key

components for selective disassembly. Although this research creates tremendous opportunities for the construction industry, a major challenge in this work was that key spatial relationships of components had to be extracted manually, which is very tedious, time-consuming and prone to errors.

While extracting geometric information from 3D objects in BIM is a relatively trivial endeavour, the development of algorithms for higher-order semantics (such as complex spatial relationships) is a challenge and remains elusive in many spheres of the construction industry [152]. To address this, the following section presents the development of a combinatorial algorithm for extracting semantic information required for disassembly planning. It functions by parameterizing objects in the principal Cartesian axes (+/-X, Y, Z directions), and through a sequence of combinatorial moves, detects relations between objects using a clash detection function. Collectively, this process provides a way to analyze spatial parameters of components automatically which is demonstrated using a real adaptive reuse project.

8.2 Combinatorial Algorithm for Disassembly Planning Semantic Enrichment

This section outlines the development of an algorithm which automatically extracts key spatial relationships between objects in a BIM automatically for the purpose of supporting automated disassembly planning. This algorithm is based on a previously developed framework by Sanchez et al. [316] for disassembly planning of buildings (Figure 53). While this framework was initially developed for use in existing buildings (where adaptive reuse is being considered), it has the ability to also be applied to industrialized buildings. This framework has five key matrices that define the underlying mechanics in terms of the spatial relationships between components in an assembly (information regarding how to obtain the 3D BIM model and how to target the disassembly components that can be found in [314]). The first matrix (component contact constraint matrix) defines the direct connectivity between components c_n'. The second matrix (component motion constraint matrix) defines the first object(s) that will obstruct an object of interest from being disassembled in a given direction. The third and fourth matrices define the contact and motion constraints for fasteners between objects. The fifth matrix (component projection constraint matrix) is an extension of the motion constraint matrix, except it includes all obstructions for an object of interest in a given disassembly direction. Most approaches simplify the procedure by considering only principal Cartesian directions i.e., x, y, z [317]. This work does not consider fastener constraints since most 3D models in construction are not developed to the level of fastener details such as nails, screws, bolts, etc.

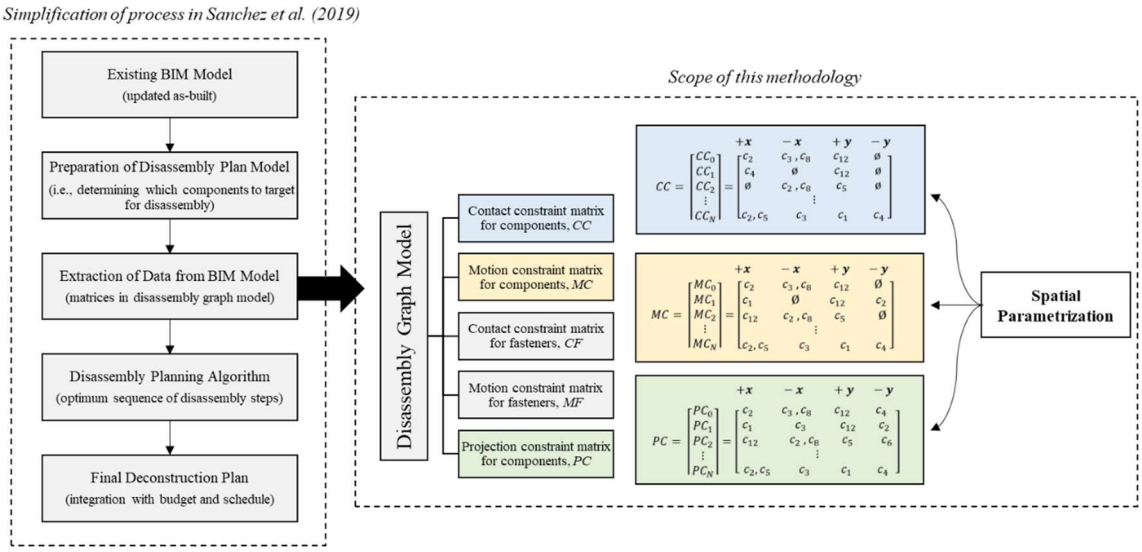

Figure 54. Summary of previous work by authors for disassembly planning and scope of this work as it relates to automating the extraction of key matrices.

8.2.1 Model initialization

The first step involves grouping CAD elements together according to their object definition. This enables all raw CAD elements (e.g., curves, surfaces, meshes, etc.) to be assigned a unique object ID. If the existing BIM model was created using a parametric software such as Autodesk® Revit, raw CAD data is often already sorted into unique groups. Apart from manually grouping elements, emerging workflows are being developed to automatically recognize and semantically segment objects [123]. The second part of model initialization is determining which objects are in direct contact with each other. Throughout this framework, clash detection is used as an event to trigger binary responses for the contact between object groups ("1" for positive clash event, "0" for no clash). All binary clash events are initially stored in an *n*-dimensional array, where *n* is the total number of objects.

8.2.2 Removing self-intersections from binary contact array

Since the process of clash detection between groups of objects will inevitably create self-intersections (each group can contain numerous CAD elements that are in contact with each other that will return positive clash events), these need to be removed from the binary contact array.

8.2.3 Constraint matrices for components

For extracting the contact constraint matrix, each object is moved iteratively in each of the ± principle Cartesian directions (+x, -x, +y, -y, +z, -z) until it is brought into a negative clash condition (no contact,

binary response of "0"). The distance in each direction to bring the objects out of contact is recorded, and the direction with the smallest distance is the disassembly direction. The motion constraint matrix is derived by iteratively moving each object in the principle Cartesian directions until the first clash event is detected. The contact object(s) in each direction are recorded in the motion constraint matrix. Finally, the projection constraint matrix is derived from the motion constraint matrix, with the only difference being that all objects in a given direction, and inside of the working-space, are recorded. For all matrices, if a given search (e.g., motion constraints for component c_1 in the $+x$ direction) turns up with a null response (i.e., no objects found), then by default a value of "-1" is inserted into the matrix. The spatial parameterization framework was programmed using Rhinoceros® software and a visual programming plugin called Grasshopper®. As a NURBS (non-uniform rational B-spline) based software, Rhinoceros® does not intrinsically have meta-data and thus all CAD elements rely on an algorithmic approach to parametrically embed intelligence. A high-level depiction of the algorithm (with over 800 script components) is shown in Appendix A, and pseudocode for each algorithm are presented below:

Algorithm 7. Semantic enrichment for disassembly planning algorithm – contact constraint matrix

Inputs: point = coordinate system origin
x_axis = vector for x axis in coordinate system
y_axis = vector for y axis in coordinate system
z_axis = vector for z axis in coordinate system
Element[] → accessed as B-rep objects with topology defined by curves, faces and vertices
Max_dist = number of move increments in a given axis direction
Distance increment = 10mm
Variables: Steps = Max_dist/distance increment
CC[][] = contact constraint matrix variables

```
01      FOR each element
02        FOR i = 1 to Steps && WHILE state = true
03          EXECUTE move element by increment in x_axis direction (both directions)
04          IF detect clash
05              state = false
06              RETURN index of element with clash as CC[i][x] && distance_x = i
08        END LOOP
09        FOR i = 1 to Steps && WHILE state = true
10          EXECUTE move element by increment in y_axis direction (both directions)
11          IF detect clash
12              state = false
13              RETURN index of element with clash as CC[i][y] && distance_y = i
14        END LOOP
15        FOR i = 1 to Steps && WHILE state = true
16          EXECUTE move element by increment in z_axis direction (both directions)
17          IF detect clash
18              state = false
19              RETURN index of element with clash as CC[i][z] && distance_z = i
20          END LOOP
21        END LOOP
22      EXECUTE construct CC[][] matrix
23      END
```

Algorithm 8. Semantic enrichment for disassembly planning algorithm – motion constraint matrix

Inputs: point = coordinate system origin
x_axis = vector for x axis in coordinate system
y_axis = vector for y axis in coordinate system
z_axis = vector for z axis in coordinate system
Element[] → accessed as B-rep objects with topology defined by curves, faces and vertices
Max_dist = number of move increments in a given axis direction
Distance increment = 10mm
Variables: Steps = Max_dist/distance increment
MC[][] = motion constraint matrix variables

```
01      FOR each element
02        FOR i = 1 to Steps && WHILE state = false
03          EXECUTE move element by increment in x_axis direction (both directions)
04          IF detect clash
05              state = true
06              RETURN index of element with clash as MC[i][x]
08        END LOOP
09        FOR i = 1 to Steps && WHILE state = false
10          EXECUTE move element by increment in y_axis direction (both directions)
11          IF detect clash
12              state = true
13              RETURN index of element with clash as MC[i][y]
14        END LOOP
15        FOR i = 1 to Steps && WHILE state = false
16          EXECUTE move element by increment in z_axis direction (both directions)
17          IF detect clash
18              state = true
19              RETURN index of element with clash as MC[i][z]
20        END LOOP
21        END LOOP
22      EXECUTE construct MC[][] matrix
23      END
```

Algorithm 9. Semantic enrichment for disassembly planning algorithm – projection constraint matrix

Inputs: point = coordinate system origin
x_axis = vector for x axis in coordinate system
y_axis = vector for y axis in coordinate system
z_axis = vector for z axis in coordinate system
Element[] → accessed as B-rep objects with topology defined by curves, faces and vertices
Max_dist = number of move increments in a given axis direction
Distance increment = 10mm
Variables: Steps = Max_dist/distance increment
PC[][] = projection constraint matrix variables

```
01      FOR each element
02        FOR i = 1 to Max_dist
03          EXECUTE move element by increment in x_axis direction (both directions)
04          IF detect clash
05              RETURN index of elements with clash as PC[i][x]
06         END LOOP
07         FOR i = 1 to Max_dist
08          EXECUTE move element by increment in y_axis direction (both directions)
09          IF detect clash
10              RETURN index of elements with clash as PC[i][y]
11        END LOOP
12        FOR i = 1 to Max_dist
13          EXECUTE move element by increment in z_axis direction (both directions)
14          IF detect clash
15              RETURN index of elements with clash as PC[i][z]
16         END LOOP
17        END LOOP
18       EXECUTE construct PC[][] matrix
19      END
```

8.2.4 Algorithm parameters

The distance for each iterative move is a parameter in the algorithm, but by default, it is set at 10 mm. Decreasing this threshold will not yield a more accurate result for object matrices but will significantly increase the computing demand (note that a smaller step value may be required for deriving fastener constraint matrices). Another algorithm parameter is tied to the motion constraint and project constraint matrices in the form of a maximum distance. In previous work [184], the authors introduced a "working-space" of 1500 mm which functions as a spatial envelope within which a construction worker can remove a given component from the assembly. This parameter is applied to both the motion and projection constraint matrices in order to define an upper bound on the iterative moves for each object.

8.2.5 Results

The spatial parameterization framework is demonstrated on a light gauge steel framing wall assembly (commonly found in industrialized building construction). An important part of this project was disassembling the construction assembly so that objects such as sinks, cabinets, and some structural

members could be either reused or properly recycled. For the purpose of determining a suitable disassembly plan, a 3D model of an interior wall was generated using Autodesk® Revit, and then subsequently imported as raw CAD elements (curves, surfaces and meshes) into Rhinoceros®, as shown in Figure 55.

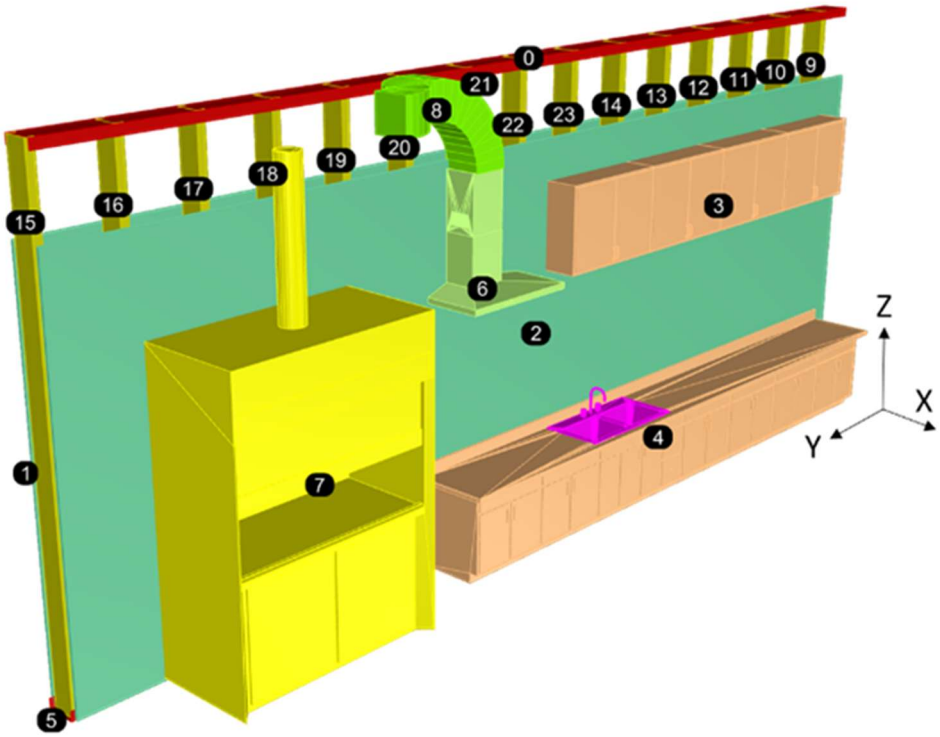

Figure 55. Construction assembly for disassembly planning. Elements categorized into groups, numerically annotated and coloured for visualization purposes. Note: the numbers in this figure only represent object labelling, and do not reflect the disassembly sequence.

Once the elements were imported, they were grouped according to their object definition (e.g., all elements corresponding to the upper cabinet – object 3 – were grouped together). Then, using the algorithm depicted in Appendix A, a contact constraint matrix, motion constraint matrix and project constraint matrix were automatically produced (Eqn. 26). The output from the algorithm is a text file, delineated by commas to represent principal Cartesian directions, which can be imported into the disassembly planning workflow. For comparison, a manual approach was employed for generating this data. The author manually isolated each component in the model and recorded the objects in direct contact, and the objects constraining motion and projection.

$$CC = \begin{bmatrix} CC_0 \\ CC_1 \\ CC_2 \\ \vdots \\ CC_{23} \end{bmatrix} = \begin{bmatrix} -1,-1,-1,-1,-1,(9,10,11,12,13,14,15,16,17,18,19,20,21,22,23) \\ 5,-1,-1,-1,-1,-1 \\ (3,4,6,7,8),5,-1,-1,-1,-1 \\ \vdots \\ -1,-1,-1,-1,0,5 \end{bmatrix}$$

$$MC = \begin{bmatrix} MC_0 \\ MC_1 \\ MC_2 \\ \vdots \\ MC_{23} \end{bmatrix} = \begin{bmatrix} 8,-1,-1,-1,-1,(9,10,11,12,13,14,15,16,17,18,19,20,21,22,23) \\ 5,-1,-1,-1,0,-1 \\ (3,4,6,7,8),5,-1,-1,0,-1 \\ \vdots \\ 2,1,22,14,0,5 \end{bmatrix}$$

$$PC = \begin{bmatrix} PC_0 \\ PC_1 \\ PC_2 \\ \vdots \\ PC_{23} \end{bmatrix} = \begin{bmatrix} 8,-1,-1,-1,-1,(9,10,11,12,13,14,15,16,17,18,19,20,21,22,23,1,2) \\ (5,9,10,11,12,13,14,15,16,17,18,19,20,21,22,23,2,3,7,8,4,6),-1,-1,-1,0,-1 \\ (3,4,6,7,8),(5,9,10,11,12,13,14,15,16,17,18,19,20,21,22,23,1),-1,-1,0,-1 \\ \vdots \\ (2,3,4),1,(22,21),(14,13),0,5 \end{bmatrix}$$

Eqn. 26

8.2.6 Results and Evaluation

Minor discrepancies between the automated and manual approaches were detected. After analysis, these differences were found to be missing constraint components in the matrices produced in manual approach, demonstrating that the automated approach is suitable of catching human errors. The automated approach was found to be 100% accurate for extracting the contact, motion and project constraints. This accuracy does however depend on having a properly configured BIM, e.g., no overlapping objects, no gaps between objects that should be in contact, etc. Of course, the accuracy suffers from bad input and an incorrectly configured BIM. Furthermore, the process of iterating principal movements, checking for collisions and cross-referencing components was found to be computationally heavy. This is likely based on the distance threshold used for iterating movements (set at 10 mm), the working space parameter (set at 1500 mm) and the level of model complexity (this 3D model contained 182 curves and 3364 mesh elements). The automated approach took 243 min to extract the contact constraint matrix, 734 min for the motion constraint matrix and 1076 min for the projection constraint matrix. With a total run time of 2053 mins, there were no direct time savings for using this algorithm over a manual approach (which took 145 mins in total). However, the benefit of an automated approach is that this process can be run in the background of other processes at very little cost. In addition, the accuracy of the extracted data can be improved. Moreover, with higher-powered processors, the algorithm run time could be reduced to become faster than the manual approach.

8.3 Conceptual Parametric Model for Product Cycling of Industrialized Building Modules

This body of work demonstrates how algorithms can be developed to promote auxiliary use of industrialized building modules in an innovative way for a circular economy. As such, this work is purely

conceptual but demonstrates the potential that having a semantically rich parametric model with assembly and disassembly information can yield. The reader is first directed to Appendix B which outlines the deployment potential of reusing the structural assemblies of industrialized buildings, considering both life cycle impact quantification and new business models.

8.3.1 Overview

Advances in industrialized building systems are creating reliable solutions for traceability across a project. However, there is an increasing demand to expand traceability to more dimensions than just the materials, processes and stakeholders involved in a project. Social demands for a circular economy, in which parts, products and materials can flow within open resource loops, are necessitating the need for lifecycle-based traceability of our built assets. This section presents a computational model for "product cycling" of modular buildings. Given their innate assembly and disassembly attributes, modular buildings offer a unique advantage to building owners and building stock managers for cycling of modules (i.e., adding modules in future adaptations, or redistributing, reusing and repurposing of modules into new assets). We present the basis for a computational model containing considerations for module topology, lifecycle costs and lifecycle impacts. We demonstrate the result of this model in a product configurator, which serves as a tool for expanding state-of-the-art traceability from being project-based to product-based across multiple lifecycles.

8.3.2 Introduction

While industrialized construction has been relied upon as a favourable approach for project delivery, modular and prefabricated assets present a unique opportunity for promoting a circular economy [318]. The nature of how modular assets are assembled in the field leads to an enhanced ability for disassembly, reuse and circular resource flows. However, current design and delivery methodologies are optimized for the singular use of modular assets. Social demands for a circular economy – global natural resource depletion, increasing waste, environmental load, energy use, etc. – require innovative approaches to constructing our built environment [319]. With significant developments being realized in the manufacturing industry regarding the circular economy [320], there is a need to expand this concept to industrialized construction. This research presents a computational model for promoting the concept of "product cycling" in modular buildings. The key to this model is optimizing design for multiple lifecycles, rather than a single lifecycle. The model contains analytical expressions for lifecycle costs and impacts, which are enumerated across multiple lifecycles (i.e., initial build, n number of adaptions and an End of Life stage). The proposed model is demonstrated in a configurator of a prototype (Figure 56).

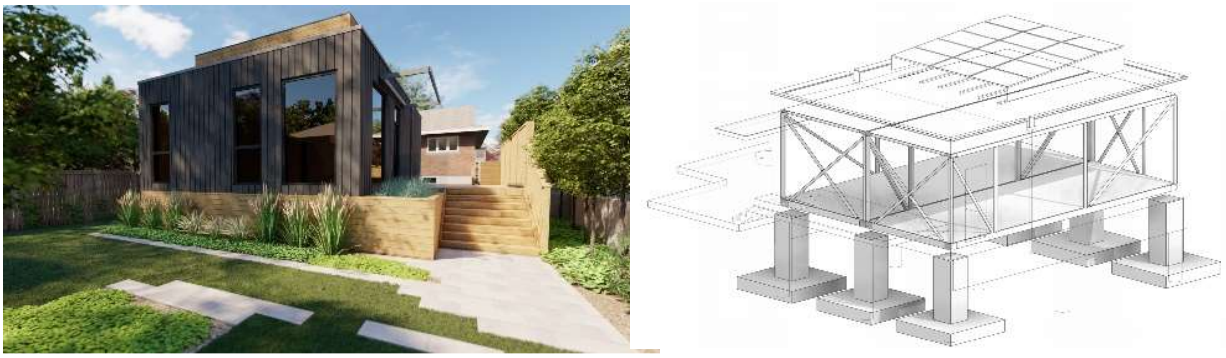

Figure 56: Two-module accessory dwelling unit used for demonstrating product cycling model

8.3.3 Background

Despite the fact that current impediments to BIM integration within modular construction and prefabrication stem largely from resistance to business change [14], this is rapidly changing, due in large part to advances from digital technologies and configuration platforms [321]. Product configurators in industrialized construction can be grouped into three typologies: (1) planning-based, (2) design-based, and (3) DfMA-based [98]. The principle of a configurator is to codify constraint-based logic for the topology of a manufacturable system, in order to define rules for how components and modules can be combined into products [322]. Since product configurators rely on computational processes to generate and iterate assemblies, they can be used across a range of projects, thus reducing project-specific effort and resources required for BIM production (i.e., since this can be largely automated). The value of codifying construction systems extends beyond just the pragmatic harmonization of complex design-to-construction relationships. Increasingly, computational processes can also be used to address vital social imperatives such as sustainable development, embodied and operational energy reduction and resource preservation.

Lifecycle Assessment (LCA) is a methodology that accounts for the materials and energy involved in a product or service along its lifecycle and quantifies its environmental impacts [323]. By applying this methodology to the building and construction industry, it is possible to make important decisions during the design stages of a building, based on a holistic approach that involves the stakeholders of a global society. LCA represents a rational standardized approach that can evolve with the development of knowledge, and it also helps stakeholders to agree upon common strategies. LCA is now considered as one of the main tools used to help achieve sustainability in the building industry [324-326]. When LCA is incorporated into the decision-making process for buildings, stakeholders can scientifically assess the lifecycle impacts of building subsystems, materials, and components, and then select alternatives that

reduce overall net environmental impacts. Several national jurisdictions already have, or plan to soon implement, requirements and building practices for reporting LCA upfront in design [327]. In some cases, monetary benefits or penalties are associated with a building's embodied energy. As LCA monetization of built assets is shifting towards being a project mandate, there is an increasing need to develop tools to forecast expected LCA impacts and costs in order to facilitate optimized lifecycle solutions.

Previous research has quantified the advantages that modular buildings have in terms of LCA impacts over traditionally constructed buildings. Modular construction is superior from both a production standpoint [18], and from an operational standpoint [23]. Despite the range of studies either documenting or improving the innate opportunities of modular assets (either from cost, time, quality or environmental perspectives), no studies to date explore multi-lifecycle scenarios for buildings. Instead of exclusively focusing effort on adapting derelict assets that may not have up-to-date asset information nor the ability for easy adaptation, there is a growing opportunity to embed adaptability upfront in new assets. In this way, we can optimize for design scenarios that facilitate product cycling of buildings that are justified from cost and LCA perspectives.

8.3.4 Approach for Developing Conceptual Parametric Model

The proposed model consists of three key components to facilitate product cycling of modular buildings: (1) codification of a reconfigurable topology (i.e., the ability for modules to be added or removed from building iterations), (2) derivation of lifecycle cost functions and (3) derivation of LCA impact functions. Collectively, these components comprise the computational core for a product cycling model for modular buildings. For demonstration purposes, the derivation of lifecycle costs and impacts in this research is done assuming modules are added to an existing building over discrete adaptations and fully disassembled at the End of Life (EoL) stage. Future research will explore mixed cases of how modules can be added or removed from existing building configurations (both in a vertical and horizontal manner). The proposed methodology is based on the existing work by Sanchez et al. [316] for the development of a multi-objective optimization approach to adaptive reuse of buildings.

8.3.4.1 Codification of Reconfigurable Topology

In order to facilitate the reconfigurability of modular buildings, key design considerations need to be derived and codified. Codification in this case refers to the development of computational logic and rules behind how modules can be added or removed from each other or to/from site interfaces. It also refers to corresponding design details required to make a building functional when adding or removing modules

(e.g., details for egress and access, details to close off or open interior spaces, details for adding or removing enclosure subassemblies, etc.). This codification is categorized into structural, constructability and architectural-based topologies.

Structural topology outlines the necessary requirements for ensuring a building can meet its load cases as required by the building code. Specifically, the configuration of structural topology relates to the structure of each module and the building substructure (foundation). In the case of adding subsequent modules to an existing building, the building substructure and existing modules need to handle the additional loads of added modules. In this way, the initial lifecycle might have an overdesigned structural topology in order to anticipate future module cycling applications. Developing structural topology in a computational manner (i.e., distilling the overall design to a series of dimensional and system-based inputs complete with necessary structural checks) is becoming common practice in structural design firms since design iterations can be computed and updated in an efficient manner [30].

Constructability topology needs to be embedded in the design to enable the easy adaptability of a modular building. This requires both design for manufacture and assembly (DfMA) and design for disassembly (DfD) principles in order to increase the flexibility and reconfigurability of modular buildings. A popular approach for this is the use of kit-of-part connections that are nearly universal in application across platform configuration [328]. Many modular companies are already investing in kit-of-part structural systems in order to optimize structural design, fabrication and onsite assembly (e.g., Z Modular's patented VectorBloc connection). It naturally follows that the use of these 'universal connections' are highly favourable for promoting the addition of more modules to a building, or for easing the processes of disassembly since processes can be repeated in a standardized manner.

Architectural topology is the last major design consideration that needs to be thoroughly examined in order to promote product cycling of modular buildings [329]. For instance, kit-of-part connectors can also be used to promote mass customization of architectural features such as doors, windows, overhangs and balconies. These connectors can be as simple as engineered structural brackets that mount to the structural system that can be used for exterior mounted assemblies or balconies. The key difference between constructability and architectural-based topology is that architectural topology outlines how a module can be reconfigured to account for varying types of product cycling. One example is how a single-story modular building can be adapted from within to have a staircase for a second-story addition in a subsequent lifecycle (this is an example of vertical adaptability). Another example is how an existing building exterior could be adapted to allow same-level module additions (this is an example of horizontal adaptability).

8.3.4.2 Lifecycle Costs

Lifecycle costs are divided into three separate functions: (1) initial capital costs (for the first lifecycle), (2) adaptation costs for each additional lifecycle, and (3) an End of Life (EoL) cost and reimbursement function. These costs are amalgamated into a net present value cost function, which can be compared against the monetization of LCA impacts.

Capital Cost Function

The initial capital cost function has components that are independent (or *quasi*-independent) of the number of modules such as costs for geotechnical evaluation, trenching/installation of building services (e.g., electrical, water, communications, etc.). Other costs are based on a minimum design case (single story, or single-module assembly) such as design, foundation, inspections/tests, and construction administration costs. Finally, certain costs are directly proportional to the number of modules, such as modular fabrication, delivery and installation. The proposed capital cost function, (C) is derived in Eqn. 27.

$$C(n,s) = (d + nD) + nM + R + F\left(\frac{n}{s}\right) + sf + O + (i + nI) + nA$$

Eqn. 27

where n is the number of modules, s is the maximum number of stories for future lifecycles (e.g., to influence the design of foundation), d are fixed design costs, D are variable design costs, M is variable costs related to module fabrication, delivery, and installation, R are costs related to supply and installation of the roof module, F are scaled costs according to building footprint (n/s), f are incremental foundation costs based on the number of stories, O are costs for building service/utility supply, i are fixed costs for tests and inspections, I are variable costs for tests and inspections, and A are variable costs for project administration.

Adaption Cost Function

Adaptation costs are derived in Eqn. 28, where modules can be added in subsequent adaptation stages.

$$A_l(n_l) = r + n_l D + n_l M + n_l A + n_l I + (s_l - s_{l-1})o$$

Eqn. 28

where l is the adaptation of interest, n_l are the number of modules added for the adaptation, s_l is the number of stories added for the adaption, o are incremental site-based costs (e.g., such as staircases/railings) and r is cost related to removal and reinstallation of the roof module. While this

function only considers the addition of modules, a future (more comprehensive) adaption cost function can be derived to account for removing modules from an existing building.

End of Life Cost Function

The EoL function (Eqn. 29) considers costs associated with disassembly, module deconstruction, and component reuse for future building applications.

$$EoL(n) = nT - nU - nV$$

Eqn. 29

where T is the deconstruction cost per module (including site disassembly, transportation to facility and costs for disassembly of all components outside of the structural system), U is the reuse value for harvesting the structural system (which can be reused in new modular buildings), and V is the salvage value for non-structural components for each module.

Amalgamated Net Present Cost Function

Finally, all cost functions can be amalgamated into a net-present cost function according to Eqn. 30.

$$NPC(n, s, n_l, i, l) = C(n, s) + \sum_{l=0}^{j} \frac{A_l(n_l)}{(1+i)^l} + \frac{EoL}{(1+k)^g}$$

Eqn. 30

where i is the compounded interest/return rate over the number of adaptation period(s) l, and k is the interest rate for the number of time periods, g, between the end of life to the present time. The purpose of this NPC function is to serve as an estimation tool to account for total lifecycle costs. As such, it assumes equal time periods between each adaptation (for simplicity), however a more complex function could be developed to anticipate different timeframes.

8.3.4.3 Lifecycle Impacts

In their work, Sanchez et al. [326] proposed an LCA BIM-based methodology for evaluating the net environmental impacts for adaptive reuse of buildings. A consequential LCA approach is used to quantify the environmental impacts per subsystem and the building's operational and construction phase is dismissed from the LCA system boundaries since the study is focused on the quantification of embodied resources. Then, the environmental impacts that are estimated and monetized are Primary Energy Demand (PED) in Mega Joules and Global Warming Potential (GWP) in equivalent kilograms of CO_2. For the purposes of this study, the same approach is used in order to estimate the environmental impacts

on the design for multiple lifecycles of modular building projects. Figure 57 shows the proposed methodology and system boundaries for evaluating the net environmental impacts. Eqn. 31 shows the derivation of net environmental impacts (EI) in the proposed LCA cradle-to-cradle framework. For a comprehensive breakdown of each component in the following equation, the reader is directed to Sanchez et al. [326] – a summarized version is provided here for succinctness.

$$EI(n,s) = LCA_{substructure} + \sum_{i=1}^{i=n} LCA_{module} + \sum_{i=1}^{i=s-1} LCA_{building}^{adaptation}$$

Eqn. 31

where n are the number of modules, s are the number of stories (assumed to correlate to the number of building adaptations), $LCA_{substructure}$ are impacts associated with the raw resources related to the building substructure (assumed to be constant over the course of multiple lifecycles), LCA_{module} are impacts associated with each additional module added to the building and $LCA_{building}^{adaptation}$ are impacts associated with the additional resources and processes associated with each building adaptation. It is important to note that within each expression in Eqn. 31 are both LCA disbursements (i.e., negative impacts) and reimbursements (i.e., benefits associated with reuse, recycling and energy recovery). While Eqn. 31 is reported for each subsystem, it can also easily be reconfigured to report LCA impacts per lifecycle stage. In addition, the impacts associated with the operation and maintenance of the building are not considered here, since the goal of this analysis is to assess embodied impacts of the physical materials and how they are used rather than incorporating the operational impacts.

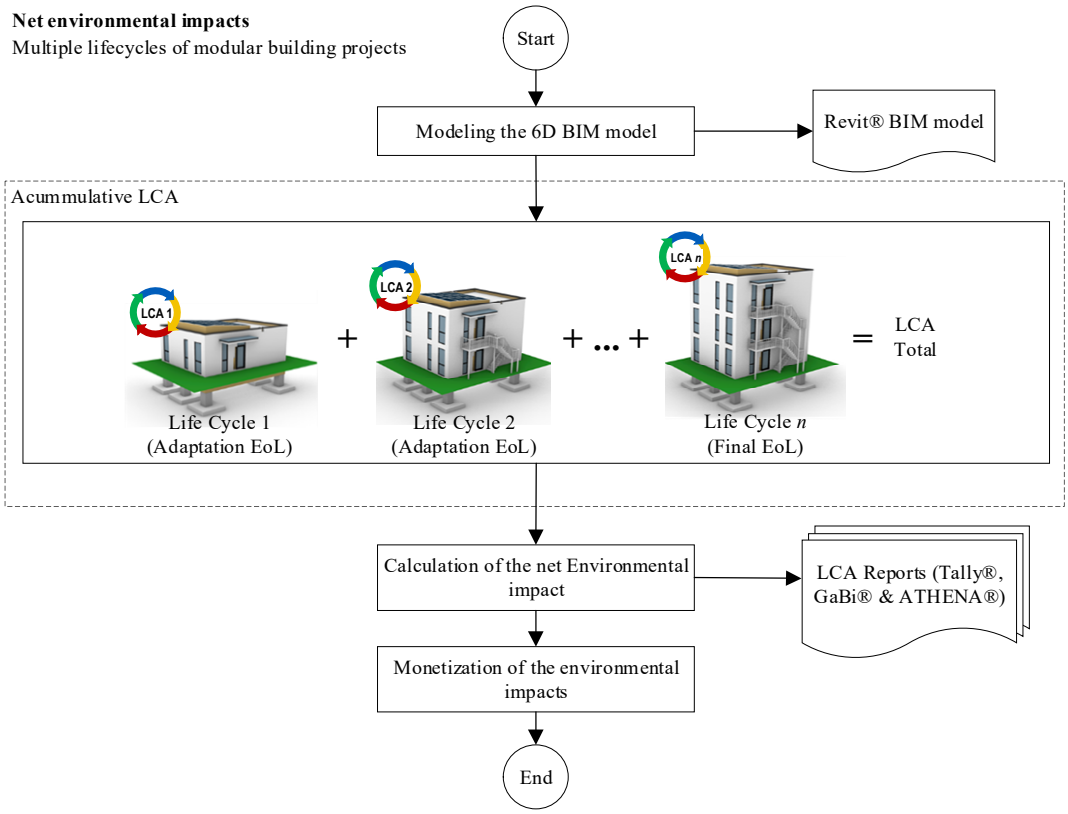

Figure 57: Methodology for evaluating the net environmental impacts in the proposed model

8.3.5 Conceptual Demonstration of Parametric Model

A modular prototype project located in Kitchener, Ontario (Canada) was carried out by Edge Architects in conjunction with Z Modular. The aim of this project was to provide supportive housing for a local non-profit organization in the form of a 2-module backyard accessory dwelling unit, while simultaneously piloting an apartment layout for an upcoming midrise affordable housing complex. Data collected from this project is used herein to develop a conceptual configurator in order to demonstrate the proposed computational model. The prototype project includes several kit-of-parts features (e.g., VectorBlocs for the structural system to enable easy stacking and connection of modules, and adaptable entryway standoffs above the door which have the ability to be used for a canopy or for supporting a balcony). While actual project costs cannot be disclosed, the values reported in this work are close to the actual values and are based on the detailed budget.

The conceptual configurator is based on a story-by-story iteration of the 2-module prototype project layout (Figure 56). This configurator was programmed using Grasshopper® visual programming interface using computational topology, and Eqn. 27 through Eqn. 31 (refer to Appendix A for depiction of this

algorithm). The configurator allows a user to select the number of stories in the first building iteration (i.e., lifecycle 1) and a maximum number of stories (i.e., lifecycle *n*). The maximum number of stories is used to computationally populate a foundation suitable for a building of this height. Then, based on the difference between the maximum number of stories and the initial number of stories, discrete adaption periods are presented to the user in terms of lifecycle costs and lifecycle impacts. Costs and LCA impacts are developed according to the material and system-outputs of the computational topology. Figure 58 depicts the configurator after a user has selected an initial building height of 1-story, with the ability to add modules in the future up to 4-stories. With these toggles selected, a rendered image of lifecycle 1 and lifecycle *n* are computationally generated. The lower part of Figure 58 has charts outlining the net-present costs and LCA impacts for each lifecycle (values in green outline LCA savings or reimbursements).

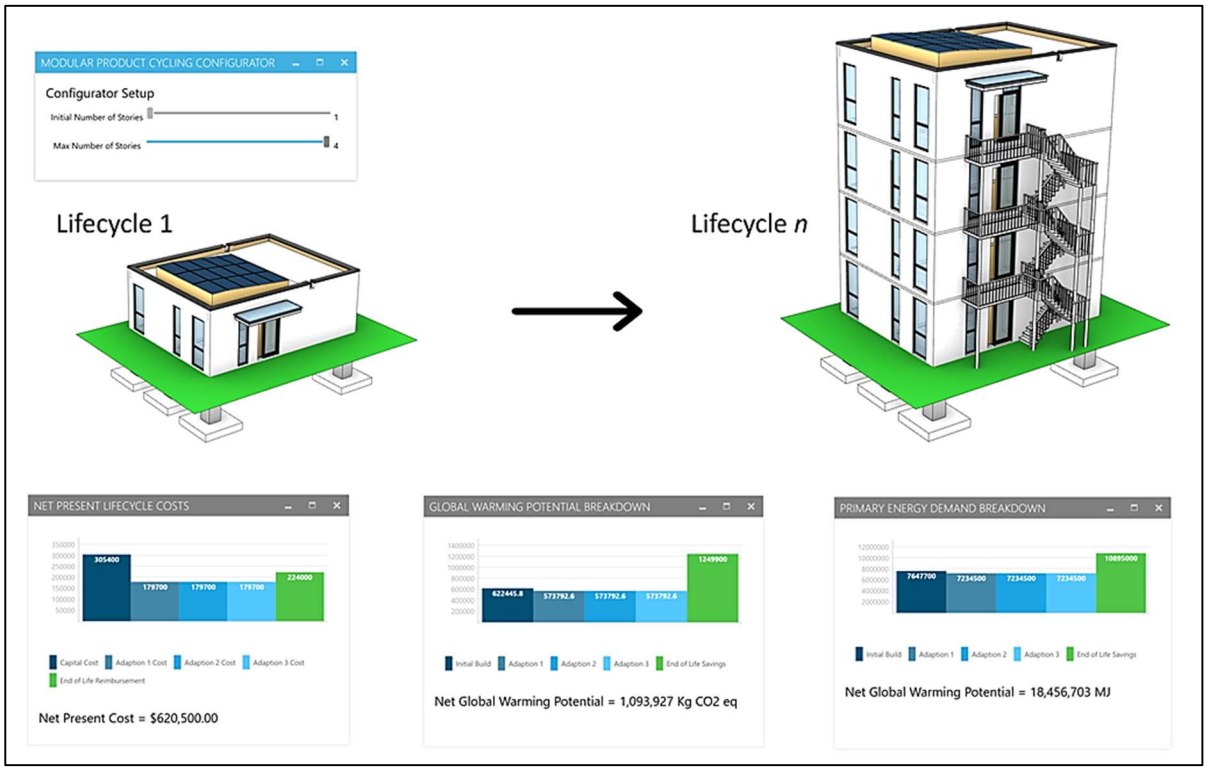

Figure 58: Product Cycling Configurator Graphical User Interface

The development of the structural topology focused on populating optimized foundations (concrete footings and piers) depending on the maximum story height since the structural system of each module (based on the kit-of-part VectorBloc connections) can facilitate stacking above the 4-story maximum height considered in this configurator. Based on geometry populated in Grasshopper®, a series of inputs are fed into a back-end spreadsheet in order to iterate, check and optimize design parameters corresponding to footing depth and area dimensions, and pier area dimensions (Figure 59).

Constructability and architectural topology are programmed to add modules vertically, by removing the roof assembly and the insulated floor assembly for each module added to the top story. Then, two different staircase assemblies are populated as needed for each additional story being added. The interior layout of each story remains identical in order to simplify the reconfiguration process for each additional lifecycle. Finally, a kit-of-parts connection above the entryway is adapted from a canopy to a balcony when a story is added. The result of all codified topology is a detail-rich and accurate building layout driven by only two user inputs (i.e., initial and maximum number of stories).

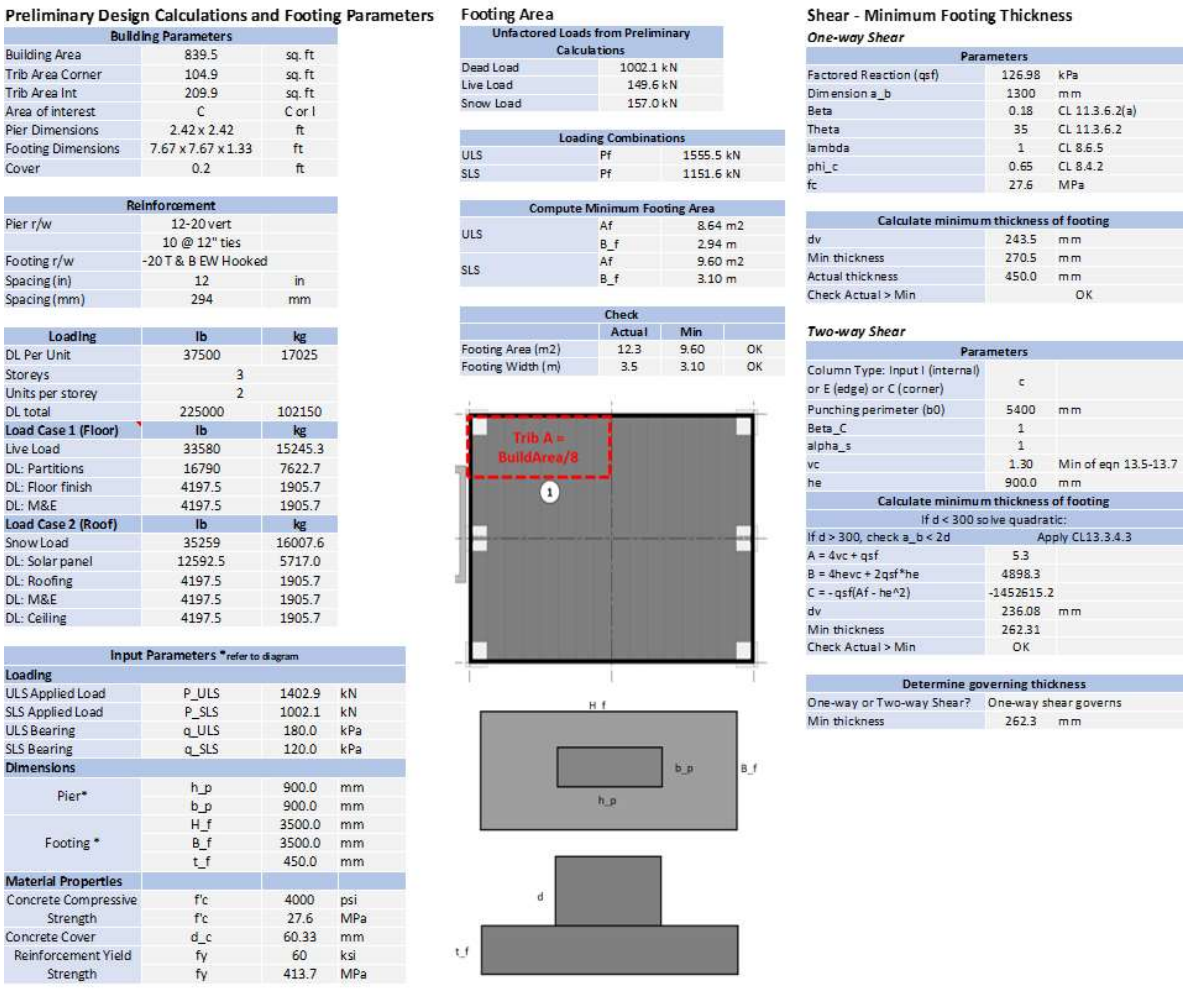

Preliminary Design Calculations and Footing Parameters

Building Parameters		
Building Area	839.5	sq. ft
Trib Area Corner	104.9	sq. ft
Trib Area Int	209.9	sq. ft
Area of interest	C	C or I
Pier Dimensions	2.42 x 2.42	ft
Footing Dimensions	7.67 x 7.67 x 1.33	ft
Cover	0.2	ft

Reinforcement		
Pier r/w	12-20 vert	
	10 @ 12" ties	
Footing r/w	-20 T & B EW Hooked	
Spacing (in)	12	in
Spacing (mm)	294	mm

Loading	lb	kg
DL Per Unit	37500	17025
Storeys	3	
Units per storey	2	
DL total	225000	102150
Load Case 1 (Floor)	**lb**	**kg**
Live Load	33580	15245.3
DL: Partitions	16790	7622.7
DL: Floor finish	4197.5	1905.7
DL: M&E	4197.5	1905.7
Load Case 2 (Roof)	**lb**	**kg**
Snow Load	35259	16007.6
DL: Solar panel	12592.5	5717.0
DL: Roofing	4197.5	1905.7
DL: M&E	4197.5	1905.7
DL: Ceiling	4197.5	1905.7

Input Parameters *refer to diagram			
Loading			
ULS Applied Load	P_ULS	1402.9	kN
SLS Applied Load	P_SLS	1002.1	kN
ULS Bearing	q_ULS	180.0	kPa
SLS Bearing	q_SLS	120.0	kPa
Dimensions			
Pier*	h_p	900.0	mm
	b_p	900.0	mm
Footing *	H_f	3500.0	mm
	B_f	3500.0	mm
	t_f	450.0	mm
Material Properties			
Concrete Compressive Strength	f'c	4000	psi
	f'c	27.6	MPa
Concrete Cover	d_c	60.33	mm
Reinforcement Yield Strength	fy	60	ksi
	fy	413.7	MPa

Footing Area

Unfactored Loads from Preliminary Calculations	
Dead Load	1002.1 kN
Live Load	149.6 kN
Snow Load	157.0 kN

Loading Combinations		
ULS	Pf	1555.5 kN
SLS	Pf	1151.6 kN

Compute Minimum Footing Area		
ULS	Af	8.64 m2
	B_f	2.94 m
SLS	Af	9.60 m2
	B_f	3.10 m

Check	Actual	Min	
Footing Area (m2)	12.3	9.60	OK
Footing Width (m)	3.5	3.10	OK

Shear - Minimum Footing Thickness

One-way Shear

Parameters		
Factored Reaction (qsf)	126.98	kPa
Dimension a_b	1300	mm
Beta	0.18	CL 11.3.6.2(a)
Theta	35	CL 11.3.6.2
lambda	1	CL 8.6.5
phi_c	0.65	CL 8.4.2
fc	27.6	MPa

Calculate minimum thickness of footing		
dv	243.5	mm
Min thickness	270.5	mm
Actual thickness	450.0	mm
Check Actual > Min	OK	

Two-way Shear

Parameters		
Column Type: Input I (internal) or E (edge) or C (corner)	c	
Punching perimeter (b0)	5400	mm
Beta_C	1	
alpha_s	1	
vc	1.30	Min of eqn 13.5-13.7
he	900.0	mm
Calculate minimum thickness of footing		
If d < 300 solve quadratic:		
If d > 300, check a_b < 2d	Apply CL13.3.4.3	
A = 4vc + qsf	5.3	
B = 4hevc + 2qsf*he	4898.3	
C = -qsf(Af - he^2)	-1452615.2	
dv	236.08	mm
Min thickness	262.31	
Check Actual > Min	OK	

Determine governing thickness		
One-way or Two-way Shear?	One-way shear governs	
Min thickness	262.3	mm

Figure 59: Output of Structural Load Calculations for Populating Optimal Foundation Design

Lifecycle costs are populated using construction costs (in CAD currency) from the prototype project and estimates for costs associated with roof removal/reinstallation, staircase assembly, reconfiguration of the canopy and additional costs associated with a larger foundation using a sliding scale based on the prototype project. EoL reimbursements are estimated according to the production cost of the structural

system of each module (since they are assumed to be directly reused in new buildings), and other reimbursements associated with the subsystems, fixtures and raw materials (i.e., wood framing, copper piping, etc.). These reimbursements are offset by estimated costs for deconstruction which include site mobilization, transportation and labour required for deconstruction processes.

LCA impacts and reimbursements are computed automatically using the plugin Tally® in Revit® (note: while the configurator is programmed in Grasshopper® which natively runs in Rhinoceros®, we employ the use of Rhino.Inside® to access Grasshopper® directly in the Revit® environment). Detailed LCA results for each lifecycle stage are computed for the substructure, modules, and building adaptation of the case study. The organization of building lifecycle stages are described according to the normativity EN 15978 (Sanchez et al., 2019): product stage (A1. raw material supply, A2. transport, and A3. manufacturing), construction stage (A4. transport), Use stage (B2. maintenance and B4. replacement), EoL stage (C2. Transport to disposal, C3. waste processing, and C4. disposal) and Module D (D. benefits and loads beyond the system boundary from reuse, recycling, and energy recovery). The environmental impact categories estimated for the purposes of this study were Global Warming Potential (GWP) reported in Kg CO_2 equivalent units and Primary Energy Demand (PED) reported in MJ.
Using the configurator, we can explore the lifecycle configurations for an initial 1-story building. By selecting various maximum story values in lifecycle n (from 2 to 4), there are three distinct lifecycle configurations (A, B, C). Configuration A, for instance, has a foundation designed to handle up to a 2-story building, and as such has two primary lifecycle stages (an initial 1-story configuration and an adapted 2-story configuration), and a secondary EoL lifecycle. In the EoL lifecycle, subsystem deconstruction, recycling and reuse of modules occur (Figure 60). This same logic can be carried out for Configuration B and Configuration C.

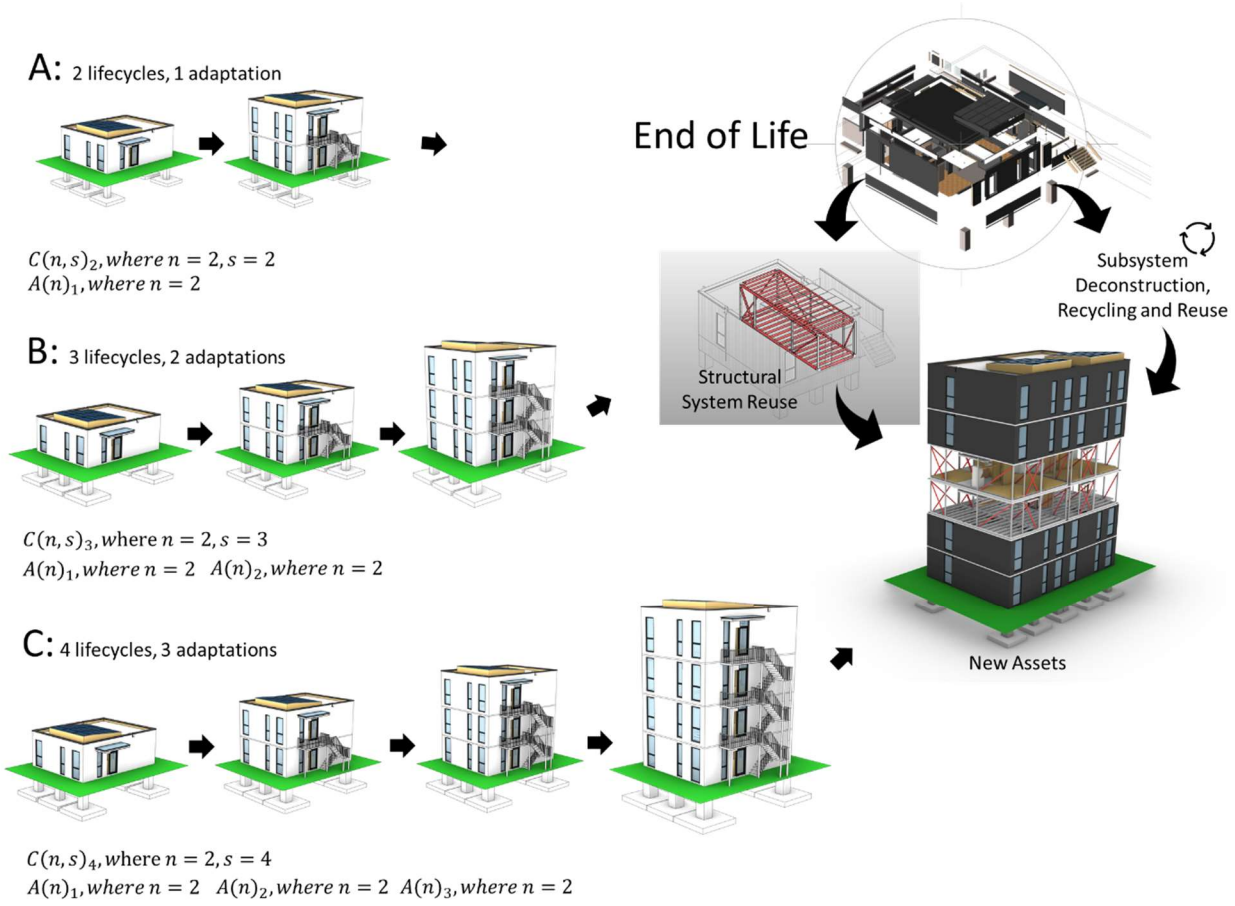

Figure 60: Lifecycle Configurations (A, B, C) for an Initial 1-Story Building Using the Configurator

Apart from exploring the potential ways in which a 1-story building can be reconfigured across multiple lifecycles, it is useful to compute the economic and environmental advantages of investing in reconfigurability. For demonstration purposes, we can compare Configuration A in Figure 60 with an alternative approach (Configuration A'): building a 1-story modular building, then deconstructing that building and foundation to erect a new 2-story building on the same site. The primary difference between Configuration A and A' is the structural topology in the foundation (both are industrialized buildings). By over-designing the foundation to allow reconfiguration which costs an additional $4,000, net savings of $66,250 can be achieved when scaling to a 2-story building (assuming the first foundation cannot be modified in-situ). In a similar manner, environmental savings of 19,295 Kg CO_2 eq. and 134,540 MJ can be achieved by investing upfront in reconfigurability as shown in Table 9.

Table 10: Comparison of Configuration A (1-Story up to 2-Story) and Configuration A' (Two Separate 1- and 2-Story Buildings) in Terms of Cost, Global Warming Potential and Primary Energy Demand.

	Item	Cost	GWP (Kg CO2 eq.)	PED (MJ)
Configuration A	1-story up to 2-story	$365,100	541,709	9,180,537
Configuration A'	1-story up to 1-story	$237,400	270,291	4,582,789
	2-story up to 2-story	$360,300	540,670	9,166,335
	Roof removal	$4,800	1,039	14,202
	Existing foundation removal	$6,250	9,873	134,918
	Existing module savings	-$177,400	-260,869	-4,583,168
	Net	$431,350	561,004	9,315,077
Savings	Configuration A over A'	$66,250	19,295	134,540

8.3.6 Conclusion

Paired with computational tools for lifecycle traceability, industrialized buildings are uniquely poised to address vital social imperatives associated with sustainability and the circular economy. This chapter proposed a "product cycling" model for industrialized buildings as one way to work towards reaching these social imperatives. The proposed model consists of computational components to generate modular topology (i.e., materials and systems), lifecycle costs and LCA impacts. The configurator developed for demonstration purposes considers a prototype modular project, in which subsequent lifecycles can be introduced by adding modules to an existing building. A comparison of distinct lifecycle configurations and their alternatives (i.e., deconstructing existing buildings and demolition foundations) is shown to result in significant economic and environmental savings. This likely stems from the fact that certain costs in the construction of foundations for industrialized buildings are not significantly influenced by the quantity of materials used (e.g., volume of concrete and quantity of rebar). Some of these quasi-independent costs include building permits, soil investigation, structural design/analysis, excavation, surveyor, etc., all of which are almost independent of the foundation structure itself. This means that over-designing the foundation to handle future addition of modules can bring some cost savings over the long run, despite the additional up-front costs. Similarly, the lifecycle impacts of adding additional materials to the current use can be distributed over many future lifecycles, lowering the overall impact. This concept of over-designing the structural system to anticipate in-situ adaption is particularly relevant for property owners who foresee the need for adaptability across their assets (i.e., single-storey applications being converted into mid-rise applications, or for home-owners who might "grow" their house as their family grows).

Chapter 9: Conclusions

9.1 Thesis Overview

Industrialized building construction (IBC) is witnessing a new wave of attention and investment within the industry principally due to advancements predicated on digital processes and technologies. Digitization[19], which is the convergence of digital and physical states – is considered to be the most powerful driver of innovation in the coming decades for the progression of technologies related to industrialization [330]. However, the construction industry is among the least digitized, according to the 2015 McKinsey Global Institute industry digitization index [331]. Developing associative data semantics and workflows for transforming data between physical and digital states is a core challenge that needs to be addressed in industrialized building construction. While automation can be developed to help embed intelligence into the data generated in digitization workflows, in many cases, manual processing and cognition are still required to produce working solutions. Furthermore, the maturity and optimization of geometric models contribute significantly to the success of industrialized building construction projects, as evidenced through high-profile litigation cases, and on recurring smaller-scale projects. Research continues to help solve many of the challenges being faced in IBC, yet a comprehensive approach for developing algorithms for geometric optimization enrichment remains elusive.

The aim of this thesis is to establish an approach for developing computational algorithms that optimize and enrich geometric models used in industrialized building construction. This is accomplished by addressed several core questions, which outline the novelty of the research approach: (1) geometric processes can be codified using the intrinsic properties of geometry and topology, aided by advanced parameterization and powerful algorithmic solvers, (2) several steps can be taken to improve the pragmatism of algorithms, predicated on using approximation approaches such as stochastic simulation, metaheuristics and combinatorial optimization, and (3) through a series of real-world experiments, it is possible to determine which types of problems are best suited for exact vs. approximate algorithms. While the aim of this thesis was not to exhaustively develop algorithms for all cases and types of geometric optimization and enrichment, the flavour and range of functional demonstrations presented here validate a rich and diverse set of algorithmic approaches that can be used in practice.

[19] Note: digitization is the North American term, while “digitalization” is the equivalent European term

In the first part of this research, a comprehensive literature review was conducted, primarily to identify the necessary and relevant background knowledge, but also to understand where current knowledge gaps exist. This resulted in the following gaps: (1) there is a need to achieve more granularity in geometric optimization than currently available methods, given the strict dimensional requirements in industrialized building construction, (2) there is a need to develop methods that preserve semantic information initially developed in models, rather than pursuing methods to recreate this information from non-parametric data (e.g., point clouds), (3) few studies compare and evaluate the performance of exact vs. approximate algorithms, and (4) there is a need to develop pragmatic approaches for algorithm development to ensure they can be feasibly implemented in practice.

The algorithms developed in this research target the main construction-related stages in an industrialized building project: design, fabrication and assembly, onsite assembly and end-of-life. The chapters outlining such algorithms have been organized in the order of these project stages. First, a new algorithm was developed to analyze and simulate dimensional tolerance accumulation. This algorithm can be used to optimize geometric models upfront during design in a prescient manner. The specific approach employed for this algorithm was based on the Monte Carlo method, which was shown to outperform prevailing tolerance analysis methods (e.g., exact methods or overtly simplified stack-up models). Next, a series of algorithms were developed to address fabrication and assembly optimization for 2D panelized assemblies. Exact vs. approximate algorithms were developed and compared for minimizing material waste for architectural panels. While this application is not explicitly related to industrialized building construction, the results are very relevant for 2D panelization (which is a form of IBC). Third, a series of parametric BIM updating algorithms were developed in order to preserve the semantic information contained in BIMs during as-built digitization processes. Such a method was deemed useful based on a chapter that explored existing geometric digital twin methods for use during fabrication and assembly in IBC. The result of the parametric BIM updating method was that a much more accurate method than currently available could be achieved and also automated. Finally, the last set of algorithms developed in this research relate to semantic enrichment tasks addressing the end-of-life stage of industrialized modular buildings. First, an automated method for determining the disassembly sequence of an assembly was developed, which was followed by a configuration platform for demonstrating how assembly modules could be ‘cycled’ or reconfigured as a way of extending the useful life of an industrialized building.

The core contributions and detailed summaries of the algorithms developed in this research are outlined in the following section.

9.2 Summary of Methods and Contributions

9.2.1 Tolerance Analysis and Optimization using Monte Carlo Simulation

Compared to other tolerance analysis methods, Monte Carlo simulation has many desirable attributes in the context of industrialized building construction. First, it is capable of handling complex three-dimensional relationships between components that other methods struggle to provide. While other tolerance analysis methods (e.g., tolerance mapping) rely on the user having a fundamental understanding of graph theory and or comprehensive manufacturing tolerance nomenclature (e.g., GD&T), tolerance simulation can be carried out using simple tolerance configurations. It can also be used as a design tool for comparing various fabrication processes in terms of quantifying risk of rework. As the uptake of virtual and computational tools continues in the construction industry, it is becoming far more favourable to solve complex geometric problems in a proactive manner through the use of simulation tools.

This work demonstrated how Monte Carlo simulation can be used to conduct tolerance analysis on large prefabricated modular steel structures. Some of the most challenging connection types to bring into proper alignment are bolted connections, due to the numerous sources of variation in a 3-D construction assembly. By utilizing process capability data in the form of statistical tolerance distributions, simulations can be used to model and subsequently predict misalignments at critical locations. Traditionally, predicting misalignments at joints was elusive due to the complex 3-D interaction between components and the inability to model tolerance accumulation in such systems. However, this work demonstrated the use of Monte Carlo simulation on a project, where misalignments up to 37 mm were successfully identified. While this magnitude of misalignment may not initially seem large enough to warrant a great amount of rework, very strict tolerance requirements are placed on modular construction assemblies [332]. Not only are these strict tolerances required to properly assemble modules offsite (during initial manufacturing), but the overall geometry of modules must comply with strict alignment demands once on site.

The framework was also used to optimize the initial project design considering the large misalignments that were identified. By tightening the tolerance associated with a key fabrication process for bolt hole creation, misalignment rework at connections was substantially reduced. While in the initial design there was essentially 100% chance of a large rework event, the optimized design with tighter tolerances had only a 34% of a small rework event. In this way, Monte Carlo simulation for tolerance analysis was also demonstrated to be a powerful tool for process optimization. Due to the complex geometric behaviour of dimensional variation and tolerances, adjustable connections are often used as a strategy in modular

construction for ensuring proper assembly requirements [333]. However, the use of virtual tools such as tolerance simulation demonstrates that other strategies can be utilized to mitigate the risk of assembly rework. In contrast with adjustable connections that may require a considerable amount of engineering and design effort, the evaluation of alternative fabrication processes can be a much more viable option in some situations. Ultimately, the proposed framework can be used as a platform for comparing these types of alternative strategies due to its versatility and ease of tolerance configuration.

9.2.2 Exact and Approximate Combinatorial Algorithms for Topology Optimization

The need to optimize the geometry and topology of construction components and assemblies can often be framed as combinatorial optimization problems (COPs). Such COPs occur throughout construction and are particularly relevant in architectural panel systems, given the complexity of panel topology, large component quantity in most projects and need to reduce waste produced during fabrication. In such applications, particularly in thin-metal panel systems, it is imperative to reduce material use during fabrication (i.e., metal coils) in order to reduce environmental impacts, improve toolpath cutting time and to decrease production costs. While the current state-of-the-art methods for panel nesting perform some degree of optimization, incorporating panel topology optimization during the unfolding process can add sizeable material savings. This work developed two combinatorial optimization algorithms for panel unfolding: one based on enumerative optimization, and one based on metaheuristic optimization. Through a series of experiments, it was found that when panel complexity is low (i.e., number of panel edges is less than 13), enumerative optimization is superior, and when panel complexity is larger, metaheuristic optimization performs better. In addition, a modified 2D cutting stock algorithm is developed to nest panels on coils. As demonstrated in a case study for a residential construction project, the material savings using both the panel unfolding and nesting algorithms, material waste during fabrication can be reduced by 11%. In general, as panel complexity and quantity increase, so do the expected material savings by adopting the proposed algorithms.

The contributions of this research are two-fold. First, the proposed algorithms provide for an automated file-to-factory system for transforming 3D panel geometry into 2D geometry that can be directly processed by a CNC router. Secondly, the proposed algorithms are shown to optimize panel topology and outperform current state-of-the-art nesting software.

9.2.3 Evaluating Geometric Digital Twinning Methods for Industrialized Building Construction: Towards Automated Parametric BIM Updating

In recent years, the concept of a digital twin has emerged as a way of capturing the complete digital status of an asset or system. The geometric framework of a digital twin, (a "geometric digital twin", or gDT) has been the focus of several research studies that employ the use of 3D scanning to obtain accurate and dense information from a physical asset. The way in which this raw data is used to produce meaningful information and to update the geometric status of an asset becomes the "twinning" method. This research explored three distinct ways that 3D scanning data can be used to produce a geometric digital twin: scan-vs-BIM, scan-to-BIM and parametric BIM updating. Each of these approaches has unique advantages and disadvantages based on the ability to capture non-rigid-body deformations, overall accuracy, fidelity or richness of semantic information, and ability to be used directly to generate an as-built BIM. This research presented the requirements for using gDTs in industrialized building construction based on geometric accuracy, semantic information, and which systems require high-fidelity twinning. Then the capabilities of each gDT approach were presented in terms of how they can be employed for distinct analyses, their ability to generate as-built BIM and enumerated factors that affect their accuracy. A case study was then used to demonstrate and compare each gDT approach.

This case study found that scan-vs-BIM produced the highest average accuracy (6.2 mm) since it eliminates potential errors accrued through reconstructive processes in twinning. Furthermore, this approach can capture non-rigid body deformations such as welding distortion. The main disadvantage of this gDT approach is that it cannot be used directly to create an as-built BIM (nor can it natively produce semantically rich information – currently this must be inferred manually). On the other hand, the parametric BIM updating gDT was found to generate the most semantically rich as-built BIM since it preserves initial semantics (the original geometry is updated parametrically). The main downside with this approach is that it relies on making several parametric assumptions, and as such, has the lowest average accuracy (21.5 mm). While this gDT method can be used directly for as-built BIM creation, it is significantly more challenging to use for generating information required for fabrication and assembly control. Finally, the scan-to-BIM gDT had balanced trade-offs with respect to the other gDTs. With an average accuracy of 16.0 mm it is similar to the accuracy of parametric BIM updating, and likewise, it can directly produce an as-built BIM (albeit not to the same semantic richness).

Based on the observed accuracies of the gDT methods in this chapter and the required dimensional tolerances for many elements in industrialized building construction, it can be concluded that even by using the most accurate laser scanners on the market, additional dimensional quantification technologies

are required (e.g., laser trackers, robotic total stations, etc.) for certain quality control tasks. Laser scanning offers a significant advantage for dimensional verification over legacy and low tech devices such as tape measures since mass-measurements can be obtained automatically and in a relatively short duration. However, in order to achieve the stipulated dimensional tolerance requirements, additional measurement techniques need to augment the digital twins created solely by laser scanning. Finally, this research demonstrated the value that a parametric BIM updating framework could have, with the only barriers for implementation being based on improving the accuracy and pursuing automation.

9.2.4 Automated Parametric BIM Updating

The ability to generate and maintain an accurate and up-to-date BIM that reflects the as-built conditions is becoming a vital necessity in industrialized building construction (and quite frankly in construction as a whole). To date, existing methods for this tend to focus solely on a re-creation process based on a 3D point cloud. The challenge with this approach is well documented in the literature: data-driven methods are often unable to recognize and generate BIMs for complex geometry, while model-driven methods require extensive *a priori* information which must be properly cross-validated for successful generation of BIMs. In addition to the geometric re-creation challenges, semantic enrichment is also a challenging endeavour, requiring extensive *a priori* expert knowledge. Rather than approaching this problem by starting with a point cloud and extracting geometric information which must then be semantically enriched, this research posited starting from an initial as-designed BIM (i.e., "proto-BIM") and updating its geometric parameters to reflect the as-built conditions, creating a dynamic, progressive and intelligent BIM (i.e., "dyna-BIM"). To do this, proto-BIMs must be parameterized to anticipate the types of deformations expected in construction. This research demonstrated how both rigid (i.e., pose) and non-rigid (i.e., shape) deformation can be parameterized efficiently for two of the most common representation schemas used in BIM (CSG and NURBS). Using a process level workflow, it was demonstrated how a parametric associative BIM and an aligned point cloud are the key inputs for obtaining an up-to-date BIM. Compared to previous related studies that use a parametric template approach for generating a CAD model, this research tailored its approach specifically for construction geometry representations. It explored and compared two of the most common metaheuristics for combinatorial optimization; namely genetic algorithm (GA) and simulated annealing (SA). A fitness function for optimization was based on the root mean square error between a given BIM element and a cropped point cloud.

There are many use-cases in construction where a tighter and more accurate as-built BIM than currently achievable is desirable. By starting with a proto-BIM from either an a-priori design source or a good scan-

to-BIM user-interface loaded with lots of "proto-objects", then filling this need with the approaches presented here is possible. The proposed approach is demonstrated using a case study for cast-in-place concrete footings, whose geometry often experiences non-negligible pose and shape deformations that affect subsequent sub-assemblies. In on-site construction, updating the BIM sequentially for critical components such as footings affords the ability to predict downstream geometric conflicts for industrialized building construction. BIM updating can be approached in stages and does not need to be conducted for each constructed component individually. For instance, an entire foundation subassembly could be scanned and updated before the industrialized superstructure is erected. The proposed approach can be easily used to generate an up-to-date BIM and to detect out of tolerance issues. Through a series of experiments, it was found that GA yielded the most reliable results, with the lowest average final deviation between the model elements and the point cloud. In cases where increased computational efficiency is required, SA achieves a similar level of accuracy in a shorter run time. Using the proposed method, the average final deviation between the as-built BIM was reduced from well over 20 mm for the initial as-designed BIM to under 5 mm.

While an alternative strategy to the proposed methodology could be using scan-to-BIM and 'copying over' the semantic information from the as-designed BIM, there is support for developing a parametric associative BIM for use cases other than as-built BIM generation. Further, there is value in exploiting the concept of model versions as part of a digital twin, to gain insight into where and why model changes occur throughout the lifecycle of a built asset (this cannot be achieved with existing scan-to-BIM approaches since entirely new models are created).

9.2.5 End-of-Life Semantic Enrichment Algorithms for Industrialized Buildings

This research demonstrated how spatial parameterization (i.e., extracting, modifying and analyzing parameters that define the spatial properties of a component) can be used as a method for automating steps in disassembly planning for industrialized buildings. The potential use cases of disassembly planning include adaptive building reuse, robotic assembly programming, reconfigurable prefabricated assemblies and selective disassembly for rehabilitation and repairs. This work presents spatial parameterization in a framework to disassemble building components via a rule-based algorithm that comprises three-dimensional Cartesian properties and clash detection between non-semantic CAD elements. Demonstration of the framework is carried out using a case study where the interior wall of a building was disassembled. A comparison of the case study results to the actual disassembly sequence demonstrates how spatial parameterization is effective for automating key steps in disassembly planning. A discussion is provided to identify key barriers to increased automation which relate to modelling

accuracy, Level of Development (LOD) for Building Information Modelling (BIM), and global spatial constraints for disassembly.

Advances in industrialized building systems are also creating reliable solutions for traceability across a project. However, there is an increasing demand to expand traceability to more dimensions than just the materials, processes and stakeholders involved in a project. Social demands for a circular economy, in which parts, products and materials can flow within open resource loops, are necessitating the need for lifecycle-based traceability of our built assets. This research also presented a computational model for "product cycling" of industrialized buildings. Given their innate assembly and disassembly attributes, industrialized building assemblies offer a unique advantage to building owners and building stock managers for cycling of modules (i.e., adding modules in future adaptations, or redistributing, reusing and repurposing of modules into new assets). The basis for a computational model was presented which contained considerations for module topology, lifecycle costs and lifecycle impacts. The result of this model was the development of a product configurator, which serves as a tool for expanding state-of-the-art traceability from being project-based to product-based across multiple lifecycles.

9.2.6 Overall Conclusions

The new algorithms in this form a rational and pragmatic approach to addressing the existing challenges in industrialized building construction. Such developments are effective for improving the status quo in the industry (i.e., improving cost, reducing project duration, and improving quality), and for facilitating continuous innovation in construction. Specifically, the new algorithms reduce rework risk during fabrication and assembly (65% rework reduction in the case study for the new tolerance simulation algorithm), reduce waste during manufacturing (11% waste reduction in the case study for the new panel unfolding and nesting algorithms), improve accuracy and automation of as-built model generation (model error reduction from 50.4 mm to 5.7 mm in the case study for the new parametric BIM updating algorithms), reduce lifecycle cost for adapting industrialized buildings (15% reduction in capital costs in the computational building configurator) and reducing lifecycle impacts for reusing structural systems from industrialized buildings (between 54% to 95% reduction in average lifecycle impacts for the approach illustrated in Appendix B). From a computational standpoint, the algorithms in this possess the following core novel traits. Complex geometric are codified solely based on the innate properties of geometry – that is, by parameterizing geometry and using methods such as combinatorial optimization, topology can be optimized and semantics can be automatically enriched for building assemblies. Such codification stands in contrast to other methods which rely on large datasets (e.g., machine learning), or on extensive expert systems. Employing the use of functional discretization (whereby continuous variable

domains are converted into discrete variable domains) is shown to be highly effective for complex geometric optimization approaches. Finally, the algorithms encapsulate and balance the benefits posed by both parametric and non-parametric schemas, resulting in the ability to achieve both high representational accuracy and semantically rich information (which has previously not been achieved or demonstrated).

One of the key findings in this work is that rather than pre-emptively determining the best suited algorithm for a given process in IBC, it is often more pragmatic to derive both an exact and approximate solution and then decide which is optimal to use for a given process. Generally, most tasks related to optimizing or enriching geometric models are best solved by approximate methods, but it should be noted that there is still value in developing and using exact approaches where possible in order to ensure the global optimum is achieved.

9.3 Limitations & Future Work

As stated in the introduction, the purpose of this thesis was not to develop algorithms that will exhaustively perform all potential geometric and enrichment demands for industrialized building construction. Accomplishing such a task is not feasible to undertake in a single body of work and since the state of IBC continues to evolve, the need for developing novel algorithms is expected to continue well into the future. However, the purpose of this thesis was to demonstrate how each of the major construction-related project stages can be supported through the development of algorithms that fall under a common theme. That theme is predicated on using approximate solving approaches, where possible, in order to achieve good solutions in a reasonable amount of time. For the most part, this was achieved, with the exception of the algorithm developed for semantic enrichment for disassembly planning, which required far more time than conducting the same process manually. However, this research can be further improved. Likewise, there are limitations across all of the algorithms developed in this research, which are presented in detail in each of the following subsections. Before outlining each of these limitations, the following general limitations apply to the research as a whole:

- Since this research focused heavily on the use of approximate algorithms, verifying global optimum solutions is very taxing, and not feasible in some cases. In general, identifying global optimum is only achieved through exact enumeration, and given the large variable domains for various problems, this can prove infeasible. As such, many of the performance metrics reported in this research rely on relative performance, rather than absolute performance.

- Much of the work in this research was established from exposure to industrialized building construction projects in the North American market. As such, many of the claims made and observations (either on performance or need for certain workflows) is based on anecdotal exposure to the North American practice. Implementing the developed algorithms in other markets may have unforeseen obstacles, barriers or nuisances affecting pragmatism or performance.

- Similar to the last point, much of this research focused on case studies for steel-framed industrialized assemblies. The author duly notes the need for algorithms for other types of material typologies such as timber, concrete, and composite systems. One notable example is the topic of dimensional tolerance control. In the author's experience in discussing this topic with industrialized timber manufacturers, there is less emphasis and attention towards the level of accuracy that is required in steel manufactured systems. Because of this, the efficacy of certain algorithms may not be as applicable in other system typologies.

- The use of metaheuristics were implemented based on guidance provided in ancillary research studies. More specifically, this research primarily investigated and compared two well-known metaheuristics: a genetic algorithm and simulated annealing. According to research, these represent two of the most common, yet opposing approaches for solving optimization problems. As such, rather than conducting a comprehensive study of multi-variate metaheuristics, the purpose of this research was to conduct a pragmatic comparison and more importantly to benchmark an approximate algorithmic approach to an exact enumerative approach.

- Throughout the range of possible algorithmic solution approaches, little attention was paid towards the use of expert systems or machine learning. It is well acknowledged that both of these types of artificial intelligence are highly efficacious for solving optimization problems, however they were considered to be outside of the scope of this research. First of all, the use of machine learning relies on having an extensive training set from which to learn and develop an appropriately trained neural network. On the other hand, the use of expert systems can be viewed as a status-quo approach already employed by industry practitioners[20]. The novelty of the algorithms in this research is that little to no external knowledge or large datasets are required for

[20] Based on the author's previous experience as a computational design specialist, many of the pre-existing computational solutions in industry can be viewed as expert systems, which rely very heavily on external knowledge in order to develop solutions, rather than relying on the innate geometric and topological properties of assemblies.

development; rather, the algorithms presented herein attempt to exploit the innate geometric and topological properties of geometry and to perform advanced forms of parameterization. As such, both of these approaches are deemed outside of the scope.

- Finally, it should be noted that a key limitation to this research is validating the efficacy of solutions across multiple projects (i.e., across identical projects as well as diverse projects). This is a valid limitation, especially for stochastic-based algorithms (Monte Carlo method and genetic algorithms) which can generate different solutions each time they are run. As such, it is difficult to gauge the overall repeatability of results across multiple projects.

9.3.1 Tolerance Analysis and Optimization using Monte Carlo Simulation

A limitation to the methodology described is that within an assembly, all non-rigid-body deformation must be "converted" into a net rigid-body effect. While the impact of this assumption was not explored in-depth in this research, many alternative tolerance analysis methods also rely on this same assumption. To overcome this limitation, future work from this research should investigate how to incorporate multi-physics capabilities such as finite element analysis (FEA) into the simulation process. By modelling realistic material behaviour, elastic deformation could be included in the simulation process as a means of gauging how flexible assemblies are for alignment purposes. In addition, "short cuts" to Monte Carlo simulation such as multiplicative dimensional reduction method as shown in [334] could also be interesting to study in future work).

9.3.2 Exact and Approximate Combinatorial Algorithms for Topology Optimization

The biggest limitation to this research is the application examined. Since architectural panel topology was examined instead of explicitly examining an industrialized building assembly, achieving the same material savings (11%) for IBC case studies cannot be claimed. In addition, the nature in which IBC assemblies are produced may not be in the same form as cutting thin-metal panels on CNC machinery. As such, future work is required to implement the proposed algorithms for more direct IBC case studies.

Future research should also include a more thorough evaluation of which metaheuristic techniques perform optimally in a series of applications. For instance, panel nesting for much larger quantities (e.g., 100s, and 1000s) should be examined compared to the 16 panels considered in this case study. Finally, exploring different coil dimensions along with a greater variety of panel geometries would be beneficial to gain further insight into the expected performance of the methods presented in this work.

9.3.3 Automated BIM Updating

Based on the experiments on cast-in-place footings, the author recommends adopting feature-based parametrization when final deviations are allowed to be on the order of centimetres, or where large occlusions exist in the point cloud data. When increased representational accuracy (on the order of millimetres) is necessary, a control point-based schema is recommended so long as the point cloud does not contain large occlusions. Furthermore, it is recommended to ensure an even density distribution of the point cloud to ensure that metaheuristic optimization has a sufficient basis for converging on global optimal solutions (i.e., the desired final geometric state), rather than locking into local optima.

Future work should focus on three areas of development. First, conducting an exploratory study on how the proposed methodology can be applied across a diverse range of industrialized material typologies. Since the case study in this research related to objects which have a non-negligible degree of rigid body (i.e., shape) deformation, the author aims to study the efficacy of metaheuristic optimization for updating objects characterized primarily by pose deformation. Examples of this include structural steel elements, offsite constructed assemblies, and precast concrete components; all of which are produced by highly controlled manufacturing processes, and thus have very low shape deformation. Second, exploring a broader range of optimization techniques for updating a parametric associative BIM. Examples of these methods include Particle Swarm Optimization, Tabu Search and Stochastic Gradient Descent. By exploring a broader range of methods, it may be feasible to identify unique cases where a given method is preferable. Finally, expanding upon the parameterization process proposed in this paper to account for more complex parameters that can be embedded in a model. One example of which is an approach for explicitly parametrizing topological parameters in a feature-based (i.e., CSG) scheme, which was not considered in this paper. While this can already be accounted for using a control point-based schema with shared interface points, topological parameters such as the association of the top of a concrete footing with the bottom of an adjoining concrete pier can be embedded into a single optimization process.

9.3.4 End-of-life Semantic Enrichment – Disassembly Planning

In the case study, many model components were not initially in direct contact that should have been (e.g., the upper horizontal frame member – component c_0 – was not in direct contact with vertical frame members – components c_9 to c_{23}). As a result, manual processing was required to improve this modelling accuracy. While this issue can be addressed upfront within parametric modellers such as Autodesk® Revit, it is much more likely to exist in non-semantic datasets where there is no active parametric control for ensuring contact between components (such as for mesh models or in NURBS-based models).

Another major challenge with the analysis of as-built data relates to uncertainty in assembly composition. For instance, if no updated model exists for a construction assembly, it is difficult to determine hidden components (e.g., not knowing what lies behind a wall before disassembly; this results from not having up-to-date BIM information). In general, data uncertainty is also very challenging for the success of disassembly planning since it can be difficult to gauge component quality and to detect defective connections that reduce the ease of disassembly.

As described in the methods section, this research does not automatically extract constraint matrices for fasteners. This is due to the lack of granularity for fastener details in most BIM models. Another limitation to the proposed algorithm is that highly interconnected (and multi-system) prefabricated assemblies such as pipe assemblies embedded in walls cannot be analyzed since the removal of certain components requires some aspect of deconstruction or "cutting". As such, the proposed algorithm can only be used for linear extraction processes.

Future work should explore methods to decrease the run time through the following aspects: reducing the model complexity (i.e., filtering only CAD elements that pertain to the geometric envelope of an object), exploring what level of detail is required for objects, and optimizing parameter presets in the algorithm (iterative distance value and working-space). Within the algorithm, other improvements can be made so that once a direction has been defined for a given component constraint, redundant processing in elapsed for-loops can be terminated. To automate the process of extracting fastener constraint matrices, future work should explore the use of heuristics to automatically embed this detail into the model, as well as to solve geometric discrepancies between components (e.g., components that should be in contact which are not). Finally, the author aims to explore use cases for the proposed algorithm in the following contexts: scan-to-BIM (through a mesh model medium), and performance comparisons between various construction sectors (e.g., residential, commercial, industrial).

9.3.5 End-of-life Semantic Enrichment – Product Cycling

An obvious point of contention when presenting economic comparisons for alternative investments is lost opportunity cost. While the author does not directly account for lost opportunity cost in the proposed model (i.e., the additional investment required to enable a modular building to be reconfigured), based on the findings, it is found that the additional investment in the foundation is low (< 2% of the total project cost). Another limitation relates to the exclusion of costs and LCA impacts related to the operation and maintenance of the building. Instead, the author has focused exclusively on capital, adaptation and EoL stages for demonstration purposes.

References

[1] Sezer, A.A., Bröchner, J., (2014). *"The construction productivity debate and the measurement of service qualities",* Construction Management and Economics. 32(6), 565-574.

[2] Goodrum, P.M., Haas, C.T., Glover, R.W., (2002). *"The divergence in aggregate and activity estimates of US construction productivity",* Construction management & economics. 20(5), 415-423.

[3] National Society of Professional Engineers, Construction Productivity in Decline, Retrieved Feb 24, 2021 from https://www.leanconstruction.org/media/docs/PEJune14_Construction.pdf (2014) 13.

[4] Sveikauskas, L., Rowe, S., Mildenberger, J.D., (2018). *"Measuring productivity growth in construction",* Monthly Lab.Rev. 141 1.

[5] Sveikauskas, L., Rowe, S., Mildenberger, J., Price, J., Young, A., (2016). *"Productivity growth in construction",* Journal of Construction Engineering and Management. 142(10), 04016045.

[6] Smith, R.E., Rupnik, I., 5 IN 5 MODULAR GROWTH INITATIVE, Modular Building Institute. (2018). https://www.modular.org/documents/document_publication/2018_1019%205in5%20Deliverable.pdf < June 6, 2020 >.

[7] MBI, Modular Advantage Report, Modular Building Institue. (2020)July-August 2020. https://edition.pagesuite-professional.co.uk/html5/reader/production/default.aspx?pubname=&edid=97296285-064e-4158-be58-5b2205d7d348 < July 9, 2020 >.

[8] Ferdous, W., Bai, Y., Ngo, T.D., Manalo, A., Mendis, P., (2019). *"New advancements, challenges and opportunities of multi-storey modular buildings–A state-of-the-art review",* Engineering Structures. 183 883-893. https://doi.org/10.1016/j.engstruct.2019.01.061.

[9] Abanda, F., Tah, J., Cheung, F., (2017). *"BIM in off-site manufacturing for buildings",* Journal of Building Engineering. 14 89-102.

[10] Hu, X., Chong, H., Wang, X., London, K., (2019). *"Understanding stakeholders in off-site manufacturing: a literature review",* Journal of Construction Engineering and Management. 145(8), 03119003.

[11] Wuni, I.Y., Shen, G.Q., (2019). *"Barriers to the Adoption of Modular Integrated Construction: Systematic Review and Meta-Analysis, Integrated Conceptual framework, and Strategies",* Journal of Cleaner Production. 119347. https://doi.org/10.1016/j.jclepro.2019.119347.

[12] Brege, S., Stehn, L., Nord, T., (2014). *"Business models in industrialized building of multi-storey houses",* Construction Management and Economics. 32(1-2), 208-226.

[13] Shahtaheri, Y., Rausch, C., West, J., Haas, C., Nahangi, M., (2017). *"Managing risk in modular construction using dimensional and geometric tolerance strategies",* Automation in Construction. 83 303-315. https://doi.org/10.1016/j.autcon.2017.03.011.

[14] Mostafa, S., Kim, K.P., Tam, V.W., Rahnamayiezekavat, P., (2018). *"Exploring the status, benefits, barriers and opportunities of using BIM for advancing prefabrication practice",* International Journal of Construction Management. 20(2), 1-11.

[15] Yin, X., Liu, H., Chen, Y., Al-Hussein, M., (2019). *"Building information modelling for off-site construction: Review and future directions",* Automation in Construction. 101 72-91. https://doi.org/10.1016/j.autcon.2019.01.010.

[16] Arashpour, M., Heidarpour, A., Akbar Nezhad, A., Hosseinifard, Z., Chileshe, N., Hosseini, R., (2019). *"Performance-based control of variability and tolerance in off-site manufacture and assembly: optimization of penalty on poor production quality",* Construction Management and Economics. 38(6), 502-514. https://doi.org/10.1080/01446193.2019.1616789.

[17] Smith, R.E., (2011).*"Prefab Architecture: A Guide to Modular Design and Construction",* John Wiley & Sons.

[18] Lawson, M., Ogden, R., Goodier, C., (2014).*"Design in Modular Construction",* CRC Press 978-0415554503.

[19] Isaac, S., Bock, T., Stoliar, Y., (2016). *"A methodology for the optimal modularization of building design",* Automation in Construction.

[20] Jaillon, L., Poon, C., Chiang, Y., (2009). *"Quantifying the waste reduction potential of using prefabrication in building construction in Hong Kong",* Waste Management. 29(1), 309-320.

[21] Orlowski, K., (2020). *"Automated manufacturing for timber-based panelised wall systems",* Automation in Construction. 109 102988.

[22] Manrique, J.D., Al-Hussein, M., Bouferguene, A., Safouhi, H., Nasseri, R., (2011). *"Combinatorial Algorithm for Optimizing Wood Waste in Framing Designs",* Journal of Construction Engineering and Management. 137(3), 188-197. 10.1061/(ASCE)CO.1943-7862.0000117.

[23] Kamali, M., Hewage, K., (2016). *"Life cycle performance of modular buildings: A critical review",* Renewable and sustainable energy reviews. 62 1171-1183.

[24] Talebi, S., (2019) Improvement of Dimensional Tolerance Management in Construction. PhD. http://eprints.hud.ac.uk/id/eprint/35070.

[25] Milberg, C.T., Tommelein, I.D., (2009). *"Tolerance and Constructability of Soldier Piles in Slurry Walls",* Journal of Performance of Constructed Facilities. 24(2), 120-127. https://doi.org/10.1061/(ASCE)CF.1943-5509.0000079.

[26] Rausch, C., (2016) Framework for the Strategic Management of Dimensional Variability of Structures in Modular Construction, http://hdl.handle.net/10012/10789. MASc.

[27] Beghini, L.L., Beghini, A., Katz, N., Baker, W.F., Paulino, G.H., (2014). *"Connecting architecture and engineering through structural topology optimization",* Engineering Structures. 59 716-726. https://doi.org/10.1016/j.engstruct.2013.10.032.

[28] de Soto, B.G., Agustí-Juan, I., Hunhevicz, J., Joss, S., Graser, K., Habert, G., Adey, B.T., (2018). *"Productivity of digital fabrication in construction: Cost and time analysis of a robotically built wall",* Automation in Construction. 92 297-311.

[29] Sawhney, A., Riley, M., Irizarry, J., (2020).*"Construction 4.0: An Innovation Platform for the Built Environment",* Routledge.

[30] Greenough, T., Smith, M., Mariash, A., (2019). *"Integrating Computational Design to Improve the Design Workflow of Modular Construction",* Modular and Offsite Construction (MOC) Summit Proceedings. 165-172.

[31] Gann, D.M., (1996). *"Construction as a manufacturing process? Similarities and differences between industrialized housing and car production in Japan",* Construction Management & Economics. 14(5), 437-450. https://doi.org/10.1080/014461996373304.

[32] Larsson, J., Eriksson, P.E., Olofsson, T., Simonsson, P., (2014). *"Industrialized construction in the Swedish infrastructure sector: core elements and barriers",* Construction Management and Economics. 32(1-2), 83-96.

[33] Lessing, J., Brege, S., (2018). *"Industrialized building companies' business models: Multiple case study of Swedish and North American companies",* Journal of Construction Engineering and Management. 144(2), 05017019.

[34] Hall, D.M., Whyte, J.K., Lessing, J., (2020). *"Mirror-breaking strategies to enable digital manufacturing in Silicon Valley construction firms: a comparative case study",* Construction Management and Economics. 38(4), 322-339.

[35] Liu, G., Nzige, J.H., Li, K., (2019). *"Trending topics and themes in offsite construction (OSC) research",* Construction Innovation.

[36] Wuni, I.Y., Shen, G.Q., (2020). *"Critical success factors for modular integrated construction projects: a review",* Building Research & Information. 48(7), 763-784.

[37] Hou, L., Tan, Y., Luo, W., Xu, S., Mao, C., Moon, S., (2020). *"Towards a more extensive application of off-site construction: a technological review",* International Journal of Construction Management. 1-12.

[38] Abdul Nabi, M., El-adaway, I.H., (2020). *"Modular Construction: Determining Decision-Making Factors and Future Research Needs",* Journal of Management in Engineering. 36(6), 04020085.

[39] Steinhardt, D., Manley, K., Bildsten, L., Widen, K., (2020). *"The structure of emergent prefabricated housing industries: a comparative case study of Australia and Sweden",* Construction Management and Economics. 38(6), 483-501.

[40] Woetzel, J., Ram, S., Peloquin, S., Limam, M., Mischke, J., (2017). *"Housing affordability: a supply-side tool kit for cities",* McKinsey Global Institute Executive Briefing, October.

[41] Enshassi, M.S., Walbridge, S., West, J.S., Haas, C.T., (2019). *"Integrated Risk Management Framework for Tolerance-Based Mitigation Strategy Decision Support in Modular Construction Projects",* Journal of Management in Engineering. 35(4),. 10.1061/(ASCE)ME.1943- 5479.0000698.

[42] Enshassi, M.S., Walbridge, S., West, J.S., Haas, C.T., (2020). *"Probabilistic Risk Management Framework for Tolerance-Related Issues in Modularized Projects: Local and Global Perspectives",* ASCE-ASME Journal of Risk and Uncertainty in Engineering Systems, Part A: Civil Engineering. 6(1), 04019022.

[43] Eastman, C., Eastman, C.M., Teicholz, P., Sacks, R., (2011).*"BIM Handbook: A Guide to Building Information Modeling for Owners, Managers, Designers, Engineers and Contractors",* 2nd ed., John Wiley & Sons, New Jersey, USA ISBN 978-0470541371.

[44] Brown, C.M., (1981). *"Some mathematical and representational aspects of solid modeling",* IEEE Transactions on Pattern Analysis and Machine Intelligence. (4), 444-453.

[45] Campbell, R.J., Flynn, P.J., (2001). *"A survey of free-form object representation and recognition techniques",* Computer Vision and Image Understanding. 81(2), 166-210.

[46] Tang, P., Huber, D., Akinci, B., Lipman, R., Lytle, A., (2010). *"Automatic reconstruction of as-built building information models from laser-scanned point clouds: A review of related techniques",* Automation in Construction. 19(7), 829-843. https://doi.org/10.1016/j.autcon.2010.06.007.

[47] Lafarge, F., Keriven, R., Brédif, M., (2010). *"Insertion of 3-D-primitives in mesh-based representations: towards compact models preserving the details",* IEEE Transactions on Image Processing. 19(7), 1683-1694.

[48] Bloomenthal, J., Byvill, B., (2000). *"Implicit surfaces",* Unchained Geometry, Seattle.

[49] Fougerolle, Y.D., Gribok, A., Foufou, S., Truchetet, F., Abidi, M.A., (2005). *"Boolean operations with implicit and parametric representation of primitives using R-functions",* IEEE Transactions on Visualization and Computer Graphics. 11(5), 529-539.

[50] Pătrăucean, V., Armeni, I., Nahangi, M., Yeung, J., Brilakis, I., Haas, C., (2015). *"State of research in automatic as-built modelling",* Advanced Engineering Informatics. 29(2), 162-171. https://doi.org/10.1016/j.aei.2015.01.001.

[51] Meadati, P., Irizarry, J., (2010). *"BIM–a knowledge repository",* 12.

[52] Jabi, W., Soe, S., Theobald, P., Aish, R., Lannon, S., (2017). *"Enhancing parametric design through non-manifold topology",* Design Studies. 52 96-114.

[53] Belsky, M., Sacks, R., Brilakis, I., (2016). *"Semantic enrichment for building information modeling",* Computer-Aided Civil and Infrastructure Engineering. 31(4), 261-274.

[54] Barazzetti, L., Banfi, F., Brumana, R., Previtali, M., (2015). *"Creation of parametric BIM objects from point clouds using NURBS",* The Photogrammetric Record. 30(152), 339-362. https://doi.org/10.1111/phor.12122.

[55] Lee, G., Sacks, R., Eastman, C.M., (2006). *"Specifying parametric building object behavior (BOB) for a building information modeling system",* Automation in Construction. 15(6), 758-776.

[56] Monedero, J., (2000). *"Parametric design: a review and some experiences",* Automation in Construction. 9(4), 369-377.

[57] Chang, K., Chen, C., (2011). *"3D shape engineering and design parameterization",* Computer-Aided Design and Applications. 8(5), 681-692.

[58] Devadas, V., (2018). "Re: Does revit use polygon or nurbs in its geometry?", AUTODESK KNOWLEDGE NETWORK. . DOI:https://forums.autodesk.com/t5/revit-architecture-forum/does-revit-use-polygon-or-nurbs-in-its-geometry/m-p/8289744#M212536.

[59] Sacks, R., Eastman, C.M., Lee, G., (2004). *"Parametric 3D modeling in building construction with examples from precast concrete",* Automation in Construction. 13(3), 291-312.

[60] Esfahania, M.E., Eraya, E., Chuoa, S., Sharifa, M., Haasa, C., (2019). *"Using Scan-to-BIM Techniques to Find Optimal Modeling Effort; A Methodology for Adaptive Reuse Projects",* 36 772-779.

[61] Reinhardt, J., Bedrick, J., (2013). *"Level of Development Specification-Draft 1 April, 19, 2013",* 0-133.

[62] AIA, Building Information Modeling Protocol Exhibit, The American Institute of Architects. Document E202 (2008). https://www.smacna.org/docs/default-source/building-information-modeling/aia-e202-building-information-modeling-protocol-exhibit-pdf.pdf?sfvrsn=333afea5_0 < 12-30-2019 >.

[63] BIMForum, Level of Development (LOD) Specification Part I & Commentary, (2018)Version: 2018.

[64] Ekici, B., Cubukcuoglu, C., Turrin, M., Sariyildiz, I.S., (2019). *"Performative computational architecture using swarm and evolutionary optimisation: A review",* Building and Environment. 147 356-371.

[65] Hu, Z., Yuan, S., Benghi, C., Zhang, J., Zhang, X., Li, D., Kassem, M., (2019). *"Geometric optimization of building information models in MEP projects: Algorithms and techniques for improving storage, transmission and display",* Automation in Construction. 107 102941.

[66] Machairas, V., Tsangrassoulis, A., Axarli, K., (2014). *"Algorithms for optimization of building design: A review",* Renewable and sustainable energy reviews. 31 101-112.

[67] Jewett, J.L., Carstensen, J.V., (2019). *"Topology-optimized design, construction and experimental evaluation of concrete beams",* Automation in Construction. 102 59-67.

[68] Xia, Y., Wu, Y., Hendriks, M.A., (2019). *"Simultaneous optimization of shape and topology of free-form shells based on uniform parameterization model",* Automation in Construction. 102 148-159.

[69] Nadal, A., Cifre, H., Pavón, J., Liébana, Ó, (2017). *"Material use optimization in 3D printing through a physical simulation algorithm",* Automation in Construction. 78 24-33.

[70] Yi, Y.K., Malkawi, A.M., (2009). *"Optimizing building form for energy performance based on hierarchical geometry relation",* Automation in Construction. 18(6), 825-833.

[71] Tuhus-Dubrow, D., Krarti, M., (2010). *"Genetic-algorithm based approach to optimize building envelope design for residential buildings",* Building and Environment. 45(7), 1574-1581.

[72] Fang, Y., Cho, S., (2019). *"Design optimization of building geometry and fenestration for daylighting and energy performance",* Solar Energy. 191 7-18.

[73] Chen, K.W., Janssen, P., Schlueter, A., (2018). *"Multi-objective optimisation of building form, envelope and cooling system for improved building energy performance",* Automation in Construction. 94 449-457.

[74] Said, H., El-Rayes, K., (2014). *"Automated multi-objective construction logistics optimization system",* Automation in Construction. 43 110-122.

[75] Le, P.L., Dao, T., Chaabane, A., (2019). *"BIM-based framework for temporary facility layout planning in construction site",* Construction Innovation.

[76] Lei, Z., Taghaddos, H., Hermann, U., Al-Hussein, M., (2013). *"A methodology for mobile crane lift path checking in heavy industrial projects",* Automation in Construction. 31 41-53.

[77] Ali, A.K., Lee, O.J., Song, H., (2020). *"Robot-based facade spatial assembly optimization",* Journal of Building Engineering. 101556.

[78] Teizer, J., Caldas, C.H., Haas, C.T., (2007). *"Real-time three-dimensional occupancy grid modeling for the detection and tracking of construction resources",* Journal of Construction Engineering and Management. 133(11), 880-888.

[79] Jergeas, G., Put, J.V.d., (2001). *"Benefits of constructability on construction projects",* Journal of Construction Engineering and Management. 127(4), 281-290.

[80] Arditi, D., Elhassan, A., Toklu, Y.C., (2002). *"Constructability analysis in the design firm",* Journal of Construction Engineering and Management. 128(2), 117-126.

[81] Zhu, M., Yang, Y., Gaynor, A.T., Guest, J.K., (2014). *"Considering constructability in structural topology optimization",* 2754-2764.

[82] Kaveh, A., Kalateh-Ahani, M., Fahimi-Farzam, M., (2013). *"Constructability optimal design of reinforced concrete retaining walls using a multi-objective genetic algorithm",* Structural Engineering and Mechanics. 47(2), 227-245.

[83] Lu, W., Tan, T., Xu, J., Wang, J., Chen, K., Gao, S., Xue, F., (2020). *"Design for manufacture and assembly (DfMA) in construction: the old and the new",* Architectural Engineering and Design Management. 1-15.

[84] Gao, S., Jin, R., Lu, W., (2019). *"Design for manufacture and assembly in construction: a review",* Building Research & Information. 1-13.

[85] Wang, J., Li, Z., Tam, V.W., (2015). *"Identifying best design strategies for construction waste minimization",* Journal of Cleaner Production. 92 237-247.

[86] Won, J., Cheng, J.C., (2017). *"Identifying potential opportunities of building information modeling for construction and demolition waste management and minimization",* Automation in Construction. 79 3-18.

[87] Banihashemi, S., Tabadkani, A., Hosseini, M.R., (2018). *"Integration of parametric design into modular coordination: A construction waste reduction workflow",* Automation in Construction. 88 1-12.

[88] Hamann, B., (1994). *"A data reduction scheme for triangulated surfaces",* Computer Aided Geometric Design. 11(2), 197-214.

[89] Wagner, A., Bonduel, M., Pauwels, P., Rüppel, U., (2020). *"Representing construction-related geometry in a semantic web context: A review of approaches",* Automation in Construction. 115 103130.

[90] Hu, Z., Zhang, X., Wang, H., Kassem, M., (2016). *"Improving interoperability between architectural and structural design models: An industry foundation classes-based approach with web-based tools",* Automation in Construction. 66 29-42.

[91] Steel, J., Drogemuller, R., Toth, B., (2012). *"Model interoperability in building information modelling",* Software & Systems Modeling. 11(1), 99-109.

[92] Ballast, D.K., (2007).*"Handbook of Construction Tolerances",* John Wiley & Sons, Hoboken (NJ) 978-0471931515.

[93] Rausch, C., Edwards, C., Haas, C., (2020). *"Benchmarking and Improving Dimensional Quality on Modular Construction Projects–A Case Study",* International Journal of Industrialized Construction. 1(1), 2-21. https://doi.org/10.29173/ijic212.

[94] Rausch, C., Zhang, L., West, J., Haas, C.H., (2016). *"Analyzing the Critical Sources of Dimensional Variability during the Lifecycle of a Steel Framed Modular Construction Project",* Modular and Offsite Construction (MOC) Summit Proceedings. 1(1),.

[95] Jensen, P., Olofsson, T., Johnsson, H., (2012). *"Configuration through the parameterization of building components",* Automation in Construction. 23 1-8. https://doi.org/10.1016/j.autcon.2011.11.016.

[96] BIMobject, The World's Leading BIM Content Platform, 2019 (2019)https://www.bimobject.com/en09/08.

[97] Farr, E.R., Piroozfar, P.A., Robinson, D., (2014). *"BIM as a generic configurator for facilitation of customisation in the AEC industry",* Automation in Construction. 45 119-125. https://doi.org/10.1016/j.autcon.2014.05.012.

[98] Cao, J., Hall, D., (2019). *"An overview of configurations for industralized construction: typologies, customer requirements, and technical approaches",* 2019 European Conference on Computing in Construction. 295-303. 10.35490/EC3.2019.145.

[99] Hall, D.M., (2018). *"CRACKS IN THE MIRROR: CONCEPTUALIZING THE ONGOING AEC INDUSTRY RE-ORGANIZATION",*.

[100] Oracle, Understanding Configurator[s], JD Edwards EnterpriseOne Applications Configurator Implementation Guide. (2014). https://docs.oracle.com/cd/E16582_01/doc.91/e15086/und_configurator.htm#EOABC00284 < 2019/09/10 >.

[101] Jansson, G., Johnsson, H., Engström, D., (2014). *"Platform use in systems building",* Construction Management and Economics. 32(1-2), 70-82. https://doi.org/10.1080/01446193.2013.793376.

[102] Yuan, Z., Sun, C., Wang, Y., (2018). *"Design for Manufacture and Assembly-oriented parametric design of prefabricated buildings",* Automation in Construction. 88 13-22. https://doi.org/10.1016/j.autcon.2017.12.021.

[103] Milberg, C., Tommelein, I., (2003). *"Role of tolerances and process capability data in product and process design integration",* 1-8. https://doi.org/10.1061/40671(2003)93.

[104] BCSA, (2017).*"National Structural Steelwork Specification (NSSS) for Building Construction",* 6th ed., The British Constructional Steelwork Association, UK ISBN 1-85073-067-9.

[105] BCA, Design for Manufacturing and Assembly (DfMA) Prefabricated Mechanical, Electrical, Plumbing (MEP) Systems, (2018). https://www.bca.gov.sg/cpc/others/MEP_Guidebook_final.pdf < April 30, 2019 >.

[106] Bryde, D., Broquetas, M., Volm, J.M., (2013). *"The project benefits of building information modelling (BIM)",* International Journal of Project Management. 31(7), 971-980. https://doi.org/10.1016/j.ijproman.2012.12.001.

[107] Tommelein, I.D., Gholami, S., *"Root causes of clashes in building information models",*. http://irep.ntu.ac.uk/id/eprint/22969.

[108] Akponeware, A.O., Adamu, Z.A., (2017). *"Clash detection or clash avoidance? An investigation into coordination problems in 3D BIM",* Buildings. 7(3), 75. https://doi.org/10.3390/buildings7030075.

[109] Park, C., Lee, D., Kwon, O., Wang, X., (2013). *"A framework for proactive construction defect management using BIM, augmented reality and ontology-based data collection template",* Automation in Construction. 33 61-71. https://doi.org/10.1016/j.autcon.2012.09.010.

[110] Kim, M., Wang, Q., Park, J., Cheng, J.C., Sohn, H., Chang, C., (2016). *"Automated dimensional quality assurance of full-scale precast concrete elements using laser scanning and BIM",* Automation in Construction. 72 102-114. https://doi.org/10.1016/j.autcon.2016.08.035.

[111] Tang, P., Anil, E., Akinci, B., Huber, D., (2011). *"Efficient and effective quality assessment of as-is building information models and 3D laser-scanned data",* Computing in Civil Engineering. 19-22. https://doi.org/10.1061/41182(416)60.

[112] Bosché, F., Ahmed, M., Turkan, Y., Haas, C.T., Haas, R., (2015). *"The value of integrating Scan-to-BIM and Scan-vs-BIM techniques for construction monitoring using laser scanning and BIM: The case*

of cylindrical MEP components", Automation in Construction. 49 201-213. https://doi.org/10.1016/j.autcon.2014.05.014.

[113] Sege, V., Balta, P., (2019) Benefits & barriers of implementing reconfigurable jigs: A study in offsite manufacturing of unique house elements in Sweden, oai:DiVA.org:hj-45194. MASc. http://hj.diva-portal.org/smash/record.jsf?pid=diva2%3A1332567&dswid=-7706.

[114] Rausch, C., Nahangi, M., Haas, C., West, J., (2017). *"Kinematics chain based dimensional variation analysis of construction assemblies using building information models and 3D point clouds",* Automation in Construction. 75 33-44. https://doi.org/10.1016/j.autcon.2016.12.001.

[115] Bloch, T., Sacks, R., (2018). *"Comparing machine learning and rule-based inferencing for semantic enrichment of BIM models",* Automation in Construction. 91 256-272. https://doi.org/10.1016/j.autcon.2018.03.018.

[116] Sacks, R., Ma, L., Yosef, R., Borrmann, A., Daum, S., Kattel, U., (2017). *"Semantic enrichment for building information modeling: procedure for compiling inference rules and operators for complex geometry",* Journal of Computing in Civil Engineering. 31(6), 04017062.

[117] Werbrouck, J., Pauwels, P., Bonduel, M., Beetz, J., Bekers, W., (2020). *"Scan-to-graph: Semantic enrichment of existing building geometry",* Automation in Construction. 119. https://doi-org/10.1016/j.autcon.2020.103286.

[118] Dimitrov, A., Gu, R., Golparvar-Fard, M., (2016). *"Non-uniform B-spline surface fitting from unordered 3D point clouds for as-built modeling",* Computer-Aided Civil and Infrastructure Engineering. 31(7), 483-498. https://doi.org/10.1111/mice.12192.

[119] Yan, J., Zlatanova, S., Aleksandrov, M., DiakitÃ©, A., Pettit, C., (2019).*"Integration of 3d Objects and Terrain for 3d Modelling Supporting the Digital Twin", .*

[120] Nguyen, C.H.P., Choi, Y., (2019). *"Triangular mesh and boundary representation combined approach for 3D CAD lightweight representation for collaborative product development",* Journal of Computing and Information Science in Engineering. 19(1), 011009.

[121] Volk, R., Stengel, J., Schultmann, F., (2014). *"Building Information Modeling (BIM) for existing buildings—Literature review and future needs",* Automation in Construction. 38 109-127. https://doi.org/10.1016/j.autcon.2013.10.023.

[122] Xue, F., Lu, W., Chen, K., Zetkulic, A., (2019). *"From Semantic Segmentation to Semantic Registration: Derivative-Free Optimization–Based Approach for Automatic Generation of Semantically Rich As-Built Building Information Models from 3D Point Clouds",* Journal of Computing in Civil Engineering. 33(4),. https://doi.org/10.1061/(ASCE)CP.1943-5487.0000839.

[123] Czerniawski, T., Leite, F., (2020). *"Automated digital modeling of existing buildings: A review of visual object recognition methods",* Automation in Construction. 113. https://doi.org/10.1016/j.autcon.2020.103131.

[124] Chen, J., Fang, Y., Cho, Y.K., (2018). *"Performance evaluation of 3D descriptors for object recognition in construction applications",* Automation in Construction. 86 44-52.

[125] Ma, J.W., Czerniawski, T., Leite, F., (2020). *"Semantic segmentation of point clouds of building interiors with deep learning: Augmenting training datasets with synthetic BIM-based point clouds",* Automation in Construction. 113 103144.

[126] Wang, Q., Kim, M., (2019). *"Applications of 3D point cloud data in the construction industry: A fifteen-year review from 2004 to 2018",* Advanced Engineering Informatics. 39 306-319.

[127] Son, H., Kim, C., Kim, C., (2015). *"3D reconstruction of as-built industrial instrumentation models from laser-scan data and a 3D CAD database based on prior knowledge",* Automation in Construction. 49 193-200.

[128] Xiong, X., Adan, A., Akinci, B., Huber, D., (2013). *"Automatic creation of semantically rich 3D building models from laser scanner data",* Automation in Construction. 31 325-337.

[129] Dimitrov, A., Golparvar-Fard, M., (2015). *"Segmentation of building point cloud models including detailed architectural/structural features and MEP systems",* Automation in Construction. 51 32-45.

[130] Xue, F., Lu, W., Chen, K., Webster, C.J., (2019). *"BIM reconstruction from 3D point clouds: A semantic registration approach based on multimodal optimization and architectural design knowledge",* Advanced Engineering Informatics. 42. https://doi.org/10.1016/j.aei.2019.100965.

[131] Sacks, R., Kedar, A., Borrmann, A., Ma, L., Brilakis, I., Hüthwohl, P., Daum, S., Kattel, U., Yosef, R., Liebich, T., (2018). *"SeeBridge as next generation bridge inspection: overview, information delivery manual and model view definition",* Automation in Construction. 90 134-145.

[132] Stojanovic, V., Trapp, M., Richter, R., Döllner, J., (2019). *"Service-oriented semantic enrichment of indoor point clouds using octree-based multiview classification",* Graphical Models. 105 101039.

[133] Bloch, T., Sacks, R., (2020). *"Clustering Information Types for Semantic Enrichment of Building Information Models to Support Automated Code Compliance Checking",* Journal of Computing in Civil Engineering. 34(6), 04020040.

[134] Zheliazkova, M., Naboni, R., Paoletti, I., (2015). *"A parametric-assisted method for 3D generation of as-built BIM models for the built heritage",* WIT Transactions on The Built Environment. 153 693-704.

[135] Sadeghineko, F., Kumar, B., (2020). *"Development of Semantically Rich 3D Retrofit Models",* Journal of Computing in Civil Engineering. 34(6), 04020039.

[136] Ribeiro Filho, J.L., Treleaven, P.C., Alippi, C., (1994). *"Genetic-algorithm programming environments",* Computer. 27(6), 28-43. 10.1109/2.294850.

[137] Blum, C., Roli, A., Sampels, M., (2008).*"Hybrid Metaheuristics: An Emerging Approach to Optimization",* Springer, Germany.

[138] Kaveh, A., (2017).*"Applications of Metaheuristic Optimization Algorithms in Civil Engineering",* Springer, Germany.

[139] Blum, C., Roli, A., (2003). *"Metaheuristics in combinatorial optimization: Overview and conceptual comparison",* ACM computing surveys (CSUR). 35(3), 268-308. https://doi.org/10.1145/937503.937505.

[140] Amiri, R., Sardroud, J.M., de Soto, B.G., (2017). *"BIM-based applications of metaheuristic algorithms to support the decision-making process: Uses in the planning of construction site layout",* Procedia Engineering. 196 558-564. https://doi.org/10.1016/j.proeng.2017.08.030.

[141] Henle, M., (1994).*"A Combinatorial Introduction to Topology",* Courier Corporation.

[142] Kacprzyk, J., Coello Coello, C.,A., Dhaenens, C., (2010).*"Advances in Multi-Objective Nature Inspired Computing",* Springer Berlin / Heidelberg, Berlin/Heidelberg 364211217X.

[143] Schrijver, A., (2005). *"On the history of combinatorial optimization (till 1960)",* Handbooks in operations research and management science. 12 1-68. https://doi.org/10.1016/S0927-0507(05)12001-5.

[144] Wäscher, G., Haußner, H., Schumann, H., (2007). *"An improved typology of cutting and packing problems",* European Journal of Operational Research. 183(3), 1109-1130. https://doi.org/10.1016/j.ejor.2005.12.047.

[145] Puchinger, J., Raidl, G.R., (2005). *"Combining metaheuristics and exact algorithms in combinatorial optimization: A survey and classification",* 41-53. https://doi.org/10.1007/11499305_5.

[146] Liao, T.W., Egbelu, P., Sarker, B., Leu, S., (2011). *"Metaheuristics for project and construction management–A state-of-the-art review",* Automation in Construction. 20(5), 491-505. https://doi.org/10.1016/j.autcon.2010.12.006.

[147] Zhou, J., Love, P.E., Wang, X., Teo, K.L., Irani, Z., (2013). *"A review of methods and algorithms for optimizing construction scheduling",* Journal of the Operational Research Society. 64(8), 1091-1105. https://doi.org/10.1057/jors.2012.174.

[148] Monizza, G.P., Bendetti, C., Matt, D.T., (2018). *"Parametric and Generative Design techniques in mass-production environments as effective enablers of Industry 4.0 approaches in the Building Industry",* Automation in Construction. 92 270-285.

[149] Svoboda, L., Novák, J., Kurilla, L., Zeman, J., (2014). *"A framework for integrated design of algorithmic architectural forms",* Advances in Engineering Software. 72 109-118.

[150] Jabi, W., (2013).*"Parametric Design for Architecture",* Laurence King Publ.

[151] Kicinger, R., Arciszewski, T., De Jong, K., (2005). *"Evolutionary computation and structural design: A survey of the state-of-the-art",* Computers & Structures. 83(23-24), 1943-1978.

[152] Lu, W., Webster, C., Chen, K., Zhang, X., Chen, X., (2017). *"Computational Building Information Modelling for construction waste management: Moving from rhetoric to reality",* Renewable and Sustainable Energy Reviews. 68 587-595.

[153] Scheurer, F., (2010). *"Materialising complexity",* Architectural Design. 80(4), 86-93.

[154] Yang, D., Ren, S., Turrin, M., Sariyildiz, S., Sun, Y., (2018). *"Multi-disciplinary and multi-objective optimization problem re-formulation in computational design exploration: A case of conceptual sports building design",* Automation in Construction. 92 242-269.

[155] A. Alwisy, M. Al-Hussein, S. Al-Jibouri, BIM approach for automated drafting and design for modular construction manufacturing, in: Anonymous Computing in Civil Engineering (2012), , 2012, pp. 221-228.

[156] Sharafi, P., Samali, B., Ronagh, H., Ghodrat, M., (2017). *"Automated spatial design of multi-story modular buildings using a unified matrix method",* Automation in Construction. 82 31-42.

[157] Baghdadi, A., Heristchian, M., Kloft, H., (2020). *"Design of prefabricated wall-floor building systems using meta-heuristic optimization algorithms",* Automation in Construction. 114 103156.

[158] Gan, V.J., Tse, K.T., Cheng, J.C., Lo, I.M., Chan, C.M., (2019). *"Site-specific modular design optimization for high-rise residential buildings",* Modular and Offsite Construction (MOC) Summit Proceedings. 544-551.

[159] Zawidzki, M., Jankowski, Ł, (2019). *"Multiobjective optimization of modular structures: Weight versus geometric versatility in a Truss-Z system",* Computer-Aided Civil and Infrastructure Engineering. 34(11), 1026-1040.

[160] Tugilimana, A., Thrall, A.P., Descamps, B., Coelho, R.F., (2017). *"Spatial orientation and topology optimization of modular trusses",* Structural and multidisciplinary optimization. 55(2), 459-476.

[161] Wikberg, F., Olofsson, T., Ekholm, A., (2014). *"Design configuration with architectural objects: linking customer requirements with system capabilities in industrialized house-building platforms",* Construction Management and Economics. 32(1-2), 196-207.

[162] Gbadamosi, A., Oyedele, L., Mahamadu, A., Kusimo, H., Bilal, M., Delgado, J.M.D., Muhammed-Yakubu, N., (2020). *"Big data for Design Options Repository: Towards a DFMA approach for offsite construction",* Automation in Construction. 120 103388.

[163] Benros, D., Duarte, J., (2009). *"An integrated system for providing mass customized housing",* Automation in Construction. 18(3), 310-320.

[164] Mullens, M.A., Armacost, R.L., Swart, W.W., (1995). *"The role of object oriented CAD in a generic simulator for the industrialized housing industry",* Automation in Construction. 4(1), 29-43.

[165] Khalili, A., Chua, D.K., (2014). *"Integrated Prefabrication Configuration and Component Grouping for Resource Optimization of Precast Production",* Journal of Construction Engineering and Management. 140(2), 4013052. 10.1061/(ASCE)CO.1943-7862.0000798.

[166] Gbadamosi, A., Mahamadu, A., Oyedele, L.O., Akinade, O.O., Manu, P., Mahdjoubi, L., Aigbavboa, C., (2019). *"Offsite construction: Developing a BIM-Based optimizer for assembly",* Journal of Cleaner Production. 215 1180-1190. https://doi.org/10.1016/j.jclepro.2019.01.113.

[167] Malik, N., Ahmad, R., Chen, Y., Altaf, M.S., Al-Hussein, M., (2019). *"Minimizing joist cutting waste through dynamic waste allocation in panelized floor manufacturing",* International Journal of Construction Management. 1-13.

[168] Liu, H., Holmwood, B., Sydora, C., Singh, G., Al-Hussein, M., (2017). *"Optimizing multi-wall panel configuration for panelized construction using BIM",* 24-29.

[169] Liu, H., Singh, G., Lu, M., Bouferguene, A., Al-Hussein, M., (2018). *"BIM-based automated design and planning for boarding of light-frame residential buildings",* Automation in Construction. 89 235-249.

[170] Said, H.M., Chalasani, T., Logan, S., (2017). *"Exterior prefabricated panelized walls platform optimization",* Automation in Construction. 76 1-13. https://doi.org/10.1016/j.autcon.2017.01.002.

[171] Kalasapudi, V.S., Tang, P., Zhang, C., Diosdado, J., Ganapathy, R., (2015). *"Adaptive 3D Imaging and Tolerance Analysis of Prefabricated Components for Accelerated Construction",* Procedia Engineering. 118 1060-1067. https://doi.org/10.1016/j.proeng.2015.08.549.

[172] Kalasapudi, V.S., Tang, P., Turkan, Y., (2017). *"Computationally efficient change analysis of piece-wise cylindrical building elements for proactive project control",* Automation in Construction. 81 300-312. https://doi.org/10.1016/j.autcon.2017.04.001.

[173] Guo, J., Wang, Q., Park, J., (2020). *"Geometric quality inspection of prefabricated MEP modules with 3D laser scanning",* Automation in Construction. 111 103053.

[174] Xu, Z., Kang, R., Lu, R., (2020). *"3D reconstruction and measurement of surface defects in prefabricated elements using point clouds",* Journal of Computing in Civil Engineering. 34(5), 04020033.

[175] Hamid, M., Tolba, O., El Antably, A., (2018). *"BIM semantics for digital fabrication: A knowledge-based approach",* Automation in Construction. 91 62-82.

[176] He, R., Li, M., Gan, V.J., Ma, J., (2020). *"BIM-enabled computerized design and digital fabrication of industrialized buildings: A case study",* Journal of Cleaner Production. 278 123505.

[177] Anvari, B., Angeloudis, P., Ochieng, W., (2016). *"A multi-objective GA-based optimisation for holistic Manufacturing, transportation and Assembly of precast construction",* Automation in Construction. 71 226-241.

[178] Shewchuk, J.P., Guo, C., (2011). *"Panel stacking, panel sequencing, and stack locating in residential construction: lean approach",* Journal of Construction Engineering and Management. 138(9), 1006-1016.

[179] Tserng, H.P., Yin, Y., Jaselskis, E.J., Hung, W., Lin, Y., (2011). *"Modularization and assembly algorithm for efficient MEP construction",* Automation in Construction. 20(7), 837-863.

[180] Taghaddos, H., Hermann, U., Abbasi, A., (2018). *"Automated Crane Planning and Optimization for modular construction",* Automation in Construction. 95 219-232.

[181] Rausch, C., Nahangi, M., Perreault, M., Haas, C.T., West, J., (2016). *"Optimum Assembly Planning for Modular Construction Components",* Journal of Computing in Civil Engineering. 04016039. https://doi.org/10.1061/(ASCE)CP.1943-5487.0000605.

[182] Hu, Z., Tian, P., Li, S., Zhang, J., (2018). *"BIM-based integrated delivery technologies for intelligent MEP management in the operation and maintenance phase",* Advances in Engineering Software. 115 1-16.

[183] Kyrö, R., Jylhä, T., Peltokorpi, A., (2019). *"Embodying circularity through usable relocatable modular buildings",* Facilities.

[184] Sanchez Andrade, B., (2019). *"Methodology for improving the net environmental impacts of new buildings through product recovery management",*.

[185] Eckelman, M.J., Brown, C., Troup, L.N., Wang, L., Webster, M.D., Hajjar, J.F., (2018). *"Life cycle energy and environmental benefits of novel design-for-deconstruction structural systems in steel buildings",* Building and Environment. 143 421-430.

[186] Iturralde, K., Linner, T., Bock, T., (2020). *"Matching kit interface for building refurbishment processes with 2D modules",* Automation in Construction. 110. https://doi.org/10.1016/j.autcon.2019.103003.

[187] An, S., Martinez, P., Al-Hussein, M., Ahmad, R., (2020). *"Automated verification of 3D manufacturability for steel frame assemblies",* Automation in Construction. 118 103287.

[188] D.H. Ballard, Generalizing the Hough transform to detect arbitrary shapes, in: Anonymous Readings in Computer Vision, Elsevier, 1987, pp. 714-725.

[189] Linsen, L., (2001).*"Point Cloud Representation",* Univ., Fak. für Informatik, Bibliothek Technical Report, Faculty of Computer ….

[190] A. Borrmann, V. Berkhahn, Principles of Geometric Modeling, in: Anonymous Building Information Modeling, Springer, 2018, pp. 27-41-41.

[191] Hartmanis, J., (1982). *"Computers and Intractability: A Guide to the Theory of NP-Completeness",* SIAM Review. 24(1), 90-91. 10.1137/1024022.

[192] Woeginger, G.J., Jünger, M., Reinelt, G., Rinaldi, G., (2003). *"Exact algorithms for NP-hard problems : A survey",* Lecture notes in computer science. 185-207.

[193] Erwig, M., Smeltzer, K., Wang, X., (2017). *"What is a visual language?",* Journal of Visual Languages & Computing. 38 9-17.

[194] Green, T.R., Petre, M., (1992). *"When visual programs are harder to read than textual programs",* 167-180.

[195] Preidel, C., Borrmann, A., (2016). *"Towards code compliance checking on the basis of a visual programming language",* Journal of Information Technology in Construction (ITcon). 21(25), 402-421.

[196] Asl, M.R., Stoupine, A., Zarrinmehr, S., Yan, W., (2015). *"Optimo: A BIM-based multi-objective optimization tool utilizing visual programming for high performance building design",*.

[197] Lilis, G.N., Giannakis, G.I., Rovas, D.V., (2017). *"Automatic generation of second-level space boundary topology from IFC geometry inputs",* Automation in Construction. 76 108-124.

[198] Seghier, T.E., Ahmad, M.H., Lim, Y., (2019). *"Automation of concrete usage index (CUI) assessment using computational BIM",* International Journal of Built Environment and Sustainability. 6(1), 23-30.

[199] Rausch, C., Nahangi, M., Haas, C., Liang, W., (2019). "Monte Carlo simulation for tolerance analysis in prefabrication and offsite construction", Automation in Construction. 103 300-314. DOI:https://doi.org/10.1016/j.autcon.2019.03.026.

[200] Milberg, C., Tommelein, I.D., Alves, T., (2002). *"Improving design fitness through tolerance analysis and tolerance allocation",*.

[201] Jin, R., Gao, S., Cheshmehzangi, A., Aboagye-Nimo, E., (2018). *"A holistic review of off-site construction literature published between 2008 and 2018",* Journal of Cleaner Production. . https://doi.org/10.1016/j.jclepro.2018.08.195.

[202] AISC, (2010).*"Steel Construction Manual.",* 14th ed., American Institute of Steel Construction 978-1564240606.

[203] Talebi, S., Koskela, L., Shelbourn, M., Tzortzopoulos, P., (2016). *"Critical Review of Tolerance Management in Construction",* 24th Annual Conference of the International Group for Lean Construction. 63-72. http://iglc.net/Papers/Details/1275.

[204] Navas, H., (2015). *"Monte Carlo Model Applied to Tolerance Analysis of Mechanical Assembly Sets",* American Journal of Mechanical Engineering and Automation. 2 55-58. http://www.openscienceonline.com/author/download?paperId=2653&stateId=8000&fileType=3 (Feb 9, 2019).

[205] Nigam, S.D., Turner, J.U., (1995). *"Review of statistical approaches to tolerance analysis",* Computer-Aided Design. 27(1), 6-15. https://doi.org/10.1016/0010-4485(95)90748-5.

[206] Hong, Y., Chang, T., (2002). *"A comprehensive review of tolerancing research",* International Journal of Production Research. 40(11), 2425-2459. https://doi.org/10.1080/00207540210128242.

[207] Gao, J., Chase, K.W., Magleby, S.P., (1998). *"Generalized 3-D tolerance analysis of mechanical assemblies with small kinematic adjustments",* IIE transactions. 30(4), 367-377. https://doi.org/10.1023/A:1007451225222.

[208] Shen, Z., Ameta, G., Shah, J.J., Davidson, J.K., (2004). *"A comparative study of tolerance analysis methods",* 471-482. https://doi.org/10.1115/1.1979509.

[209] Lin, C., Huang, W., Jeng, M., Doong, J., (1997). *"Study of an assembly tolerance allocation model based on Monte Carlo simulation",* Journal of Materials Processing Technology. 70(1-3), 9-16. https://doi.org/10.1016/S0924-0136(97)00034-4.

[210] Yan, H., Wu, X., Yang, J., (2015). *"Application of Monte Carlo method in tolerance analysis",* Procedia CIRP. 27 281-285. https://doi.org/10.1016/j.procir.2015.04.079.

[211] Ramnath, S., Haghighi, P., Chitale, A., Davidson, J.K., Shah, J.J., (2018). *"Comparative Study of Tolerance Analysis Methods Applied to a Complex Assembly",* Procedia CIRP. 75 208-213. https://doi.org/10.1016/j.procir.2018.04.073.

[212] Huang*, S.H., Liu, Q., Musa, R., (2004). *"Tolerance-based process plan evaluation using Monte Carlo simulation",* International Journal of Production Research. 42(23), 4871-4891. https://doi.org/10.1080/00207540420002646O8.

[213] Sleath, L.C., (2014) The dimensional variation analysis of complex mechanical systems. The dimensional variation analysis of complex mechanical systems. Eng.D. https://dspace.lboro.ac.uk/2134/13996.

[214] Henzold, G., (2006).*"Geometrical Dimensioning and Tolerancing for Design, Manufacturing and Inspection: A Handbook for Geometrical Product Specification using ISO and ASME Standards",* Butterworth-Heinemann 978-0750667388.

[215] Yang, K., Basem, S., El-Haik, B., (2003).*"Design for Six Sigma: A Roadmap for Product Development",* McGraw-Hill New York 978-0071412087.

[216] O'Connor, P., Kleyner, A., (2012).*"Practical Reliability Engineering",* John Wiley & Sons 978-0470979815.

[217] Cvetko, R., Chase, K.W., Magleby, S.P., (1998). *"New metrics for evaluating Monte Carlo tolerance analysis of assemblies",*. http://adcats.et.byu.edu/WWW/Publication/98-2/CvP1-2col__6=30=98.PDF (Feb 2, 2019).

[218] AISC, Specification for Structural Steel Buildings (ANSI/AISC 360-10), (2010). https://www.aisc.org/globalassets/aisc/publications/standards/a360-16-spec-and-commentary.pdf < Feb 2, 2019 >.

[219] Shahtaheri, M., Haas, C.T., Salimi, T., (2017). *"A multi-dimensional joint confidence limit approach to mixed mode planning for round-the-clock projects",* Engineering, Construction and Architectural Management. 24(1), 40-60. https://doi.org/10.1108/ECAM-10-2015-0165.

[220] Rausch, C., Sanchez, B., Haas, C., (2021). *"Topology optimization of architectural panels to minimize waste during fabrication: algorithms for panel unfolding and nesting",* Journal of Construction Engineering and Management. . 10.1061/(ASCE)CO.1943-7862.0002089.

[221] M. Eigensatz, M. Kilian, A. Schiftner, N.J. Mitra, H. Pottmann, M. Pauly, Paneling architectural freeform surfaces, in: Anonymous Acm Siggraph 2010, , 2010, pp. 1-10.

[222] Castaneda, E., Lauret, B., Lirola, J., Ovando, G., (2015). *"Free-form architectural envelopes: Digital processes opportunities of industrial production at a reasonable price",* Journal of Facade Design and Engineering. 3(1), 1-13. 10.3233/FDE-150031.

[223] Naqash, M.T., (2019). *"Design and Fabrication of Aluminum Cladding and Curtain Wall of a Sports Club",* Open Journal of Civil Engineering. 9(01), 1. 10.4236/ojce.2019.91001.

[224] Taborianski, V.M., Prado, R.T., (2012). *"Methodology of CO2 emission evaluation in the life cycle of office building façades",* Environmental Impact Assessment Review. 33(1), 41-47. https://doi.org/10.1016/j.eiar.2011.10.004.

[225] Montali, J., Sauchelli, M., Jin, Q., Overend, M., (2019). *"Knowledge-rich optimisation of prefabricated façades to support conceptual design",* Automation in Construction. 97 192-204. https://doi.org/10.1016/j.autcon.2018.11.002.

[226] Yahya, M., Saka, M., (2014). *"Construction site layout planning using multi-objective artificial bee colony algorithm with Levy flights",* Automation in Construction. 38 14-29. https://doi.org/10.1016/j.autcon.2013.11.001.

[227] Kandil, A., El-Rayes, K., El-Anwar, O., (2010). *"Optimization Research: Enhancing the Robustness of Large-Scale Multiobjective Optimization in Construction",* Journal of Construction Engineering and Management. 136(1), 17-25. 10.1061/(ASCE)CO.1943-7862.0000140.

[228] Wu, K., de Soto, B.G., Zhang, F., (2020). *"Spatio-temporal planning for tower cranes in construction projects with simulated annealing",* Automation in Construction. 111 103060.

[229] Li, H., Love, P., (1997). *"Using improved genetic algorithms to facilitate time-cost optimization",* Journal of Construction Engineering and Management. 123(3), 233-237. https://doi.org/10.1061/(ASCE)0733-9364(1997)123:3(233).

[230] Anagnostopoulos, K.P., Koulinas, G.K., (2010). *"A simulated annealing hyperheuristic for construction resource levelling",* Construction Management and Economics. 28(2), 163-175. https://doi.org/10.1080/01446190903369907.

[231] Agirbas, A., (2019). *"Façade form-finding with swarm intelligence",* Automation in Construction. 99 140-151. https://doi.org/10.1016/j.autcon.2018.12.003.

[232] Pantazis, E., Gerber, D., (2018). *"A framework for generating and evaluating façade designs using a multi-agent system approach",* International Journal of Architectural Computing. 16(4), 248-270. https://doi.org/10.1177%2F1478077118805874.

[233] Deng, M., Gan, V.J.L., Tan, Y., Joneja, A., Cheng, J.C.P., (2019). *"Automatic generation of fabrication drawings for façade mullions and transoms through BIM models",* Advanced Engineering Informatics. 42 100964. https://doi.org/10.1016/j.aei.2019.100964.

[234] Di Giuda, G.M., Giana, P.E., Masera, G., Seghezzi, E., Villa, V., (2019). *"A BIM-based approach to façade cladding optimization: Geometrical, economic, and production-control in a DfMA perspective",* 1 324-331. http://doi.org/10.35490/EC3.2019.156.

[235] Ali, A.K., Lee, O.J., Song, H., (2021). *"Robot-based facade spatial assembly optimization",* Journal of Building Engineering. 33 101556. 10.1016/j.jobe.2020.101556.

[236] Lee, A.D., Shepherd, P., Evernden, M.C., Metcalfe, D., (2018). *"Optimizing the architectural layouts and technical specifications of curtain walls to minimize use of aluminium",* 13 8-25. https://doi.org/10.1016/j.istruc.2017.10.004.

[237] Xu, Y., (2016). *"An efficient heuristic approach for irregular cutting stock problem in ship building industry",* Mathematical Problems in Engineering. 2016. https://doi.org/10.1155/2016/8703782.

[238] Cui, Y., Cui, Y., Yang, L., (2014). *"Heuristic for the two-dimensional arbitrary stock-size cutting stock problem",* Computers & Industrial Engineering. 78 195-204. https://doi.org/10.1016/j.cie.2014.10.009.

[239] Kierkosz, I., Luczak, M., (2014). *"A hybrid evolutionary algorithm for the two-dimensional packing problem",* Central European Journal of Operations Research. 22(4), 729-753. https://doi.org/10.1007/s10100-013-0300-0.

[240] Salem, O., Shahin, A., Khalifa, Y., (2007). *"Minimizing Cutting Wastes of Reinforcement Steel Bars Using Genetic Algorithms and Integer Programming Models",* Journal of Construction Engineering and Management. 133(12), 982-992. 10.1061/(ASCE)0733-9364(2007)133:12(982).

[241] Boschetti, M.A., Montaletti, L., (2010). *"An exact algorithm for the two-dimensional strip-packing problem",* Operations research. 58(6), 1774-1791. https://doi.org/10.1287/opre.1100.0833.

[242] Shalaby, M.A., Kashkoush, M., (2013). *"A particle swarm optimization algorithm for a 2-D irregular strip packing problem",* 3(2), 268-278. DOI:10.4236/ajor.2013.32024.

[243] AXYZ, CNC Router for ACM Fabricated Panels: PANELBuilder, 2020 (2020)https://www.axyz.com/us/product/panelbuilder/08/17.

[244] Camp, C.V., Bichon, B.J., Stovall, S.P., (2005). *"Design of steel frames using ant colony optimization",* Journal of Structural Engineering. 131(3), 369-379. https://doi.org/10.1061/(ASCE)0733-9445(2005)131:3(369).

[245] Said Hisham M., Prathyaj, K., (2018). *"Performance Measurement of Building Sheet-Metal Ductwork Prefabrication under Batch Production Settings",* Journal of Construction Engineering and Management. 144(2), 04017107. 10.1061/(ASCE)CO.1943-7862.0001423.

[246] Sherif, S.U., Jawahar, N., Balamurali, M., (2014). *"Sequential optimization approach for nesting and cutting sequence in laser cutting",* Journal of Manufacturing Systems. 33(4), 624-638. https://doi.org/10.1016/j.jmsy.2014.05.011.

[247] Zani, A., Andaloro, M., Deblasio, L., Ruttico, P., Mainini, A.G., (2017). *"Computational design and parametric optimization approach with genetic algorithms of an innovative concrete shading device system",* Procedia engineering. 180 1473-1483. https://doi.org/10.1016/j.proeng.2017.04.310.

[248] Rausch, C., Sanchez, B., Esnaashary Esfahani, M., Haas, C., (2020). *"Computational Algorithms for Digital Twin Support in Construction",* Construction Research Congress 2020. . https://doi.org/10.1061/9780784482865.021.

[249] Dyckhoff, H., (1990). *"A typology of cutting and packing problems",* European Journal of Operational Research. 44(2), 145-159. https://doi.org/10.1016/0377-2217(90)90350-K.

[250] Evtimov, G., Fidanova, S., (2017). *"Heuristic algorithm for 2D cutting stock problem",* 350-357. https://doi.org/10.1007/978-3-319-73441-5_37.

[251] Carravilla, M.A., Ribeiro, C., Oliveira, J.F., (2003). *"Solving nesting problems with non-convex polygons by constraint logic programming",* International Transactions in Operational Research. 10(6), 651-663. 10.1111/1475-3995.00434.

[252] Rutten, D., (2013). *"Galapagos: On the logic and limitations of generic solvers",* Architectural Design. 83 132-135. https://doi.org/10.1002/ad.1568.

[253] Rausch, C., Lu, R., Talebi, S., Haas, C., (2021). *"Deploying 3D scanning based geometric digital twins during fabrication and assembly in offsite manufacturing",* International Journal of Construction Management. . https://doi.org/10.1080/15623599.2021.1896942.

[254] Zhang, J., Long, Y., Lv, S., Xiang, Y., (2016). *"BIM-enabled modular and industrialized construction in China",* Procedia engineering. 145 1456-1461.

[255] A. Parrott, L. Warshaw, Industry 4.0 and the digital twin, 2020 (2017) 1-17https://www2.deloitte.com/us/en/insights/focus/industry-4-0/digital-twin-technology-smart-factory.htmlNov 26.

[256] Lim, K.Y.H., Zheng, P., Chen, C., (2019). *"A state-of-the-art survey of Digital Twin: techniques, engineering product lifecycle management and business innovation perspectives",* Journal of Intelligent Manufacturing. 18 1-25.

[257] Söderberg, R., Wärmefjord, K., Carlson, J.S., Lindkvist, L., (2017). *"Toward a Digital Twin for real-time geometry assurance in individualized production",* CIRP Annals. 66(1), 137-140.

[258] Akcamete, A., Akinci, B., Garrett Jr, J.H., (2008). *"Towards a formal approach for updating building information models",* 5th International Conference on Innovation in AEC 2008. . Obtained 2020-10-31 from https://www.researchgate.net/profile/Asli_Akcamete/publication/260056260_Towards_a_formal_approach_for_updating_building_information_models/links/54fefb000cf2672e2240e557/Towards-a-formal-approach-for-updating-building-information-.

[259] Akcamete, A., Akinci, B., Garrett, J., James H, (2009). *"Motivation for computational support for updating building information models (BIMs)",* International workshop on computing in civil engineering (2009). 523-532-532. https://doi.org/10.1061/41052(346)52.

[260] Nahangi, M., Haas, C.T., (2014). *"Automated 3D compliance checking in pipe spool fabrication",* Advanced Engineering Informatics. 28(4), 360-369. https://doi.org/10.1016/j.aei.2014.04.001.

[261] Nguyen, C.H.P., Choi, Y., (2018). *"Comparison of point cloud data and 3D CAD data for on-site dimensional inspection of industrial plant piping systems",* Automation in Construction. 91 44-52.

[262] ARUP, Digital Twin: Towards a Meaningful Framework, (2019)https://www.arup.com/perspectives/publications/research/section/digital-twin-towards-a-meaningful-frameworkSeptember 16.

[263] Lu, R., Brilakis, I., (2019). *"Digital twinning of existing reinforced concrete bridges from labelled point clusters",* Automation in Construction. 105 102837.

[264] M. Grieves, J. Vickers, Digital twin: Mitigating unpredictable, undesirable emergent behavior in complex systems, in: Anonymous Transdisciplinary Perspectives on Complex Systems, Springer, 2017, pp. 85-113.

[265] Lu, Q., Xie, X., Parlikad, A.K., Schooling, J.M., (2020). *"Digital twin-enabled anomaly detection for built asset monitoring in operation and maintenance",* Automation in Construction. 118 103277. https://doi.org/10.1016/j.autcon.2020.103277.

[266] Brilakis, I., Lourakis, M., Sacks, R., Savarese, S., Christodoulou, S., Teizer, J., Makhmalbaf, A., (2010). *"Toward automated generation of parametric BIMs based on hybrid video and laser scanning data",* Advanced Engineering Informatics. 24(4), 456-465.

[267] Wang, Q., Sohn, H., Cheng, J.C., (2018). *"Automatic as-built BIM creation of precast concrete bridge deck panels using laser scan data",* Journal of Computing in Civil Engineering. 32(3), 04018011.

[268] Ochmann, S., Vock, R., Klein, R., (2019). *"Automatic reconstruction of fully volumetric 3D building models from oriented point clouds",* ISPRS journal of photogrammetry and remote sensing. 151 251-262.

[269] Anil, E.B., Tang, P., Akinci, B., Huber, D., (2013). *"Deviation analysis method for the assessment of the quality of the as-is building information models generated from point cloud data",* Automation in Construction. 35 507-516. https://doi.org/10.1016/j.autcon.2013.06.003.

[270] Martinez, P., Ahmad, R., Al-Hussein, M., (2019). *"A vision-based system for pre-inspection of steel frame manufacturing",* Automation in Construction. 97 151-163. https://doi.org/10.1016/j.autcon.2018.10.021.

[271] FARO, FARO BuildIT Construction Software Techsheet, FARO Technologies, Inc. 2020 (2019)https://insights.faro.com/buildit-construction/techsheet-faro-buildit-construction?_ga=2.89244312.2089616917.1606401423-684408283.1602100014Nov 26.

[272] Sacks, R., (2004). *"Evaluation of economic impact of three-dimensional modeling in precast concrete engineering",* Journal of Computing in Civil Engineering. 18(4), 301-312.

[273] Lu, Q., Chen, L., Li, S., Pitt, M., (2020). *"Semi-automatic geometric digital twinning for existing buildings based on images and CAD drawings",* Automation in Construction. 115. https://doi-org.proxy.lib.uwaterloo.ca/10.1016/j.autcon.2020.103183.

[274] Gao, T., Akinci, B., Ergan, S., Garrett, J., (2015). *"An approach to combine progressively captured point clouds for BIM update",* Advanced Engineering Informatics. 29(4), 1001-1012. https://doi.org/10.1016/j.aei.2015.08.005.

[275] Kim, M., Wang, Q., Li, H., (2019). *"Non-contact sensing based geometric quality assessment of buildings and civil structures: A review",* Automation in Construction. 100 163-179. https://doi.org/10.1016/j.autcon.2019.01.002.

[276] Wang, Q., Kim, M., Cheng, J.C., Sohn, H., (2016). *"Automated quality assessment of precast concrete elements with geometry irregularities using terrestrial laser scanning",* Automation in Construction. 68 170-182. https://doi.org/10.1016/j.autcon.2016.03.014.

[277] Iwashita, T., Packer, J.A., Oliveira, J.d., (2012). *"Defect tolerance for cast steel connections in braced frames",* Journal of Structural Engineering. 138(12), 1455-1464.

[278] Maalek, R., Lichti, D.D., Ruwanpura, J.Y., (2019). *"Automatic Recognition of Common Structural Elements from Point Clouds for Automated Progress Monitoring and Dimensional Quality Control in Reinforced Concrete Construction",* Remote Sensing. 11(9), 1102.

[279] ACI, ACI Committee 117, Commentary on Standard Specifications for Tolerances for Concrete Construction and Materials, ACI 117-06 (2002).

[280] CONSTRUCT, National structural concrete specification for building construction. 4th edition. (2010). https://construct.org.uk/wp-content/uploads/2017/01/NSCS-Edition-4.pdf.

[281] Government of Ontario, (2018). "Building Code Act, 1992, S.O. 1992 c. 23",.

[282] Xiao, Y., (2017) Three-Dimensional Reconstruction and Modeling Using Low-Precision Vision Sensors for Automation and Robotics Applications in Construction, Three-Dimensional Reconstruction and Modeling Using Low-Precision Vision Sensors for Automation and Robotics Applications in Construction. PhD.

[283] Rebolj, D., Pučko, Z., Babič, N.Č, Bizjak, M., Mongus, D., (2017). *"Point cloud quality requirements for Scan-vs-BIM based automated construction progress monitoring",* Automation in Construction. 84 323-334.

[284] FARO, FARO Laser Scanner LS 840/880, <http://www2.faro.com/FaroIP/Files/File/Techsheets%20Download/IN_LS880.pdf>. 2016 (2007) 2http://www2.faro.com/FaroIP/Files/File/Techsheets%20Download/IN_LS880.pdfFeb 2.

[285] R. Lu, C. Rausch, M. Bolpagni, I. Brilakis, C.T. Haas, Geometric accuracy of digital twins for Structural Health Monitoring, in: Anonymous Bridge Engineering, IntechOpen, 2020.

[286] Rausch, C., Haas, C., (2021). *"Automated shape and pose updating of building information model elements from 3D point clouds",* Automation in Construction. 124 103561. https://doi.org/10.1016/j.autcon.2021.103561.

[287] Lin, Y., Lin, C., Hu, H., Su, Y., (2018). *"Developing final as-built BIM model management system for owners during project closeout: A case study",* Advanced Engineering Informatics. 36 178-193. https://doi.org/10.1016/j.aei.2018.04.001.

[288] Zvietcovich, F., Castaneda, B., Perucchio, R., (2015). *"3D solid model updating of complex ancient monumental structures based on local geometrical meshes",* Digital Applications in Archaeology and Cultural Heritage. 2(1), 12-27. https://doi.org/10.1016/j.daach.2015.02.001.

[289] Bosché, F., Guillemet, A., Turkan, Y., Haas, C.T., Haas, R., (2013). *"Tracking the built status of MEP works: Assessing the value of a Scan-vs-BIM system",* Journal of Computing in Civil Engineering. 28(4),. https://doi.org/10.1061/(ASCE)CP.1943-5487.0000343.

[290] Bosché, F., (2010). *"Automated recognition of 3D CAD model objects in laser scans and calculation of as-built dimensions for dimensional compliance control in construction",* Advanced engineering informatics. 24(1), 107-118. https://doi.org/10.1016/j.aei.2009.08.006.

[291] Buonamici, F., Carfagni, M., Furferi, R., Governi, L., Lapini, A., Volpe, Y., (2018). *"Reverse engineering of mechanical parts: A template-based approach",* Journal of computational design and engineering. 5(2), 145-159. https://doi.org/10.1016/j.jcde.2017.11.009.

[292] Buonamici, F., Carfagni, M., Furferi, R., Volpe, Y., Governi, L., (2020). *"Reverse engineering by CAD template fitting: study of a fast and robust template-fitting strategy",* Engineering with Computers. 1-19. https://doi.org/10.1007/s00366-020-00966-4.

[293] Shah, G.A., Polette, A., Pernot, J., Giannini, F., Monti, M., (2020). *"Simulated annealing-based fitting of CAD models to point clouds of mechanical parts' assemblies",* Engineering with Computers. 1-19. https://doi.org/10.1007/s00366-020-00970-8.

[294] Yonekura, K., Watanabe, O., (2014). *"A shape parameterization method using principal component analysis in applications to parametric shape optimization",* Journal of Mechanical Design. 136(12),. https://doi.org/10.1115/1.4028273.

[295] Samareh, J.A., (1999). *"A survey of shape parameterization techniques",*. NAS 1.55:209136/PT1.

[296] Qin, H., Terzopoulos, D., (1996). *"D-NURBS: a physics-based framework for geometric design",* IEEE Transactions on Visualization and Computer Graphics. 2(1), 85-96. https://doi.org/10.1109/2945.489389.

[297] Piegl, L., (1989). *"Modifying the shape of rational B-splines. part 1: curves",* Computer-Aided Design. 21(8), 509-518. https://doi.org/10.1016/0010-4485(89)90059-6.

[298] Piegl, L., (1989). *"Modifying the shape of rational B-splines. part 2: surfaces",* Computer-Aided Design. 21(9), 538-546. https://doi.org/10.1016/0010-4485(89)90014-6.

[299] Piegl, L., Tiller, W., (2012).*"The NURBS Book",* Springer Science & Business Media ISBN 978-3-540-61545-3.

[300] Barazzetti, L., (2016). *"Parametric as-built model generation of complex shapes from point clouds",* Advanced Engineering Informatics. 30(3), 298-311. https://doi.org/10.1016/j.aei.2016.03.005.

[301] Che, X., Liang, X., Li, Q., (2005). *"G1 continuity conditions of adjacent NURBS surfaces",* Computer Aided Geometric Design. 22(4), 285-298. https://doi.org/10.1016/j.cagd.2005.01.001.

[302] Zheng, J., Wang, G., Liang, Y., (1995). *"GCn continuity conditions for adjacent rational parametric surfaces",* Computer Aided Geometric Design. 12(2), 111-129. https://doi.org/10.1016/0167-8396(94)00005-D.

[303] Lowe, D.G., (1991). *"Fitting parameterized three-dimensional models to images",* IEEE Transactions on Pattern Analysis & Machine Intelligence. 441-450. https://doi.org/10.1109/34.134043.

[304] Tam, G.K., Cheng, Z., Lai, Y., Langbein, F.C., Liu, Y., Marshall, D., Martin, R.R., Sun, X., Rosin, P.L., (2012). *"Registration of 3D point clouds and meshes: A survey from rigid to nonrigid",* IEEE Transactions on Visualization and Computer Graphics. 19(7), 1199-1217. https://doi.org/10.1109/TVCG.2012.310.

[305] Van Kaick, O., Zhang, H., Hamarneh, G., Cohen-Or, D., (2011). *"A survey on shape correspondence",* 30 1681-1707. https://doi.org/10.1111/j.1467-8659.2011.01884.x.

[306] Elbeltagi, E., Hegazy, T., Grierson, D., (2005). *"Comparison among five evolutionary-based optimization algorithms",* Advanced engineering informatics. 19(1), 43-53.

[307] Johnson, D.S., Aragon, C.R., McGeoch, L.A., Schevon, C., (1989). *"Optimization by simulated annealing: An experimental evaluation; part I, graph partitioning",* Operations research. 37(6), 865-892.

[308] Zwierzycki, M., Evers, H.L., Tamke, M., (2016). *"Parametric architectural design with point-clouds",* 2.

[309] Rausch, C., Sanchez, B., Haas, C., (2019). *"Spatial Parameterization of Non-Semantic CAD Elements for Supporting Automated Disassembly Planning",* Modular and Offsite Construction (MOC) Summit Proceedings. 108-115. 10.29173/mocs83.

[310] Rausch, C., Sanchez, B., Edwards, C., Haas, C., (2020). *"A computational model for product cycling of modular buildings",* EG-ICE 2020 Workshop on Intelligent Computing in Engineering. 304-313. https://doi.org/10.14279/depositonce-9977.

[311] Jaillon, L., Poon, C., (2014). *"Life cycle design and prefabrication in buildings: A review and case studies in Hong Kong",* Automation in Construction. 39 195-202.

[312] Geissdoerfer, M., Savaget, P., Bocken, N.M., Hultink, E.J., (2017). *"The Circular Economy–A new sustainability paradigm?",* Journal of Cleaner Production. 143 757-768.

[313] Korhonen, J., Honkasalo, A., Seppälä, J., (2018). *"Circular economy: the concept and its limitations",* Ecological Economics. 143 37-46.

[314] Sanchez, B., Haas, C., (2018). *"A novel selective disassembly sequence planning method for adaptive reuse of buildings",* Journal of Cleaner Production. 183 998-1010.

[315] S. Vongbunyong, W.H. Chen, General Disassembly Process, in: Anonymous Disassembly Automation, Springer, 2015, pp. 9-24.

[316] Sanchez, B., Rausch, C., Haas, C., Saari, R., (2020). "A selective disassembly multi-objective optimization approach for adaptive reuse of building components", Resources, Conservation and Recycling. 154 104605. DOI:https://doi.org/10.1016/j.resconrec.2019.104605.

[317] Smith, S., Smith, G., Chen, W., (2012). *"Disassembly sequence structure graphs: An optimal approach for multiple-target selective disassembly sequence planning",* Advanced engineering informatics. 26(2), 306-316.

[318] Minunno, R., O'Grady, T., Morrison, G., Gruner, R., Colling, M., (2018). *"Strategies for applying the circular economy to prefabricated buildings",* Buildings. 8(9), 125.

[319] Adams, K., Osmani, M., Thorpe, T., Thornback, J., (2017). *"Circular economy in construction: current awareness, challenges and enablers",*.

[320] Lieder, M., Rashid, A., (2016). *"Towards circular economy implementation: a comprehensive review in context of manufacturing industry",* Journal of Cleaner Production. 115 36-51.

[321] Smith, R.E., Rupnik, I., (2019). *"10 Productivity, innovation and disruption",* Offsite Production and Manufacturing for Innovative Construction: People, Process and Technology.

[322] Jensen, P., (2010) Configuration of modularised building systems, Configuration of modularised building systems. PhD. http://www.diva-portal.org/smash/record.jsf?pid=diva2%3A999331&dswid=7490.

[323] International Standard Organization, (1997).*"ISO 14040: Environmental Management-Life Cycle Assessment-Principles and Framework",* .

[324] Cabeza, L.F., Rincón, L., Vilariño, V., Pérez, G., Castell, A., (2014). *"Life cycle assessment (LCA) and life cycle energy analysis (LCEA) of buildings and the building sector: A review",* Renewable and sustainable energy reviews. 29 394-416.

[325] Azari, R., Abbasabadi, N., (2018). *"Embodied energy of buildings: A review of data, methods, challenges, and research trends",* Energy and Buildings. 168 225-235.

[326] Sanchez, B., Esfahani, M.E., Haas, C., (2019). *"A methodology to analyze the net environmental impacts and building's cost performance of an adaptive reuse project: a case study of the Waterloo County Courthouse renovations",* Environment Systems and Decisions. 39(4), 419-438.

[327] TAF, Embodied Carbon in Construction: Policy Primer for Ontario, The Atmospheric Fund. (2017). http://taf.ca/wp-content/uploads/2018/04/Embodied-Carbon-in-Construction.PRIMER-FINAL.pdf.

[328] Jensen, P., Lidelöw, H., Olofsson, T., (2015). *"Product configuration in construction",* International Journal of Mass Customisation. 5(1), 73-92.

[329] Nunez, J.G., (2010). Prefab the FabLab: rethinking the habitability of a fabrication lab by including fixture-based components.

[330] H. Kagermann, Change through digitization—Value creation in the age of Industry 4.0, in: Anonymous Management of Permanent Change, Springer, 2015, pp. 23-45.

[331] Agarwal, R., Chandrasekaran, S., Sridhar, M., (2016). *"Imagining construction's digital future",* MCKINSEY INSIGHTS REPORT, MCKINSEY & COMPANY AND MCKINSEY GLOBAL INSTITUTE, JUN.

[332] M. Lawson, R. Ogden, C. Goodier, Chapter 16: Construction issues in modular systems, in: Anonymous Design in Modular Construction, CRC Press, 2014, pp. 211-224. 978-0415554503.

[333] Sharafi, P., Mortazavi, M., Samali, B., Ronagh, H., (2018). *"Interlocking system for enhancing the integrity of multi-storey modular buildings",* Automation in Construction. 85 263-272. https://doi.org/10.1016/j.autcon.2017.10.023.

[334] Zhang, X., Pandey, M.D., Zhang, Y., (2014). *"Computationally efficient reliability analysis of mechanisms based on a multiplicative dimensional reduction method",* Journal of Mechanical Design. 136(6),.

[335] Kanters, J., (2020). *"Circular Building Design: An Analysis of Barriers and Drivers for a Circular Building Sector",* Buildings. 10(4), 77.

[336] Rose, C.M., Stegemann, J.A., (2018). *"Characterising existing buildings as material banks (E-BAMB) to enable component reuse",* 172 129-140.

[337] Kirchherr, J., Reike, D., Hekkert, M., (2017). *"Conceptualizing the circular economy: An analysis of 114 definitions",* Resources, Conservation and Recycling. 127 221-232.

[338] Minunno, R., O'Grady, T., Morrison, G.M., Gruner, R.L., (2020). *"Exploring environmental benefits of reuse and recycle practices: A circular economy case study of a modular building",* Resources, Conservation and Recycling. 160 104855.

[339] Brütting, J., De Wolf, Catherine Elvire L, Fivet, C., (2019). The reuse of load-bearing components.

[340] Brütting, J., Senatore, G., Fivet, C., (2019). *"Form follows availability–Designing structures through reuse",* Journal of the International Association for Shell and Spatial Structures. 60(4), 257-265.

[341] Yeung, J., Walbridge, S., Haas, C., (2015). *"The role of geometric characterization in supporting structural steel reuse decisions",* Resources, Conservation and Recycling. 104 120-130.

[342] Yeung, J., (2016). *"Development of analysis tools for the facilitation of increased structural steel reuse",.*

[343] Becqué, R., Mackres, E., Layke, J., Aden, N., Liu, S., Managan, K., Nesler, C., Mazur-Stommen, S., Petrichenko, K., Graham, P., (2016). *"Accelerating building efficiency: Eight actions for urban leaders",* World Resources Institute, Washington, DC.

[344] Bullen, P.A., Love, P.E., (2010). *"The rhetoric of adaptive reuse or reality of demolition: Views from the field",* Cities. 27(4), 215-224.

[345] Shahi, S., Esfahani, M.E., Bachmann, C., Haas, C., (2020). *"A Definition Framework for Building Adaptation Projects",* Sustainable Cities and Society. 102345.

[346] Rakhshan, K., Morel, J., Alaka, H., Charef, R., (2020). *"Components reuse in the building sectorâ€“A systematic review",* Waste Management & Research. 38(4), 347-370.

[347] Huuhka, S., Kaasalainen, T., Hakanen, J., Lahdensivu, J., (2015). *"Reusing concrete panels from buildings for building: Potential in Finnish 1970s mass housing",* Resources, Conservation and Recycling. 101 105-121.

[348] Dorsthorst, B.t., Kowalczyk, T., (2005). *"State of Deconstruction in the Netherlands",* CIB Report, Publication. 300 162-180.

[349] Diyamandoglu, V., Fortuna, L.M., (2015). *"Deconstruction of wood-framed houses: Material recovery and environmental impact",* Resources, Conservation and Recycling. 100 21-30.

[350] Gorgolewski, M., (2008). *"Designing with reused building components: some challenges",* Building Research & Information. 36(2), 175-188.

[351] Spector, S., (2003). *"Creating Schools and Strengthening Communities through Adaptive Reuse.",*.

[352] Yung, E.H., Chan, E.H., (2012). *"Implementation challenges to the adaptive reuse of heritage buildings: Towards the goals of sustainable, low carbon cities",* Habitat International. 36(3), 352-361.

[353] Esnaashary Esfahani, M., Rausch, C., Haas, C., Adey, B.T., (2020). *"Prioritizing Preproject Planning Activities Using Value of Information Analysis",* Journal of Management in Engineering. 36(5), 04020064.

[354] SCI, Protocol for reusing structural steel, Steel Construction Institute. (2019). https://steel-sci.com/assets/downloads/steel-reuse-protocol-v06.pdf < July 9, 2020 >.

[355] Hollberg, A., Ruth, J., (2016). *"LCA in architectural design—a parametric approach",* The International Journal of Life Cycle Assessment. 21(7), 943-960.

[356] Tingley, D.D., Davison, B., (2012). *"Developing an LCA methodology to account for the environmental benefits of design for deconstruction",* Building and Environment. 57 387-395.

[357] Treloar, G.J., Love, P.E., Holt, G.D., (2001). *"Using national input/output data for embodied energy analysis of individual residential buildings",* Construction Management and Economics. 19(1), 49-61.

[358] Webster, M., Costello, D., (2006). Designing structural systems for deconstruction.

[359] Jurkait, K., Stiglmair, J., (2019). *"Cradle-to-Cradle in Building Services",* E&ES. 225(1), 012013.

[360] Tingley, D.D., Davison, B., (2011). *"Design for deconstruction and material reuse",* Proceedings of the institution of civil engineers-energy. 164(4), 195-204.

[361] Rios, F.C., Grau, D., (2019). *"Circular Economy in the Built Environment: Designing, Deconstructing, and Leasing Reusable Products",*.

[362] Iacovidou, E., Purnell, P., (2016). *"Mining the physical infrastructure: Opportunities, barriers and interventions in promoting structural components reuse",* Science of the Total Environment. 557 791-807.

[363] Ross, B.E., Chen, D.A., Conejos, S., Khademi, A., (2016). *"Enabling adaptable buildings: Results of a preliminary expert survey",* Procedia Engineering. 145(Supplement C), 420-427.

[364] Nijs, J.C., Durmisevic, E., Halman, J.I., (2011). *"Interface design for open systems building",* open house international. 36(1), 35.

[365] AIA, BUILDINGS THAT LAST: DESIGN FOR ADAPTABILITY, DECONSTRUCTION, AND REUSE, The American Institute of Architects. (2020). http://content.aia.org/sites/default/files/2020-03/ADR-Guide-final_0.pdf < July 10, 2020 >.

[366] Ellen MacArthur Foundation, (2015). *"Towards a circular economy: Business rationale for an accelerated transition",*.

[367] Sehnem, S., Campos, L.M., Julkovski, D.J., Cazella, C.F., (2019). *"Circular business models: level of maturity",* Management Decision.

[368] Lewandowski, M., (2016). *"Designing the business models for circular economy—Towards the conceptual framework",* Sustainability. 8(1), 43.

[369] Planing, P., (2015). *"Business model innovation in a circular economy reasons for non-acceptance of circular business models",* Open journal of business model innovation. 1(11), 1-11.

[370] Carra, G., Magdani, N., (2017). *"Circular business models for the built environment",* Arup, BAM & CE100: London, UK.

[371] Mendoza, J.M.F., Gallego-Schmid, A., Azapagic, A., (2019). *"Building a business case for implementation of a circular economy in higher education institutions",* Journal of Cleaner Production. 220 553-567.

[372] Ünal, E., Urbinati, A., Chiaroni, D., Manzini, R., (2019). *"Value Creation in Circular Business Models: The case of a US small medium enterprise in the building sector",* Resources, Conservation and Recycling. 146 291-307.

[373] Leising, E., Quist, J., Bocken, N., (2018). *"Circular Economy in the building sector: Three cases and a collaboration tool",* Journal of Cleaner Production. 176 976-989.

[374] Vihola, J., Edelman, H., (2016). *"Life-cycle economics of rentable prefabricated school facility units in municipal real estate procurement",*.

[375] Kim, D., (2008). Preliminary Life Cycle Analysis of Modular and Conventional Housing in Benton Harbor, MI.

[376] Kamali, M., Hewage, K., Milani, A.S., (2018). *"Life cycle sustainability performance assessment framework for residential modular buildings: Aggregated sustainability indices",* Building and Environment. 138 21-41.

[377] Faludi, J., Lepech, M.D., Loisos, G., (2012). *"Using life cycle assessment methods to guide architectural decision-making for sustainable prefabricated modular buildings",* Journal of green building. 7(3), 151-170.

[378] Aye, L., Ngo, T., Crawford, R.H., Gammampila, R., Mendis, P., (2012). *"Life cycle greenhouse gas emissions and energy analysis of prefabricated reusable building modules",* Energy and Buildings. 47 159-168.

[379] Geldermans, R., (2016). *"Design for change and circularityâ€“accommodating circular material & product flows in construction",* Energy Procedia. 96 301-311.

[380] Koutamanis, A., van Reijn, B., van Bueren, E., (2018). *"Urban mining and buildings: A review of possibilities and limitations",* Resources, Conservation and Recycling. 138 32-39.

[381] CORDIS, Buildings as Material Banks: Integrating Materials Passports with Reversible Building Design to Optimise Circular Industrial Value Chains, European Commission. 2020 (2020)https://cordis.europa.eu/project/id/64238407/06.

[382] Gepts, B., Meex, E., Nuyts, E., Knapen, E., Verbeeck, G., (2019). *"Existing databases as means to explore the potential of the building stock as material bank",* 225 1755-1315.

[383] Bragança, L., (2019). *"SBE19 Brussels-BAMB-CIRCPATH: Building As Material Banks: a pathway for a circular future",*.

[384] Akbarieh, A., Jayasinghe, L.B., Waldmann, D., Teferle, F.N., (2020). *"BIM-Based End-of-Lifecycle Decision Making and Digital Deconstruction: Literature Review",* Sustainability. 12(7), 2670.

[385] Brand, S., (1995).*"How Buildings Learn: What Happens After they'Re Built",* Penguin.

[386] Bertram, N., Fuchs, S., Mischke, J., Palter, R., Strube, G., Woetzel, J., (2019). *"Modular construction: From projects to products",* McKinsey & Company: Capital Projects & Infrastructure. 1-34.

[387] Bertin, I., Mesnil, R., Jaeger, J., Feraille, A., Le Roy, R., (2020). *"A BIM-Based Framework and Databank for Reusing Load-Bearing Structural Elements",* Sustainability. 12(8), 3147.

[388] Salama, T., Salah, A., Moselhi, O., Al-Hussein, M., (2017). *"Near optimum selection of module configuration for efficient modular construction",* Automation in Construction. 83 316-329.

[389] Peters, M., Ribeiro, A., Oseyran, J., Wang, K., Buildings as Materials Banks and the Need for Innovative Business Models, Horizon 2020 Framework Programme of the European Union. (2017). https://www.bamb2020.eu/wp-content/uploads/2017/11/BAMB_Business-Models_20171114_extract.pdf < July 16, 2020 >.

[390] Srisangeerthanan, S., Hashemi, M.J., Rajeev, P., Gad, E., Fernando, S., (2020). *"Review of performance requirements for inter-module connections in multi-story modular buildings",* Journal of Building Engineering. 28 101087.

[391] Finkbeiner, M., Inaba, A., Tan, R., Christiansen, K., Klüppel, H., (2006). *"The new international standards for life cycle assessment: ISO 14040 and ISO 14044",* The international journal of life cycle assessment. 11(2), 80-85.

[392] ASTM, Environmental Product Declaration: Fabricated Steel Structural Sections, ASTM International. 122 (2019). https://www.astm.org/CERTIFICATION/DOCS/469.EPD_for__Structural_FINAL_20191212.pdf < July 22, 2019 >.

[393] PE International AG, LCA Background Report for Steel Specialty Products: Life cycle assessment background report in support of an Environmental Product Declaration (EPD) for steel specialty products. Ceilings and Interior Systems Construction Association. (2014). http://www.gordon-inc.com/literature/pdf/cisca%20epd%20background%20report%20(fe)%202014-11-25.pdf < July 22, 2019 >.

Appendix A: Visual Programming Language Based Algorithms Developed in this Research

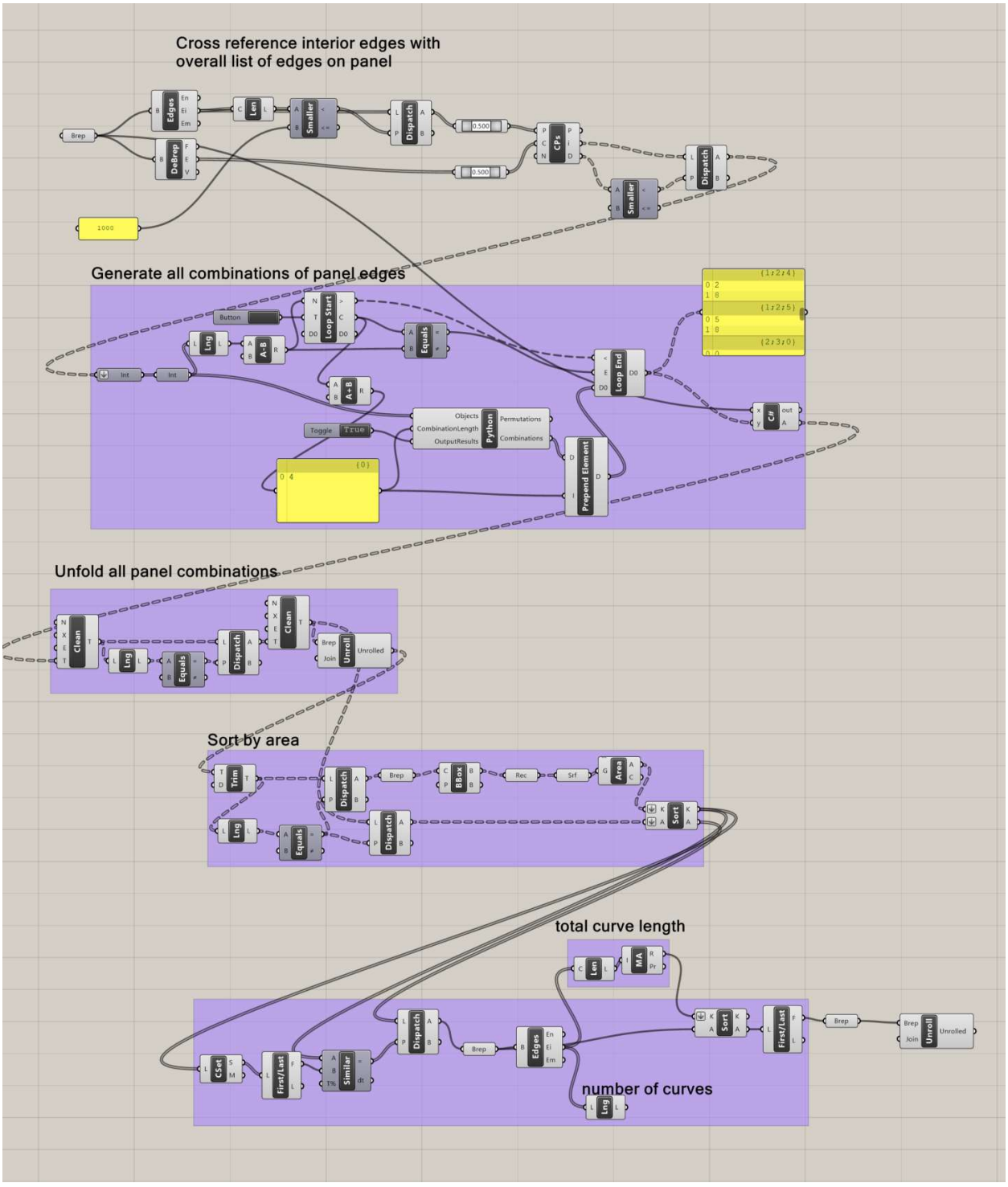

Figure 61: Grasshopper script for Algorithm 2 (Chapter 5)

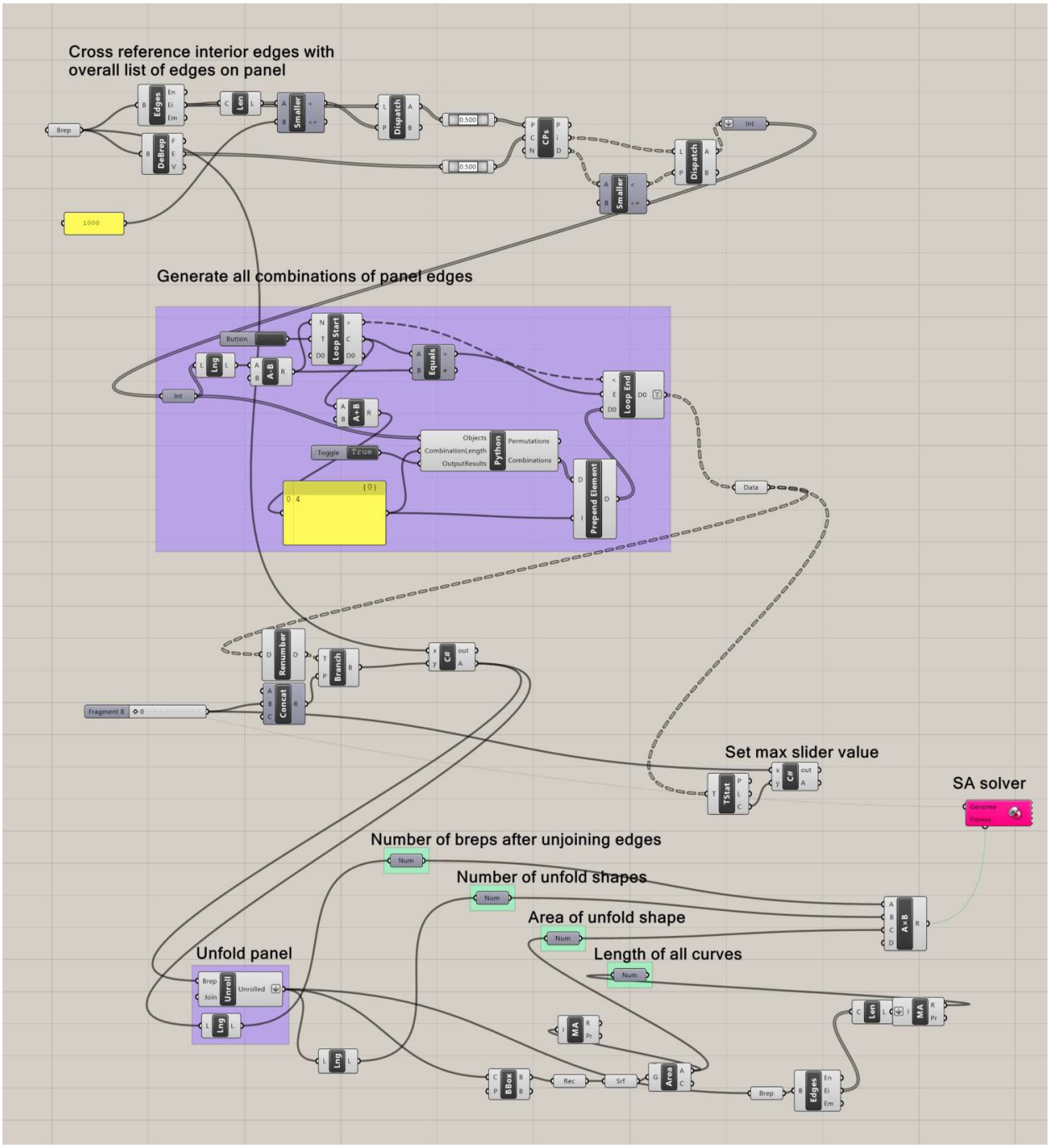

Figure 62: Grasshopper script for Algorithm 3 (Chapter 5)

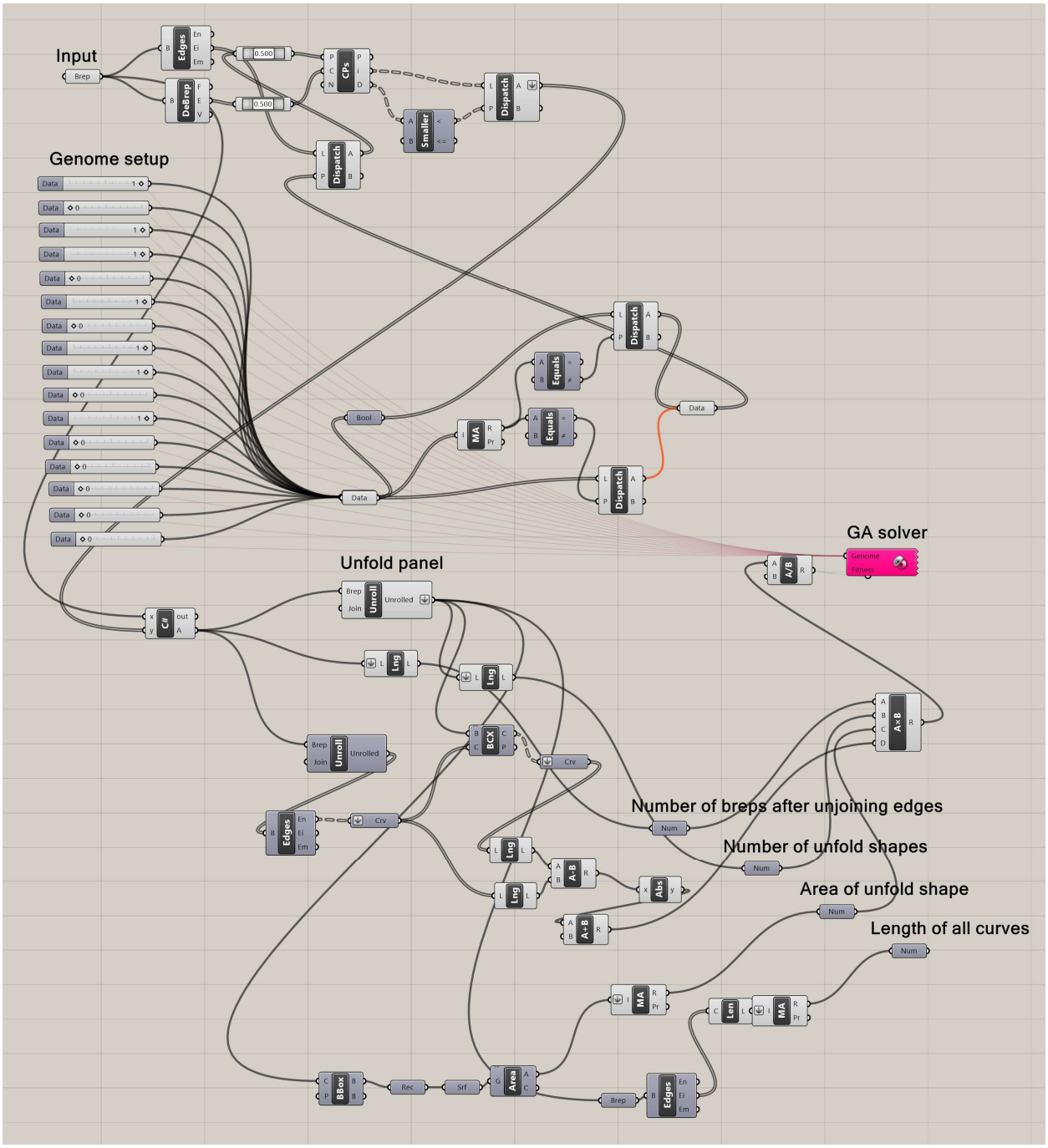

Figure 63: Grasshopper script for Algorithm 4 (Chapter 5)

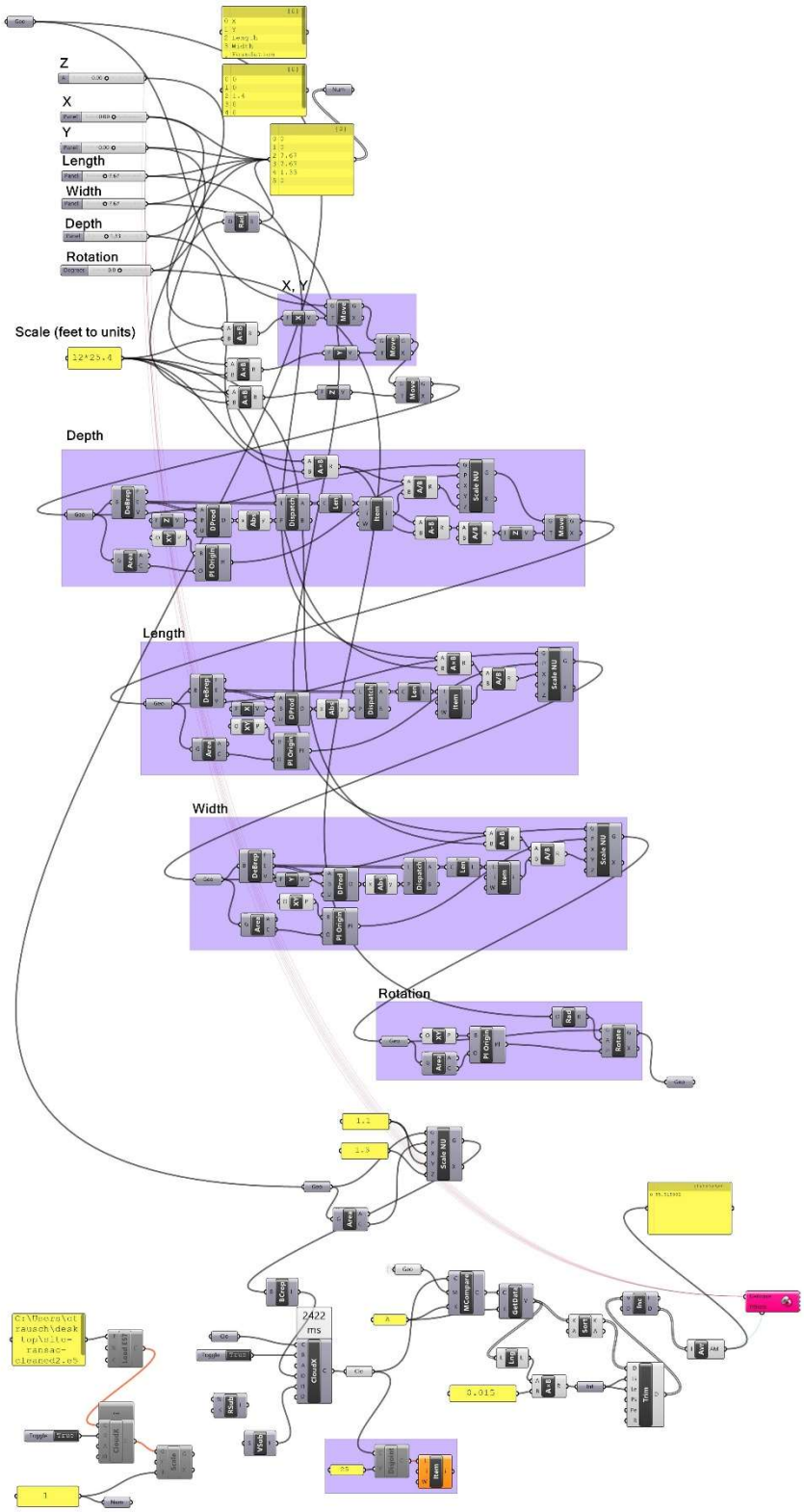

Figure 64: Grasshopper script for feature-based parameterization algorithm (Chapter 7)

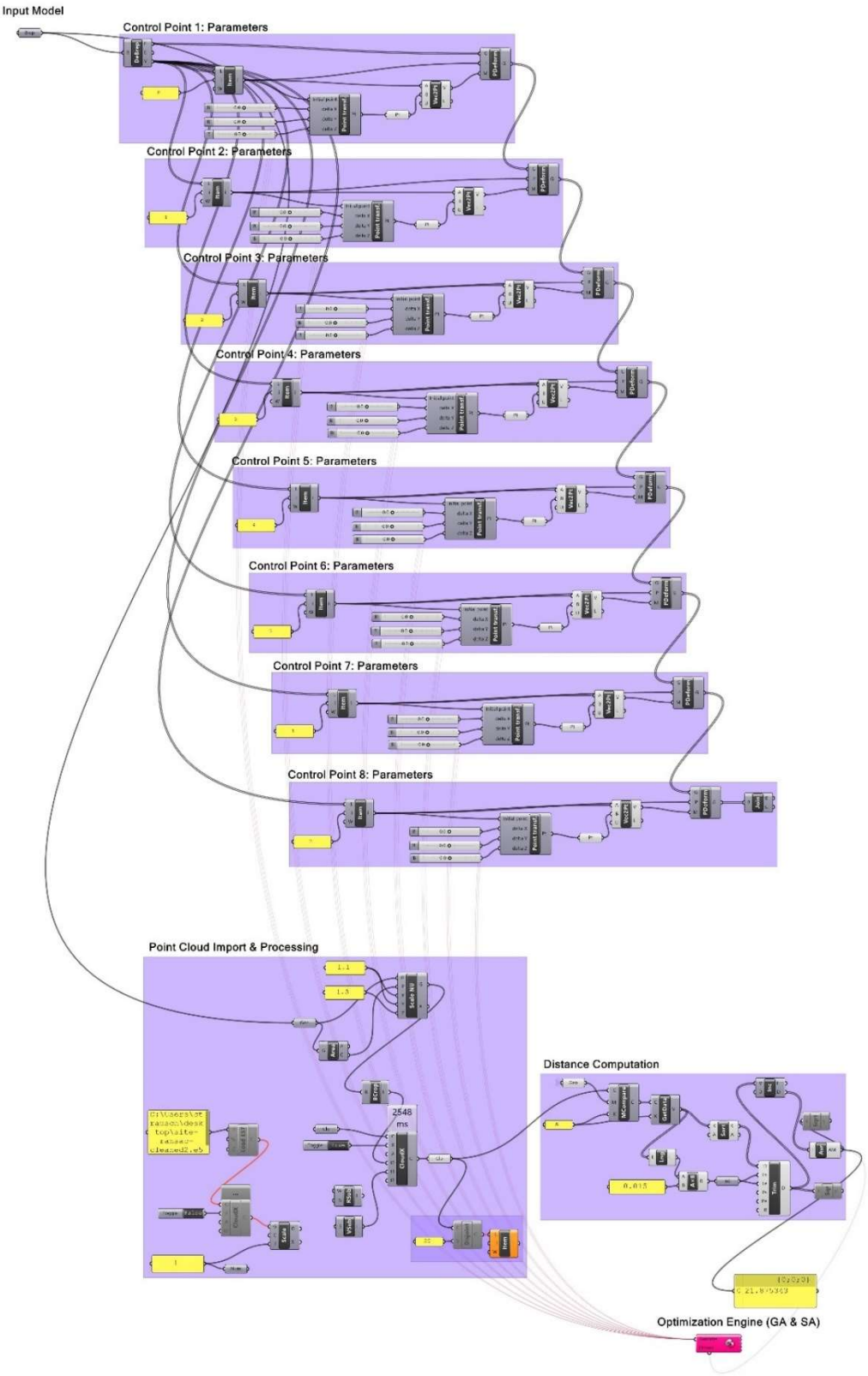

Figure 65: Grasshopper script for control point based parameterization algorithm (Chapter 7)

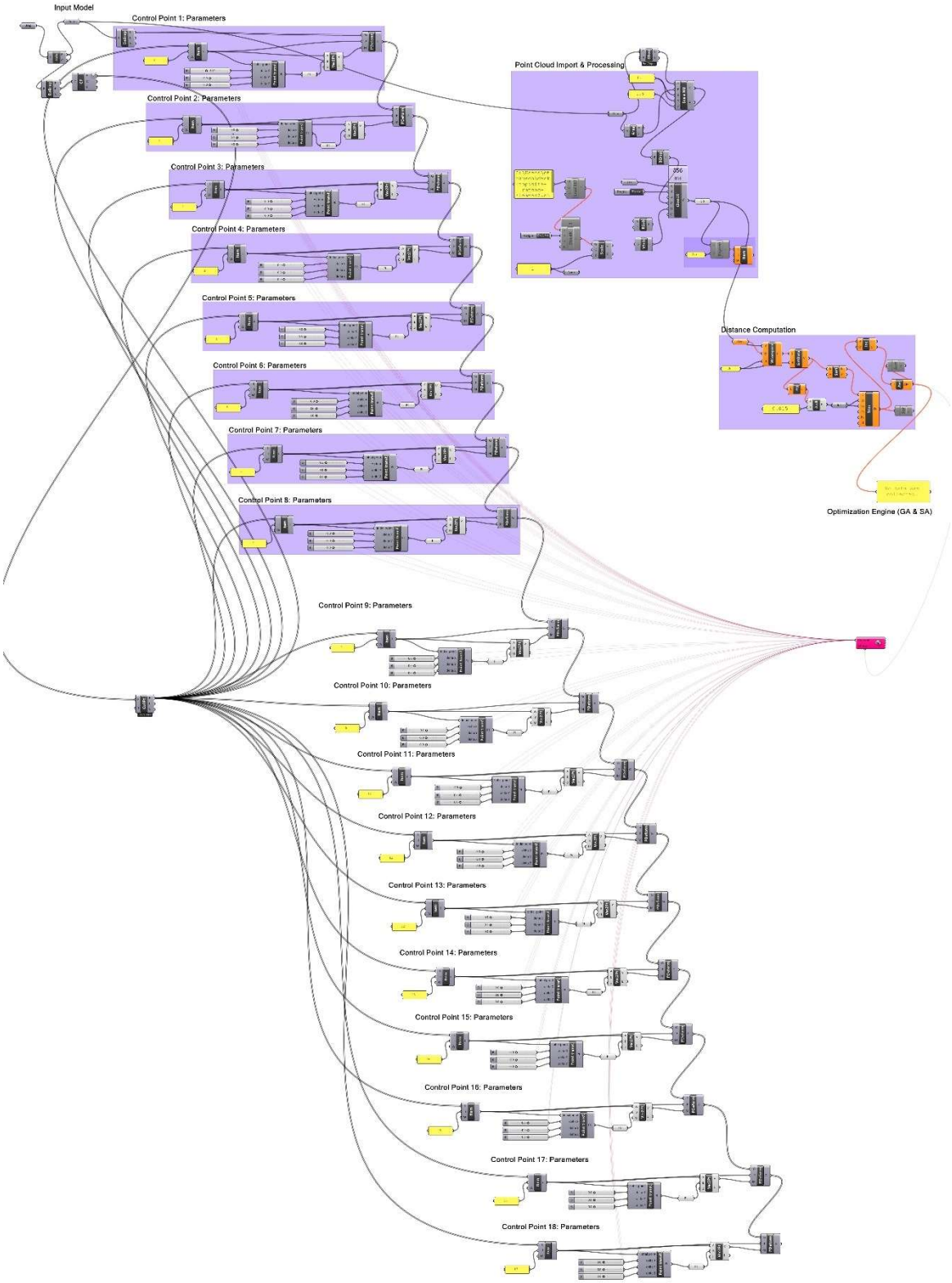

Figure 66: Grasshopper script for midpoint discretized parameterization algorithm (Chapter 7)

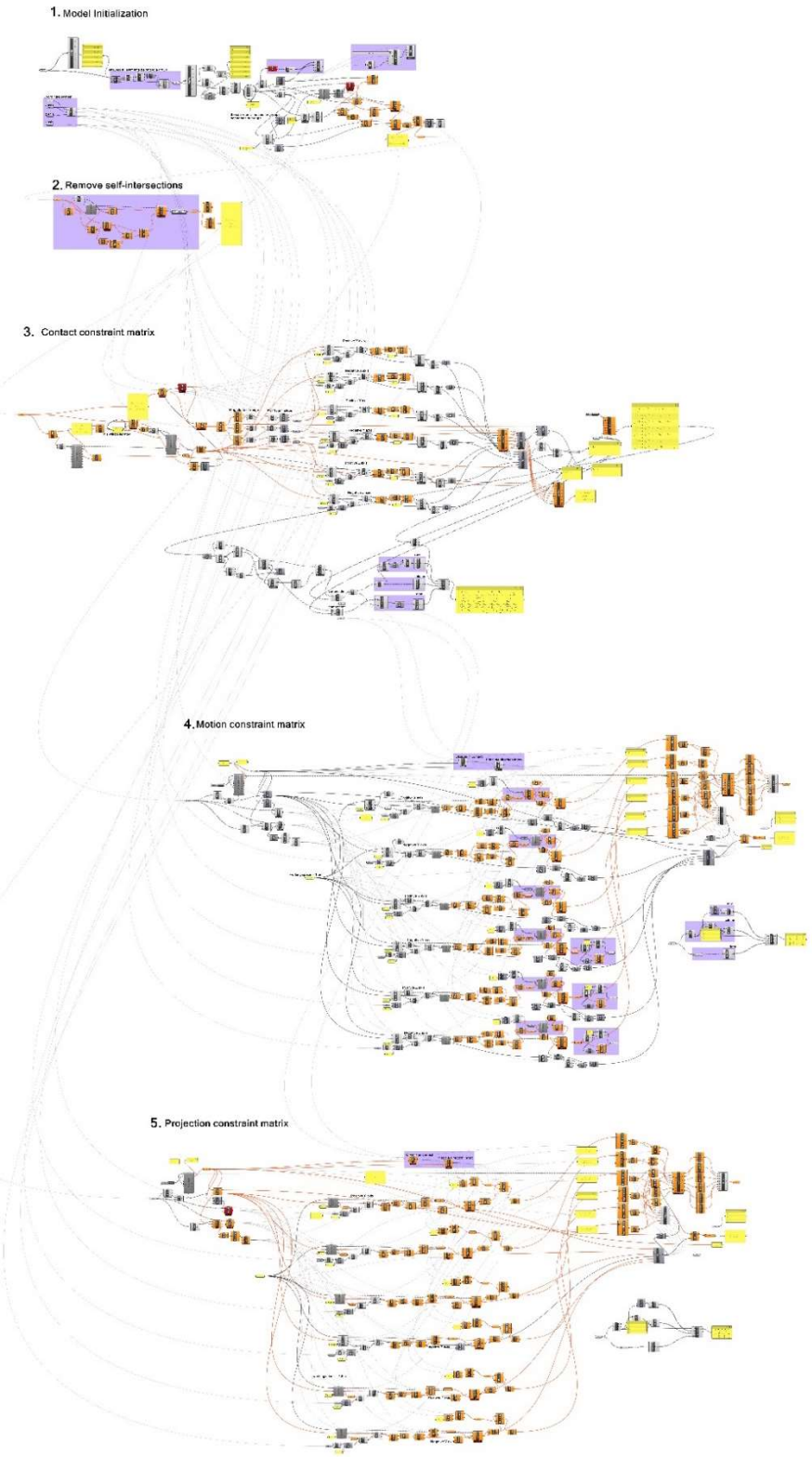

Figure 67: Grasshopper script for disassembly planning algorithm (Chapter 8). For clarity, each of the modules in this algorithm are shown below.

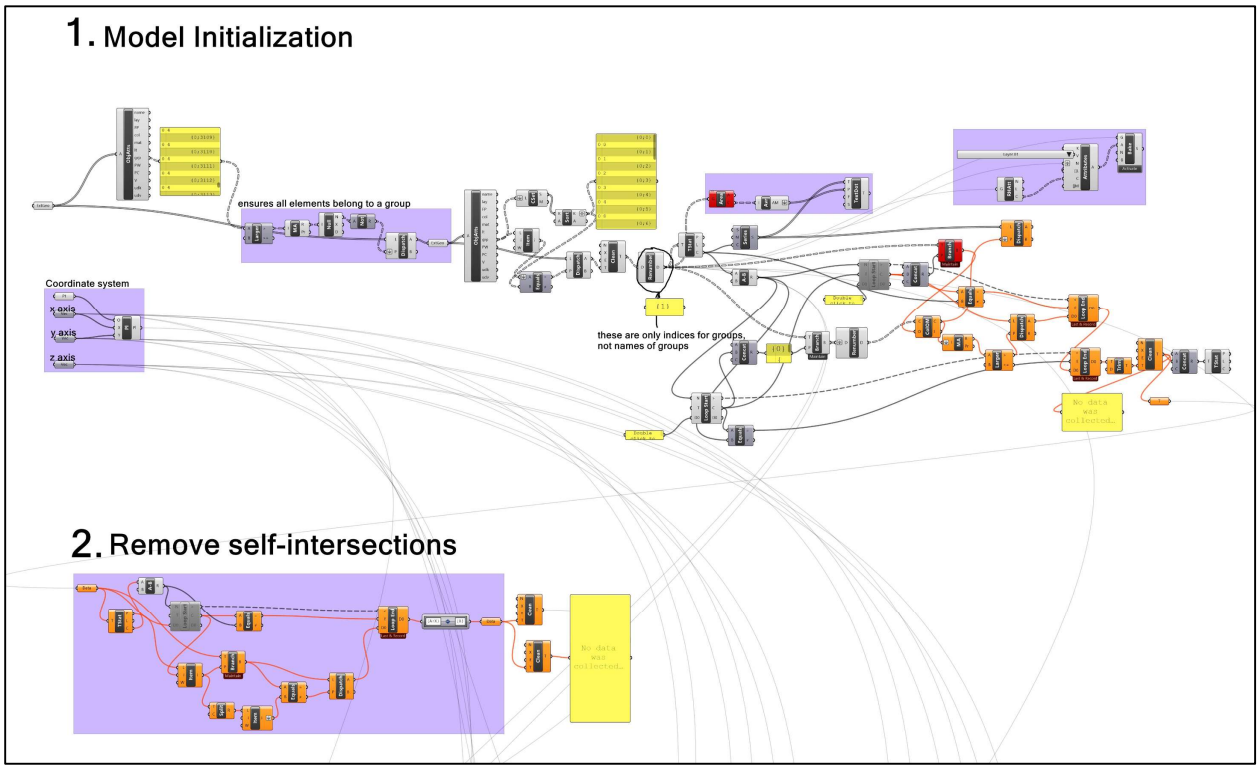
1. Model Initialization
ensures all elements belong to a group
Coordinate system
x axis
y axis
z axis
these are only indices for groups, not names of groups
No data was collected.
2. Remove self-intersections
No data was collected.

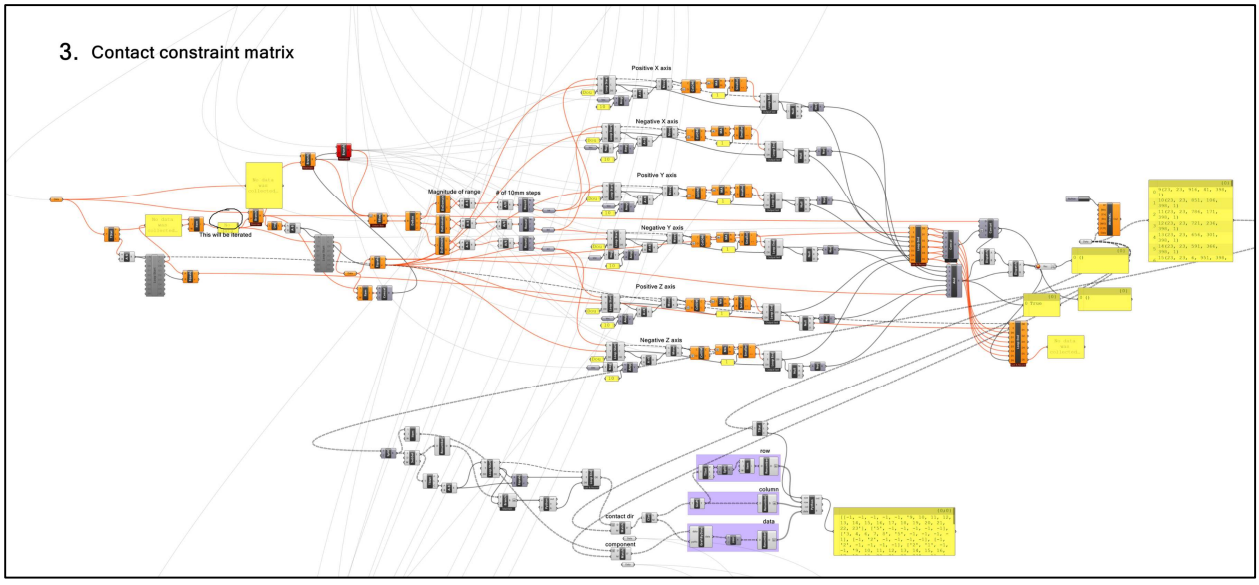
3. Contact constraint matrix
Positive X axis
Negative X axis
Positive Y axis
Negative Y axis
Positive Z axis
Negative Z axis
Magnitude of range
# of 10mm steps
This will be filtered
row
column
data
contact dir
component

4. Motion constraint matrix

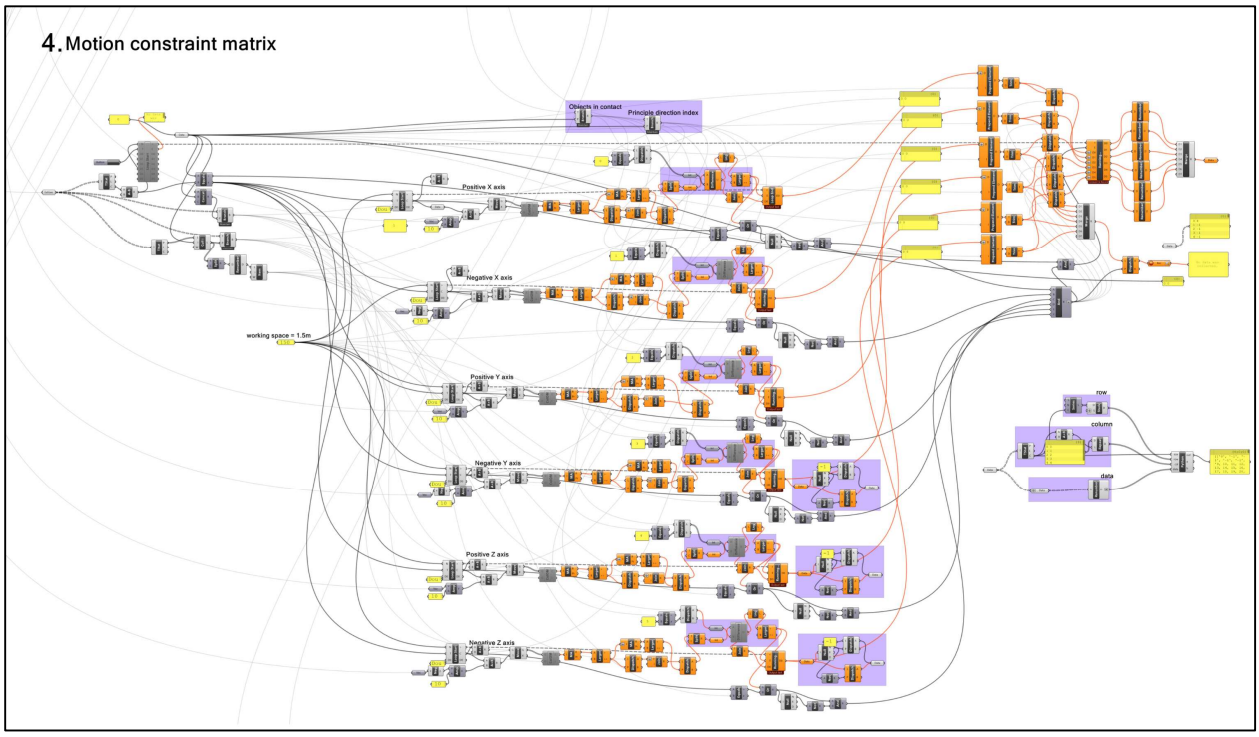

5. Projection constraint matrix

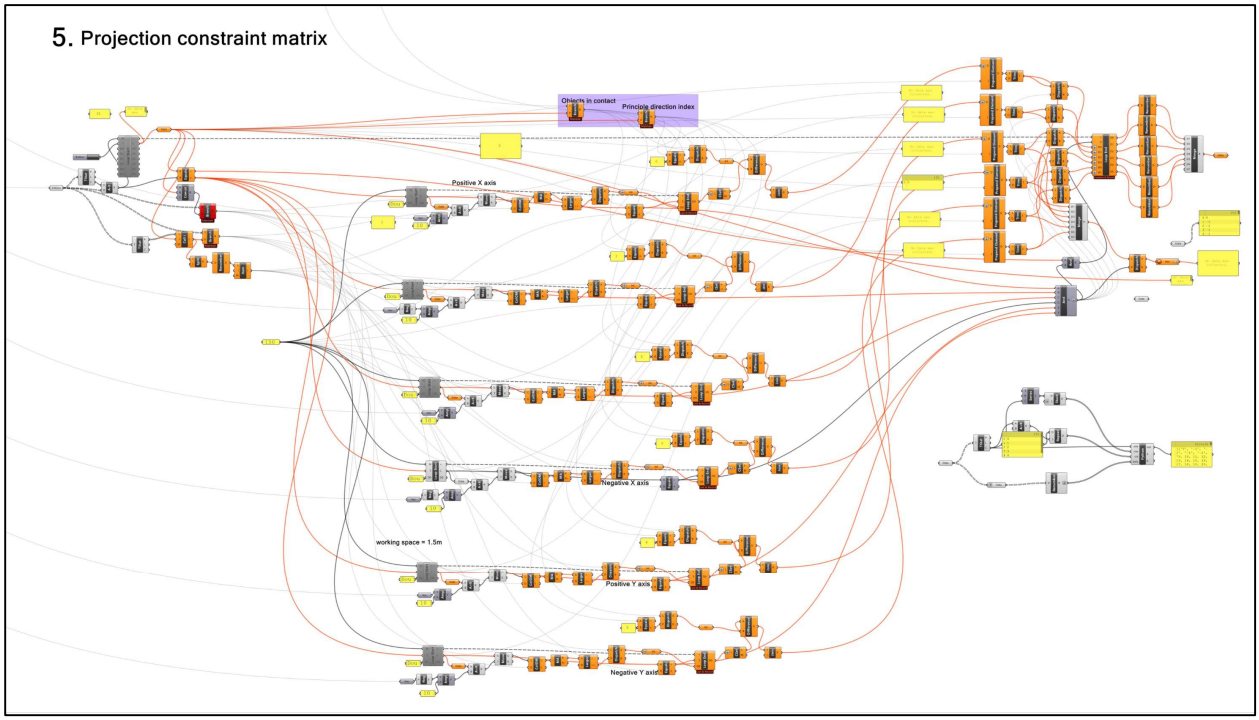

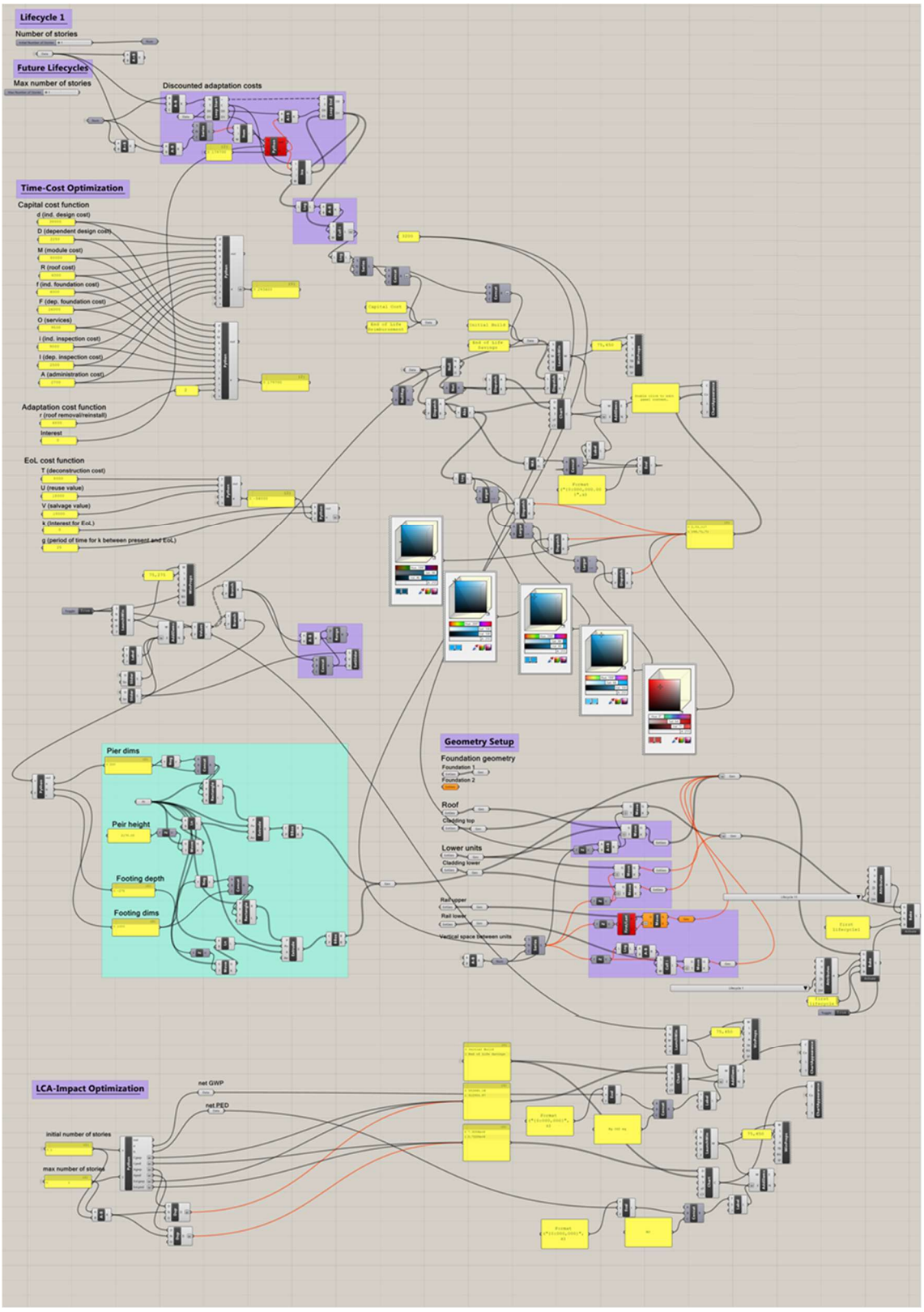

Figure 68: Grasshopper script for the product cycling configurator (Chapter 8).

Appendix B: Deploying Industrialized Buildings as Structural Assembly Banks for a Circular Economy

Emergent circular economy principles are at the forefront of societal priorities in the near to mid-term horizon. Concepts such as *Building as Materials Bank* (BAMB) promote circularity by shifting from a linear use of materials to closed-loop material flows, where building assets can be reused across multiple life cycles. Enabling circularity within buildings is often founded upon principles of modularity so that components can be easily disassembled and reused. This appendix explores how such a concept can be applied to the broader market of industrialized buildings. Since structural systems can comprise the majority of embedded impacts in buildings, this study specifically focuses on the reuse potential of modular structural assemblies. A case study comprising several life cycle analyses is conducted for a industrialized building to quantify expected life cycle savings for deploying industrialized buildings as structural assembly banks. In addition, new business strategies are presented to illustrate how such a concept can be realized from a supply chain standpoint within the market. This research helps inform and frame the context for using industrialized buildings in a more circular manner, thereby creating tangible solutions for the built environment with respect to societal priorities.

B.1 Introduction

Closing material-loops has been traditionally difficult to achieve within the construction industry. This is primarily because buildings are often custom made by a large group of participants and lack fundamental rules for supporting circularity such as ensuring buildings can be suitably deconstructed and enabling products to be easily reused [311]. This is predominately where industrialized buildings offer sizeable advantages. Given the nature in which industrialized buildings are brought together at the job site, they also have desirable attributes for disassembly. Even apart from the inherent advantages of disassembly, simply the ability to relocate modular assets has been shown to improve circularity by facilitating extended usability, and thus providing an alternative to otherwise hastened linear material flows [183].

Innovative approaches to building design are creating tangible propositions for a circular economy. Among these approaches is the *Building as Materials Bank (BAMB)* model, where buildings are viewed merely as temporary configurations of materials, and once at the end of their useful lifespan, materials contained within are directly reused in new building configurations [335,336]. Research on the circular economy often focuses on material use efficiencies in order to reduce, reuse, or recycle materials that would otherwise end of up in landfills (i.e., linear use) [337,338]. Among the principles required to achieve this is the concept of adaptability. This is said to be best achieved through modularity and

standardization, which are also core tactics employed in prefabricated building construction [319]. As such, there is a natural set of shared principles between BAMB and industrialized building construction. Structural systems of buildings tend to contribute the greatest to overall material mass and embodied impacts [339]. As such, they have great potential for being targeted for reuse. However, a large challenge of reusing structural components in a new building is that the design is subject to material availability and existing geometric form [340,341]. Furthermore, it is difficult to assess the structural integrity of individual components; it becomes invariably more difficult to assess integrity of an overall system of varying degrees of reused components [342]. For these reasons, designing the structural system upfront for deconstruction and direct reuse can overcome some of the prevailing reuse challenges.

This research applies the *Building as Materials Bank (BAMB*) model to industrialized buildings to evaluate reuse potential of structural assemblies. The ability to close material loops for these types of assets is evaluated in terms of increasing degrees of circularity with respect to the percent reuse of structural assemblies. This work is structured as follows. First, a literature review is conducted for end-of-life management of industrialized buildings and for current opportunities afforded by BAMB. Then, a case study is conducted to assess the reuse potential of structural assemblies from an existing modular accessory dwelling unit. New business strategies are then presented, based on BAMB and existing supply chain models from literature. Finally, the implications and future research are presented.

B.2 Background

B.2.1 Strategies for Supporting the Circular Economy in the Building Industry

Often, the circular economy is equivocated with the *3-R's*: reduce, reuse, recycle [337]. In the context of the built environment, the 3R's are often approached through existing building end-of-life management, new design strategies for new buildings, and lucrative business models.

B.2.1.1 End-of-Life Management for Existing Building Stock

The ability to reduce the amount of materials ending up in landfills is a principle target in the management of end-of-life for existing buildings, since the built environment is said to contribute 40% to overall volumetric contributions to landfills [343]. Often, buildings are disposed of simply because they no longer meet the needs of owners and occupants [344]. Adaptive reuse of buildings is becoming a burgeoning practice to extend the life of buildings. In their collation of various building adaptation typologies, Shahi et al. [345] present the distinction between refurbishment (retrofitting, renovation, or

rehabilitation) and adaptive reuse (conversion, or material reuse). A further classification considers whether these adaptation methods relate to the structural or non-structural systems of a building.
The key circular choices for end-of-life management at the component level center on either recycling or reuse. Of course, this stands in sharp contrast to simply disposing of materials via landfills. On one hand, recycling is still the dominant circular end-of-life pathway, yet reuse is far more preferable since it involves significantly less emissions and embodied energy impacts [346]. Components reuse has been heavily studied in literature, and applications span across the main building material groups: concrete, steel and timber construction [342,347-349]. In order to reuse building components, additional costs and time are required to employ deconstruction practices as compared to demolition. A study by Gorgolewski [350] showed that while deconstruction costs were 21% higher than demolition of six buildings, the net costs were in fact 37% lower when factoring in reuse savings. As such, reuse of components has tremendous potential financial benefits.

Despite the best efforts to extend the functional life of buildings and subsystems, adaptive reuse and building refurbishment face several challenges. In order to extend the functional life of buildings, numerous criteria must first be evaluated. Spector [351] present some of this criteria as assessing the structural integrity, energy efficiency, building services conditions, health and safety concerns, and potential environmental concerns. This can be a daunting task, especially when existing conditions information is non existing nor kept up to date (which happens in many projects). Furthermore, several studies reveal the chief barrier in adaptive reuse projects lies with economic uncertainty and inability to achieve required cost efficiencies [342,346,352]. Further, Esnaashary et al. [353] detail how adequate pre-project planning must be based on cost-optimal selection of methods to collect required information and to mitigate potential risks which are unique to adaptive reuse projects.

Lack of, or low confidence in the information for existing conditions of reuse building components also creates significant technical challenges related to design. Architectural design must be much more flexible in accommodating the unique geometric and structural constraints of reused components. In some cases, the strength of reused components is in fact compromised, but more common is the difficulty or hesitancy in certifying the structural capacity and integrity of reused components [346]. As such, design guidelines are slowly beginning to emerge to outline the modifications to various structural design processes (e.g., changes to buckling resistance factors) that can be used to design with reused materials safely, and confidently [354]. However, it remains that designing and building with reused components is a very challenging practice to undertake. As such, strategies are also being pursued in the design of new buildings to ensure they can more efficaciously manage the end-of-life stage.

B.2.1.2 New Design Strategies

By explicitly planning upfront for circular-centric buildings, prevailing challenges with managing existing building stock (e.g., how to obtain accurate as-built information, how to address deconstruction, and how to achieve required cost efficiencies etc.) can be assuaged. The first and obvious design approach that has emerged has been the assessment and optimization of life cycle impacts associated with material choices. Often the preliminary architectural design, complete with choices such as number of stories, building orientation, massing, and general assembly composition has the largest impact on overall LCA impacts [355]. But by selecting materials and configuring them diligently, it is possible to significantly reduce the embodied and operational impacts of buildings.

Apart from preliminary material selection and building configuration, specific design strategies can be incorporated to aid in end-of-life management; specifically, to enable reuse of components. Design for disassembly (DfD), which is often synonymous with design for deconstruction, involves selecting durable materials and designing specialized connections that enable efficient disassembly for recycling and reuse of legacy components. While circularity can be pursued through recycling, reuse is far superior, since recycling of building materials still incurs large environmental burdens compared with direct reuse. As such, DfD is not merely concerned with how to take a component out of an existing building, but it should also incorporate flexible design attributes to facilitate use across a range of applications. Recently, consideration of DfD has been incorporated into LCA [356], however it is important to note that any savings from reuse are allocated to the building with the reused components, and not the initial building from which those components originate from [357]. DfD has been applied to building structures, since they can comprise the majority of a building's mass [358], and has been applied for other subsystems (e.g., MEP system and façade) [359,360]. Yet, despite the potential of DfD, there are only a small number of buildings based on this design principle [361]. Some of the barriers for DfD include high costs for design, planning and actual deconstruction, supply chain uncertainty (i.e., mismatched demand and supply flows), consumer perception of salvaged components, lack of standards, lack of financial incentives, little to no monetization of LCA impacts, conditions monitoring and maintenance of information databases [361,362]. Another design-based strategy which can promote circularity is design for future adaptability (DfFA). This is often synonymous with other related concepts such as design for change, open building systems, and design for adaptability. The idea with this approach is to arrange and configure buildings in an architectural manner suitable for spatial reconfiguration over time; e.g., using large open interior spaces [338], or layering and separating building systems so that for instance the structure could be accessed and adapted separately from the MEP system [363,364]. The challenge with designing for future circularity is risk that the additional upfront factors may not be recovered in terms of

expected economic and environmental benefits. The AIA report *Buildings that last: design for adaptability deconstruction and reuse* [365] outline some further risks being economic (higher soft and hard costs upfront), environmental (more materials may be required), and process (early buy-in from owner and a long term commitment from stakeholders to realize expected benefits).

B.2.1.3 New Business Models

Aside from the technical methods to support a circular economy, it is equally imperative to develop market-based models to facilitate tangible solutions and realization [366]. Circular business models provide a way to understand, describe and predict how things work in the real world using abstract representations of supply chains and systems [366,367]. Lewandowski [368] outline the key types of business models as those which regenerate, share, optimize, loop, virtualize, or exchange products, services or processes. Furthermore, they present key components to a circular business model: partners, activities, resources, value proposition, customer relations, channels, cost structure, revenue streams, take-back system and adoption factors. One of the emerging practices within circular business models is the shift from ownership to access for products, through Product-Service-System (PSS) [368,369] which optimizes the functional use of products until no longer desired. This approach also places the onus back on the producer to manage the end-of-life for products. To work successfully, circular business models need to provide explicit financial incentives and create value propositions for the key stakeholders required in developing circular solutions. For instance, in the context of reclaimed materials, reselling materials at a higher value than demolition costs create a financial incentive and potential value proposition for reclamation specialists who can re-introduce those materials back into the market.

A recent review of circular business models revealed that the majority of existing practices are within the services industry, focusing on the optimization of technology and systems [e.g., smart thermostats], with only 5% being related to the construction industry [367]. Documented examples of circular business models in the built environment tend to focus on the provision of materials and components in buildings (e.g., carpets, millwork, doors, windows, tiles, interior lighting, appliances, etc.) as operational expenditures rather than capital expenditures (i.e., PSS) [370,371]. PSS both warrant and allow for new roles in the supply chain through deconstruction/disassembly capabilities, product/asset reconfiguration, and recycling/downcycling/reclamation through incentivization schemes (Figure 61). Other business models include local supply chains between demolition contractors, reclamation ‘agencies’, reuse design specialists and reused material suppliers who extend the lifecycle of otherwise derelict materials and components [372,373]. Finally, new approaches are being developed for circular financial models. Reducing the burden of capital expenditure such as through lease-and-reuse models [361], rentable

buildings [374], and relocatable buildings [183] are not only economically sensible, but have particular relevance for the circularity of modular buildings.

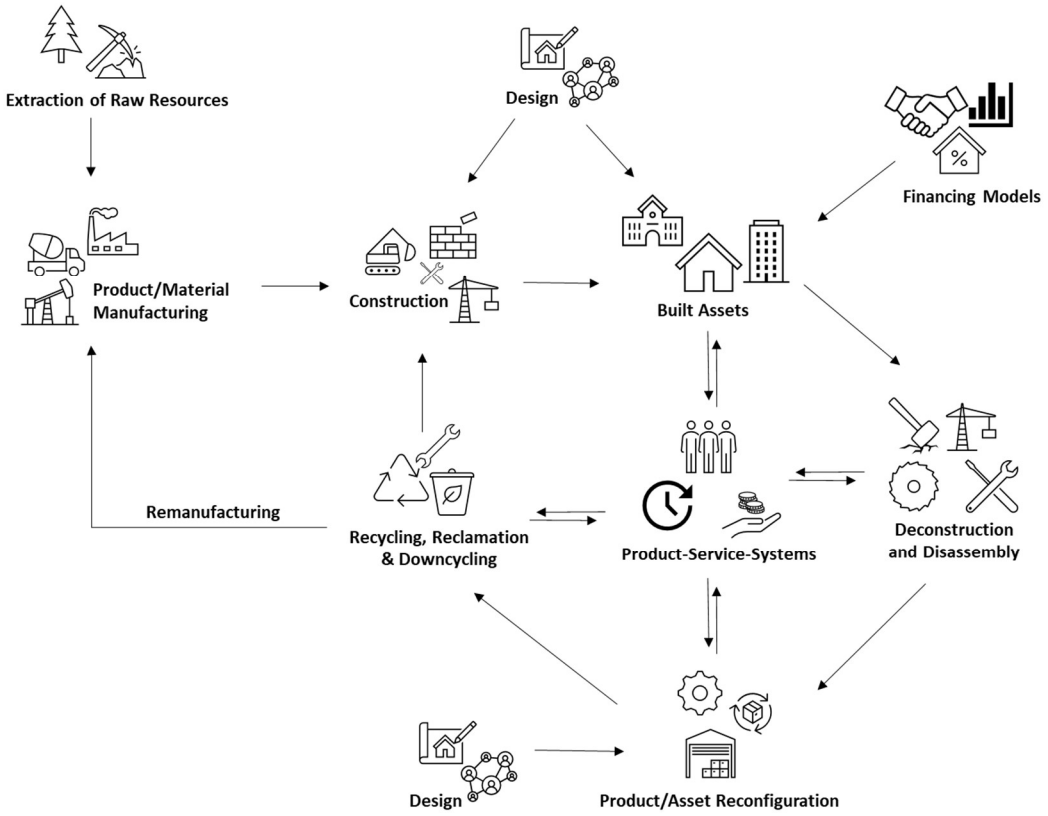

Figure 69: Ecosystem for Enacting Circular Business Model Strategies in the Built Environment

B.2.2 Circular Economy Research for Industrialized Buildings

Research on how industrialized building construction can support the circular economy is often focused on the LCA attributes of the production and operations stages and presents comparisons with conventionally built counterparts. Studies such as [375] reveal how modular buildings often experience the majority of their life cycle impacts during the operations stage (which is also true for conventionally built assets). This is largely dependent on the material selection and energy efficiency of a building. Modular buildings often have more materials on a strict comparison to their conventional counterparts (up to 15% more [376]) due to additional structural members required at matelines to self-support modules during transportation and handling. However, the life cycle impacts produced from these additional materials are more than compensated for by material waste savings due to the manufacturing efficiency in offsite construction (which can be as significant as 2.5 times less waste) [375,377]. Furthermore, as buildings become more energy efficient and the realization of initiatives such as net-zero energy

efficiency become a reality, the focus for reducing the life-cycle impacts will shift towards other life cycle stages. For this reason, numerous studies on life cycle impacts of modular construction have quantified and compared the production stage with traditional stick-built construction.

In addition to examining the production and operations life cycle impacts, a handful of studies have specifically examined the LCA benefits of prefabricated and modular buildings at the end of life stage. In their review of how prefabricated construction can support the circular economy, Minunno et al. [318] outline seven core strategies. Among these, two are specifically directed towards the end of life stage: design toward disassembly of goods into components to be reused, and design for recycling of construction materials. Eckelman et al. [185] conducted a series of tests to quantify the energy and environmental savings of combining prefabrication and DfD. Their analysis of reusable composite floor systems found that while additional costs and environmental impacts are required upfront for a DfD based building, there are statistically less impacts compared to non-DfD buildings after just one reuse, and up to 70% reductions after 3 reuses. In an earlier study, Jailon and Poon [311] explored the combination of DfD and Industrialized, Flexible and Demountable (IFD) building systems in prefabricated precast construction as a way of promoting circularity through sustainable life-cycle design. Ultimately, while the study presented numerous advantages of DfD and IFD, the ability to harvest and reuse prefabricated concrete elements had impediments with respect to in-situ connections. This conclusion was also echoed in another study by Aye et al. examining the life-cycle savings (in terms of energy and emissions) for prefabricated steel, concrete and timber building modules [378]. This study concluded that steel has the highest circularity potential for reuse of modules (up to 81% savings in embodied energy), with timber modules being the second best (up to 51% savings in embodied energy) and concrete only being practical for downcycling within a circular context. The most recent study for end of life of prefabricated and modular buildings was conducted by Minunno et al. [338], where two attributional life cycle assessments were carried out to compare recycling vs. reuse in a modular building. A prototype building constructed from heavy gauge steel chassis and columns and light gage steel walls was built with DfD in mind to enable ease of disassembly at the end of life. A comparison with a traditional non-circular building found that designing for disassembly and reuse can attribute up to 88% savings in global warming potential and up to 87% savings in acidification potential, among other benefits.

Existing studies demonstrate how industrialized buildings have great potential for end of life savings. Yet, despite the currently available studies, there remains a gap to assess the use of these assets as banks of materials for reuse in terms of higher levels of assembly aggregation (and thereby higher levels of circularity). By reusing a higher aggregation level in a building (i.e., entire structural assemblies as opposed to just single parts) greater savings of LCA impacts and costs can be achieved. Furthermore, it is

not only necessary to explore the reuse potential of industrialized construction from a life cycle perspective, but also from a market perspective, in order to enact pragmatic implementations.

B.2.3 Buildings as Material Banks (BAMB)

The notion of viewing buildings as materials banks (BAMB) was arguably posited by Cradle-to-Cradle®, but has been garnered by many other sources in various forms [379]. While the concept of urban mining has existed for quite some time [380], it is applied to existing buildings, whereas BAMB is a new paradigm premised on purposed-built assets that can be disassembled for increased component reuse. In 2015, a Horizons 2020 project was carried out under the topic of BAMB; receiving nearly €10,000,000 in support and comprising 15 industry and academic stakeholders [381]. Several reports generated by this project document successful prototype projects, technologies and processes required to make BAMB a widespread practice [339,382,383]. The overall goal of BAMB is to recover value from building materials, which is principally achieved through design methodologies (e.g., DfD, *build reversible in conception*, etc.), tracking mechanisms for tracing material condition, value and reuse potential (e.g., materials passports), and new business models.

The challenges, so far, with BAMB are that some elements will inevitably have cosmetic and "acute" problems, not to mention storage and logistic challenges of material inventories, as alluded to by Akbarieh et al. [384]. For these reasons, materials in BAMB must be assessed in terms of their structural and environmental attributes rather than aesthetic qualities. A simple example is reused pressure treated wood; while it quickly loses its aesthetic quality due to weathering, it may still be structural sound and fit for reuse. BAMB is also challenged by materials that can be 'locked-in' to the structure if concepts such as open buildings systems are not employed. Frequency of material availability is often not balanced across building subsystems. According to the *6S* hierarchy of buildings systems by Stewart Brand (i.e., Stuff, Space Plan, Services, Structure, Skin, Site) [385], when "stuff" is available for reuse, often the structure or skin is not and this can be problematic when trying to target specific elements for reuse. During disassembly, structural analyses may be required to ensure structural component removal does not comprise the integrity of the building. Individual structural components would need to be assessed and then integrated into a new system. Whereas entire structural system extraction could be salvaged easier. Finally, BAMB faces challenges with its supply chain requirements. The current low volume of buildings designed for deconstruction [361] means that available BAMB stock will remain elusive until widespread adoption. It is a complex task to link demand in the market with supply [336], and while materials passports and digital marketplaces present opportunities, supply chain logistics will remain a barrier for BAMB in the foreseeable future.

B.2.4 Summary of Knowledge Gap

The gaps in literature, and where the contributions of this work lie are as follows:

- Reusing individual structural components from existing buildings requires extensive planning, revised design code provisions, among other factors, which lead to unreasonable costs.
- Relying on diverse building stocks for component recovery presents challenges for logistics, temporary materials storage and digital marketplaces that warrant a substantive timeframe before ubiquitous materials recovery from buildings can become a reality.
- While immensely promising, BAMB is still in its infancy, and needs greater market saturation before tangible solutions can be realized.
- Industrialized buildings have unique characteristics that enable efficient deconstruction and do not warrant extensive structural analyses during materials recovery, since entire (self-supported) modules can be removed in the reverse manner to assembly.

B.3 Deploying Industrialized Buildings as Structural Assembly Banks

To evaluate the deployment potential of industrialized buildings to function as structural assemblies banks, this research concentrates on three key topics: (1) necessary design considerations, (2) quantification of LCA potential, and (3) proposition of new business models.

B.3.1 Design Considerations

There are a wide variety of industrialized buildings, ranging in typology from single custom modular homes, to multi-unit high-rise buildings. To reuse the structural systems from modular buildings, it is advantageous to target buildings with a high degree of standardization. In general, 3D volumetric modularization through multi-unit and high-rise buildings enable the greatest potential for standardization of assemblies [386]. In general, reuse calls for maximizing the number of repeatable, easily disassembled components or assemblies, which is why multi-unit and high-rise buildings have been previously identified as good reuse candidates due to their high degree of assembly repetition [387]. However, standardized modules have been viewed as a design constraint in modular construction [19], and efforts have been made to instead focus on standardized connections. This of course presents a unique trade-off, with specific implications for reuse. In modular design, it is well regarded that the number of connections between modules be reduced, since more connections elicit increased construction and maintenance costs

[388]. However, the discretization of a building into smaller pieces (i.e., more connections) is efficacious for circularity since there is increased flexibility in how those pieces can be used [311]. Standardization of discretized components is also a key target for increasing reuse potential and market fluidity [348]. However, as already alluded to, BAMB, which warrants scaled standardized parts inventories, is still very much in its infancy. The question then remains, where should standardization in design be directed - on components, modules or connections?

Figure 62 shows industrialized typologies with respect to degrees of standardization. At one end of the scale is *Singularity*, where modules are entirely bespoke in composition. *Commonality* (as presented in [363]) encompasses standardization within a given building. Singularity and commonality are best suited for reuse solely in the form of relocation, and any other form (i.e., harvesting the structural system), requires extensive analysis, design and modifications. At the other end of the scale in Figure 62, *Modularity* (standardized modules across a fleet of buildings produced by a vendor or a specific supply chain) and *Universality* (i.e., off-the-shelf standardization, across vendors and supply chains) engender greater reuse potential since standard modular blocks have larger inventory, and a diverse supply chain.

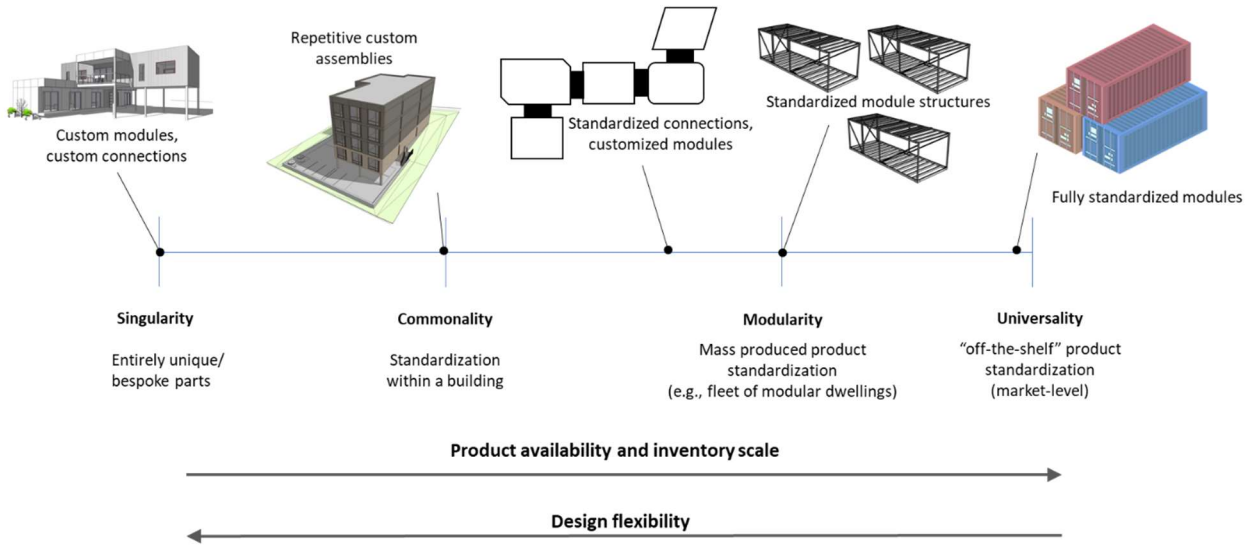

Figure 70: Standardization vs. Design Flexibility within Industrialized Construction Typologies

In many respects, industrialized construction already uses standardized structural components. For instance, in the authors' experience working with several large North American modular contractors, the use of W-flange steel, hollow structural sections (HSS), and standardized dimensional lumber (i.e., standard off-the-shelf components) is the De Facto approach compared to customized components. Where more customization has been observed is in other subsystems such as wall systems, where light-gage steel framing for instance, can be custom produced. In general, designing with standardized components

reduces engineering design/analysis demands and reduces potential challenges associated with building inspections.

Whereas the automotive and electronics industry have adopted standardized connections to facilitate optimized disassembly and components replacement, the same standardization within buildings has not seen the same adoption [389]. However, within modular systems, much more attention has been directed towards standardization of connections. Standardized connections seems to address this dichotomy [19] by giving more flexibility to the form of modules, while not sacrificing important constructability requirements. In their comprehensive review of connections in modular buildings, Srisangeerthanan et al. [390] present three distinct connection types: inter-module (enable formation of key structural system for whole building through vertical and horizontal connectivity between modules), intra-module (assist in forming the structural frame of modules, and for lateral resistivity), and foundation. The development of inter-module connections is arguably the most complex connection type since they need to consider gravity framing, lateral force resistivity and diaphragm actions. Manufacturing and constructability performance requirements for inter-module connections requires they be comprised of simple geometry (less unique), using off-the-shelf systems where possible for ease of production, be self-aligning as well as having the ability to be easily demounted for repair.

While existing design approaches allow intra-module connections to be conventionally produced (i.e., welded), this research posits that certain intra-module connections must also be carefully designed for reuse capabilities (i.e., bolted) in order to enable the reconfiguration of modules across use cases. While many DfD guides call for near exclusive use of bolted connections, these guides tend to assume an assembly must be 100% disassembled and are not directed towards reuse of 'core' structural assemblies. As such, this research proposes developing standard 'core' structural assemblies (using standardized connections), that can be subsequently customized from both a structural and architectural standpoint using a system of bespoke components Figure 63. This requires careful design of both inter-module and specific intra-module connections; both of which need to be demountable. In steel systems, these connections are best attained through bolted connections. The notion of *Modularity* as depicted in Figure 62 is specifically targeted in this work to accomplish the present needs of architecture and manufacturing, while also providing useful reuse capabilities.

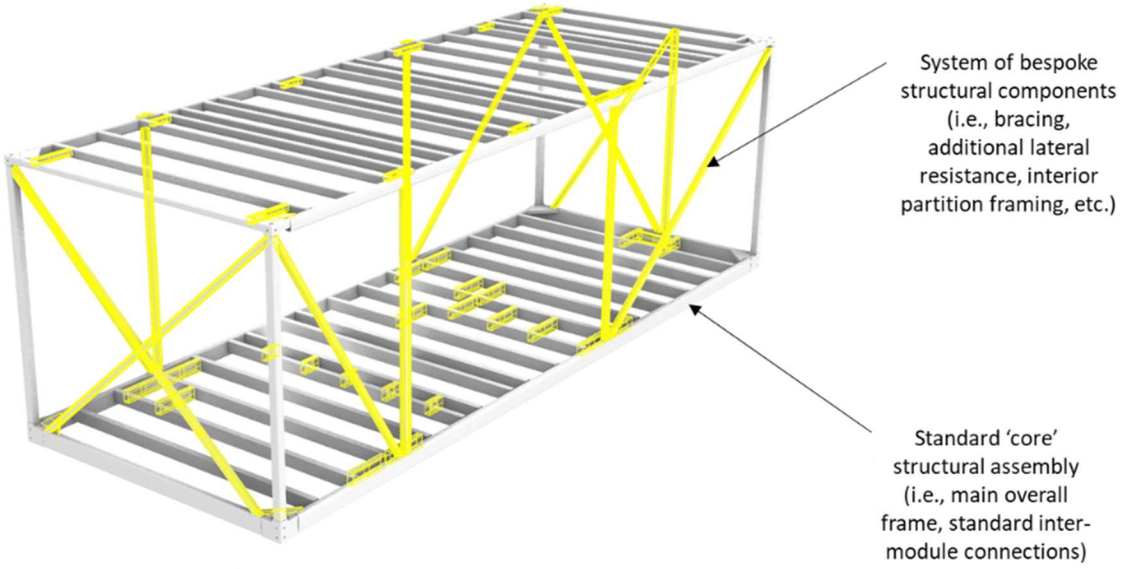

Figure 71: Discretization of Module Structure into a Standard 'Core' Assembly, and System of Bespoke Components for Individual Module Needs on a Given Project

Finally, reuse of structural frames relies on having adequate structural reserve. This could be achieved by over-designing modules upfront to anticipate future reuse cases, or through "vertical-downcycling" based on load capacity, i.e., taking modules from an 8-story building with higher loads and using them in a 6-story building where loads are lower. Structural reserve adds additional weight to a structure, which inevitably increases cradle-to-gate impacts for the first module. It also increases transportation impacts of each reuse case due to increased weight. However, it is expected that these additional life cycle impacts are minimal in comparison to the savings provided by reuse.

B.3.2 Case Study: LCA Quantification for Reuse of Steel-Framed Module Structures

This case study examines the life cycle savings for harvesting structural steel frames from an existing modular building for reuse in a new building. In a recent project, the author worked as a project coordinator for an architect (Edge Architects) on the construction of a single story modular accessory dwelling unit (ADU), located in Kitchener, Ontario, CA. This modular ADU has a 70m^2 footprint, is comprised of two steel chassis frames, with light gauge steel framing, 5" (127mm) thick sandwich panel insulation, timber cladding and sits on concrete piers and footings. This project was undertaken as a prototype to test, develop and validate flexible design solutions to be employed in both single-unit and multi-unit residential construction applications. As such, numerous design and construction efficiencies were realized with respect to the dimensions and composition of the structural system, interior space

layout and building service (mechanical, electrical, plumbing) coordination. A key component to the structural design of modules was targeting a sufficient level of structural reserve so that modules could be used in a multi-story application (i.e., up to 4 stories) or for single story ADUs. While this increases the cost and materials for ADUs, it enables manufacturing efficiencies for mass production of residential units and creates the circular opportunities for reusing modular frames in the future.

Figure 72: Modular Accessory Dwelling Unit

An attributional LCA was first carried out to quantity the contribution stemming from the module structural system. At the end-of-life for the modular ADU, the modules can be disassembled on site, transported to an offsite facility, where the timber cladding can be removed, insulation panels demounted, interior wall systems deconstructed and the structural system exposed. Since each module has unique bracing requirements depending on load paths, window supports, interior partition walls, doors, and MEP routing, each module has slight variations in its structural system. However, all modules have the same main overall structural members (columns, kit-of-part connections at corners, and frame purlins). As a result, a necessary step at the end-of-life is removing the unique bracing (shown as blue in Figure 65), which can either be designated for recycling or catalogued into a bank from which to reuse in future bracing layouts.

According to ISO 14040, LCA is a technique for assessing the environmental impacts of a product by evaluating its system inputs and outputs and interpreting the results in terms of distinct life cycle stages [391]. For brevity, this work does not delve into all the details of an LCA, but rather presents the results obtained from using a software plugin OneClick® within Revit®. Key assumptions are discussed to provide a basis for the results obtained. The life cycle impacts (LCI) considered in this study include global warming potential (GWP), acidification (AFC), eutrophication (EUT), ozone depletion (OD), formation of tropospheric ozone (FTO), fossil fuel primary energy demand (FFPED) and total primary energy demand (TPED). Despite anticipating and planning for future reuse upfront in the initial ADU, it is necessary to conduct a consequential LCA to realize the environmental benefits associated with reuse

of structural assemblies and components. This is because according to LCA methodology, if a material is harvested and reused after its initial use, the building that uses the reused components can receive a credit for the embodied energy savings and reduction (or elimination) of other LCA impacts, but not the building from which the reused components originate [357]. For this study, a steel frame chassis from a new multi-story building was obtained and used to analyze the life cycle impacts associated with reuse from a chassis in the modular ADU. Four unique scenarios are evaluated in the consequential LCA:

- Scenario A considers all steel in the new module is from *generic* sources (i.e., 20% recycled content and a global warming potential of 2.051 kg CO_2e/kg). This scenario functions as a worse-case condition and the least circular outcome.

- Scenario B considers only the base frame from the modular ADU is reused, and any additional bracing is from *generic* sources.

- Scenario C considers the base frame from the modular ADU is reused, and the additional bracing requirements come from 100% recycled sources.

- Scenario D considers 100% reuse: the base frame from the modular unit, and selective bracing elements are harvested from a bank of catalogued components.

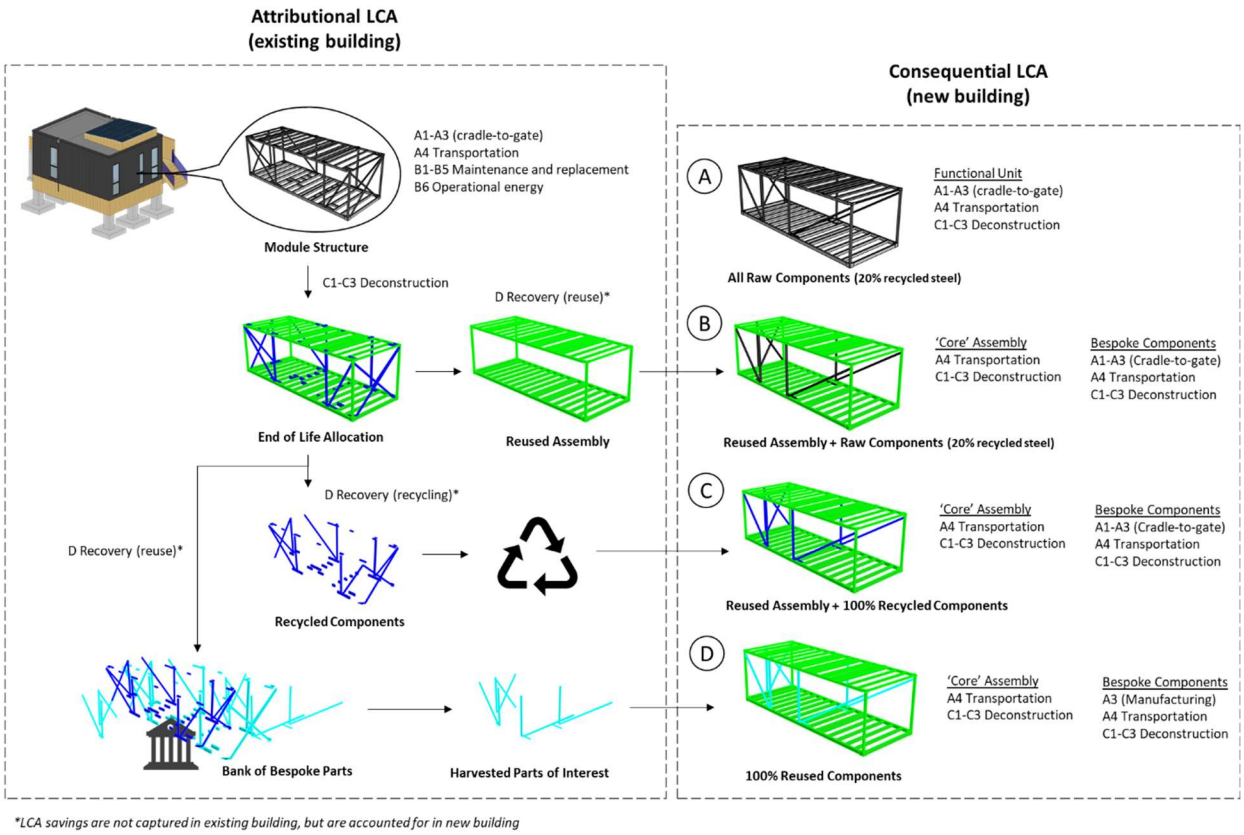

Figure 73: System Boundary for Attributional and Consequential Life Cycle Analyses for Reuse of Structural Module Assemblies.

B.3.2.1 Attributional LCA

The attributional LCA examines the comprehensive life cycle of the building by considering modules A1-A3 (cradle-to-gate), module A4 (transportation to site), maintenance and material replacement (modules B1-B5), operational energy (module B6) and end-of-life impacts (modules C1-C4). OneClick®'s *default* and *generic* material classifications are used based on the location of this project (Ontario, Canada). The transportation distance was set at 930km to reflect the fact that several manufactured materials were transported across provinces and from the United States. The material lifespans were set to the *default* values generated by OneClick®, which primarily correspond to the life of this building (50 years). Operational energy use was determined using an annual energy use of 7000 kwh and a lifespan of 50 years. The end-of-life considers deconstruction, transport, and waste processing. All material recovery benefits (module D) are not captured in this LCA but are transferred to the consequential LCA via a cradle-to-cradle process. In terms of the total material inputs, the foundation comprises the majority of the mass, since large concrete footings and piers were used. The third largest mass category, at 12% total

mass, relates to “Columns and load-bearing vertical structures” which correspond to the modules allocated for reuse (Figure 66).

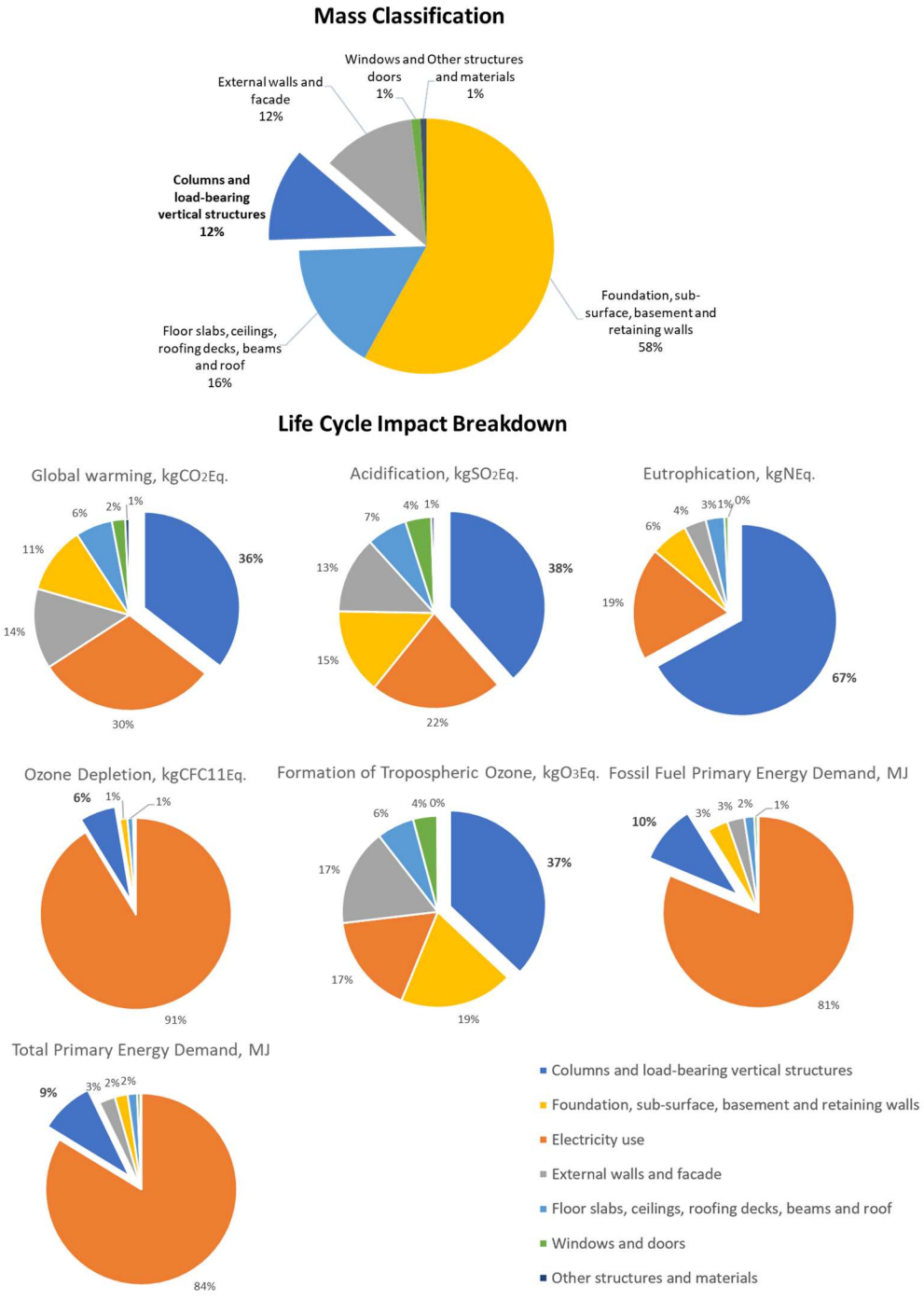

Figure 74: Mass Classification and Percent Contribution of Life Cycle Impacts for Structural Module Frames (i.e., “Columns and load-bearing vertical structures”) with Respect to Overall Building.

The total LCIs of this project are as follows: 70,700 kg CO_2e GWP, 259 kg SO2e AFC, 200 kg Ne EUT, 0.0296 kg CFC11e OD, 3,390 kg O3e FTO, 3.87×10^6 MJ FFPED, and 4.39×10^6 MJ TPED. While the module structure comprises just 12% of the material mass, it contributes to 36% of the GWP, 38% of the AFC, 67% of the EUT and 37% of the FTO contributions, even when accounting for the operational energy demand of this building (Figure 66). When removing the operational energy impacts, the LCIs associated with the module structure are the largest across all categories. This finding supports previous studies that investigate LCI associated with building material typologies which show that steel carries more impacts than wood or concrete [378]. However, the reuse potential of the steel structure in this building carries significant savings in reuse, which is observed and quantified in the consequential LCA.

B.3.2.2 Consequential LCA

Following the system boundary shown in Figure 65, four different LCAs were carried out: one for the functional unit (i.e., a new module constructed from raw materials) labelled as Design "A", and three cases of varying degrees of circularity, labelled Designs "B", "C", and "D". The functional unit is constrained to cradle-to-gate impacts (i.e., modules A1-A3), transportation from the offsite facility to project site (i.e., module A4), and end-of-life deconstruction impacts (i.e., modules C1-C3). Although this new module could be reused in subsequent applications, to be conservative, it is assumed that LCA modules C1-C3 follow typical recycling processes for steel (which increases the environmental impacts compared to reuse). No use-stage impacts (i.e., modules B1-B7) are considered in this consequential LCA, in order to exclusively evaluate the impacts associated with reuse and recycling of the structural 'core' assembly and additional bespoke components. Design B has all of the same LCA components as Design A except for cradle-to-gate impacts of the 'core' assembly. It is assumed that any transportation of reused module components or structural 'core' assemblies are applied the same default distance as the attributional LCA (930km). Design C has all of the same LCA components as Design B except that the bespoke components are sourced from 100% recycled sources, as opposed to the *generic* 20% recycling sources. Finally, Design D has all of the same LCA components as Design C except that only module A3 (i.e., manufacturing processes) is considered during the product stage since modules A1 and A2 (i.e., raw material supply) are averted due to reuse. The assumptions used for developing A3 impacts for Design D are based on the following approximate percent contributions of module A3 to all cradle-to-gate impacts as identified in literature: 8% of global warming potential, 9% of acidification potential, 9% of eutrophication potential, 91% ozone depletion potential, 8% tropospheric ozone formation potential, 0% fossil fuel primary energy (i.e., no fossil fuels are burned during manufacturing since all electric equipment can be utilized), and 20% primary energy demand [392,393]. The LCI results for the

functional unit are shown in Table 10. From these impacts, a percentage reduction profile can be generated for each of the subsequent design cases compared to Design A. As shown in Figure 67, compared with Design A, Design B, C, and D result in an average LCI reductions of 78%, 91%, and 95% respectively.

Table 11: Life Cycle Impacts of the Functional Unit for the Case Study

	Life Cycle Stage	Global warming, kgCO2Eq.	Acidification kgSO2Eq.	Eutrophication, kgNEq.	Ozone Depletion, kgCFC11Eq.	Formation of Tropospheric Ozone, kgO3Eq.	Fossil Fuel Primary Energy Demand, MJ	Total Primary Energy Demand, MJ
Design A – 'Core' Assembly	A1-A3	10351	42.659	52.25165	7.08E-04	502.3328	157660	166070
	A4	153.12	0.8738	0.12207	4.04E-05	24.75	4363	4374
	C1-C4	36.7	0.2282	0.007817	0.00E+00	4.781	1040.8	1043.9
Design A – Bespoke Components	A1-A3	2424.8	10.0145	12.212122	1.66E-04	118.0177	37040	38828
	A4	35.99	0.2045	0.0287	9.48E-06	5.811	1022.9	1025.9
	C1-C4	8.607	0.05343	0.0018292	0.00E+00	1.1211	243.9	245
Total		13,010.22	54.03	64.62	9.24E-04	656.81	201,370.60	211,586.80

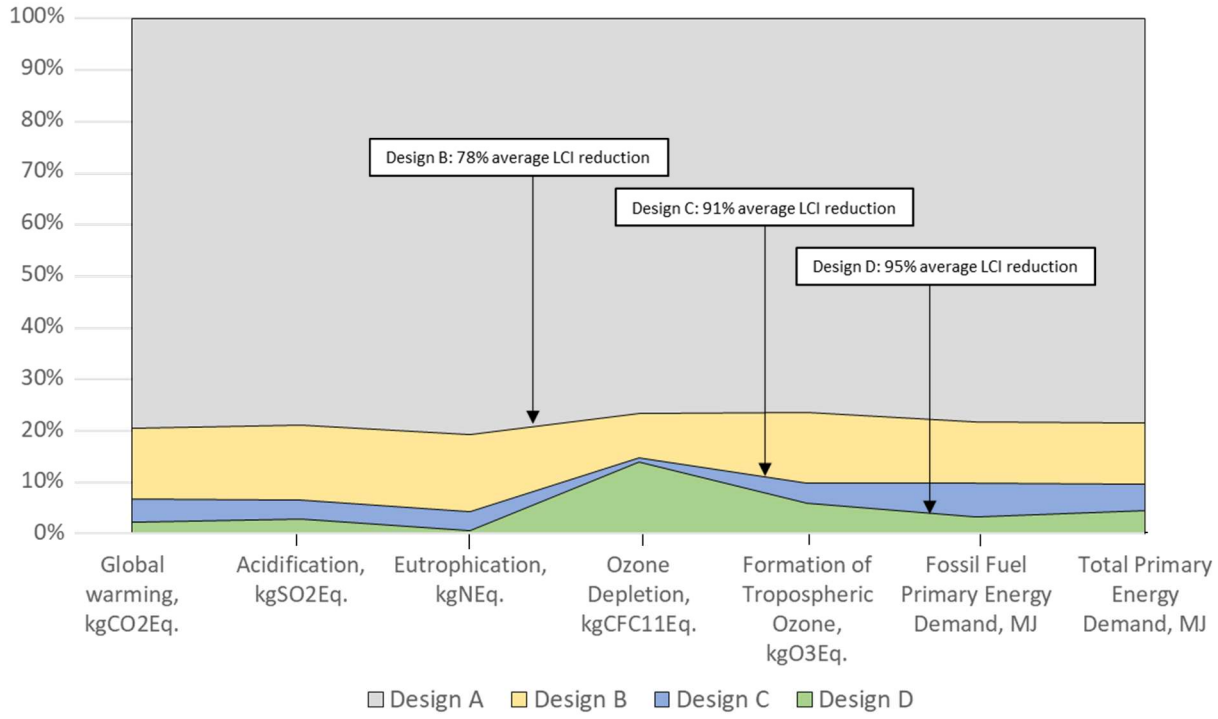

Figure 75: Life Cycle Impact Percent Reduction Profile for Varying Module Structure Reuse Cases

Analyzing the results of the consequential LCA, the following conclusions should be noted. First, just reusing the structural 'core' assembly and using new raw materials for the bespoke components (Design B) has the most significant LCA savings. The marginal percent reduction when analyzing Design C and D compared to Design A is only 13% and 17% respectively. However, when comparing the percent reduction in LCIs between each iterative design option, much more significant relative reductions are achieved. For instance, comparing Design B to Design C has a 60% reduction in LCI and comparing Design C to Design D has a 54% reduction (Table 11). These values are important, since they become the basis for evaluating whether there is potential viability from a business standpoint for only reusing the structural 'core' (Design B), reusing the 'core' and using 100% recycled bespoke components (Design C), or 100% reuse of both 'core' and bespoke components (Design D).

Table 12: Percent Reduction in Average LCIs for all Design Options (Reductions between Iterative Design Options are Shown in Bold for Emphasis)

		Benchmark Design			
		Design A	Design B	Design C	Design D
Selected Design	Design A	0%	-	-	-
	Design B	**78%**	0%	-	-
	Design C	91%	**60%**	0%	-
	Design D	95%	79%	**54%**	0%

B.3.3 Stakeholder Value Propositions

Using industrialized buildings as structural assembly banks opens new value propositions for financing building stock. Reusing components has been shown to yield in to cost savings for materials [346]. Design for deconstruction increases cost savings for material reuse by enabling the owner of an original building to easily harvest and sell components to the owner of a new building at a discounted price compared to raw materials [185]. To promote industrialized buildings as structural assembly banks, these cost savings need to be directed into new business flows for additional stakeholders required such as facility managers, and component reuse suppliers and marketplaces.

The presented business models specifically address reuse of module structural systems, which is more complex than simply relocating modular buildings as a whole. For demonstration purposes, two unique business models are considered, which reflect variations in supply chain complexity and capital vs. leasing opportunities.

B.3.3.1 Vertically Integrated Leasing Business Model

The first proposed business model is based on a lease structure between a vertically integrated modular producer (i.e., complete with design, production, commissioning, and financing services) and a series of end-users. Such a business model is uniquely posed to address the affordable housing crisis being felt in many countries globally, where a modular dwelling can be leased to a private or public agency to reduce the burden of ownership (since many of these agencies have strict operational budgets from which to work with). This concept has been directly asserted to support circularity and has already been demonstrated in practice. It functions similar to other PSS models throughout the built environment and while reference to this business model first appears in a recent study [183], it is adapted here to demonstrate its validity and value proposition. As shown in Figure 68, a modular producer configures an initial modular building, and leases it to *End user A* for a set period of time, T_A. Then, the building is returned to the modular producer, where it undergoes disassembly, harvesting of the structural core assembly, and any additional repairing, recycling and downcycling of non-structural components is performed. Any reclaimed materials can be fed back into the resource production supply chain for use in the next building configuration. The modular producer can then perform this reconfiguration process for a series of N subsequent cycles.

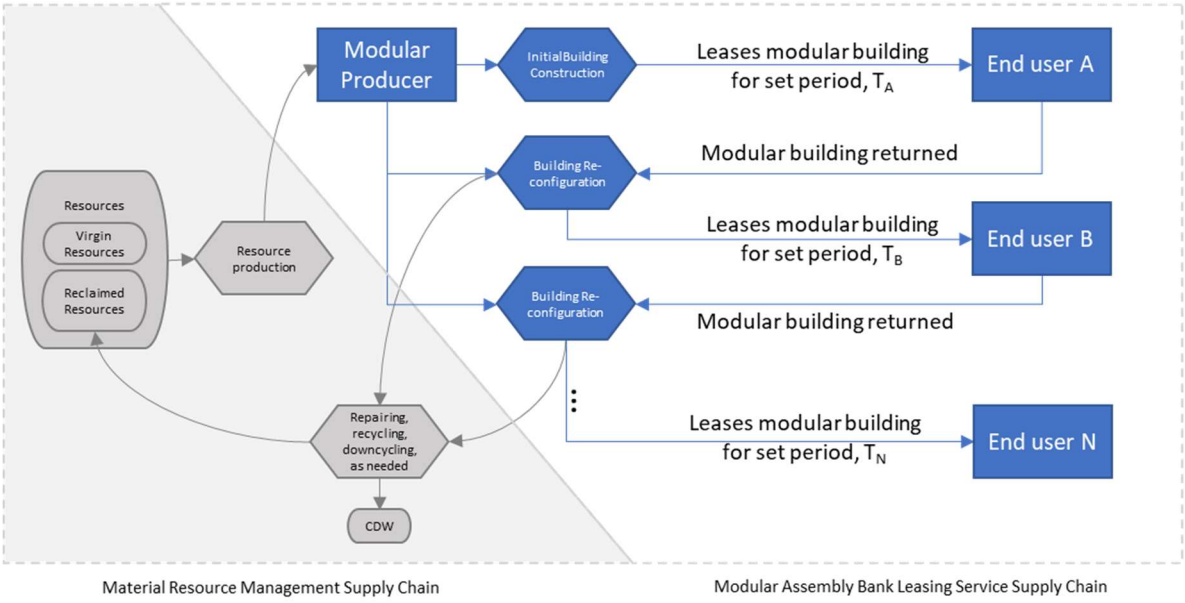

Figure 76: Vertically Integrated Modular Producer and End-user Leasing Business Model

To clarify, this business model is more than a modular building that is rented out to end users. There are many instances where a building is constructed for general commercial or residential leasing (e.g., strip mall complexes or multi-unit apartment buildings). This business model is instead geared towards

specialized use cases. For instance, numerous government agencies were recently challenged with medical isolation needs in light of the novel coronavirus COVID-19 pandemic. An organization in the United States (Modular Mobilization Coalition) proposed deploying modular buildings that could be initially configured as medical isolation units, and when no longer needed, be converted into permanent affordable and supportive housing. Such a unique condition is only possible by designing the initial modular building to function as a structural assembly bank. A government could for instance lease a fleet of medical isolation units for a set duration, after which a permanent building for homelessness support could be configured from several isolation units and then leased for a new period of time.

The value proposition for this business model is formulated as follows. First, the ownership burdened is shifted from an end user to the producer. This of course brings a new risk to the producer, which is managed through an agreement with *End user A* for a set lease period, T_A. Lease A is calculated as

$$Lease\ A = \frac{MB_A - S_A + LCC_A}{T_A} + M$$

Eqn. 32

where MB_A is the cost for producing building A, S_A is the expected salvage value of building A, LCC_A is the life cycle cost for the end-of-life (which is primarily allocated to construction demolition waste, CDW), and M is a set markup for the producer (i.e., to cover overhead, profit margin, etc.). After T_A, a new building is configured and leased to *End user B* for a lease period, T_B. The virgin resources from building A are much higher than the virgin resources for building B since the structure can be salvaged along with other building components. Since Lease A discounts the salvage value of building A, the life cycle costs can be logically monetized. In building B, since the cost to produce the building is offset by the salvage value from building B, no discount is provided for the salvage value of building B (i.e., since $MB_B < MB_A$). As such, Lease B is calculated as

$$Lease\ B = \frac{MB_B + LCC_B}{T_B} + M$$

Eqn. 33

The clever value proposition here is that the producer is incentivized after a second lease period to keep salvaging and reusing the structural system within its built product since what would otherwise be an additional salvage value for building B (i.e., S_B) is not discounted to an end-user. Instead, it becomes straight profit for the producer. If the salvage value is close to the life cycle cost of the modular building configurations, Lease A and Lease B should be close to the same numerical value, which establishes long term financial predictability.

The inherent benefit of this business model is removing the burden of capital expenditure for end users of modular buildings. While banks and lenders could also provide this service, the unique feature with this business model is creating an incentivization scheme for a modular producer to manage the structural assembly assets over time through new value propositions associated with reuse.

B.3.3.2 Conventional Supply Chain Capital Business Model

A second business model illustrates how a conventional supply chain could also support modular buildings as structural assembly banks. As opposed to a simpler model with a fully vertically integrated modular producer, this business model distinguishes unique roles for conventional entities (e.g., engineering, architecture, general contracting and material suppliers) as well as new roles (e.g., reuse material suppliers, DfD specialist and building asset manager). Rather than presenting how this supply chain could facilitate a leasing approach, a more conventional capital expenditure model is explored.

Figure 69 presents the overall supply chain for material resource management and modular building procurement. An initial building is designed by a team of engineers, architects and a DfD specialist. The modular producer then established a supply chain with a reuse material supplier (for structural 'core' assemblies and bespoke structural components), and with a conventional material supplier for raw or generic materials (which could also encompass recycled materials). Then, a modular building is commissioned by a general contractor, who along with the architect has a contract with an owner. A key role also emerges for the management of the modular asset, who ensures a materials passport and maintenance record is kept up to date during the lifecycle of the building. The need for a dedicated asset manager is heavily supported by the BAMB model. At the end-of-life, the modular building is disassembled, where the reuse material supplier salvages key components for a bank of structural 'core' assemblies and bespoke components.

The value proposition with this business model is formulated as follows. Revenue generation lies with recuperated costs from salvaging materials, S_M. These savings (compared with capital expenses for new materials) are used to offset the LCC for the building and for establishing the three new roles: reuse material supplier, modular asset manager and DfD specialist. In order to rationalize this value proposition, the following condition needs to be met:

$$S_M > LCC + DfD + RS + AM$$

Eqn. 34

where LCC is the life cycle costs, DfD is the fee for a DfD specialist, RS is the markup on supply of reused materials and AM is the cost for asset management over the lifespan of the building. Since the initial building will have a higher LCC than subsequent designs (since reuse savings is not attributed to the first building), costs for reuse material supply will take effect in the second building configuration (unless a pre-existing bank of structural 'core' assemblies and bespoke parts exists).

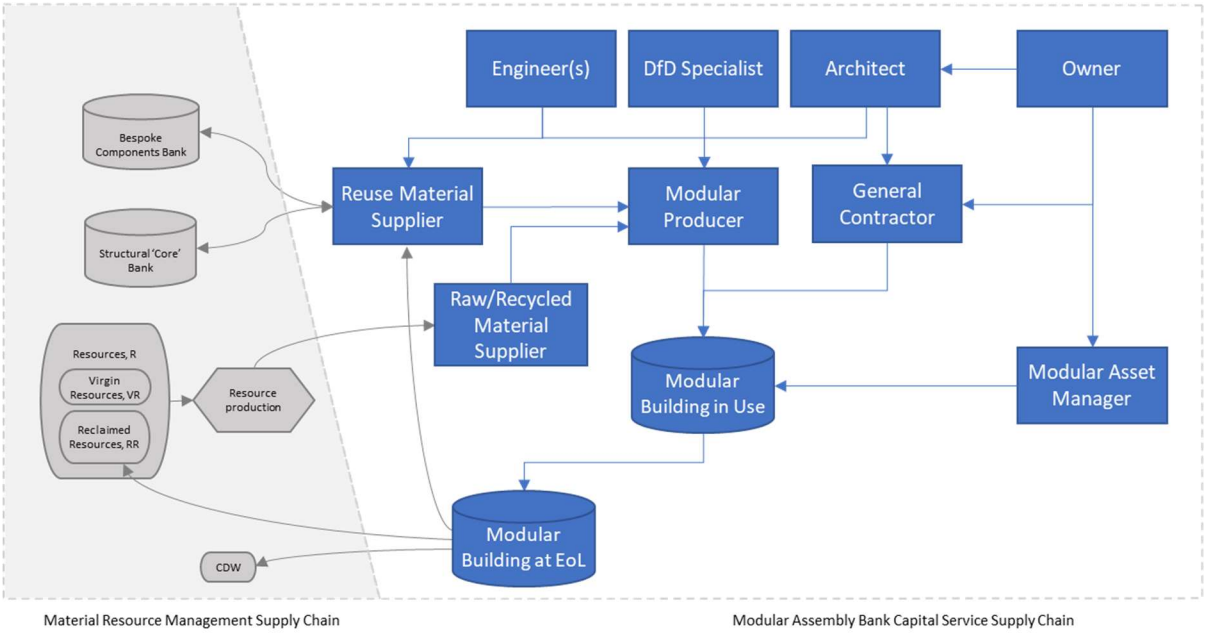

Figure 77: Conventional Supply Chain and Owner Capital Financing Business Model

B.4 Conclusions

With respect to closing material loops in the construction industry, industrialization of structural systems provides several key opportunities. First, as opposed to reuse of individual structural components which are difficult to validate their structural integrity and invariably more challenging to design an entire system of reuse components, industrialized structural systems can be engineered for reuse. In the case of modular buildings, most structural systems have some degree of reserve capacity embedded in them, since additional materials are often required to self-support modules and along matelines. Since these additional materials contribute to more life cycle impacts, it is efficacious to reuse components and assemblies as much as possible. The challenge with existing buildings as material bank (BAMB) models is that they often encompass a diverse range of building components. In order to facilitate dynamic marketplaces, supply chains will rely on having a large inventory of 'banked buildings' in order to suit the needs of new building configurations. Alternatively, industrialized buildings have very similar dimensional properties, which are often dominated by transportation constraints.

This work explored the concept of deploying industrialized buildings as structural assembly banks. The proposed concept relies on having a structural 'core' assembly: configured as a generic frame that could be across a range of buildings. Then additional bespoke components are inserted in order to serve unique structural and architectural needs of each module. It is important to note that reusing structural systems requires important design considerations premised on design for disassembly. While it is generally expected that inter-module connections be standardized in modular buildings, it is also necessary to standardize key intra-module connections. This enables bespoke components to be salvaged more easily and with lower life cycle impacts across use cases.

A case study of a modular accessory dwelling unit was conducted to quantify expected life cycle savings for varying degrees of reuse. An attributional LCA revealed that while the structural assembly comprised 12% of the building mass, the LCIs ranged up to 67% of total cradle-to-grave impacts. However, these impacts are recuperated when considering distinct degrees of reuse. It was found through a consequential LCA that reusing only the structural 'core' assembly (and using raw bespoke components) could reduce LCIs by 78%. Reusing the 'core' assembly along with 100% recycled bespoke components could reduce LCIs by 91%. Finally, reusing the entire structural assembly could reduce LCIs by up to 95%. The remaining LCIs are associated with activities connected with disassembly, transportation from the existing site to the material handling facility and for reconstruction of a new building.

In addition to quantifying the expected life cycle savings, it is key to develop pragmatic business models to support the notion of industrialized buildings as structural assembly banks. This research presented two unique approaches, based on a vertically integrated supply chain, and on a more conventional discretized supply chain. Furthermore, a leasing model vs. a capital expense model were considered. In the lease model, life cycle costs for a modular building are monetized as part of the lease value. The modular producer is incentivized to harvest the structural system by recuperating the salvage value in as little of two cycles. By financing the structural system, the modular producer establishes a lucrative interest in managing not only the delivery of a modular building, but its multi-life cycle existence. End-users in this business model are not burdened by traditional capital expenditure, and depending on the lease duration, the building can be optimally configured to match the functional utility. In the more conventional business model, the salvage value of reusing the structural system in a modular building is used to create new stakeholder roles in the deliver process; specifically, a dedicated DfD specialist, modular asset manager, and reuse material supplier. In such a business model, the expected reuse savings are also used to offset the life cycle costs.